EUNAseis

a seismic model for Moho and crustal structure in Europe, Greenland, and the North Atlantic region

Artemieva, Irina; Thybo, Hans

Published in:
Tectonophysics

DOI:
10.1016/j.tecto.2013.08.004

Publication date:
2013

Document version
Publisher's PDF, also known as Version of record

Tectonophysics 609 (2013) 97–153

Contents lists available at ScienceDirect

Tectonophysics

journal homepage: www.elsevier.com/locate/tecto

Review Article

EUNAseis: A seismic model for Moho and crustal structure in Europe, Greenland, and the North Atlantic region ☆

Irina M. Artemieva *, Hans Thybo

IGN, University of Copenhagen, Denmark

ARTICLE INFO

Article history:
Received 27 November 2012
Received in revised form 18 July 2013
Accepted 4 August 2013
Available online 15 August 2013

Keywords:
Moho
Crustal thickness
Crystalline crust
Sedimentary cover
Pn velocity
Crustal evolution

ABSTRACT

We present a new digital crustal model for Moho depth and crustal structure in Europe, Greenland, Iceland, Svalbard, European Arctic shelf, and the North Atlantic Ocean (72W–62E, 30N–84N). Our compilation is based on digitization of original seismic profiles and Receiver Functions from ca. 650 publications which provides a dense regional data coverage. Exclusion of non-seismic data allows application of the database to potential field modeling. EUNAseis model includes Vp velocity and thickness of five crustal layers, including the sedimentary cover, and Pn velocity. For each parameter we discuss uncertainties associated with theoretical limitations, regional data quality, and interpolation.

By analyzing regional trends in crustal structure and links to tectonic evolution illustrated by a new tectonic map, we conclude that: (1) Each tectonic setting shows significant variation in depth to Moho and crustal structure, essentially controlled by the age of latest tectono-thermal processes; (2) Published global averages of crustal parameters are outside of observed ranges for any tectonic setting in Europe; (3) Variation of Vp with depth in the sedimentary cover does not follow commonly accepted trends; (4) The thickness ratio between upper-middle (Vp < 6.8 km/s) and lower (Vp > 6.8 km/s) crystalline crust is indicative of crustal origin: oceanic, transitional, platform, or extended crust; (5) Continental rifting generally thins the upper-middle crust significantly without changing Vp. Lower crust experiences less thinning, also without changing Vp, suggesting a complex interplay of magmatic underplating, gabbro-eclogite phase transition and delamination; (6) Crustal structure of the Barents Sea shelf differs from rifted continental crust; and (7) Most of the North Atlantic Ocean north of 55°N has anomalously shallow bathymetry and anomalously thick oceanic crust. A belt of exceptionally thick crust (ca. 30 km) of probable oceanic origin on both sides of southern Greenland includes the Greenland–Iceland–Faeroe Ridge in the east and a similar "Baffin Ridge" feature in the west.

Contents

* Corresponding author. Tel.: +45 35322473; fax: +45 35322501.
E-mail address: irina@geo.ku.dk (I.M. Artemieva).

0040-1951/$ – see front matter © 2013 The Authors. Published by Elsevier B.V. All rights reserved.
http://dx.doi.org/10.1016/j.tecto.2013.08.004

1. Introduction

The crust in most parts of continental Europe has been studied in detail, primarily during the past half a century. Details of the development of crustal studies may be found in Prodehl et al. (2013–this volume). The first controlled source seismological experiment was carried out near Dublin in the mid 19th century by Mallet (1852), who determined the velocity of granites in the upper crust. The refraction seismic method came into use following *Mintrop's* developments in the 1920s and the first observations of normal-incidence reflections from the Moho were published by Beloussov et al. (1962), Kosminskaya and Riznichenko (1964), Liebscher (1964), Dohr and Fuchs (1967), Meissner (1967) and Clowes et al. (1968). During the late 20th century, several large scale seismic experiments provided the dense data coverage of the structure of the European crust, e.g. a series of EGT sub-projects, BABEL, POLONAISE and the Celebration'2000/Alps2000 projects, as well as the extensive activities by various national seismic programs (e.g. DEKORP, ECORP, and BIRPS).

The results have earlier been summarized as maps of the depth to Moho for specific areas of Europe (e.g. Behm et al., 2007; Beloussov et al., 1991; Burollet, 1986; Dezes et al., 2004; Garkalenko, 1970; Neprochnov et al., 1970; Pavlenkova, 1996; Sollogub, 1970; Thybo, 1997; Volvovski, 1973; Volvovsky and Volvovsky, 1975), and for the whole of western Europe (Artemieva and Meissner, 2012; Grad et al., 2009; Meissner et al., 1987a,b; Tesauro et al., 2008; Ziegler and Dezes, 2006). Two of them (Grad et al., 2009; Tesauro et al., 2008) additionally cover substantial areas outside of western Europe (Fig. 1) and are available in digital form, which makes them a useful tool for many geophysical studies. The models differ by the spatial coverage and include significantly different information on the crustal structure (Table 1): Grad et al. (2009) published a map of depth to the Moho in the European plate, whereas EuCRUST-07 model (Tesauro et al., 2008) includes information on the internal structure of the crust. Methodologically, both models are based on an extensive selection of original interpretations of seismic profiles, published maps and also use gravity data, tectonic regionalization, and interpolation to fill-in gaps between incorporated compilations. For example, gravity models, tectonic considerations and interpolations, such as often used in the crustal models of Russian geophysical organizations GEON (1979-1994), are inherited in the crustal model by Grad et al. (2009), where the Russian compilations (Erinchek and Milstein, 2006; Kostyuchenko, 1999) form an integral part.

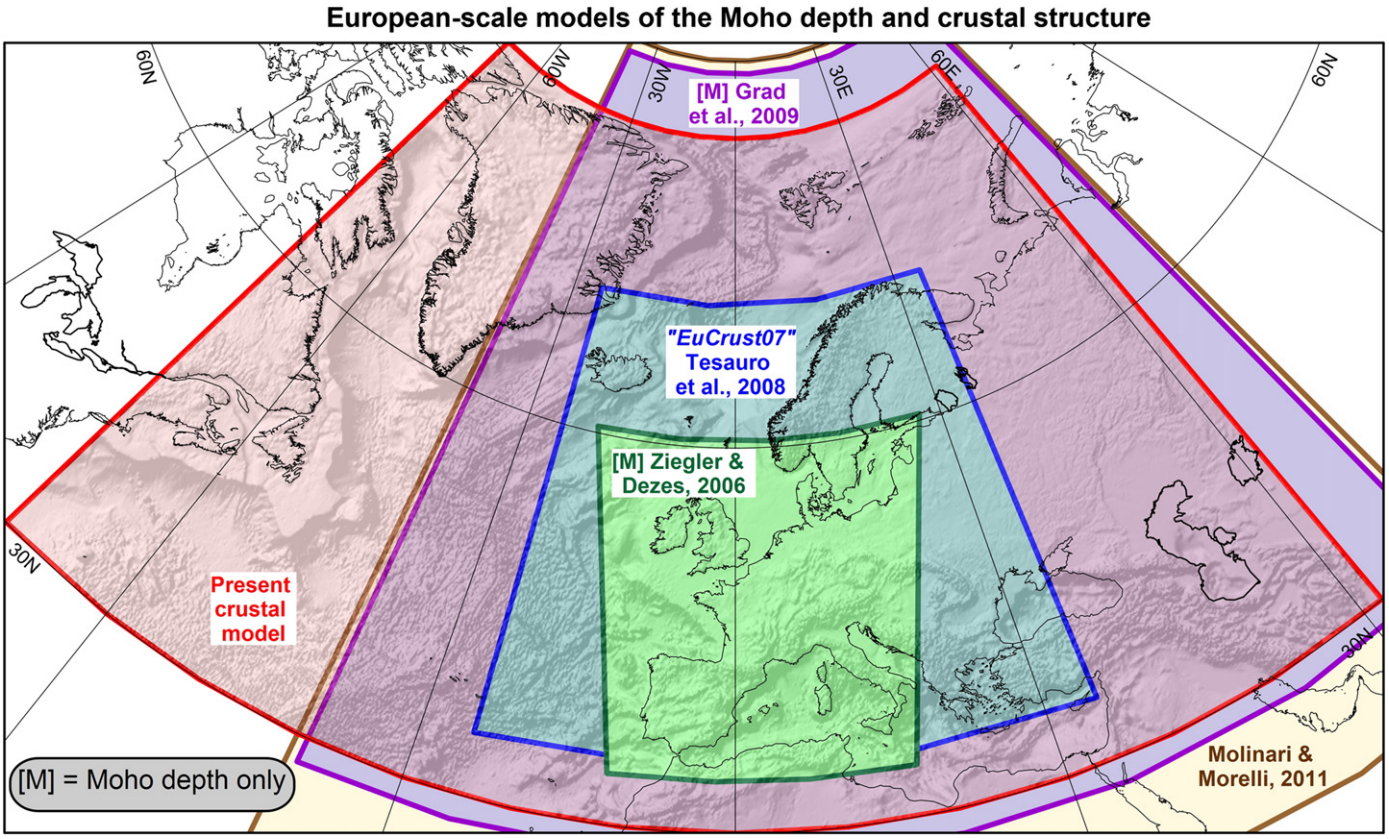

Fig. 1. Coverage of the European continent and the adjacent areas by continent-scale models of Moho depth (Grad et al., 2009; Ziegler and Dezes, 2006) and crustal structure (Tesauro et al., 2008; Molinari and Morelli, 2011; present study).

In contrast, another recent crustal model for the European plate (Molinari and Morelli, 2011) builds not on original crustal models as constrained by seismic and gravity interpretations, but incorporates eight previous global and regional compilations. To resolve problems arising from inconsistency of regional compilations by different authors, they introduce a data weighting factor, which is proportional to the number of crust-specifying parameters in original models. Thus, the European part of global crustal model CRUST2.0 (Bassin et al., 2000), which is partially constrained by geological similarity rather than by geophysical data, got the highest weight since it includes the largest number of parameters (18 as compared, for example, to 1 parameter (Moho depth) in three high resolution regional seismic models for the Iberian Peninsula (Díaz and Gallart, 2009), the Italian Peninsula (Agostinetti and Amato, 2009), and southern Norway (Stratford et al., 2009) and to 7 parameters in the EuCRUST-07 model (Tesauro et al., 2008)). The approach may be questioned since there is no reason why the number of parameters in a database and the accuracy of constraints of each parameter should be correlated. We further address this problem in Section 6.1.4 where we show that there is a significant difference between CRUST2.0 (Bassin et al., 2000) and regional seismic models for large parts of the study region.

Here we adopt an alternative approach to use only original seismic results from the region (reflection and refraction profiles, Receiver Function (RF) interpretations, and some tomography models in regions where no other seismic data are available, see Table 1 for details) as constraints for our model of the crustal structure (Electronic Supplements 1 and 2). Thereby, we ensure that our results can be used as independent constraints for interpretations of potential field (e.g. gravity) data, in addition to being valuable for understanding the implications from various tectonic and geological events in the region for crustal structure and evolution. The EUNAseis model also includes a broader range of crustal parameters than any existing regional model (Table 1) and extends further westwards (Fig. 1). In the east, the new crustal model links to a recently released new crustal model SibCrust for Siberia (Cherepanova et al., 2013–this volume); both models are constrained by the same methodology and thus can be easily merged.

We present a new, consistent regional digital model of the crust and uppermost mantle structure, based on original seismic interpretations. The results are summarized in a series of maps of lateral variation in crustal and sedimentary cover thicknesses, average Vp seismic velocity variations in the crust and in the sub-Moho mantle (Pn). We next use our new model EUNAseis to review the crustal structure in an area which extends from the Atlantic coast of North America in the west to the Urals in the east and encompasses Europe, Greenland, and Iceland. We focus on on-shore areas, but the adjacent parts of the North Atlantic Ocean are included into the discussion to constrain a continuous regional model. We correlate regional variations in crustal thickness and velocity heterogeneity with regional tectonics and plate tectonic processes since the Archean. Five cross-sections further illustrate heterogeneity of the regional crustal structure.

2. Tectonic evolution: an overview

2.1. Preamble

The topography and bathymetry of the study region (72W–62E, 30N–84N) (Fig. 2) show several characteristic aspects. Within the on-shore part of the region, the Precambrian part of the European continent (the East European craton (EEC) which outcrops in the Baltic and Ukrainian shields) is flat with topography commonly less than 300 m, whereas Precambrian Greenland shows stronger topographic variation with heights of 2000 m and the central parts below sea level. Isostasy

Table 1
Summary of continent-scale crustal models for Europe.

Continent-scale crustal models	Ziegler and Dezes (2006)	Tesauro et al. (2008) (EuCRUST-07)	Grad et al. (2009)	Molinari and Morelli (2011) (EPcrust)	Present model (EUNAseis)
Area	34°N–61°N, 20°W–25°E	35°N–71°N, 25°W–35°E	28°N–88°N, 40°W–70°E	20°N–90°N, 40°W–70°E	30°N–84°N, 70°W–62°E
Methodology					
Seismic models	No specific information	Compilation based on ca. 15 previous regional compilations for various crustal parameters, complemented by 134 papers on the crustal structure and 44 papers on Moho depth	Compilation based on 39 previous regional compilations, complemented by 112 papers on Moho depth (in total more than 250 datasets from individual seismic profiles)	Compilation based on 8 previous global and regional compilations, complemented by RF models and 4 global and regional compilations for Moho depth	Compilation "from scratch" based on ca. 650 papers on the seismic crustal structure and additionally ca. 200 RF models for Moho depth
Discretization of seismic model	No information	No information on compilation strategy, compilation includes digitized contour maps	No information, compilation includes digitized contour maps	Weighted merging and averaging of all datasets (weight depends on the number of crustal parameters in incorporated models)	Along seismic profiles digitized with less than 50 km spacing
Potential field data	No information, might be included	Included through use of previous regional compilations	Explicitly included	Included through use of previous regional compilations	Excluded
Geological data	No information, might be included	Included, no specific information on the details	Included through use of previous regional compilations	Included through use of previous compilations (e.g. CRUST2.0)	Bathymetry used to assign only Moho depth on deep-water side along parts of the shelf–ocean transition without seismic data
Model parameterization					
Moho depth	Yes	Yes	Yes	Yes	Yes
Sedimentary cover	n/a	Thickness; depth to the basement	n/a	Thickness based on weighted averaging of compiled models; average Vp in layer is determined from regional dependence on sediment thickness; Vs and density are derived from Vp using a Nafe–Drake regression	Thickness, depth to the basement, average Vp in the sedimentary layer extracted from seismic models without other assumptions
Crustal layers within the crystalline crust	n/a	2 layers (upper crust and lower crust)	n/a	2 layers (upper crust and lower crust)	4 layers (upper, middle, lower, and high-Vp lower) crust
Parameters for crustal layers	n/a	Thickness; Vp	n/a	Thickness; average Vp in layer (Both thickness and Vp are based on weighted averaging of compiled models); Vs and density derived from Vp using a Nafe–Drake regression	Thickness; Vp (Both parameters derived from seismic models)
Average crustal Vp in crystalline crust	n/a	Vp calculated as weighted average	n/a	n/a	Vp calculated as weighted average and through travel times
Average crustal Vp (incl. sediments)	n/a	n/a	n/a	n/a	Vp calculated as weighted average and through travel times
Upper mantle Pn velocity	n/a	n/a	n/a	Yes	Yes
Availability in digital form	n/a	Yes [T]	Yes [G]	Yes [M]	Yes [A]

Web-sites with electronic versions of databases:

[T] GRL web-site and http://onlinelibrary.wiley.com/doi/10.1029/2007GL032244/suppinfo
[G] http://www.seismo.helsinki.fi/mohomap/
[M] http://www.bo.ingv.it/~molinari/EPcrust_solar/download.html
[A] www.lithosphere.info.

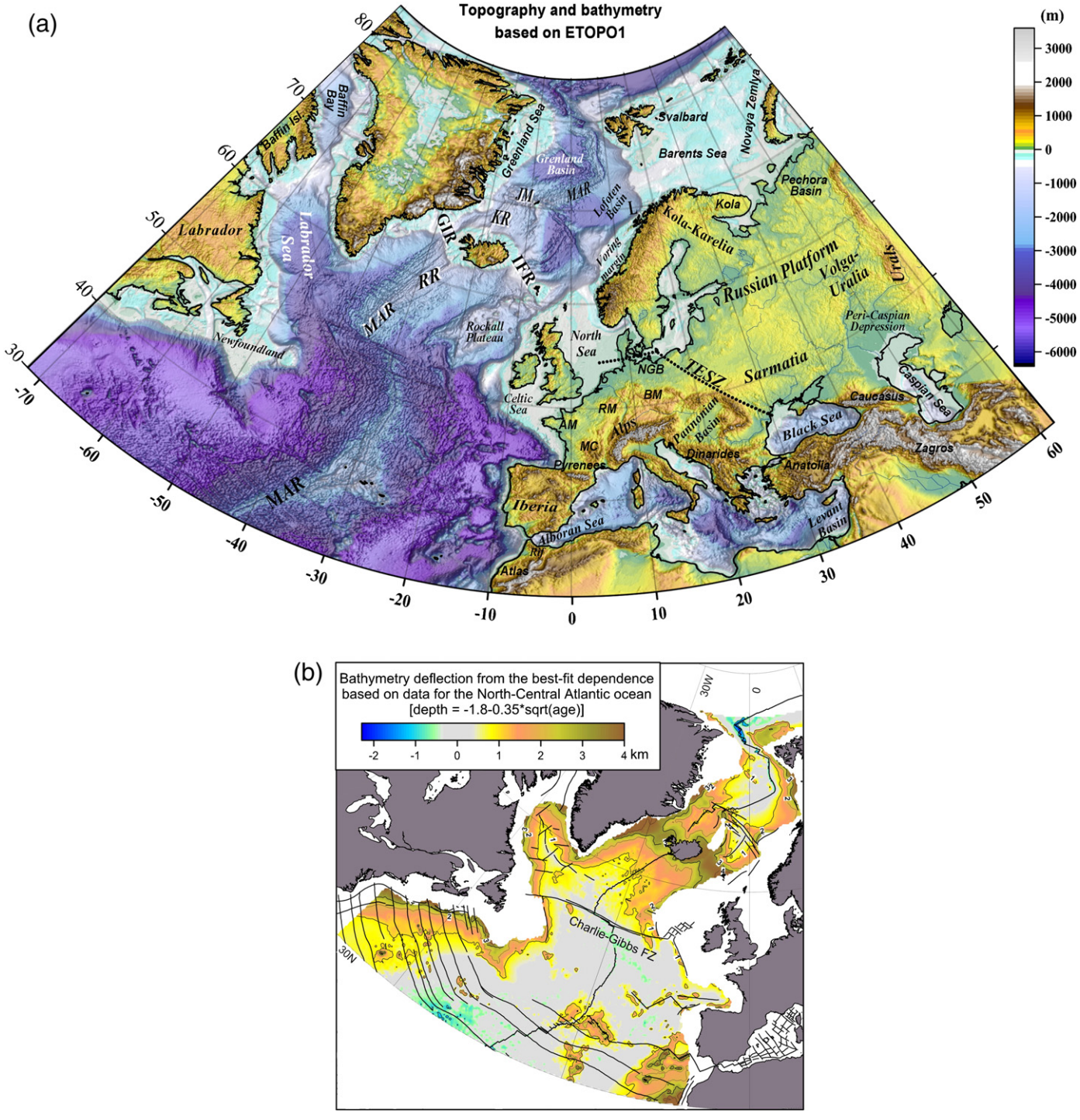

Fig. 2. (a) Topography and bathymetry of Europe, Greenland, and the North Atlantic Ocean based on ETOPO1 data (NOAA, 2011). Dotted line — Trans-European Suture Zone (TESZ), which separates the Precambrian East European craton from Phanerozoic Europe. Abbreviations: AM — Armorican massif, BM — Bohemian massif, GIR — Greenland–Iceland Ridge, IFR — Iceland–Faeroe Ridge, JM — the Jan Mayen microcontinent, KR — Kolbeinsey Ridge, L — the Lofoten block, MAR — Mid-Atlantic Ridge, MC — Massif Central, NGB — North German basin, RM — Rhenish massif, RR — Reykjanes Ridge. Topography of Greenland is shown for bedrock, i.e. without ice (ice thickness increases inland and reaches ca. 3.8 km in the center). (b). Anomalous bathymetry of the North Atlantic Ocean based on ETOPO1 data (NOAA, 2011) for bathymetry and ages of the oceanic crust based on a global compilation (Müller, 2002). For the North-Central Atlantic ocean the best-fit square-root-of-age dependence (as predicted by the cooling half-space model) is estimated for the ocean floor younger than 80 Ma. Most of the ocean floor in the North-Central Atlantic ocean south of the Charlie–Gibbs fracture zone follows the square-root-of-age prediction of the cooling half-space model (gray shading). With few exceptions, all of the North Atlantic ocean north of the Charlie–Gibbs fracture zone is anomalous. Off-shore regions without magnetic anomalies (continental shelves), as well as the Mediterranean Sea are shown in white. Black lines — major fracture zones.

may explain the negative bedrock topography in central Greenland by balancing the load of the ice cap, as the thickest ice sheet (close to 4000 m thick) is observed at the deepest depression of the bedrock topography (Bamber et al., 2001).

All topography in western-central Europe is young and shows high elevations in Cenozoic orogens with the highest peaks in the Caucasus, Alps, and orogenic belts around the Mediterranean Sea. Notably, Precambrian areas, Paleozoic orogens and Mesozoic volcanics close to the

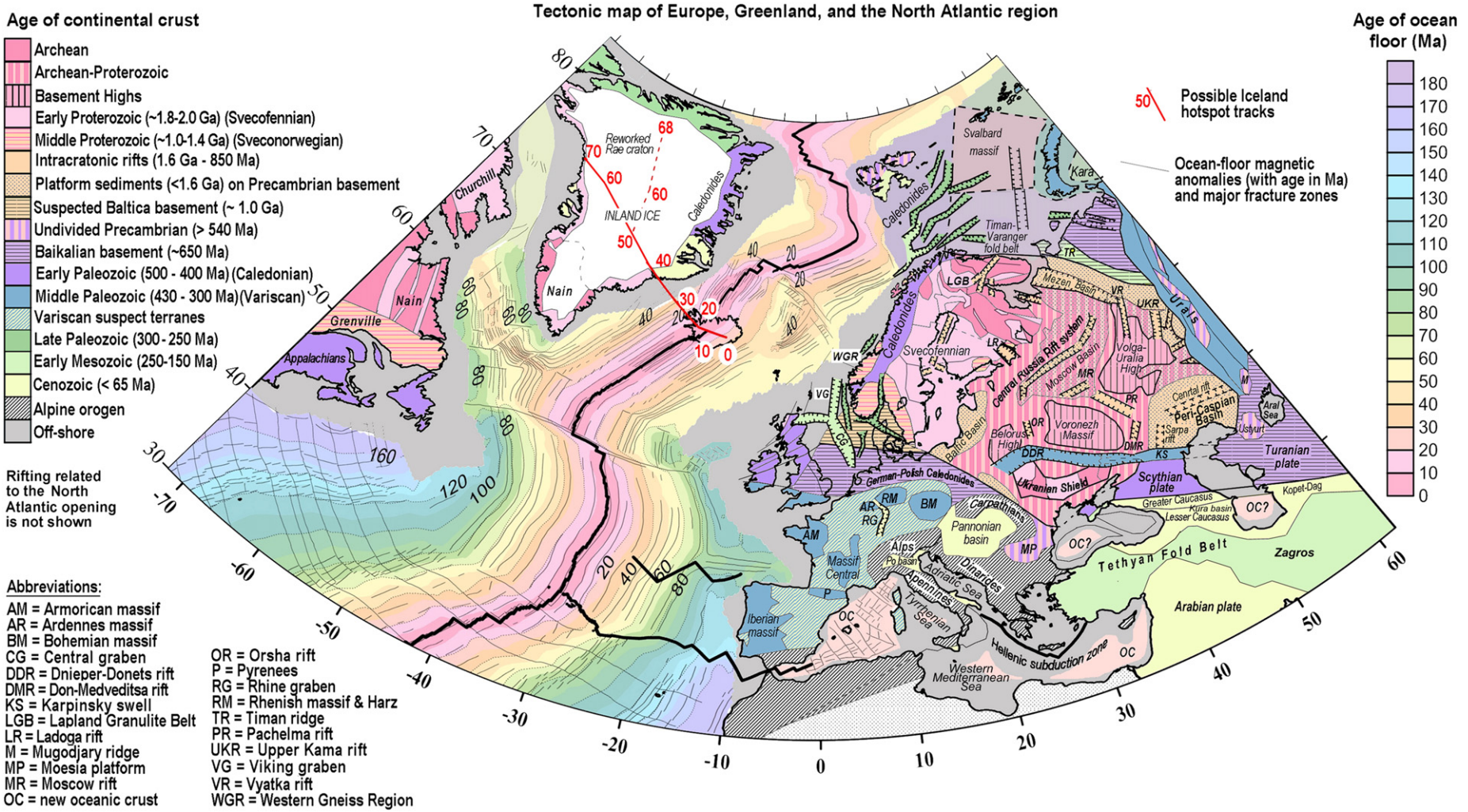

Fig. 3. Tectonic map of Europe, Greenland, and the North Atlantic Ocean (compilation based on various sources). The color codes for the Phanerozoic continents and oceans are adjusted to facilitate comparison. For the continents, the map shows tectono-thermal (not juvenile) ages of the crust (updated from different sources and modified after Artemieva et al., 2006). Ages of the oceanic crust are based on a global compilation of Müller (2002). Suspected oceanic crust in the western Black Sea and the southern Caspian Sea is marked by question marks (Beloussov et al., 1988; Zonenshain and Le Pichon, 1986). Red lines — proposed tracks of Iceland hotspot (numbers — ages in My): solid line — for fixed hotspot (Lawver and Muller, 1994) and dashed line — for moving hotspots in a corrected paleomagnetic frame (Torsvik et al., 2008).

Off-shore regions without magnetic anomalies (the shelves with bathymetry typically shallower than 400 m) are shaded gray. Inferred terranes of the Barents Sea shelf (Pre-Neoproterozoic Svalbard massif and White Sea, Neoproterozoic Timan-Varanger Fold belt, Caledonian West Barents Sea, and Early Mesozoic Novaya Zemlya Fold belt) are after Drachev et al. (2010).

Greenland and Norwegian coasts of the North Atlantic have high elevation as well (up to ca. 3700 m) despite the fact that the Caledonian orogen may once have been eroded to sea level (Japsen and Chalmers, 2000). The cause of the present-day high topography on both sides of the North Atlantic Ocean is the subject of debate (e.g. Anell et al., 2009 and references therein).

Much of the water covered parts of the region are of continental origin with wide continental shelves along the coasts of Norway and Greenland and in the Barents Sea, and shallow water seas around the British Isles, the North Sea and the Baltic Sea (Fig. 2a). The bathymetry of the North Atlantic Ocean shows characteristic deepening away from the spreading ridges. However, much of the North Atlantic Ocean is anomalous (Fig. 2b) with shallow waters most notable in the Iceland–Faeroe and Greenland–Iceland Ridges, and also at the presumed continental slivers such as at the East Greenland Ridge, the Jan Mayen microcontinent and the Rockall plateau (Døssing et al., 2008; Gernigon et al., 2009; Klingelhofer et al., 2005). A similar shallow water "ridge" crosses the Baffin Bay (hereafter referred to as the Baffin Ridge). New oceanic crust is interpreted to be present in the western Mediterranean (e.g. Müller, 2002). The nature of the crust in the eastern Mediterranean (the Levant basin south of Cyprus) is still debated, and in our new tectonic map (Fig. 3) we adopt the results which favor its oceanic origin (e.g. Ben-Avraham et al., 2002; Khais and Tsokas, 1999). New oceanic crust may also be present in the western Black Sea and the southern Caspian Sea (both the Black and the Caspian seas include two independent basins). The ridge which separated the northern (shallow) and the southern (deep) basins of the Caspian Sea and served as a part of the ancient Silk Route became submerged recently, after the 1895 Krasnovodsk earthquake (M = 7.9) (Ivanovsky, 1896; Kondorskaya and Shebalin, 1977).

The Europe–North Atlantic–Greenland region comprises a unique mosaic of crustal terranes covering ca. 4 Ga of continental and ca. 170 Ma of oceanic crustal history. Its evolution has been influenced by a long series of tectonic events, starting from formation of the early crust in Greenland and in the East European Craton in the Archean, followed by Proterozoic terrane accretion, orogenesis and subduction, and subsequent Phanerozoic continent–continent collision at the edges of the cratons and at plate boundaries, subduction, rifting, volcanism, and basin formation, as well as formation of new crust at the Mid-Atlantic Ridge and in Iceland. Naturally the latest evolution is known in most detail. We refer to the map in Fig. 3 for tectono-thermal ages of the upper part of the lithosphere (note that tectono-thermal ages refer to the time of the last major tectonic event, whereas the geological ages refer to the time of crustal formation by differentiation from the mantle). In discussion of the Precambrian tectonics of the East European Platform, we follow the still widely-used Russian Proterozoic stratigraphic scheme (Semikhatov, 1991), since all regional geotectonic studies are based on it. The correspondence between this scheme and the International Time Scale is given in Fig. 4.

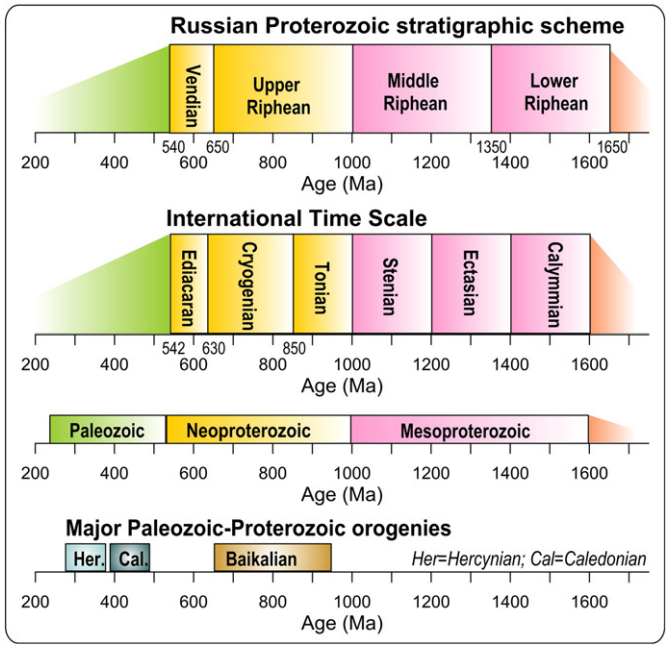

Fig. 4. Sketch showing the correspondence between the still widely-used Russian Proterozoic stratigraphic scheme (Semikhatov, 1991) and the International Time Scale (Gradstein et al., 2012). Bottom axis shows time intervals for major Paleozoic–Proterozoic orogenies discussed in the text.

2.2. Precambrian basement

The oldest crust in the Europe–North Atlantic–Greenland region is located in the northern and eastern continental parts which include Greenland and the East European craton (in the following termed "Norden"). It is mainly of Precambrian age and is primarily made of crust from the two palaeocontinents: Baltica (most of present day Baltic Shield together with parts of the EEC) and Laurentia (much of North America and Greenland), which have been accreted several times, at least as parts of the Neoarchean Kenorland, Neoproterozoic Rodinia, Palaeozoic–Mesozoic Pangea supercontinents, and the Laurasia supercontinent after the break-up of Pangaea in the late Mesozoic. Additionally, three large subcratons separated by Riphean rifts (sutures?) are recognized within the East European Craton: Baltica to the north of the Central Russia rift system, Sarmatia (including the Ukrainian shield and the Voronezh massif) to the west of the Pachelma rift, and Volgo–Uralia in the eastern part of the East European Craton, north of the Peri-Caspian depression (Fig. 3).

Rocks from the shield areas have been substantially dated due to the easy access, whereas in most of the East European Craton basement sampling for dating is complicated by Phanerozoic sedimentary sequences (up to 15–25 km in thickness on the continental shelves and around the North Sea area), as well as by the ice cover of Greenland. In Greenland only samples of the crust in the vicinity of the coast have been dated due to the presence of the ice cap. The oldest known, well-preserved crustal fragments, ca. 3.8 Ga old, are found in the Itsaq Gneiss Complex of southern West Greenland (Nutman et al., 1993). The crust is believed to be mainly of Archean to Palaeoproterozoic age, and Archean rocks have been dated at both the eastern and western coasts of southern Greenland (Kalsbeek, 1993).

The Ukrainian Shield is made of Archean granulite gneisses and greenstone belts and Paleoproterozoic crustal blocks (Fig. 3) which are traced in the Archean–Paleoproterozoic Voronezh massif separated from the Ukrainian shield by the Paleozoic Dnieper–Donets paleorift. Basement outcrops in the Ukrainian Shield (the Sarmatia subcraton) have Paleoarchean age (ca. 3.6–3.0 Ga) (Stepanyuk et al., 1998). Similar ages were reported also in the southernmost part of the Karelian Province of the Baltic Shield (the Vodlozero terrane south of the Ladoga Lake), although the age of the oldest crust of the Baltic shield proper (in the Kola–Karelian province) is significantly younger, ca. 3.1–2.5 Ga (e.g. Gaal and Gorbatschev, 1987). A similar age (3.1–2.8 Ga) is found in the Lewisian Gneiss Complex in northern Scotland; these rocks have later been metamorphosed and deformed in a major tectonothermal event at 2.7–2.5 Ga (Macdonald and Fettes, 2006).

The basement of the East European Platform is buried under 3–6 km cover of Riphean–Mesozoic sediments (Bronguleev et al., 1975; Nalivkin, 1976). As a result, its age is not well known, but data from thousands of deep boreholes indicate mostly Palaeoproterozoic ages (2.1–1.8 Ga), although Paleoarchean crust may be present. The oldest basement rocks of the East European Craton have been sampled in the deep boreholes in the Volga–Uralia subcraton, where Hf and Nd isotope dating of zircons indicate a Paleo- to Eoarchean protolith with model ages up to 3.8 Ga

(Bogdanova et al., 2010). Basement samples from deep boreholes in the Middle Volga granulite–gneiss domain indicate ages of 3.3–2.9 Ga (and perhaps also 3.7–3.3 Ga), although they were subject to later large-scale amphibolite-facies metamorphism at 2.8–2.6 Ga which could have reset the isotope systems (U–Pb and Sr–Nd dating, Bibikova et al., 2008). About eight large greenstone belts are recognized in the (mostly granulite gneissic) basement of the East European Craton (Lobach-Zhuchenko, 1988). They form a sublongitudinal belt which extends from the Black Sea coast to the Kola Peninsula with ages ranging from ca. 3.2–3.0 Ga in the south to ca. 2.7–2.5 Ga in the north. The Archean–Proterozoic basement of Fennoscandia probably extends into the Barents Sea area, where (a part of?) the Svalbard archipelago in the north-west is of Proterozoic (and locally, Archean) age (Harland, 1997).

A series of terranes were accreted to the Archean provinces of the Baltic Shield during the Svecofennian orogeny in the late Proterozoic (2.0–1.8 Ga) (Gaal and Gorbatschev, 1987). Subsequently, the Sveconorwegian (coeval with the Grenvillian) orogeny (1.1–0.9 Ga) deformed the southern part of the Baltic Shield during the assembly of Rodinia. Sets of dipping reflections from the mantle are imaged laterally over distances of up to 100 km at 40–110 km depths by high-resolution seismic reflection experiments in the Bothnian Gulf and Bay, in onshore Sweden, in the southern Baltic Sea, and in the Skagerrak Strait. These reflections are interpreted as relics of paleosubduction associated with the Svecofennian and Sveconorwegian orogenies (Abramovitz et al., 1997; BABEL WG, 1990, 1993a,b; Dahl-Jensen et al., 1987; Lassen and Thybo, 2004; Lie et al., 1990).

The Riphean (1.35–1.05 Ga) tectonics of the East European Craton is marked by emplacement of rapakivi granites in its north-western part and subsequent subsidence of the Baltic Sea (Gaal and Gorbatschev, 1987). The Riphean is also marked by the formation of a craton-scale rift system across the East European (Russian) Platform (Fig. 3) which is well expressed in the thickness of the sedimentary cover and in the structure of the basement (Artemieva, 2007; Kostyuchenko et al., 1999). This rift system may have developed in the paleosutures between three autonomous crustal megablocks/subcratons (Baltica in the north, Sarmatia in the south-west, and Volga–Uralia in the south-east) which were assembled into the East European Craton (Gorbatschev and Bogdanova, 1993).

Devonian rifting in the southern parts of the Russian platform (with peak magmatism at ca. 350 Ma) led to the formation of the ca. 1000 km long Pripyat–Dnieper–Donets rift. The rift continues further eastwards to the Peri-Caspian depression. The central part of the depression was probably formed by Riphean rifting, followed by Devonian rifting that may have led to the formation of the oceanic or magmatic crust at the intersection of two rift systems (the Riphean Pachelma rift and the Devonian Sarpa and Central paleorifts), which are both characterized by positive gravity anomalies (Zonenshain and Le Pichon, 1986).

2.3. Palaeozoic orogens

The last collision between Baltica and Laurentia took place during the Caledonian orogeny (500–400 Ma, Caledonia is the Latin name of Scotland) along the present western margin of the Baltic Shield and the eastern margin of Greenland. Further to the south, a micro-continent or a series of accreted terranes (Avalonia) collided at a triple junction with Baltica and Laurentia in the North Sea area (Lassen et al., 2001; Lyngsie and Thybo, 2007; MONA LISA Working Group, 1997a,b).

The major geologic and tectonic boundary in Europe is the Trans-European Suture Zone (TESZ), which separates the East European Craton from the Caledonides and Variscides of western Europe and marks the western margin of the craton. The accretion of a series of terranes during the Caledonian (500–400 Ma) and the Variscan (Hercynian, 430–300 Ma) orogenies took place in a ca. 3000 km long and a 700–1000 km wide belt along the cratonic margin (Pharaoh, 1999; Sengör, 1990; Thybo et al., 1999, 2002; Ziegler, 1986, and references therein; Winchester and the PACE Network Team, 2002). The oldest of the accreted terranes are the Neoproterozoic–Paleopaleozoic Massif Central and the Bohemian, Brabant, Armorican, Iberian and the Ardennes massifs (Bosse et al., 2005; Dallmeyer and Tucker, 1993; Dewey, 1982; Grauert et al., 1973; Guerrot, 1989; Tichomirowa et al., 2005). Detrital zircons from some of these terranes even indicate Archean to Mesoproterozoic ages (e.g. Fernandez-Suarez et al., 2002; Gutierrez-Alonso et al., 2005).

Subduction, orogeny, and crustal shortening affected the accreted terranes of the Hercynian belt by deformation and metamorphism during the Variscan closure of paleo-oceans (Dubuisson et al., 1989; Matte, 1986; Ziegler, 1986). During the late stages of the Variscan orogeny, intensive melting of thickened continental crust (anatexis) created widespread granite intrusions in the crust. Following orogenesis and crustal shortening, late Palaeozoic large-scale normal faulting and crustal extension followed, which led to thinning, perhaps analogous to the modern Basin and Range province (Artemieva and Meissner, 2012; Menard and Molnar, 1988). Significant tectonic activity took place along the northern segment of the TESZ in the late Palaeozoic–Mesozoic, as observed from faults and rifts with associated magmatism in a system of rifts which included the Oslo rift and the Central Graben in the North Sea (Olsen, 1995; Thybo, 1997).

The geographic boundary between Europe and Asia is the Ural mountain belt, which marks the eastern margin of the East European Craton. The Uralides orogen is partly exposed in the Ural mountain belt, the Novaya Zemlya archipelago, and the Taimyr peninsular in the Polar East Siberia; a substantial part of the orogen is buried under the sedimentary cover of the West Siberian basin. The Uralides is the only Palaeozoic orogen which has remained intact with preserved lithospheric structure since the Palaeozoic, being trapped within stable continental interior since its formation. Its Precambrian nucleus is exposed locally in the Northern Urals (1.7 Ga), Central Urals (2.9–2.0 Ga, SHRIMP U–Pb zircon dating, rocks from the Taratash block), and Southern Urals (1.63 Ma) (Puchkov, 2010 and references therein).

Accretion of microcontinents, island arcs, volcanic complexes and fold belts to the passive (and later, in Silurian–early Devonian, active) margin of the East European Craton during its collision with the Siberian–Kazakhstan plate gave birth to the Uralides orogen at 450–385 Ma (main phase) (Zonenshain et al., 1990). The early-middle Paleozoic tectonic evolution of the Urals included: continental and oceanic rifting at ca. 500 Ma, a passive continental margin stage at ca. 450–320 Ma, and the development of several Silurian–Devonian subduction systems (including east-dipping subduction of the Baltica plate), which have different timing in different parts of the Uralides orogen. Two major island arc complexes (although there are several others known) include the Tagil arc in the Middle Urals (60–64N) formed at ca. 460–400 Ma (there is some indication for later subduction reversal when the Alapaevsk island arc and active continental margin were formed in the Middle Urals, Kashubin et al., 2006) and the Magnitogorsk arc in the Southern Urals (50–58N) formed at ca. 400–360 Ma with its likely continuation in the Mugodjary Ridge to the south (Fig. 2a).

Late Paleozoic was marked by active compressional tectonics as indicated by collision-related granitic plutons. The Uralides fold belt was formed at the final stages of the plate collision (320–250 Ma), when the oceanic plate between the European and the Siberian–Kazakhstan plates subducted eastwards (Hamilton, 1970; Sengör et al., 1993). The orogeny ceased by ca. 260–250 Ma in the Southern Urals, but it still continued in the Middle Urals. The Triassic uplift of the orogen, coeval with scattered basaltic trap magmatism (250–230 Ma), is attributed to a mantle plume since no Triassic deformation is documented (Puchkov, 1997). In the Middle Jurassic to Miocene (ca. 170–20 Ma), the Uralides underwent a platform stage of evolution with sedimentation in the West Uralian and East Uralian zones (similar zones, the Fore-Uralian and the Trans-Uralian, are recognized in the Polar Urals). The present day topography came into existence in the Tertiary–Quaternary (Lider, 1976). The past 5 Ma are marked by a new, on-going orogenic activity which is responsible for the present topography of the Urals (Lider,

1976; Puchkov, 2010). This topography is as enigmatic as the origin of high topography in the Norwegian and Greenland coastal ranges (e.g. Anell et al., 2009).

2.4. Meso-Cenozoic tectonics

The convergence of the European and African plates began at ca. 120 Ma and has led to plate collision, subduction (at 65 Ma), and regional uplift (after 25 Ma) in south-western Europe (Castellarin and Cantelli, 2000; Schmid et al., 1996). The Alpine deformation extends from the Pyrenees to the Zagros mountains and includes the fold belts of the Alps, the Caucasus, the Apennines, and other mountain ranges around the Mediterranean Sea (see reviews by Blundell et al., 1992; Cavazza et al., 2004; Coward et al., 1987; Pfiffner et al., 1997). This deformation zone is still active as a result of the collision of the European and African lithosphere plates which still continues with a convergence rate of ca. 9 mm/y. The formation of the Carpathians and the Pannonian Basin may be significantly controlled by the continuous lithosphere deformation in the Alpine zone (Cloetingh et al., 2004).

The collision of Europe and Africa has affected the tectonic evolution of the Variscides, as expressed by tectono-magmatic events in the Central European Rift system that extends from the North Sea to the Atlas mountains in northern Africa and includes the Rhine graben, the Rhenish Massif, and the Massif Central in France. Tectonic models that explain geophysical, petrological, and tectonic observations along the Central European Rift system include plume-related active rifting, passive rifting associated with Europe–Africa collisional events, back-arc rifting, slab pull from the Alpine subduction zone, and asthenospheric flow from the Mediterranean (for reviews see Artemieva et al., 2006; Merle and Michon, 2001; Prodehl et al., 1995; Ziegler, 1992).

The Mediterranean Sea is underlain by oceanic crust in many parts, consisting of young oceanic crust in the western to central areas, whereas the oceanic crust in the eastern parts may originate from the Tethys Ocean (e.g. Müller, 2002). Northward subduction has taken place in the eastern Mediterranean since the Cretaceous and has resulted in continental collision leading to the Taurus and Caucasian ranges (Okay and Tüysüz, 1999; Papanikolaou et al., 2004; Stampfli and Borel, 2004). Results from seismic tomography indicate that the subducting slab beneath the Aegean region may extend as deep as 1500 km over a horizontal distance of 2400 km (Bijwaard et al., 1998). The dextral North Anatolian Fault Zone became active during the Miocene (Burchfiel et al., 2000; Nikishin et al., 2001; Yilmaz et al., 2000). The late Miocene initiation of the sinistral Levant (Dead Sea) transform fault (Mart et al., 2005) decoupled the Arabian indenter from the African plate, including the continental Sinai–Levant and the oceanic (?) East-Mediterranean domains.

Whereas there is general consensus that the western part of the Mediterranean Sea is of oceanic origin, the origin of the crust below the Alboran Sea is still under discussion. It has been speculated if there has been northward subduction below the Iberian peninsula since the late Cretaceous as indicated by high pressure metamorphic rocks (Faccenna et al., 2001; Zeck, 1999). Simultaneously, the Pyrenean collision began with northward subduction of continental Iberian lithosphere beneath Europe and southward subduction of the oceanic Bay of Biscay beneath Iberia (e.g. Dezes et al., 2004).

2.5. Oceans

Opening of the southern Atlantic ocean began at 170 Ma and at 80 Ma reached the latitude of southern Greenland where initial spreading took place along the western margin of Greenland forming the Labrador Sea and Baffin Bay basins (Müller et al., 2008). The Caledonian margins of Greenland and Baltica were rifted apart during opening of the North Atlantic Ocean which began at about 65 Ma. At ca. 55 Ma

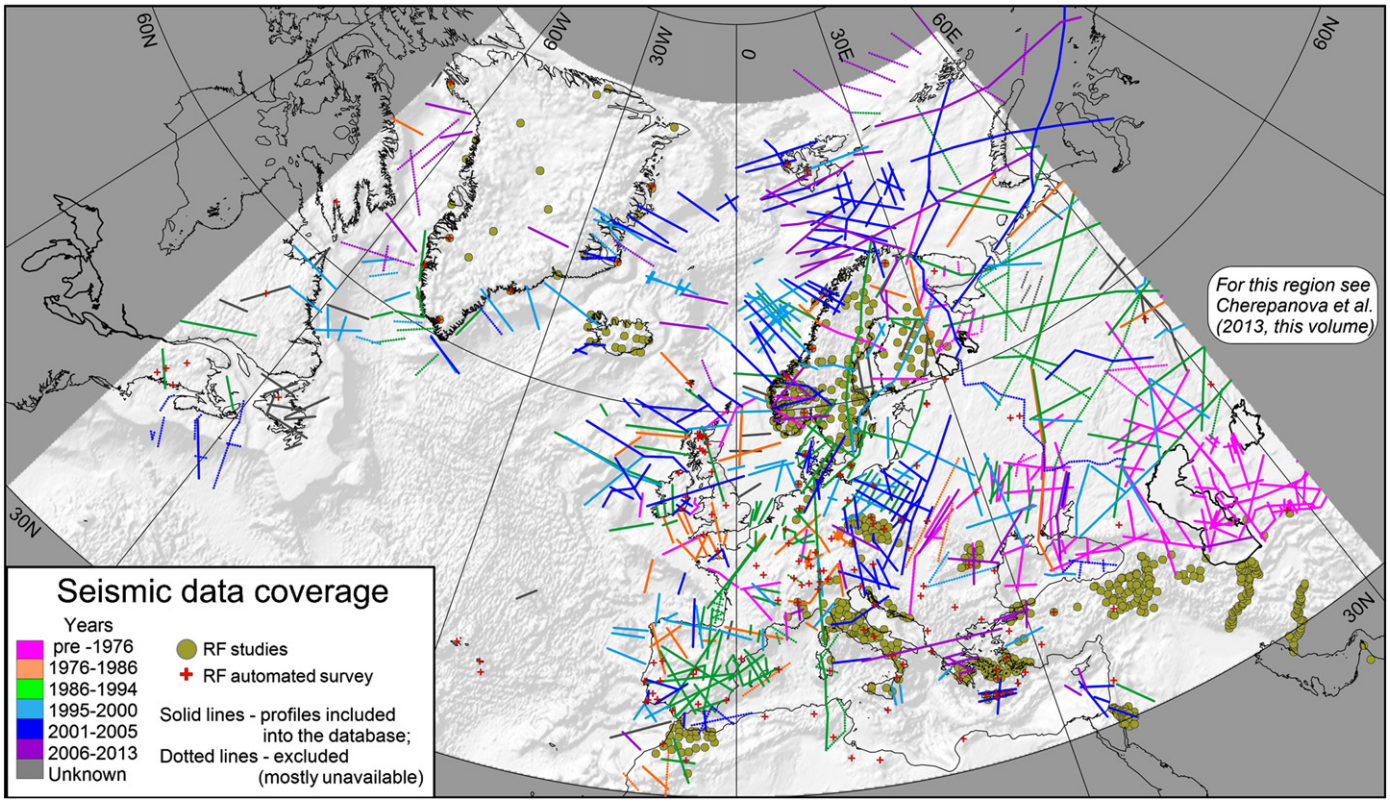

Fig. 5. Major seismic profiles in Europe, Greenland and adjacent regions, which reach Moho. Colors refer to the year when crustal models, used in this study, were published. Note that for many profiles multiple interpretations exist; in such cases the more recent or more reliable models were used. Not all of the on-shore seismic profiles are shown; for off-shore regions we show mostly profiles within the shelf areas. For regions, where only few seismic profiles exist, we show the locations of seismic stations for which Receiver Function (RF) models are available. See Table 2 for details.

Table 2
Summary of some of the seismic profiles. Due to the enormous number of publications used in the compilation of the crustal structure and Moho depth in the study area (see Fig. 5 for data coverage), this table lists (a) only the key profiles and (b) only the key references.

Location	Project name	Data type	Maximal depth	V_p accuracy	Key references
Greenland, W. North Atlantic					
Greenland–Senja Fracture Zones		Refraction, CDP	40 km	2%	Engen et al. (2008), Døssing et al. (2008)
Central E. Greenland		Refraction	50 km	2%	Voss and Jokat (2007), Schmidt-Aursch and Jokat (2005a,b)
E. Greenland margin	SIGMA	Refraction, CDP	50 km	2%	Holbrook et al. (2001)
Southern E Greenland margin	ICE	Refraction, CDP	50 km	2%	Dahl-Jensen et al. (1998)
Greenland	GLATIS	RF	50 km	4%	Dahl-Jensen et al. (2003), Kumar et al. (2007)
N & central Greenland		RF	50 km	4%	Dahl-Jensen et al. (2012)
Central E interior Greenland	TopoGreenland	Refraction	50 km	2%	Shulgin et al. (2012), Thybo and Shulgin (in prep.)
W Greenland		Refraction	40 km	3%	Gohl and Smithson (1993)
W Greenland margin		Refraction	50 km	3%	Chian and Louden (1992, 1994)
N. American Margin		Refraction	40 km	3%	Chian and Louden (1992), Lizarralde and Holbrook (1997)
Labrador Sea		Refraction	40 km	3%	Chian et al. (1995a,b)
Canadian Margin		Refraction	40 km	3%	Reid and Keen (1990)
Baffin Bay		Refraction	40 km	3%	Reid and Jackson (1997)
Baffin Bay, Davies strait	AWI	Refraction	40 km	3%	Skaarup et al. (2006), Suckro et al. (2012), Funck et al. (2012)
Iceland, Central North Atlantic					
Iceland		Refraction; RF	50 km	2%	Gebrande et al. (1980), Palmason (1986), Darbyshire et al. (2000), Du et al. (2002), Foulger and Anderson (2005) Tilmann and Dahm (2008)
Faeroe–Iceland–Greenland Ridge	FIRE	Refraction, CDP	40 km	2%	FIRE WG (1996), Ljones et al. (2004), Parkin and White (2008), Staples et al. (1997)
Faeroe islands	FLARE	Refraction	40 km	3%	Richardson et al. (1998)
Mid-Atlantic Ridge		Refraction	20 km	4%	Canales et al. (2000)
Gakkel Ridge		Refraction	20 km	4%	Jokat and Schmidt-Aursch (2007)
Knippovich Ridge		Refraction	20 km	4%	Ljones et al. (2004), Kandilarov et al. (2008)
North Atlantic transects		Refraction	30 km	3%	Mjelde et al. (2008c)
Kolbeinsey Ridge		Refraction	30 km	3%	Kodaira et al. (1997)
Reykjanes Ridge		Refraction	15 km	3%	Angenheister et al. (1980), Weir et al. (2001)
Jan Mayen		Refraction	25 km	3%	Kodaira et al. (1998), Raum et al. (2006), Breivik et al. (2012)
E. North Atlantic					
Lofoten		Refraction	40 km	2%	Mjelde et al. (1992), Kodaira et al. (1995), Tsikalas et al. (2005)
Norwegian Shelf		Refraction, CDP	40 km	2–4%	Planke et al. (1991), Grevemeyer et al. (1997), Gomez et al. (2004), Raum et al. (2006), Mjelde et al. (2008a,b)
Voring area		Refraction	40 km	2%	Mjelde et al. (1998, 2001, 2005), Raum et al. (2002), Breivik et al. (2011)
S Norwegian Shelf		Refraction	40 km	3%	Eldholm and Grue (1994)
Faeroe islands	iSIMM	Refraction and reflection	40 km	2%	White et al. (2008)
Edoras Bank		Refraction	30 km	3%	Barton and White (1997)
Goban Spur		Refraction	30 km	2%	Bullock and Minshull (2005)
Barents Sea and Svalbard					
Spitzbergen		Refraction	40 km	3%	Baturin et al. (1994), Breivik et al. (2003, 2005), Czuba et al. (2005), Czuba (2007), Czuba et al. (2008, 2011), Minakov et al. (2012)
Barents Sea, Spitzbergen	PETROBAR-07	Refraction/reflection	50 km	2%	Clark et al. (2013)
West Barents Sea		Refraction and reflection	40 km	2%	Mjelde et al. (2002), Breivik et al. (2005), Ritzmann et al. (2007)
Hovgard Ridge		Refraction	40 km	3%	Ritzmann et al. (2004)
West Barents Sea		Compilation	40 km	Variable	Faleide et al. (2008)
East Barents, Kara Seas	1-AR (1440 km) 2-AR (935 km) 3-AR (2400 km) 4-AR (1370 km)	Refraction/reflection (DSS/CDP)	50 km	2%	Ivanova et al. (2011), Roslov et al. (2009)
Novaya Zemlya	3-AR (2400 km) 2-AR (935 km)	Refraction/reflection	50 km	2%	Ivanova et al. (2006), Ivanova et al. (2011)
Scandinavia					
Baltic Shield, Sweden	FENNOLORA	Refraction/DSS	260 km	2%	Stangl (1990), Guggisberg et al. (1991), Perchuc and Thybo (1996)
Central Finland	BALTIC	Refraction/DSS	80 km	2%	Luosto et al. (1990), Azbel et al. (1993b)
Central Finland	SVEKA	Refraction/DSS	65 km	2%	Grad and Luosto (1987)
Kola–Karelia	Pechenga–Kostomuksha	Refraction data	45 km	2%	Luosto et al. (1990), Sharov et al. (1990)
Kola–Karelia	Pechenga–Umbozero–Rybachiy	Refraction data	45 km	2%	Sharov et al. (1990), Azbel et al. (1993a)
Kola-Karelia	Kalevala-White Sea	Refraction data	45 km	2%	Sharov et al. (2010)
Finnish Kola–Karelia	FIRE	Refraction data	80 km	2%	Kukkonen and Lahtinen (2006)
Finland	SVEKALAPKO	RF	50 km	4%	Kozlovskaya et al. (2008), Olsson et al. (2007)

Table 2 (*continued*)

Location	Project name	Data type	Maximal depth	V_p accuracy	Key references
Scandinavia					
Lapland Granulite Belt	POLAR	Refraction/DSS	80 km	2%	Behrens et al. (1989), Luosto et al. (1989), Walter and Flueh (1993)
Lapland–Kola	POLAR, HUKKA, FIRE-4	Reflection/refraction		2%	Janik et al. (2009)
Baltic Sea	BABEL, Profiles A and B	Reflection/refraction	80 km	2%	BABEL Working Group (1993a), Abramovitz (1997), Meissner et al. (2002)
Bothnian Gulf	BABEL, Profiles 1–7	Reflection/refraction	61 km	2%	BABEL Working Group (1993b),
			55 km	2%	Ohlander et al. (1993). Korja et al. (2001)
			56 km	2%	
S. Baltic shield	Oslo–Helsinki–Leningrad	Refraction data	200 km	2%	Ryaboy (1990)
Norway, Lofoten		Reflection/gravity	40 km		Tsikalas et al. (2005)
Norway–Sweden	Blue Norma	Refraction	50 km	4%	Avedik et al. (1984)
Norway	Blue Road	Refraction	50 km	4%	Hirschlebar et al. (1975)
Oslo Graben		Refraction	40 km	4%	Tryti and Sellevoll (1977)
S Norway		Refraction	40 km	5%	Sellevoll and Warrick (1971),
			40 km	2%	Stratford et al. (2009)
Norway		RF	50 km	4%	Ottemoller and Midzi (2003), Svenningsen et al. (2007), Frassetto and Thybo, 2013
Scandinavia		Compilation	60 km	Var.	Korsman et al. (1999)
S.Scandinavia		Compilation	50 km	Var.	Kinck et al. (1993)
East European platform					
Baltic States	Sovetsk–Riga–Kohtla Jarve	Refraction/DSS	80 km	4%	Ankudinov et al. (1991)
Kola–Polar Urals	Murmansk–Kyzyl	Refraction data	60 km	4%	Kostyuchenko et al. (2004)
EEP, Kola to the Black Sea	1-EB (3700 km long NS profile)	CDP	80 km	4%	Mints et al. (2007)
Mezen–Timan–Pechora basins	3-AR (2400 km long profile, NW–SE)	Refraction/reflection	50 km	2%	Lobkovsky et al. (1996), Ivanova et al. (2011)
Mezen–Timan–Pechora Basins		DSS	40 km	4%	Kostyuchenko and Romanyuk (1997), Ismail-Zadeh et al. (1997)
EEP, Precambrian Rifts		Seismic/gravity	50 km	5%	Kostyuchenko et al. (1999)
NE EEP	QUARTZ, KRATON, and other	PNE	500 km	4%	Egorkin (1991)
NE EEP	QUARTZ	PNE, Refraction/ DSS	500 km	4%	Mechie et al. (1993), Ryberg et al. (1996), Morozova et al. (2000)
NE EEP	KRATON	PNE, Refraction	500 km	4%	Nielsen et al. (1999), Nielsen and Thybo (2006)
EEP		Reflection/refraction data for many profiles	50 km	Var.	Volvovsky and Volvovsky (1975), Zverev and Kosminskaya (1980), Beloussov et al. (1991), Egorkin (1999)
EEP	GEON and VSEGEI data	Compilations based on reflection/refraction, borehole & potential field data, tectonic similarity	60 km	4%	Kostyuchenko (1999), Erinchek and Milstein (2006), Kostyuchenko et al. (2004)
Volga–Uralia	Tatseis-2003	Reflection	60 km	5%	Trofimov (2006)
EEC, SW–NE	Kineshma–Kupiansk (EEGT)	Reflection/refraction data	450 km	2%	Yurov (1980)
EEC, SW–NE	E–W profile	DSS-based composite profile	50–80 km	Variable	Pavlenkova and Yegorkin (1983)
EEC, Lithuania to Ukraine	EUROBRIDGE	Refraction/DSS	55 km	2%	EUROBRIDGE Seismic Working Group (1999, 2000, 2001), Thybo et al. (2003)
Ukraine and Ukrainian Shield		Reflection/refraction	60 km	5%	Sollogub (1980), Ilchenko (1990), Burianov et al. (1985), Grad and Tripolsky (1995)
Dnieper–Donets rift	DOBRE	Reflection/refraction	70 km	2%	DOBREfraction'99 Working Group (2003), Lyngsie et al. (2007)
Dnieper–Donets rift		Reflection/refraction	50 km	5%	Chekunov et al. (1992, 1993), Ilchenko (1996), Stovba et al. (1995)
DonBas foldbelt		Reflection/refraction	60 km	5%	Lobkovsky et al. (1996), Maystrenko et al. (2003)
Pripyat Trough		Reflection/refraction	60 km	5%	Juhlin et al. (1996b);Thybo et al. (2003)
SW EEC		Refraction	60 km	2%	Grad et al. (2006a,b)
S EEC (Karpinsky swell)		Reflection, CDP	70 km	2%	Brodsky and Voronin (1994)
Southern Urals	URSEIS	Reflection, CDP	70 km	2%	Carbonell et al. (1996, 2000), Puchkov (1997), Steer et al. (1998a,b), Brown et al. (1998), Suleimanov (2006)
Southern Urals	R114, R115	Reflection	70 km	2%	Brown et al. (1998), Steer et al. (1995)
Middle Urals	ESRU	Reflection	75 km	2%	Juhlin et al. (1996a), Druzhinin et al. (1997), Brown et al. (1998), Knapp et al. (1998), Kashubin et al. (2006)
Middle Urals	R17, UWARS	Reflection	70 km	2%	Druzhinin et al. (1990), Juhlin et al. (1996a), Thouvenot et al. (1995)
Caspian sea, Peri-Caspian basin		DSS/refraction/ compilation	40 km	5%	Neprochnov et al. (1975), Beloussov et al. (1988), Artemjev and Kaban (1994), Leonov and Volozh (2004)
Caucasus–Caspian–Turanian plate		DSS/compilation	50 km	Variable	Kunin et al. (1992)

(*continued on next page*)

Table 2 (*continued*)

Location	Project name	Data type	Maximal depth	V_p accuracy	Key references
North Sea Region					
SW Baltic Shield	Eugeno-S	Refraction/DSS	130 km	2%	EUGENO-S Working Group (1988), Gregersen (1991), Thybo (1990, 2001), Thybo and Schonharting (1991)
SW Baltic Shield	MOBIL Search	CDP/refraction	100 km	4%	Lie et al. (1990), Lie and Andersson (1998)
SW Baltic Shield	EUGENO-S, BABEL	CDP/refraction	40 km	2%	Thybo et al. (1998), Thybo (2000)
North Sea	MONA LISA	CDP/refraction	100 km	2%	MONA LISA Working Group (1997a,b), Abramovitz et al. (1998, 2000), Nielsen et al. (2000)
Danish Basin	ESTRID	Refraction	40 km	2%	Sandrin and Thybo (2008a,b), Sandrin et al. (2008)
N. Europe	BASIN'96	Reflection, Refraction	50 km	2%	Bleibinhaus et al. (1999), Bayer et al. (2002)
Central Graben		Refraction	40 km	3%	Barton and Wood (1984)
E North Sea		Refraction	40 km	3%	Sellevol (1973), Christie (1982)
E North Sea	SWABS	Refraction	40 km	3%	McCaughey et al. (2000)
S North Sea		Reflection	40 km	4%	Rijkers et al. (1993), Rijkers and Duin (1994)
Netherlands		Reflection	40 km	4%	Duin et al. (1995, 2006)
British Isles					
Scotland–Shetland	NASP-D	Refraction	40 km	4%	Smith and Bott (1975)
Scotland	MAVIS	Refraction	40 km	3%	Dentith and Hall (1989)
W of Scotland	PUMA	Refraction	40 km	3%	Powell and Sinha (1987)
Around Scotland		Refraction	40 km	3%	White et al. (1982), Jones et al. (1984)
England–Scotland	LISPB, LISB IV	Refraction	100 km	3%	Bamford et al. (1976), Barton (1992), Maguire et al. (2011)
SW of England		Refraction	40 km	4%	Holder and Bott (1971)
Rockall	Rockall	Refraction	30 km	4%	Roberts and Ginzburg (1984)
Rockall	RAPIDS	Refraction	30 km	3%	O'Reilly et al. (1995, 1996)
Rockall	AMP, BANS	Refraction	30 km	3%	Klingelhofer et al. (2005)
British Isles	BIRPS	Reflection	40 km	–	Snyder and Hobbs (1999)
Ireland	VARNET	Refraction	50 km	2%	Abramovitz et al. (1999), Masson et al. (1999), Landes et al. (2003)
Porcupine Ridge		Refraction	40 km	5%	Whitmarsh et al. (1974)
Porcupine Sea		Refraction	40 km	3%	Makris et al. (1988)
Hatton bank, Porcupine		Refraction	40 km	2%	Morgan et al. (1989), Vogt et al. (1998), England and Hobbs (1997), O'Reilly et al. (2006)
British Isles		Compilation	40 km	Variable	Chadwick and Pharaoh (1998)
British Isles		Compilation	40 km	Variable	Kelly et al. (2007)
Central Europe					
N. German Caledonides	EUGENO-S	Refraction	100 km	5%	EUGENO-S WG (1988), Gregersen (1991), Grad et al. (1991), Perchuc and Thybo (1996), Yoon et al. (2009)
Baltic Shield to Italy	EGT	Refraction	40 km	2%	Blundell et al. (1992), Ye et al. (1995)
Variscan Europe	EUGEMI	Refraction	40 km	2%	Aichroth (1990), Aichroth et al. (1992)
Poland, across TESZ	POLONAISE'97	Refraction/DSS	~45 km	2%	Guterch et al. (1999), Jensen et al. (1999), 2002)
	Profile 1				
	Profile 2		~45 km	2%	Janik et al. (2002)
	Profile 3		57 km	2%	Sroda et al. (1999)
	Profile 4		~45 km	2%	Grad et al. (2003)
	Profile 5		~45 km	2%	Grad et al. (2005)
	Profile TESZ		~45 km	2%	Wilde-Piorko et al. (2002)
TTZ in Poland	TTZ	Refraction/DSS	50 km	2%	Grad et al. (1999), Janik et al. (2005)
	CELEBRATION 2000	Reflection/refraction data			Guterch et al. (2003), Malinowski et al. (2005), Hrubcova et al. (2005), Ruzek et al. (2006), Sroda et al. (2002, 2006)
Belgium		RF	50 km	4%	Zhang and Langston (1995)
Belgium		Broad-band reflection data	40 km	6%	Sichien et al. (2012)
Variscides Germany, Poland and France	DEKORP ECORS	Refraction, CDP	50 km	variable	Matte and Hirn (1988), Meissner and Bortfeld (1990), Zeis et al. (1990), Brun et al. (1992), Prodehl et al. (1992), Zeyen et al. (1997), Jensen et al. (2002)
N Germany	ZIPE	Refraction	40 km	2%	Rabbel et al. (1995)
Rhine Graben	ECORS-DEKORP	Refraction CDP	40 km	2%	Gajewski et al. (1987), Fuchs et al. (1987), Brun et al. (1992)
Central Europe		Compilation	60 km	Var.	Dezes et al. (2004)
Brittany		Refraction	40 km	3%	Bitri et al. (1997)
Brittany Coast		Refraction	30 km	2%	Grandjean et al. (2001)
Massif Central		Refraction	40 km	4%	Sapin and Prodehl (1973)
Massif Central		Refraction	40 km	3%	Zeyen et al. (1997)
Romania		Refraction	40 km	3%	Hauser et al. (2007)
Bohemian Massif	-	RF	50 km	4%	Geissler et al., (2012)
Romania		CDP/refraction	40 km	3%	Mucuta et al. (2006)
Hungary	PGT-1	Reflection data	70 km	2%	Posgay et al. (1995)
Pannonian Basin		Refraction	40 km	3%	Weber (2002)
Carpathians, Vrancea	VRANCEA	Refraction, CDP	40 km	2%	Hauser et al. (2001, 2007), Knapp et al. (2005)

Table 2 (*continued*)

Location	Project name	Data type	Maximal depth	V_p accuracy	Key references
Central Europe					
Vrancea		RF	60 km	4%	Ivan (2011)
Carpathians, Pannonian Basin, EEP	CELEBRATION'2000	Refraction	50 km	2%	Grad et al. (2006a,b), Janik et al. (2011)
Carpathians, Pannonian Basin, EEP	PANCAKE	Refraction	60 km	2%	Starostenko et al. (2013)
Alpine Region					
Pyrenees	ECORS	Reflection, Refraction	50 km	2–3%	ECORS Pyrenees Team (1988), Gallart et al. (1985), Souriau et al. (2008)
E Alps		Refraction	50 km	4%	Scarascia and Cassinis (1997)
Austria E Alps	Alps 2000, 2002	Refraction	60 km	2%	Bruckl et al. (2003, 2007), Behm et al. (2007)
Austria	Transalps	Reflection Refraction	60 km	2%	Bleibinhaus and Gebrande (2006), Luschen et al. (2004, 2006), Millahn et al. (2006), TRANSALP Working Group, 2002
E Alps		Compilation	60 km	2–4%	Cassinis (2006)
Swiss Alps	EUGEMI	Refraction	60 km	3%	Ye et al. (1995)
W.Alps	NRP 20	Reflection, Refraction	60 km	2%	Pfiffner et al. (1997), Schmid et al. (1996)
SW Alps		Integrated study	50 km	3%	Lardeaux et al. (2006)
SW Alps		Wide-angle refl.	50 km	4%	Thouvenot et al. (2007)
French Alps		Broad band	60 km	5%	Bertrand and Deschamps (2000)
N Appenines		RF	50 km	5%	Mele and Sandvol (2003), Agostinetti et al. (2008)
C Appenines		RF	50 km	5%	Mele et al. (2006), di Bona et al. (2008)
Dinarides, Croatia		RF	60 km	4%	Stipcevic et al. (2011)
Iberia					
Bay of Biscay		Refraction	30 km	3%	Ginzburg et al. (1985)
Bay of Biscay		Refraction	30 km	2%	Lefort and Agarwal (2000)
Bay of Biscay	MARCONI	Reflection and refraction	30 km	4%	Fernandez-Viejo et al. (1998), Ferrer et al. (2008)
Bay of Biscay	Norgasis	Refraction	30 km	2%	Thinon et al. (2003)
Iberian Peninsula	ILIHA	Refraction	100 km	2–3%	ILIHA DSS Group (1993), Díaz et al. (1996)
Iberian Peninsula		Compilation	Var.	Var.	Díaz and Gallart (2009)
Iberia		Refraction, compilation	40 km	Var	Banda (1988)
NW Iberia		RF	100 km	4%	Díaz et al. (2009, 2012)
NW Spain		Refraction	40 km	4%	Tellez and Cordoba (1996)
Cantabria	ECSIN	CDP/refraction	40 km	3%	Pulgar et al. (1996), Alvarez-Marron et al. (1996), Pedreira et al. (2003)
C Spain		Refraction	40 km	4%	Surinach and Vegas (1988)
Betic Codillera		Refraction	50 km	4%	Medialdea et al. (1986)
Betic Codillera		Reflection	50 km	4%	Garcia-Duenas et al. (1992)
Betic Codillera		Refraction	50 km	4%	Banda et al. (1993)
Betic Codillera		Refraction, integrated	50 km	3%	Carbonell et al. (1998)
SW Iberia	IBERSEIS	Refraction	40 km	2%	Flecha et al. (2006), Schmelzbach et al. (2008)
Ibrian Margin		Refraction	30 km	4%	Whitmarsh et al. (1990)
Abyssal plain		Refraction	30 km	4%	Minshull et al. (1998), Chian et al. (1999)
Gulf of Cadiz		Refraction	30 km	3%	Gonzalez-Fernandez et al. (2001)
N. Morocco		RF	50 km	4%	de Lis Mancilla et al. (2012)
Mediterranean Region					
Moroccan Margin		Reflection	30 km	4%	Maillard et al. (2006)
Moroccan Margin		RF	40 km		de Lis Mancilla et al. (2012)
Atlas Mountains		Refraction	40 km	3–5%	Wigger et al. (1992), Mickus and Jallouli (1999)
Alboran Sea		Tomography	30 km	5%	Calvert et al. (2000)
Calabrian Sea		Refraction	30 km	4%	Cernobori et al. (1996)
Ligurian Sea		Refraction	30 km	4%	Ginzburg et al. (1986), Makris et al. (1999)
Corsica–Sardinia		Refraction	30 km	2–4%	Egger et al. (1988), Sartori et al. (2004)
Tyrrhenian Sea		Refraction	30 km	3%	Duschenes et al. (1986), Contrucci et al. (2005)
NW Med. Basin		Refraction	30 km	3%	Mauffret et al. (1995)
Italy		Refraction, Reflection		–	Scrocca et al. (2004), Scarascia et al. (1994)
Italy		RF			Mele et al. (2006), Agostinetti and Amato (2009), Miller and Agostinetti (2012)
Gulf of Corinth		CDP/refraction	30 km	3%	Clement et al. (2004), Zelt et al. (2005)
Gulf of Saronikis		Refraction	30 km	3%	Drakatos et al. (2005)
Ionian islands		CDP/refraction	30 km	3–4%	Hirn et al. (1996)
Ionian margin		Refraction	30 km	3%	Nicolich et al. (2000)
Ionian sea		Refraction	30 km	5%	Makris et al. (1986)
Aegean sea		Surface waves	40 km	10%	Karagianni et al. (2002)
Aegean plate		RF	40 km	15%	Zhu et al. (2006), Sodoudi et al. (2013)
E Mediterranean		RF	40 km	10%	Marone et al. (2003)
E Mediterranean		Refraction	40 km	5%	Makris et al. (1983)
Hellenic subduction zone		Refraction and reflection	40 km	3%	Clement et al. (2000), Bohnhoff et al. (2001)
Hellenic subduction zone		RF	40 km	5%	Li et al. (2003)
Hellenic subduction zone		Regional tomography	50 km	5–10%	Marone et al. (2003)

(*continued on next page*)

Table 2 (*continued*)

Location	Project name	Data type	Maximal depth	V_p accuracy	Key references
Black Sea, Caucasus, Middle East					
Black Sea Basins		Refraction/Gravity	40 km	5%	Starostenko et al. (2004)
Black Sea Basins		Tomography	40 km	5–8%	Sayil and Osmansahin (2000)
Black Sea		DSS/refraction	40 km	5%	Neprochnov et al. (1970, 1975), Beloussov et al. (1988)
E. Black Sea		Reflection	20 km	3%	Minshull et al. (2005), Afanasenkov et al. (2007)
Caucasus		DSS	50 km	?	Yegorkin and Matushkin (1970)
Caucasus		Compilation	50 km	Var.	Krasnopevtseva (1984), Artemjev et al. (1985)
South Caspian		RF	40 km	5%	Mangino and Priestley (1998)
Turkey		RF	40 km	5%	Zor et al. (2003), Angus et al. (2006)
Turkey		Tomography	40 km	5–8%	Gok et al. (2007)
Tuz Golu Basin, Turkey		Refraction	40 km	4%	Gurbuz and Evans (1991)
Iraq		RF	40 km	5%	Gök et al. (2008)
Iran		Refraction	40 km	?	Giese et al. (1984)
Zagros, Iran	Zagros01; Zagros03	RF	40 km	5%	Doloei and Roberts (2003), Taghizadeh-Farahmand et al. (2010), Paul et al. (2010), Vergés et al. (2011)
Dead Sea region		Refraction	40 km	2–5%	Ginzburg et al. (1981), Mechie et al. (2005)
Dead Sea region		RF	40 km	5%	Mohsen et al. (2005)
Levant Basin		Refraction	40 km	4%	Ben-Avraham et al. (2002), Netzeband et al. (2006)

Abbreviations: CDP = Common Depth Point; RF = Receiver Function; DSS = Deep Seismic Sounding; PNE = Peaceful Nuclear Explosions; Var. = variable; TESZ = Trans-European Suture Zone; TTZ = Teisseyre–Tornquist Zone.

the mid-ocean ridge jumped to the eastern margin of Greenland. Later, a westward jump of the spreading axis took place at ca. 30 Ma when the North Atlantic opening reached the Jan Mayen microcontinent (Mosar et al., 2002); the latter separated from East Greenland and other continental fragments, such as the East Greenland Ridge, rifted from the European side (Døssing et al., 2008; Figs. 2, 3). The Fram Strait between the North Atlantic and the Arctic Ocean may finally have opened in the Miocene between 20 and 10 Ma as indicated by plate reconstructions (Engen et al., 2008).

Long lasting extension that led to the formation of the northern Atlantic ocean may have formed the economically important Central-Viking Graben system in the North Sea as well as the very wide continental shelves along the Greenland and European margins. Along the coasts on both sides of the North Atlantic ocean, structures of the Caledonian orogeny are identified onshore in up-to 200 km wide zones and probably extend off-shore into the 100–600 km wide continental shelves (Olesen et al., 2002). In particular, the Barents Sea shelf north of the European continent experienced strong stretching throughout the time from the Caledonian orogeny until break-up, as evidenced by the many rift-like basins in the region (Faleide et al., 2008). However, the basement in the Barents Sea is much older than Caledonian and the continental crust of the shelf is believed to consist of Palaeoproterozoic cratonic and Palaeozoic accreted crust, covered by a several kilometers thick carbonate and siliciclastic sequence of Neoproterozoic, Palaeozoic and Mesozoic–Cenozoic ages (Fig. 3). Possible outlines of the boundaries between these crustal domains and their tectonic relationships are highly controversial due to thick sedimentary cover of the Arctic shelf (Drachev et al., 2010 and references therein). Similarly the western continental shelf of Norway has been extending since the late Palaeozoic or early Mesozoic, with resulting deep hydrocarbon containing basins; for a review we refer to Mjelde et al. (2003) and Faleide et al. (2008).

Break-up of the North Atlantic Ocean was accompanied by intensive magmatism and volcanism which led to the formation of the North Atlantic Igneous Province (NAIP) which has been estimated to cover an area of 1.3×10^6 km^2 and totaling a volume of 6.6×10^6 km^3 (Eldholm and Grue, 1994). It is mainly observed in eastern Greenland as much of the magmatic material of the NAIP is today concealed under water and covered by sediments and as underplated material at the margins of the North Atlantic (Eldholm et al., 2002; Faleide et al., 2008; Saunders et al., 1997). It has a spectacular expression in central eastern Greenland, where the volcanic rocks are found up to high elevation, including the highest mountain in Greenland, Gunnbjørn Fjeld with its peak at 3707 m above sea level. A large area of 65,000 km^2 is covered by volcanic sequences around Gunnbjørn Fjeld and it is believed that the sequence may be up to 7 km thick (Brooks, 2011). The eruptions apparently took place close to sea level, which would indicate substantial uplift of eastern Greenland after the break-up. The exceptionally extensive volcanism in eastern Greenland could have been caused by the proposed mantle plume, which may now be situated below Iceland (Lawver and Muller, 1994; Waight and Baker, 2012). The Arctic shelf of the Barents Sea hosts one more igneous province, flood basalts of Franz Josef Land and Eastern Svalbard, which erupted at ca. 125–100 Ma probably as a result of a plume-related magmatic event (Amundsen et al., 1998).

Iceland is situated at the intersection of two major tectonic structures: the oceanic spreading zone of the North Atlantic Ocean, diverging at a rate of 2 cm/y, and the Greenland–Iceland–Faeroe Ridge of shallow bathymetry, transversing the North Atlantic at ca. 65N (Sigmundsson and Schmundsson, 2008; Fig. 2a). Young (<16 Ma, Björnsson et al., 2005) onshore crust in the study area is found in Iceland, where the spreading ridge has migrated eastwards with spreading on two parallel ridges during the last 17 Ma, or perhaps even 26 Ma (Foulger and Anderson, 2005). Due to a distinct depleted component it is possible that recycled oceanic crust forms part of the Icelandic basalts in the axial rift zone of Iceland (Chauvel and Hemond, 2002). Alternatively, an iron-enriched component derived either from a chiefly eclogitic source (Foulger et al., 2005) or from an ancient OIB seamount structure (McKenzie et al., 2004) may explain the depleted component. Fragments of Caledonian or older continental lithosphere may also be present (Korenaga and Kelemen, 2000). A major positive geoid anomaly (+60 m) has its maximum at Iceland. Together with positive free air gravity values and elevated surface topography (attaining surface elevations of up to 1000 m) this may indicate significant dynamic support from the mantle of the bathymetry and topography in a wide zone around Iceland.

3. Seismic data coverage and existing models of the European crust

3.1. The European continent

A dense network of seismic profiles exists over most of Europe, including the continental margins and shelves, whereas the seismic data coverage is sparse in the rest of the study area, including the oceans, Greenland and Iceland (Fig. 5). Intensive acquisition of crustal seismic

data in continental Europe took place in the 1980s and continued in the 1990s, with a very intensive program in central-eastern Europe at around the turn of the century (POLONAISE, Celebration'2000, Alps'2000 and Alps'2002) and dense profiling in the Barents Sea during the past decade. Different techniques (refraction, normal-incidence and wide-angle reflection, P- and S-wave Receiver Functions (RF), as well as some application of surface waves) are being used. Due to the large number of important publications on the structure of the European crust we will abstain from providing a review of them, but instead refer to the reviews by Blundell et al. (1992), Artemieva et al. (2006) and Prodehl et al. (2013–this volume).

The European continent is unique by being covered by a dense network of seismic profiles acquired over more than 40 years by numerous research teams from different countries. The long time span also implies high variability in the quality of the seismic data and models, resulting in significant discrepancies in crustal models published by different research groups for the same regions or even along the same profiles. Given progress in seismic instrumentation and data processing, time of data acquisition and interpretation provides a rough assessment of model quality (Fig. 5). However, it is worth noting that some recent controlled-source seismic experiments, such as in southern Norway (e.g. Stratford et al., 2009), have confirmed findings of the early seismic studies in the region (e.g. Sellevoll and Warrick, 1971), clearly indicating that many crustal models of the 1970s and 1980s provide adequate and highly reliable models of the crustal structure.

In general, station density, and thereby resolution, has increased with time. The interpretation techniques have also improved substantially with time. A significant advancement in the ability to model waveforms and amplitudes arose by the introduction of the reflectivity method (Fuchs and Muller, 1971). Detailed modeling of traveltimes and amplitudes was enabled by the introduction of ray-tracing algorithms (e.g. Cerveny et al., 1982), and algorithms that enable assessment of parameter uncertainties (Zelt and Smith, 1992). Due to these advances, there are sometimes significant differences between old and recent models along the same seismic profiles, although old results are also often reliable, in particular concerning crustal thickness. Therefore our compilation of crustal structure and Moho depth is based primarily on results derived since 1980, supplemented by earlier results where needed in order to fill in voids. This is, particularly, the case for the southern parts of the East European Craton, the Caucasus, and the areas around and within the Black and the Caspian seas, although a somewhat similar situation exists for France. Besides, there are some large areas which are poorly covered by seismic data on the crustal structure and the Moho depth; they include most of the Dinarides and the Balkans, Turkey, Italy (only Moho depth is constrained by RFs), Central Russia, parts of western Europe, the Baltic States, and Belarus (Fig. 5). The situation is now changing with new seismic surveys (including RF studies) providing data on the crustal structure of the Mediterranean and of the Tethys mountain belt (e.g. Gok et al., 2007; Hatzfeld et al., 2003; Saunders et al., 1998; Sodoudi et al., 2013; Zhu et al., 2006; Zor et al., 2003).

3.2. Greenland, Iceland, and off-shore regions

The coverage by crustal seismic profiles in the North Atlantic Ocean is coarse and still almost no seismic data are available for the northern-central Atlantic ocean south of Iceland. Most seismic data in the North Atlantic Ocean have been acquired in oceanic regions with anomalous bathymetry (compare Figs. 2b and 5) and thus with anomalous crustal structure (along the Greenland–Iceland and Iceland–Faeroe Ridge, around the Jan Mayen microcontinent, at the Kolbeinsey Ridge, at the Azores, and at the margins).

The margins of the British Isles and Norway, including the Arctic shelf are covered by an exceptionally dense network of recent seismic profiles (Table 2). The number of seismic surveys along the Greenland margins, as well as in the Labrador Sea, the Davies Strait and the Baffin Bay (largely acquired by AWI) is also growing fast, and at the time of the publication the results of interpretations are available only for some of them (in some cases, only as preliminary models). New seismic data has been acquired recently by AWI across the continent–ocean transition at the Arctic shelf; however the results are not yet available (Fig. 5). Some crustal seismic profiles have been acquired at the southern margins of east and west Greenland (Fig. 5).

Only one crustal seismic refraction profile has been acquired in central onshore Greenland in the summer of 2011 as part of the TopoGreenland project (Shulgin et al., 2012; Thybo and Shulgin, preparation) and has been included into the present compilation. Otherwise the onshore crustal seismic information is from the GLATIS broad band seismological experiment (Dahl-Jensen et al., 2003; Kumar et al., 2007), which has provided estimates of the crustal thickness at about 20 locations by Receiver Function (RF) analysis. The number of stations used for RF studies has been expanded recently by new observations from the northern part of Greenland (Dahl-Jensen et al., 2012) and these preliminary results are also included into the present compilation. Most of the seismic stations were deployed close to the coast, but some locations are within the central part of the ice cover (Fig. 5). At three stations, two published models of crustal thickness based on RF analysis differ by up-to 11 km, with the S-wave RF results of Kumar et al. (2007) showing systematically smaller values for all but one station than the P-wave RF results by Dahl-Jensen et al. (2003). The recent refraction seismic profile shows that the deeper values are probably correct in the center of Greenland, and similar indication is found from comparison to a profile from Scoresbysund Fjord (Schmidt-Aursch and Jokat, 2005a). In the present model we therefore adopted the larger values of crustal thickness from the RF (see also the discussion in Section 6).

The structure of the crust in Iceland has been intensively studied by numerous controlled-source seismic surveys since the 70s–80s (Table 2) complemented by a more recent RF study of the crustal thickness (Darbyshire et al., 2000; Du et al., 2002). Although the velocity structure of the Icelandic crust is well established, the total crustal thickness gives rise to a strong controversy despite being based on the same or very similar seismic data; different petrologic interpretations are possible for the nature of a high-velocity layer at around the crust–mantle transition, which may be considered as gabbroic "lower crust" (e.g. Menke and Levin, 1994) or an anomalous peridotite mantle (Schmeling, 1985) (see Section 8.3.4 for further discussion). Clearly, the interpreted depth to Moho depends on the choice of petrologic interpretation. We favor the former interpretation as more consistent with seismic and heat flow data and our compilation includes Moho depths according to the "thick crust model". A similar controversy about the Moho nature has been discussed recently for passive margins (Mjelde et al., 2012). For these regions, we adopt depth to Moho as interpreted in the original publications.

4. New regional crustal model EUNAseis: methodology

4.1. Sampling procedure

4.1.1. Seismic profiles

Here we extend a crustal model of the East European craton (Artemieva, 2007) to cover the whole study region (including the European shelves and margins, Greenland, Iceland, and the adjacent parts of the North Atlantic Ocean and of Asia Minor). The crustal model EUNAseis of the Europe–North Atlantic–Greenland region presented here is based solely on first order seismic observations of the crustal structure (Fig. 5, Table 2). Overall exclusion of gravity data from our crustal compilation, in contrast to other recent crustal models for the European plate (Table 1), makes it a valuable tool for potential data modeling.

The new crustal database is based primarily on seismic refraction/wide-angle reflection profiles (Fig. 5). Additionally, seismic normal-

incidence profiles and Receiver Function interpretations have been used in areas that are sparsely sampled by seismic refraction profiles (cf. Table 2). For the Turanian plate where all seismic data are old (Fig. 5), we have included interpolated data for the Moho depth and thickness of sediments (Artemjev and Kaban, 1994) based on a large number of regional Soviet seismic profiles (Godin, 1969; Kunin et al., 1973; Ryaboy, 1966).

Most of the available seismic profiles were digitized to obtain a dense coverage of the study area (for complete reference list to all seismic data included in the database see Electronic Supplement 1). Given the immense amount of seismic models available for the region, we do not implement any kind of quality assessment, as we do in the companion study for Siberia (Cherepanova et al., 2013–this volume). In cases, where multiple interpretations are available for the same seismic data, only one (usually most recent) interpretation has been included in the database. Similar approach is used in those rare cases where several seismic surveys have been acquired basically along the same line. In case of alternative seismic models (e.g. for Iceland, see Section 3.2), independent information (such as gravity-based models) is used, where possible, to choose between them.

Model completeness (see Cherepanova et al., 2013–this volume, for details) varies substantially regarding information on the crustal structure provided by different seismic studies. While recent interpretations provide detailed information on the structure of all crustal layers, many old profiles could reliably resolve only the major velocity contrasts, i.e. at the top of the basement and at Moho. We do not include information on model completeness in Fig. 5; but an indirect indicator is provided by the time of interpretation.

4.1.1.1. Refraction/wide-angle reflection profiles. The sampling interval for the initial digitization of the refraction profiles was based on the variability (wavelength of the Moho depth or velocity changes) of the profile in concern. This means that the sampling interval is large (ca. 30–50 km) where the Moho depth and internal crustal velocity structure remain constant, and very dense (down to 5 km lateral distance) where abrupt changes occur either in the Moho depth or in velocity. This strategy ensures that the individual profiles are adequately sampled for the subsequent interpolation onto a regular grid.

The Vp-velocity structure of the crust is based solely on the refraction profiles (Vs-velocities are available only for very few profiles and are not included in the compilation). The database includes information on individual crustal layers; each layer is specified by Vp-velocity and thickness; additionally the upper mantle Pn velocity (>7.8 km/s) is included (lateral, vertical, and amplitude resolution of different parameters is discussed in Sections 5.1, 6.1, and 7.1). For continental crust, the following traditional subdivision has been adopted:

(i) sedimentary cover with Vp < 5.6–5.8 km/s (see Section 5.1 for details);
(ii) upper crust typically with Vp < 6.4 km/s;
(iii) middle crust typically with 6.4 < Vp < 6.8 km/s;
(iv) lower crust typically with 6.8 < Vp < 7.2 km/s;
(v) high-velocity lower crustal layer with Vp > 7.2 km/s.

Importantly, along many refraction/wide-angle reflection profiles, seismic velocities reported for various crustal layers between first-order reflectors fall outside the above listed Vp ranges (the reason the word "typically" is used above). As such, these "typical" boundary velocities are used as "guidelines" to separate the crustal layers only where the published models do not include clear first-order reflections to define the startigraphy and do not include information of the boundaries between the crustal layers.

Similar strategy was adopted for oceanic and transitional crust, i.e. our subdivision of the crust into individual layers follows published original interpretations. For the sake of model simplicity and consistency, parameters (Vp and thickness) specifying layers in oceanic and transitional crust from top to bottom are put into the same categories (columns) as for layers of the continental crust, from top to bottom, even though Vp velocity and composition of these layers in the crust of different origin are essentially different.

4.1.1.2. Normal-incidence reflection profiles. Seismic normal-incidence profiles have been interpreted for depth to Moho along selected profiles, where no refraction profiles are available. The base of reflectivity from the crust mostly coincides with the wide-angle reflection defined Moho, which may also coincide with a coherent, continuous normal-incidence reflection, as demonstrated in many profiles from various tectonic settings (e.g. Abramovitz and Thybo, 2000; BABEL Working Group, 1993a; Mooney and Brocher, 1987).

We applied these principles for digitizing depth to Moho along the selected normal-incidence reflection profiles. However, we have avoided interpretation where gaps appear in the coverage of an otherwise well resolved Moho reflection or reflectivity interval, thus effectively introducing a long-wavelength smoothing where there is no evidence for short-wavelength changes. Such gaps may be caused by intrusion of mafic magma into the crust, representing effectively a magmatic underplated layer (e.g. Thybo and Artemieva, 2013). Short-wavelength variations in the Moho depth have been included into the database when there is clear evidence in the normal-incidence reflection seismic data for such abrupt change.

4.1.2. Receiver Functions

4.1.2.1. Authored interpretations. Receiver Function (RF) estimates of the Moho depth have been introduced into the database (at ca. 1000 locations in total at the time of the publication), particularly in regions where the coverage by seismic refraction/wide-angle reflection profiles is sparse. This information is crucial mostly for Greenland, Italy and Asia Minor (Fig. 5), but it is also important for mapping short-wavelength variations in the Moho depth in many other regions. In some regions (e.g. central Greenland), there is a significant discrepancy between the results reported by different interpretations. In such cases, we use independent constraints such as from seismic refraction profiles to choose between the alternative models (see Section 3.2).

RF estimates are included as point data, assuming that the seismic conversion point is below the seismic station. This approach is not fully correct as the conversion points are offset from the station, but given that most published Receiver Function interpretations only provide one stacked value at each station, without considering back-azimuth variation, this is the best possible approach. Given the relatively steeply traveling P-waves after conversion, the uncertainty introduced by this approach is negligible, considering the lateral scale we are interested in. No velocity information has been included from RF interpretations.

4.1.2.2. Automated RF estimates. In addition to traditional, "manual" RF interpretations, we have included automated Receiver Function surveys which, within our study area, are available through the IRIS website for 243 stations (Electronic Supplement 2). These estimates provide valuable, although probably not always well-constrained, information on the Moho depth in numerous "white spots" (Fig. 5).

Following the approach of Zhu and Kanamori (2000), the IRIS website shows the Hk space for each station for determining simultaneously the parameters that best explain the observed Moho conversions: the Moho depth (H) and average crustal Vp/Vs ratio (k). We use this information to check manually the Hk solutions for all stations with complexity of the Hk-pattern greater than 0.5. For many of these stations, the automatic solution gives extreme Vp/Vs ratio (<1.65 or >1.9). As a result, 70 stations are not included in the database, and for 19 stations automatic Moho estimates are replaced by alternative manually picked Hk pairs. The following strategy has been adopted.

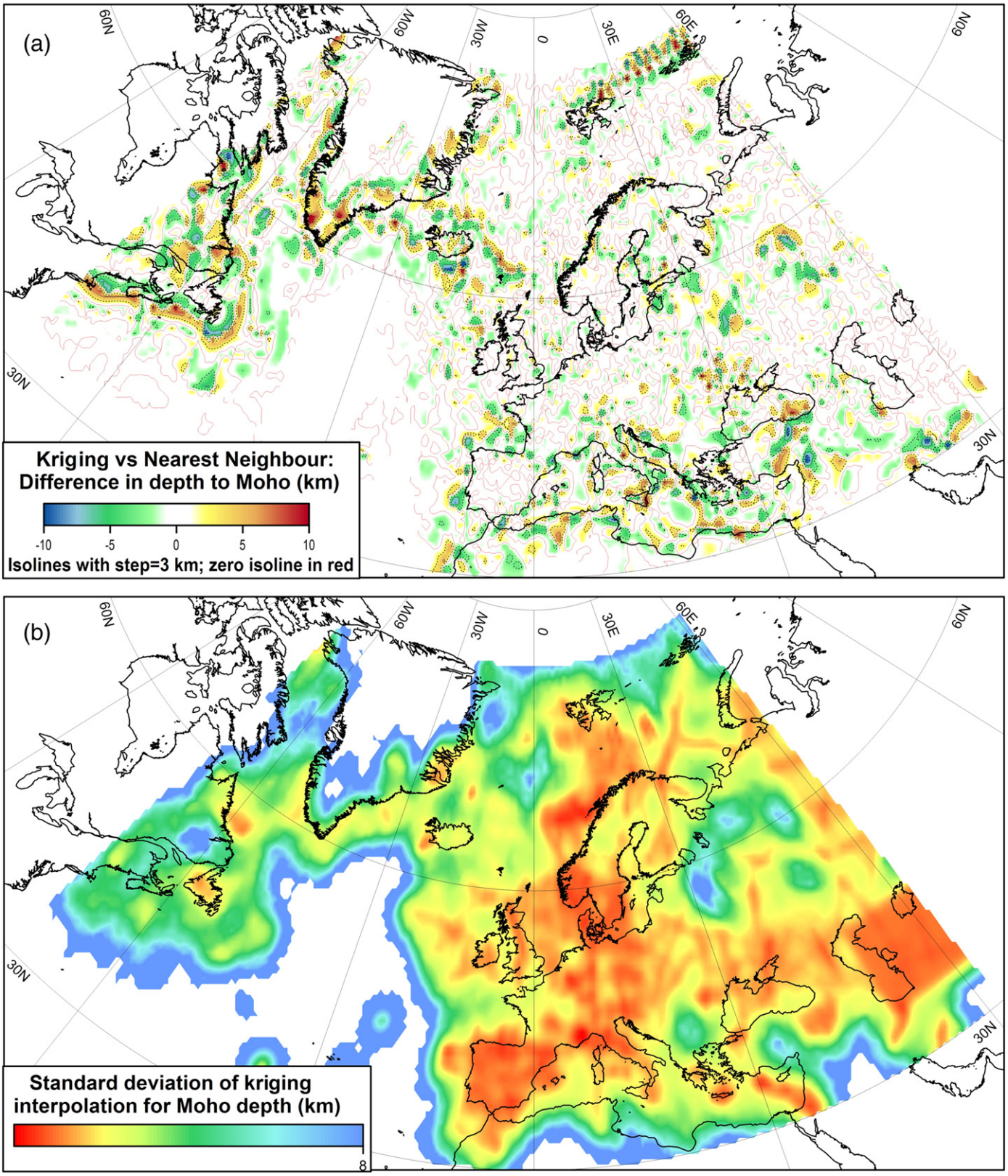

Fig. 6. Uncertainty associated with interpolation. (a) Difference between depth to Moho based on kriging and "nearest neighbor" methods. In both cases interpolation radius is 3°. (b) Standard deviation of interpolation for the depth to Moho, interpolation radius is 3°. The same interpolation parameters are used to produce Fig. 10. In regions with very dense data coverage the uncertainty of interpolation is 1–2 km. Total uncertainty for the Moho depth sums up from the uncertainty of seismic models (1–2 km for good profiles and 2–4 km for RF), an unknown uncertainty due to discrepancies between models produced by different authors, and the uncertainty added by data interpolation. The total uncertainty can hardly be assessed and in some cases it can reach ca. 5 km or more, particularly in regions with sparse seismic data coverage where interpolation alone produces uncertainty of up to 8 km.

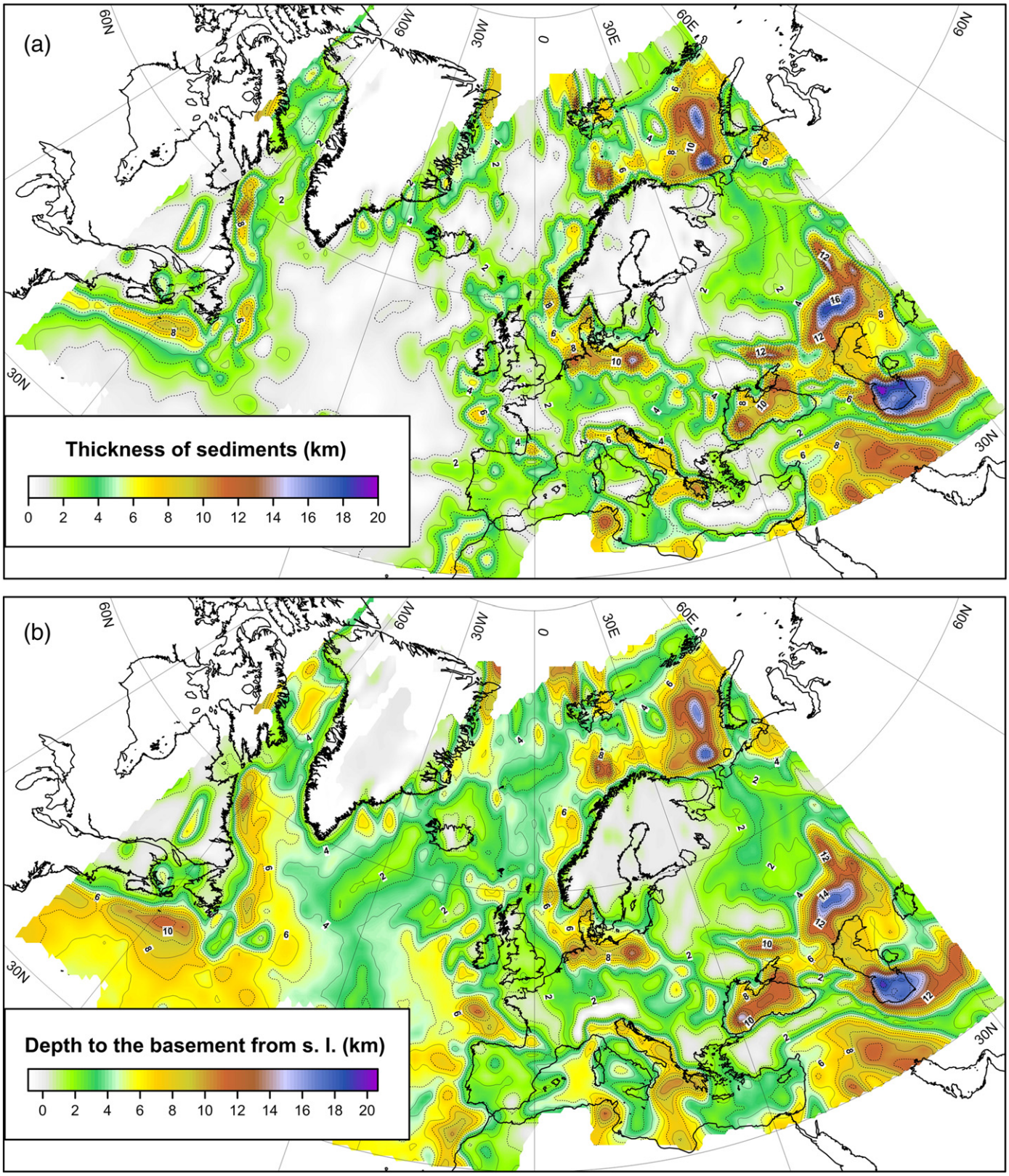

Fig. 7. Thickness of sediments (a) and depth to the basement from sea level (b), constrained with interpolation radius 3°. The major difference between the maps is for deep-water parts of the Atlantic ocean. Isolines are shown with a 2 km spacing. Gray shading — regions with less than 1 km of sediments. White shading — regions with no data or excluded from the study. Off-shore regions are constrained by a 5′ NGDC global compilation (Divins, 2008) updated and corrected by recent seismic data, in particular, for the continental shelves of Greenland/Newfoundland (see Table 2 for details) and the Barents Sea (Drachev et al., 2010). For the continental part, the sedimentary thickness is constrained by seismic data complemented by data from EXXON (1985) based on high-resolution regional seismic surveys and drilling. Both maps are constrained with a 3° × 3° interpolation. Although the interpolation method has been chosen to preserve the magnitudes, many details may be missing, in particular due to averaging in regions with a highly variable thickness of sediments.
Thickness of sediments in the Arabian plate is after Konert et al. (2001) and in the Turanian plate after Babadzhanov and Kunin (1991).

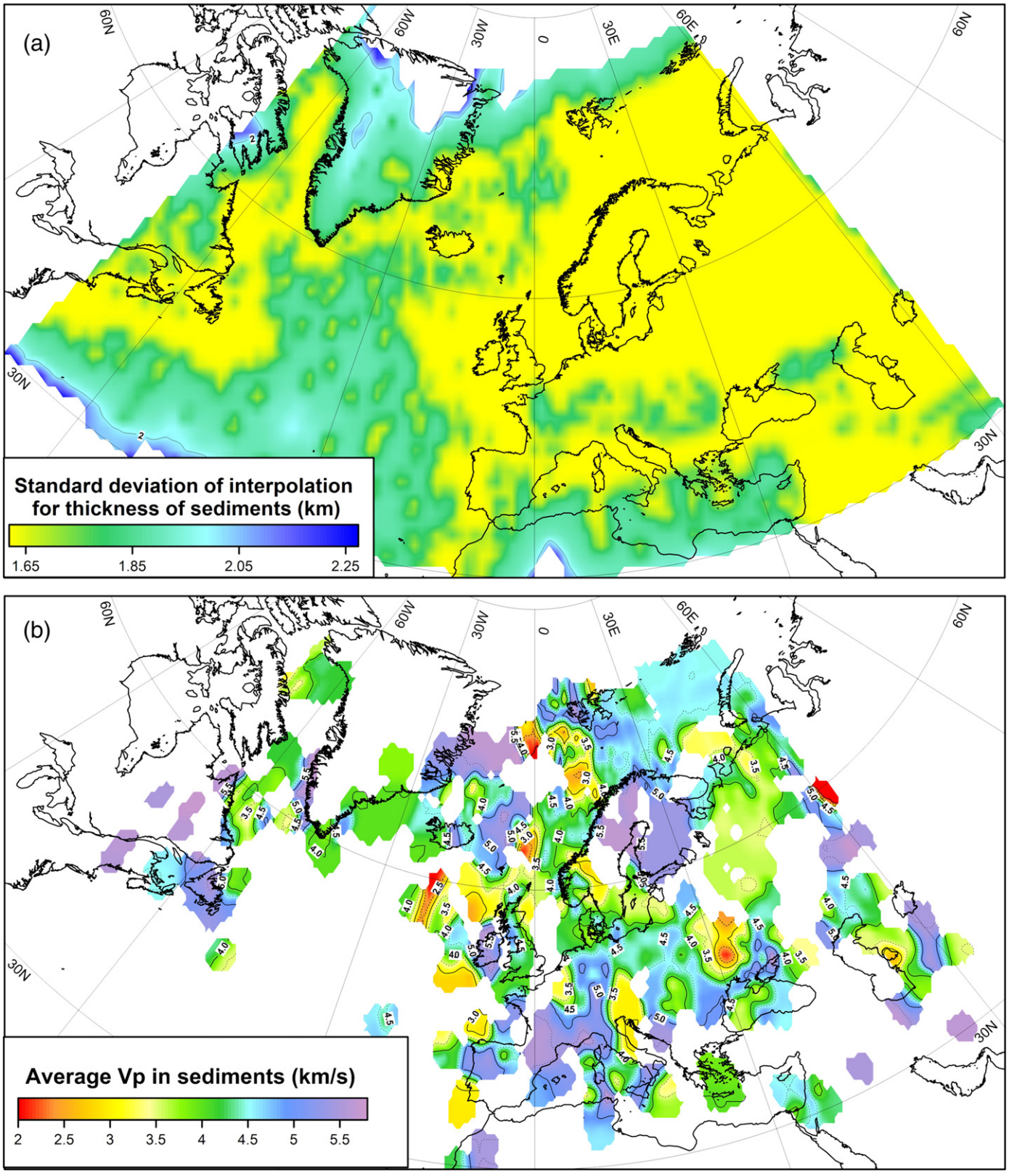

Fig. 8. Standard deviation of interpolation for thickness of sediments (a). The map is constrained with the same interpolation parameters as used to produce Fig. 7. Thickness of sediments is constrained better than depth to Moho due to a large amount of borehole data and shallow exploration studies. (b) Average Vp velocity in the sedimentary cover. The map is constrained with a 1° × 1° interpolation, given strong variability in the parameter. Given incomplete information on the structure of the sedimentary cover in our database (see caption to Fig. 7), this map illustartes only general trends.

- Stations with less than 10 earthquakes are excluded, except for stations located in "white spots" where seismic data are lacking (e.g. station GFA in Tunisia with only 2 processed events);
- Out of 54 stations with complexity >0.75, 33 are excluded either due to multiple choice for the solution or unrealistic Hk pairs. The remaining stations are kept either because they are located in areas with no

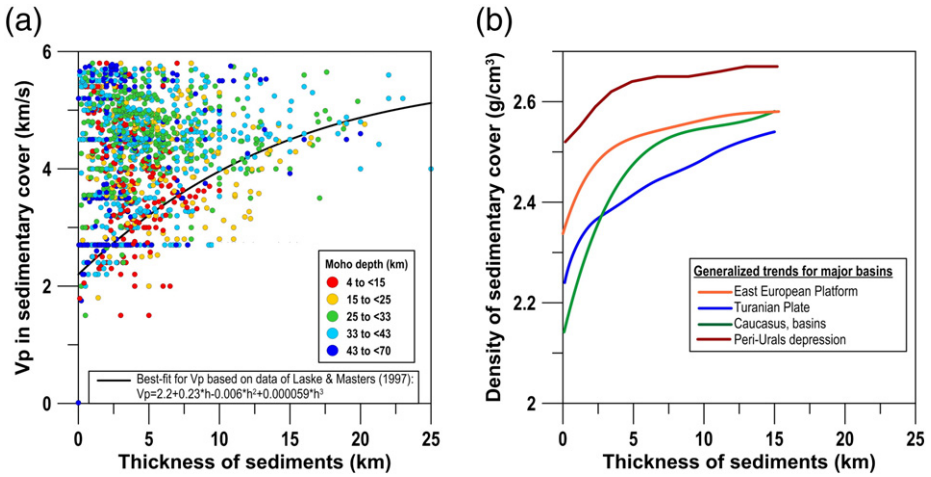

Fig. 9. Average Vp velocity (a) and density (b) in the sedimentary layer of the European region as a function of layer thickness. Vp is based on seismic data for the entire region included into the crustal database. Color code indicates depth to Moho. Solid line shows the best polynomial fit to data based on data by Laske and Masters (1997) and used by Molinari and Morelli (2011) to constrain Vp structure of the sedimentary layer in Europe. The regression fit reflects mostly the effect of compaction, and apparently does not account for lateral variations in composition and metamorphic state (e.g. from complex burial history) of the sedimentary cover. (b) General trends of density variation with depth in some major sedimentary basins of the ex-USSR (Avchan and Oserskaya, 1985; Oserskaya and Podoba, 1967) clearly demonstrate that, depending on regional tectonics, there are significant differences in density structure of different basins.

other seismic data, or the estimated Moho depth is in agreement with other existing seismic models in the vicinity of these stations;
- Stations for which the automated RF solution contradicts regional seismic models (e.g. station MELI in Northern Morocco with a Moho depth of 51 km in the automatic solution vs 23–29 km in regional studies) are excluded;
- In case of duplicate data (manual and automated) for the same station (e.g. Summit station SUMG in Greenland), we keep the values based on manual interpretations.

As a result, Moho depth estimates are added for 173 stations (Electronic Supplement 2). This permitted us to close "white spots" (i.e. regions with otherwise no seismic data on the crustal structure) such as in the Central Russia (the Moscow region), parts of France and Germany, the Apennines, the Balkans, eastern Mediterranean, northern Africa, and the Azores (Fig. 5).

4.2. Interpolation and map presentation

4.2.1. Interpolation strategy

The database (EUNAseis crustal model) is constrained by point data along seismic profiles and (for RFs) at seismic stations, and is available as interpolation on a regular grid. Given the uneven data coverage, very dense in some parts and very sparse in other parts of the region, our choice of interpolation radius is governed by the following considerations:

(i) to provide a continuous coverage of the entire region, avoiding "white spots"; this would allow for an easy application of the database in various regional studies where crustal correction is needed;
(ii) to preserve amplitudes and variation of all of the parameters (Vp and thickness) for individual crustal layers, depth to Moho, and Pn velocity; this would additionally allow for regional analysis of links between crustal structure and tectonic setting.

To address consideration (i), parts of the Mediterranean Sea with no seismic data and with bathymetry greater than 2 km (the suspected oceanic crust (Fig. 3)) are assigned 8 km thickness of the crust (the Eastern Mediterranean Sea and the deep-water basins south of the Hellenic subduction zone in the Western Mediterranean Sea). This value is to some degree arbitrary since, with few exceptions, no seismic profiles cross these deep-water basins. A seismic refraction profile across the 2.5–3.5 km deep basin of the Tyrrhenian Sea shows a total crustal thickness of 6–8 km (Duschenes et al., 1986) and thus by analogy a crustal thickness of 8 km is assumed for other deep-water parts of the Mediterranean Sea.

We prefer to leave most of the southern part of the North Atlantic Ocean blank, given that in much of the area the bathymetry does not follow predictions for "normal oceans" (Fig. 2b) and the oceanic crust may be anomalous. Particularly, for the Azores, Moho depth estimated by automated RFs is ca. 20 km (Electronic Supplement 2).

4.2.2. Implementation and uncertainty analysis

Consideration (i) dictates the choice of interpolation radius. In continental Europe, the largest gap between seismic models (in the Moscow region) can be almost closed by a 3° interpolation distance; similar gap exists in the northern part of the Atlantic ocean. Given the scarcity of seismic data in Greenland, we decided to leave this region with white spots.

To address consideration (ii), several interpolation methods and strategies have been tested to determine the method and the parameters which allow for preservation of amplitudes and shapes of all parameters in the database (Fig. 6a). For control, the difference between seismically determined and interpolated values has been routinely analyzed for all model parameters. The "nearest neighbor" interpolation method has shown to be the best in preservation the shapes and the amplitudes, particularly in regions with large lateral gradients in crustal properties.

We quantify the uncertainty associated with interpolation (also see Sections 5.1 and 7.1); its value depends on the density of seismic data coverage and is comparable to the resolution of the seismic methods for most of the study area. We use a cross-validation procedure for kriging interpolation based on data-constrained variograms (Fig. 6b). Since data cross-validation cannot be directly used for the "nearest neighbor" interpolation method, the parameters of both interpolation procedures have been adjusted to achieve very close similarity between the methods and between the observations and the seismic models (Fig. 6a). The largest uncertainties are in regions with sparse seismic data coverage where interpolation uncertainty is up to 8 km for thickness (depth).

In relation to consideration (ii) we also consider how to prevent uncontrolled interpolation "leakage" to regions without seismic data.

Given the dense data coverage in most of the European continent, no artificial effort is made for this area. However, we "damp" interpolation "leakage" across the ocean–continent transition in regions without seismic data by artificially assigning 8 km thick crust in a narrow corridor on the oceanic side of the transition from the shelf to deep water. This includes four tectonic regions: western North Atlantics around Newfoundland, the Arctic part of the North Atlantics, the southern coasts of the Black Sea and the Mediterranean Sea.

In summary, the following interpolation strategy is adopted for the production of maps illustrating the new EUNAseis crustal database. All maps illustrating crustal structure in the European–North Atlantic region are produced by the "nearest neighbor" interpolation method with a 3° search radius and are sampled on a 0.5° × 0.5° grid. Short wavelength sampling allows for preservation of small scale variations in the crustal structure, and only very limited regions in the study area have adequate coverage by seismic models (Fig. 5) to justify coarser sampling. We emphasize that neither a 3° search radius nor a 0.5° sampling grid correspond to the true resolution of the EUNAseis crustal model which is controlled by the seismic data coverage (Fig. 5).

Finally, high-frequency "noise" unsupported by seismic data (such as "bull's-eye" anomalies produced by interpolation) has been removed by low-pass filtering. Random comparison of gridded data with seismic models shows preservation of the seismic information during the interpolation procedure. However, as with any interpolation, small-scale anomalies are significantly smeared in amplitude and size, similar to smearing of tall but laterally small mountain peaks on topographic maps.

5. Sedimentary cover

5.1. Preamble

Thickness of the sedimentary cover and the depth to the basement are illustrated in Fig. 7; clearly the major difference between the two maps is for deep oceans. Note that for Greenland we do not include ice into the sedimentary cover; information on inland ice thickness can be found at the NOAA web-site and is shown by Artemieva and Thybo (2008). For normal oceans (i.e. oceans where the bathymetry follows the square-root-of-age dependence) (Schroeder, 1984), the sedimentary thickness is based on a 5′ NGDC global compilation (Divins, 2008). For the continental part and the continental shelves, the sedimentary thickness is constrained by seismic data (Electronic Supplement 1), complemented by data from the EXXON map (1985); the latter incorporates results from high-resolution regional seismic surveys and drilling. Given that a large amount of recent (post-EXXON map) borehole data and high-resolution regional seismic data has been acquired for commercial purposes and is not publically available, our model for the sedimentary cover can be missing many details. Sedimentary thickness in the Barents Sea is adopted largely from Drachev et al. (2010) with some modifications in accordance with available seismic profiles (Electronic Supplement 1), when in conflict. The seismic Vp velocity structure of the sedimentary layer is discussed in Section 5.7.

Seismic definition of the top of the crystalline crust is not unique. Given typical composition of sediments, in western Europe it is usually defined as the depth where the seismic velocity reaches 5.4–5.6 km/s, whereas in most of the East European Platform covered by a thick sequence of high-velocity carbonates and metasediments the top of the basement is usually associated with Vp ~ 5.8 km/s (Beloussov et al., 1991), while in the southern parts of the East European Platform (e.g. the Donbas coal region) it may correspond to the depth where the Vp velocity even reaches 6.0–6.2 km/s (Kostyuchenko et al., 2004). These differences in the boundary velocity at the sediment–basement transition are adopted in the present study when no direct information on the depth to the basement is reported in original publications.

Given a significant amount of commercial seismic and borehole data, thickness of the sedimentary cover is well constrained in many regions, in particular in regions with oil and gas deposits. There are, however, large regions (e.g. deep-water Mediterranean Sea) where no seismic or borehole data are available. As a result, the uncertainty of the maps (Fig. 7a, b) is rather non-uniform. Additional uncertainty arises from the interpolation of the available data. Its value depends on the density of data coverage and is ca. 1.5 km for most on-shore areas and ca. 2 km for off-shore areas (Fig. 8a), given that the density of available data is uneven for most of the region. Note that these values do not incorporate the true uncertainty in the thickness of sediments as estimated by geophysical methods. While for most of the area interpolation uncertainty for the Moho depth is comparable to the resolution power of seismic methods, the interpolation uncertainty for the thickness of sediments is significant and in some cases may reach 30–50% of the true value.

5.2. Key patterns

Major observations that follow from the maps of the depth to the basement (Fig. 7a) and thickness of the sedimentary cover (Fig. 7b) are the following (further details are provided in Sections 5.3–5.7):

- The sedimentary cover is less than 1 km thick in the shield areas which are of Archean–Mesoproterozoic age.
- Sedimentary basins formed on the Variscan crust are relatively shallow (2–3 km deep) and similar in thickness to much of the platform cover in Proterozoic Europe.
- Deep basins, with more than 10 km sediment, are found in large parts of the European region. Most of them are located on Precambrian crust and the deepest (with ca. 20 km of sediment) formed in the Paleozoic. Main depocentres are observed in the southern part of the East European Platform (including the Caspian Sea region), along the craton margins (including the Polish–German Caledonides), and in the Paleozoic rifts (including the Peri-Caspian basin and the Dnieper–Donets rift). Thick sequences of sediments are in the foreland basins (such as the Aquitaine and Po basins), on the continental shelves (most notable in the eastern Barents Sea), in the intramountain depressions (e.g. the Kura basin in the TransCaucasus), and in the Black Sea.
- The sedimentary cover is less than 1 km thick in many of the collisional orogens and mountain ranges (the Alps, the Apennines, the Caledonian ranges of Norway, Greenland and North America, the Urals). However, a thick (8–10 km) layer of sediments is reported for the Zagros mountains to the west of the Main Zagros Fault (Vergés et al., 2011).
- The young ocean floor of the North Atlantic ocean lacks sediments, except for the anomalous crust around Iceland and the Jan Mayen microcontinent.
- The Vp velocity structure of the sedimentary layer is highly heterogeneous with short wavelength variations (Fig. 8b).
- As a rule, average Vp velocities in sedimentary layer are better correlated with the tectonic age rather than with basin depth (Fig. 9a). No correlation is observed between average Vp in the sedimentary sequence and Moho depth. Significant differences in Vp structure of the sedimentary successions occur in different basins even at local scale (cf. Section 5.7).

5.3. Cratonic crust

The shield areas of the East European Craton (the Baltic Shield, the Ukrainian Shield and the Voronezh massif) and Greenland are almost void of sedimentary cover. In most of the East European Platform the thickness of the sedimentary cover is between 2 and 7 km, showing a general eastward increase from ca. 2–3 km in the central part of the platform to 5–7 km in the graben structures at the western margin of the Urals. Deposition of a thick sequence of sediments along the Ural mountains may have been caused by a dynamic downflexure of the cratonic lithosphere in response to the Urals orogeny with a west-dipping

subduction (Mitrovica et al., 1996). The southern parts of the platform continue to subside during the latest 200 Ma (Nalivkin, 1976) as a result of a dynamic flexure associated with the collision of the Arabian (Turkish) plate and the Scythian plate and the Africa–Eurasia collision. Alternatively, or additionally, the post-Devonian subsidence of the cratonic lithosphere may have a compositional origin caused by metasomatic enrichment of depleted cratonic lithosphere mantle by Fe-rich heavy basaltic melts caused by the Devonian magmatism (Artemieva, 2003), as suggested by the spatial correlation between the areas of Meso-Cenozoic subsidence and areas with a compositionally dense lithospheric mantle as constrained by lithospheric buoyancy and by Vp/Vs ratio in global and regional seismic tomography models (Artemieva et al., 2006).

5.4. Rifted cratonic crust

The East European Craton is cut into three parts by two trans-cratonic Riphean rift systems: the SW–NE stretching Central Russia rift system which from west to east includes the Orsha, Valday, and Soligalich rifts and a roughly perpendicular rift system which separates Sarmatia from Volga–Uralia and includes the Don–Medveditsa rift at the edge of the Peri-Caspian depression and the Pachelma–Saratov trough (rift) bordering the Voronezh massif in the east; at the northern end the rift turns westwards forming the Moscow branch with the rift junction roughly beneath Moscow (Fig. 3). These Riphean rifts mark the suture zones along which three Archean–Paleoproterozoic subcratons were amalgamated in the Proterozoic (Gorbatschev and Bogdanova, 1993). A number of seismic surveys have been acquired across them (e.g. Kostyuchenko et al., 2004). The results show that the rifts are well expressed in the structure of the sedimentary cover, with sedimentary sequences there 1–3 km thicker (e.g. 4–5 km in the Pachelma rift) than in the adjacent areas of the East European Platform (where sedimentary cover is ca. 1.5–2 km thick).

Palaeozoic (Devonian) rifting in the southern parts of the East European Craton created the Dnieper–Donets rift and rifted the Peri-Caspian basin (Leonov and Volozh, 2004). The sedimentary successions of the Dnieper–Donets Rift are 4–5 km thick in the north-western part (chiefly chalk and mergels, with salt in the lowermost horizons), 10–12 km in the south-eastern part, and up-to 20–24 km thick locally in the central part of the rift. In the Donbas coal region in the south-central part of the rift, the sedimentary successions which include thick coal deposits with high seismic velocity (5.6–5.8 km/s) are more than 10 km, and in places 20 km, thick (DOBREfraction'99 Working Group, 2003; Maystrenko et al., 2003).

The very deep Peri-Caspian depression apparently formed on Precambrian basement in the southern part of the Volga–Uralia subcraton. The oldest sediments reached by deep drilling are from the Middle Ordovician. The central, post-rift basin of the Peri-Caspian depression is filled with 16–20 km (locally 22–26 km) of sediments as indicated by results from interpretations of seismic refraction and wide-angle seismic reflection data (Bush and Kaz'min, 2008; Effimoff, 2002; Segalovich et al., 2007; Volozh et al., 1996). The thickness of sediments in the peripheral parts of the Peri-Caspian depression is ca. 7–10 km. The northward extension of the belt of thick sedimentary cover fills the Urals Foredeep.

5.5. Phanerozoic crust

The main geologic–tectonic border in Europe (TESZ) is marked by a chain of basins with at least 5 km of sedimentary rocks. Although in places (e.g. the Polish Trough and the Danish and the North German Basins) they reach up to 20–25 km in thickness, commonly sedimentary thickness in the Danish–Norwegian Basin is 5 to 10 km (Grad et al., 2003; Jensen et al., 1999; Lassen and Thybo, 2012; Thybo, 1997). However, in most of central (Variscan) Europe, including the Paris basin, the sedimentary cover is generally only ca. 2–3 km thick. Similarly, in large parts of the Pannonian basin the thickness of sediments is 2–3 km, increasing to ca. 5 km (locally more) in the Great Hungarian Plain and the Transylvanian basins (Horvath et al., 2006).

Notable exceptions are the deep foreland basins such as the asymmetric Aquitaine basin (with more than 11 km of sediments accumulated in the southern part along the northern edge of the Pyrenees), the Ebro basin in north-eastern Iberia, and the Po basin in northern Italy with at least 6 km of Pliocene sediments lying above 3–4 km thick Mesozoic carbonate sequence (Haan and Arnott, 1991). In the Caucasus, the foredeeps and inter-mountainous basins are more than 8 km deep, with the deepest succession (ca. 16 km) accumulated in the Kura basin (Trans Caucasus).

5.6. Off-shore regions

Deep sedimentary basins continue westwards from the German and Danish Basins into the North Sea, where very deep (locally reaching 20 km, e.g. in the Skagerrak graben where sedimentation could have begun already in the late Proterozoic) small-size pre-Permian basins are present (Lassen and Thybo, 2012). Typically, the thickness of sediments in the North Sea is the largest in the Central graben (locally up to ca. 10 km) with ca. 3 km (locally up to 5–6 km) in the North and South Viking grabens, and thinning to 1–3 km towards the coasts.

The continental shelf of the Barents Sea area formed on Archean–Proterozoic basement. Main subsidence occurred during the Mesozoic in the eastern Barents Sea where the South and North Basins have sedimentary thicknesses around 20 km (Engen et al., 2008; Ritzmann et al., 2007). In the western Barents Sea, continuous subsidence took place in small basins since Middle Carboniferous rifting. Presently these basins contain up to 10–12 km of sediments (for overview see Ritzmann et al., 2007; Drachev et al., 2010).

In the North Atlantic ocean, the thickness of sediments increases towards the coasts, but is close to zero in the young oceanic crust. Anomalous oceanic crust around Iceland has locally 2–4 km of sediments, similar to the coastal areas around Greenland and the Baffin Bay.

In the Black Sea, the thickness of sediments is larger than 16 km in the Western Black Sea depression, and 8–11 km in its Eastern depression (Beloussov et al., 1988; Minshull et al., 2005). The thickness of the sedimentary successions in the basement depression of the South Caspian Sea is 22–24 km decreasing to ca. 16 km in the North Caspian Sea and to 10–12 km in the Central Caspian block.

The amount of seismic data on sedimentary thickness in the Mediterranean Sea remains very limited. A number of seismic profiles have been recorded during the VALSIS experiment along the eastern Iberian margin (e.g. Maillard and Mauffret, 2011). They document a strong short-scale variability in thickness of sediments which ranges from ca. 2–3 km in the Valencia Basin and the Alicante shelf to ca. 1 km or less in the Ibiza channel. Thick Meso-Cenozoic sequences (ca. 6 km) are reported for the Adriatic Sea, reaching ca. 10 km in its oil-bearing northern part (Mattavelli et al., 1991). Gravity modeling along a NS profile between southern Italy and Africa suggests the presence of a ca. 8 km of sediments beneath the Sirte basin which decrease in thickness to ca. 5 km beneath the deep-water part of the Ionian Sea (Cowie and Kusznir, 2012). In the eastern Mediterranean (the Levant continental margin) seismic refraction data indicates the presence of 10–14 km thick sedimentary sequence (Ben-Avraham et al., 2002); no seismic data have been found by the authors for the deep-water basins of the Mediterranean Sea.

5.7. Average Vp in sedimentary layer

The sampling density in the sedimentary basins is lower for seismic Vp velocity than for the thickness of the sedimentary succession because most seismic data, targeting basins, is based on the normal-incidence seismic reflection method, which does not provide reliable information on seismic velocity. We include all available data on the thickness of the

sedimentary successions from seismic reflection and refraction investigations, and complement it by information from other sources (see Section 5.1), whereas for the seismic velocity of the sedimentary successions we only rely on the results from seismic refraction investigations and acoustic logging in boreholes, where available. Due to incompleteness of information on the seismic velocity structure of the sedimentary layer, we do not distinguish soft and hard sediments, but instead incorporate average P-wave velocity (Vp) in the sedimentary layer (calculated as average weighted by thickness) in cases where details on Vp structure in sedimentary successions are provided in original seismic models.

This approach leads to a map of average seismic Vp in the sedimentary basins which shows large short-wavelength variation (Fig. 8b) and clearly indicates that seismic velocity and thickness of sedimentary basins do not correlate with each other (Fig. 9a). Overall there is a large scatter between average seismic Vp velocity in the sedimentary strata and total thickness of the sedimentary successions. The same plot also shows a large scatter in the cross-plot between thickness of the sedimentary succession and Moho depth. Some extremely deep basins (with thicknesses of about 20 km or more), such as the Peri-Caspian Basin and the Eastern Barents Sea, have very high average velocity (up to 4.5–5 km/s), whereas other deep basins with more local extent (e.g. the Polish Trough and the North Sea) have relatively low Vp velocity. In shallow basins, the average velocity covers the entire range from about 2 to 5.8 km/s, and is probably mainly controlled by basin age and burial history of the basin fill as indicated by some regional studies (e.g. Japsen, 1998; Nielsen et al., 2011). Although deep basins are generally characterized by high seismic velocity, there is substantial scatter even for 10 km deep basins and the range of average velocity narrows out only to the deepest (>10 km) basins.

A direct relation between average seismic velocity and thickness of sedimentary basins has been suggested by Molinari and Morelli (2011) based on a correlation study of a global digital database of sediment thickness (Laske and Masters, 1997), even though the latter is in part constrained by geological similarity rather than by geophysical data. Although these authors find that there is substantial scatter in the actual point distributions, they use the empirical relation between Vp and thickness to estimate the former from the latter (Molinari and Morelli, 2011). The shape of their relation between average Vp and thickness of sedimentary basin suggests that sediment compaction is the major control of density (and Vp) increase with depth. However, our results demonstrate that such simple correlation does not exist and factors other than compaction play important role in controlling Vp and density structure of sedimentary basins.

Our database, constrained by direct observations of seismic velocity and basin depth, shows that any direct relation between the average Vp and thickness of sedimentary basin is unlikely (cf. Fig. 9a). It is evident that a general, direct relation between the two parameters cannot exist, considering the huge differences in depositional history between old (Proterozoic to Paleozoic) platform covers with high average velocity and young basins (many of Mesozoic and Cenozoic age) with low average velocity in sediments. In general, most areas show some correlation between basin age and average sediment velocity, instead of correlation between basin depth and velocity. Clearly, the burial history (including composition and metamorphic state of the sediments and sedimentary rocks) also influences the actual average sediment velocity. This may be a major reason that the old platform covers in general have extremely high velocity, caused by long term metamorphosis and possible deep burial since deposition. These considerations explain the large differences between the map of average sediment velocity based on the assumption of a direct relation between thickness and velocity (Molinari and Morelli, 2011) and our map (Fig. 9a), which is based on actual seismic Vp measurements in the various sedimentary basins and platform covers. For example, in sediments of the Baltic Shield, the Vp velocity is ca. 2 km/s according to Molinari and Morelli (2011) and 5.4–5.7 km/s according to seismic models (e.g. Guggisberg et al., 1991). Generalized plots for the relation between Vp and sediment thickness based on regional geological data confirm that, although the overall relation between density (and Vp) in sedimentary layer is similar to the one adopted by Molinari and Morelli (2011), there are significant differences between different basins of Eurasia (Fig. 9b).

6. Crystalline crust

6.1. Preamble

The following section discusses the structure of the crust in the Europe–Greenland–North Atlantic region. It includes the depth to Moho (Figs. 10a, 11) compared to other available crustal models (Fig. 12), the thickness of crystalline crust (Fig. 10b), the interior structure of the crystalline crust as defined by Vp seismic velocities (Figs. 13–16), including thicknesses of the individual crustal layers and their average Vp velocities, as well as average Vp velocities in the crystalline crust and in the entire crust (Fig. 17). We further compare the regional crustal model with other available global and regional models for the structure of the crust in the Europe–Greenland–North Atlantic region (Fig. 18). Pn-velocities at the top of the mantle are discussed in the next section (Fig. 19). Five crustal-scale cross-sections are chosen to illustrate major tectonic structures in the region (Fig. 20).

The summary of the crustal structure in Europe, Greenland, Iceland, the North Atlantic and adjacent regions focuses on controversies in the existing interpretations, rather than on providing a comprehensive description of the model of the crust. Details of specific areas and the European continent can be found in a series of reviews and crustal compilations (e.g. Artemieva and Meissner, 2012; Artemieva et al., 2006; Blundell et al., 1992; Burollet, 1986; Dezes et al., 2004; Foulger et al., 2005; Grad et al., 2009; Jensen et al., 2002; Kelly et al., 2007; Meissner, 1986; Meissner et al., 1987b; Pavlenkova, 1996; Prodehl et al., 1995; Ritzmann et al., 2007; Tesauro et al., 2008; Thybo, 1997; Ziegler and Dezes, 2006). Prior to discussion of specific details on the structure of the crystalline crust in Europe–Greenland–North Atlantic region, we list the key patterns for each of the crustal characteristics and provide some comments related to the resolution and uncertainties of the crustal model and its visual presentation. This is followed by a brief discussion (with the key references) of the crustal structure for major tectonic provinces in the region (Section 8).

6.2. Depth to Moho and thickness of crystalline crust

6.2.1. Uncertainties in crustal thickness

It is hardly possible to provide a realistic estimate of the uncertainty for the depth to Moho (Fig. 10a) and thickness of the crystalline crust (Fig. 10b). While the uncertainty for the Moho depth as calculated in regional crustal models is 1–2 km for good quality seismic profiles and 2–4 km for the RF models, the overall uncertainty for the entire region cannot be estimated due to a significant controversy between crustal models produced by different authors. As it is discussed for Greenland and Iceland (Sections 3.2, 8.1 and 8.3), one of the problems arises in interpretations of the nature of the high-velocity (>7.2 km/s) layer at the depth where the base of the crust may be expected (e.g. Mjelde et al., 2012). Depending on petrological interpretation of this layer (high-velocity (partially eclogitized) lower crust, low-velocity (partially molten) upper mantle, or a crust–mantle mixture), the difference in the calculated Moho depth may reach ca. 10 km (Thybo and Artemieva, 2013–this volume). In some regions with a complex tectonic evolution, double Moho can exist (e.g. caused by two subduction systems as under the Alps). In such cases the choice of the shallow, Adriatic (Tesauro et al., 2008) or the deeper, European Moho as the base of the crust is subjective, and here the deeper of two Mohos is incorporated into the EUNAseis database.

Additional uncertainty which arises from the interpolation is addressed in detail in Section 4.2 (also see Fig. 6). To compensate for uneven data coverage in the study area, for visualization purpose the

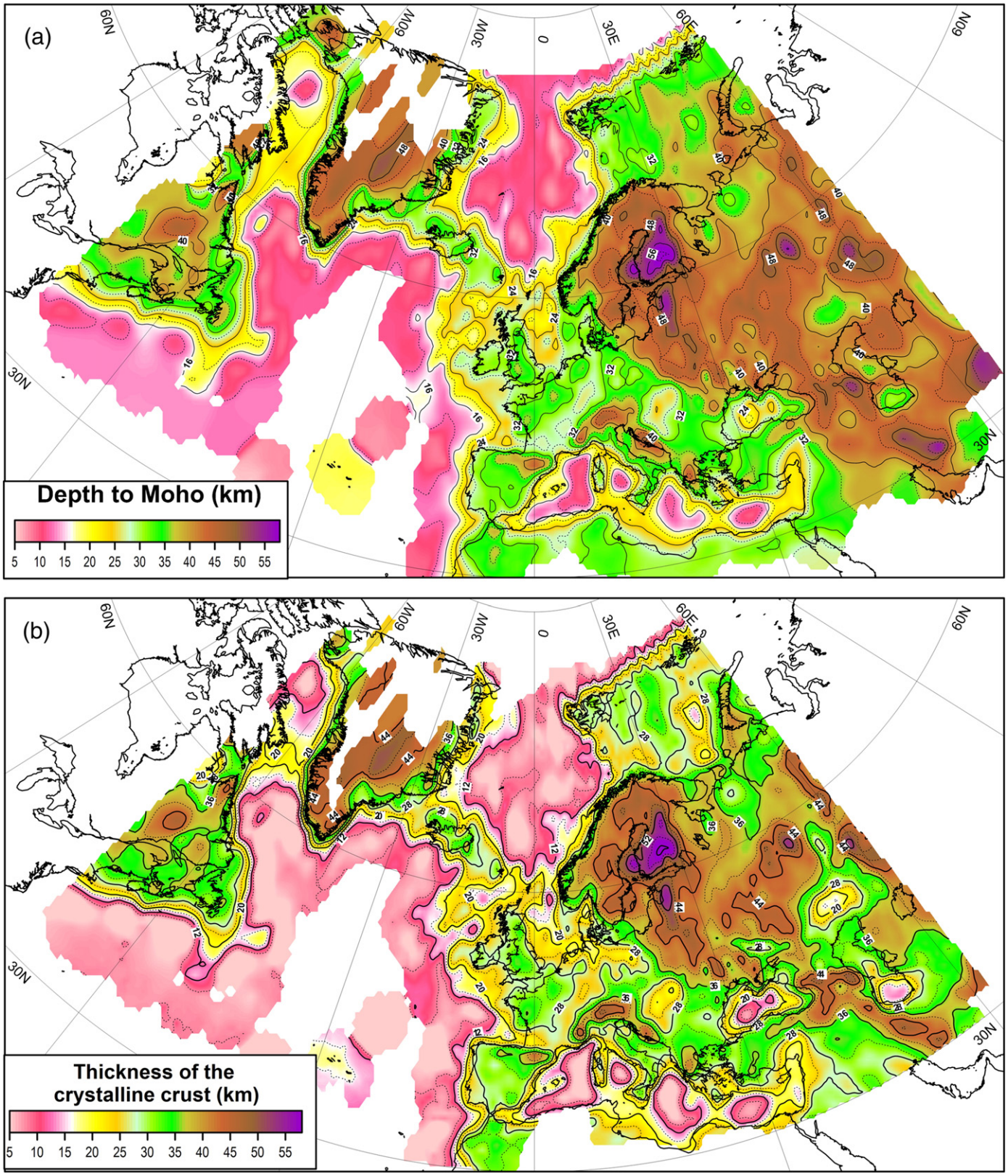

Fig. 10. Depth to Moho from sea level (a) and thickness of the crystalline crust (b). Moho depth is constrained by seismic data (see Fig. 5 for data coverage and Table 2 for some details); thickness of sediments is constrained as specified in Fig. 7. Both maps are constrained with a 3° interpolation radius chosen to preserve the magnitudes; however, in regions with highly variable crustal and sedimentary thicknesses many details can be missing due to interpolation averaging. (c, d) Depth to Moho based on the same seismic data but constrained with a 0.5° and 1° interpolation radius. Assumed values along the western North Atlantics and Arctics, used in a 3° interpolation to "damp" interpolation "leakage" across the ocean–continent transition in regions with no seismic data, are removed (see Section 4.2 for details).

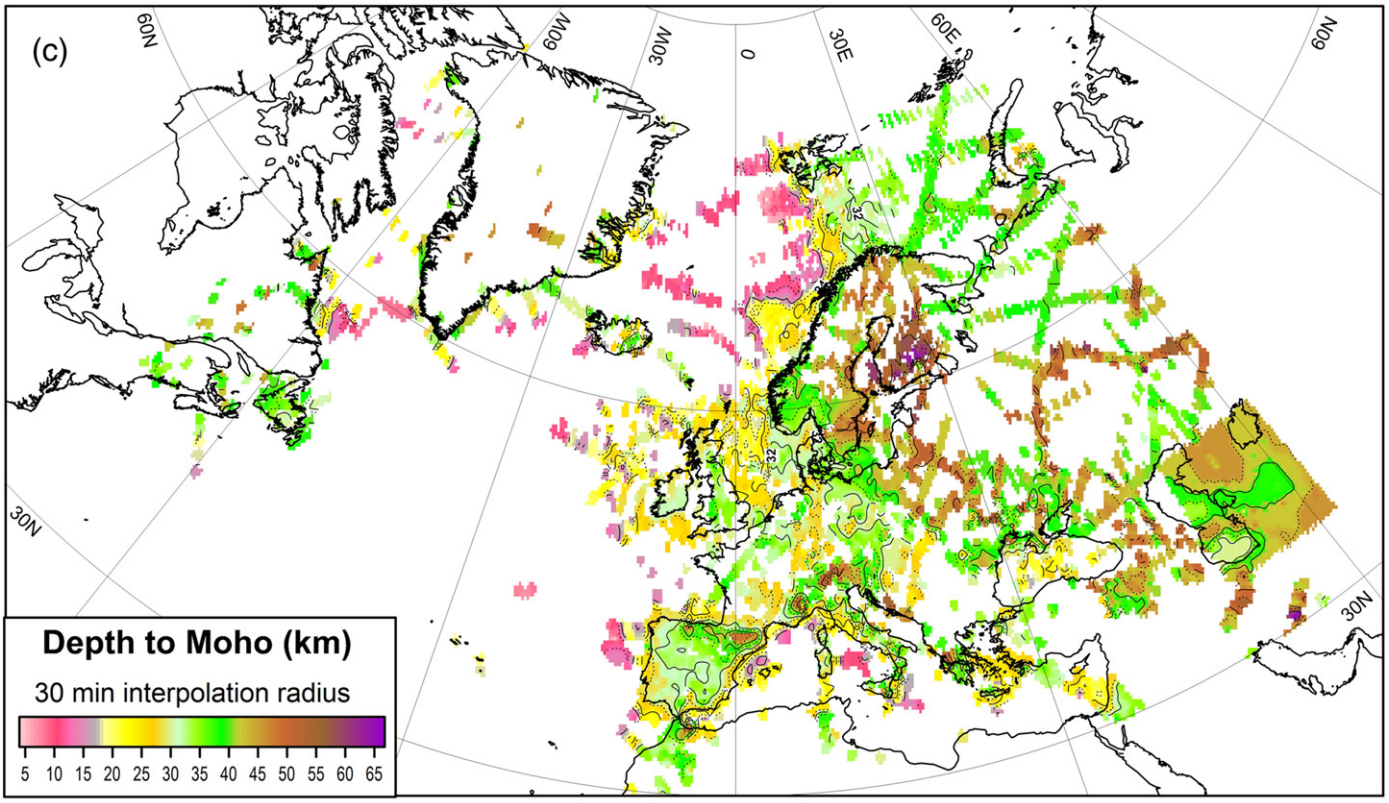

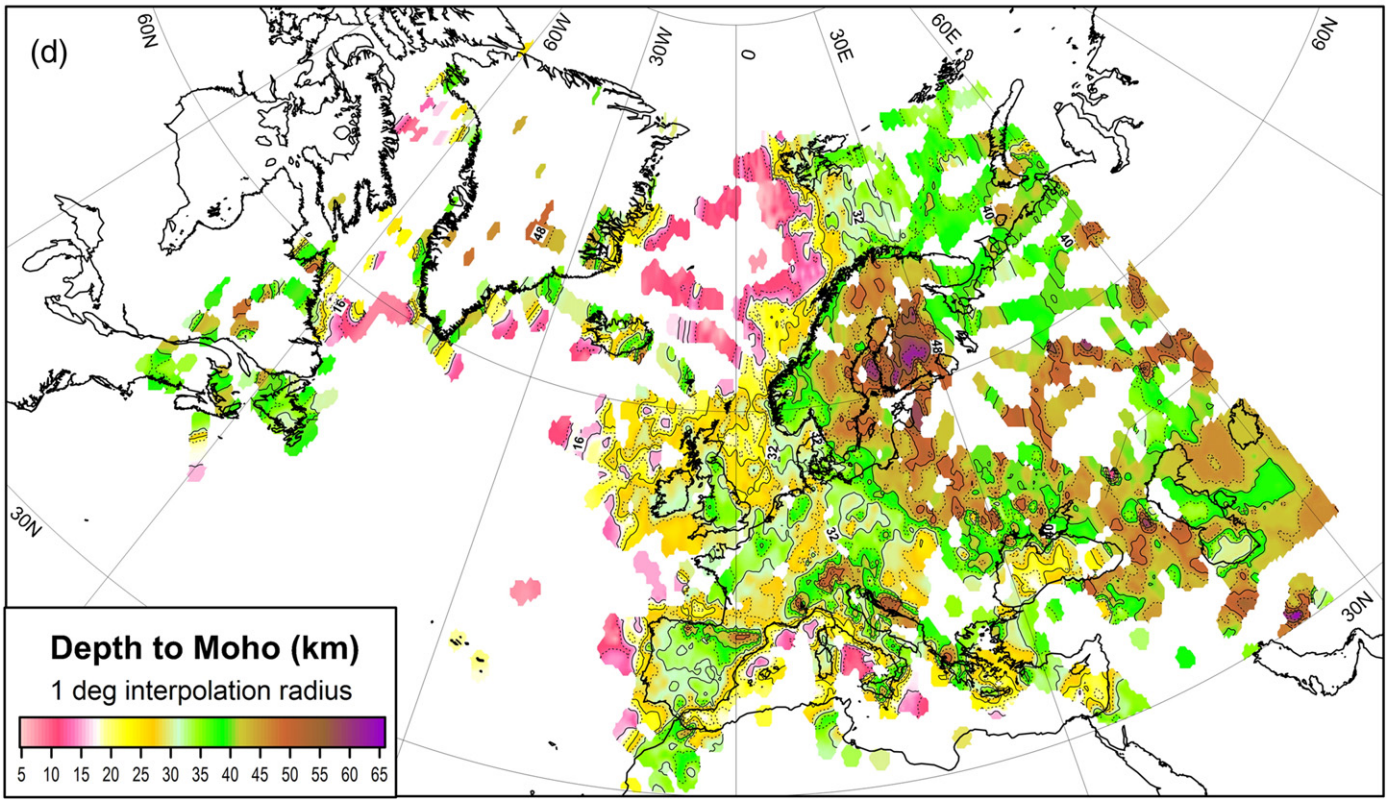

Fig. 10 (*continued*).

Moho depth is interpolated within a 3° radius which allow for a continuous mapping in all regions except for Greenland. Although the interpolation method has been chosen to preserve the magnitude of the Moho depth variations, the resulting maps (Fig. 10ab) do not include all small-scale details present in our crustal database and shown in regional crustal maps, such as for central-western Europe in the area defined by 16W–24E and 35N–61N (Dezes et al., 2004) or in the area 25W–35E, 35N–71N covered by the crustal model EuCRUST-07 (Tesauro

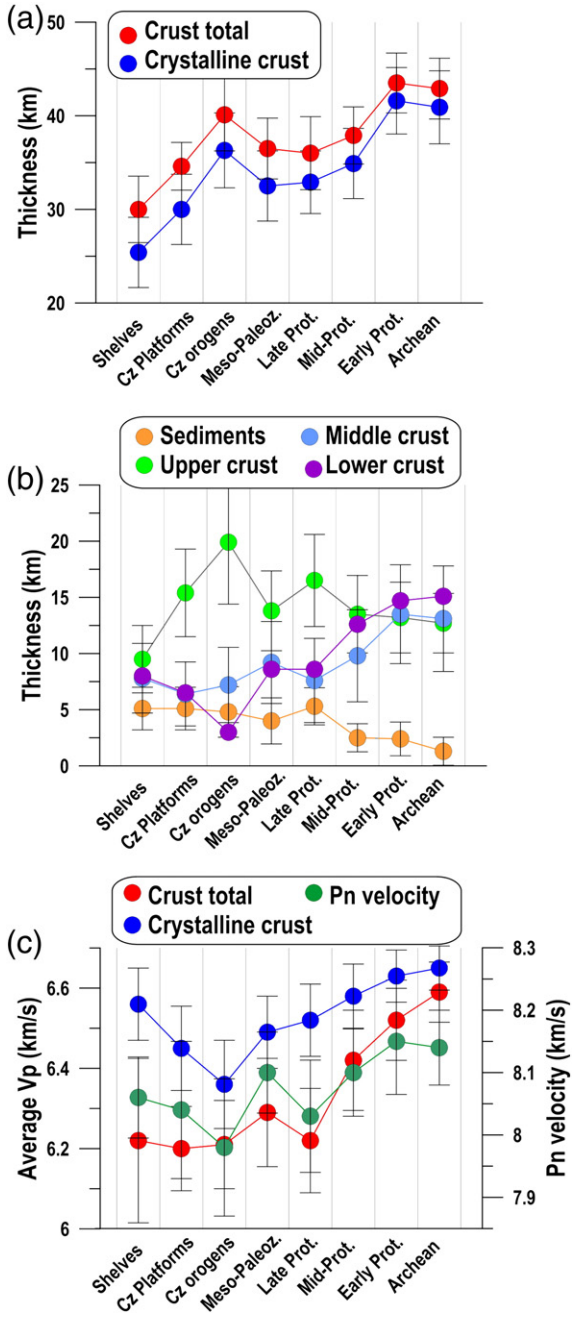

Fig. 11. Statistical properties of the European continental crust (on-shore and shelves) for different tectonic settings and as function of crustal tectono-thermal age. (a) Thickness of the crust (including sediments) and its crystalline part; (b) Thickness of four crustal layers (high-velocity lower crust is included as a part of the lower crust); (c) Average Vp velocity (calculated by weighted averaging of layer thickness) in the crust (including sediments) and in its crystalline part; also shown is Pn velocity at the top of the mantle. Vertical lines — standard deviation of the parameters. Tectonic settings follow the categories in Table 3, that also provides futher details.

et al., 2008). Note that the true resolution of our crustal model as constrained by seismic data is finer than 3° × 3°, as is illustrated by Fig. 10c where interpolation radius of 0.5° is used. This map also demonstrates that the claimed uniform lateral resolution of 15′ ×15′ in the EuCRUST-07 model (Tesauro et al., 2008) or 0.5° × 0.5° in the EPcrust model (Molinari and Morelli, 2011) is not supported by the existing seismic data coverage for a significant part of the area, unless gaps in seismic data coverage are filled by gravity constraints, tectonic considerations, and interpolation.

Although our database for the off-shore regions is significantly more extensive than other published compilations, a particular problem with seismic data coverage exists in the North Atlantic Ocean (Fig. 5). This problem is discussed in Section 4.2. While anomalous regions (where bathymetry is not proportional to the square root of age, Fig. 2b) of the North Atlantic Ocean north of 50N are well covered by seismic data (Fig. 5), the region south of Iceland largely lacks seismic studies. In contrast to the EuCRUST-07 and EPcrust models (Molinari and Morelli, 2011; Tesauro et al., 2008), where the parts of the North Atlantic ocean not covered by seismic models are assigned Moho depth from the global CRUST2.0 model (Bassin et al., 2000), we decided to leave these regions blank, given that substantial parts of the region may have anomalous crustal structure.

6.2.2. Key patterns for Moho depth

Major observations that follow from the map of the depth to Moho (Fig. 10a) are the following:

- The Precambrian crust of the cratons (including the Archean–Paleoproterozoic crust) has highly variable thickness. Depth to Moho varies from less than 40 km in rifted parts of the East European Craton to ca. 60 km at the Archean–Paleoproterozoic suture in the Baltic shield.
- Thick crustal roots (50–60 km) are typical for Archean–Paleoproterozoic terranes and are documented for the Karelian province of the Baltic Shield and the Volga–Uralia subcraton. In both cases, thick crustal roots are apparently associated with ancient sutures (collisional zones).
- The craton to noncraton transition across the TESZ is marked by a sharp (ca. 10 km) decrease in the Moho depth over a short lateral distance of less than 100 km.
- Young (Phanerozoic) crust has as variable thickness as the ancient crust. Its thickness ranges over more than 20 km, from ca. 30 km in the Variscides to more than 50 km in the young orogens of the Alpine belt. Note that due to their small lateral dimensions, areas with thick crust in these orogens and with thin crust in some deep basins (e.g. grabens of the North Sea) cannot be resolved by the presented interpolated maps, although the variation is preserved in the compiled EUNAseis database.
- The shelves appear to have a rather uniform depth to Moho of ca. 32–36 km in the Arctic shelf and ca. 20–24 km along the margins of Greenland, western Norway and the British Isles.
- The shelf to ocean transition is narrow and commonly occurs within a 50 km wide zone.
- The Greenland–Iceland and the Iceland–Faeroe Ridges have anomalous crustal thickness. Early interpretations favored an oceanic affinity. The belt of anomalous crust may continue at about the same latitude to the west of Greenland across the Baffin Bay (termed here as the "Baffin Ridge").
- Anomalously thin crust in some parts of the Mediterranean, western Black Sea and southern Caspian Sea, where seismic data exist, may be indicative of oceanic origin.

6.2.3. Key patterns of the thickness of the crystalline crust

Additional conclusions can be derived from the map of the thickness of crystalline crust (Fig. 10b):

- The thickness of crystalline crust shows greater variations than depth to Moho. In particular, variations in thickness of crystalline crust in the East European Craton span from ca. 60 km in the Baltic Shield to less than 15 km in the deepest parts of the Peri-Caspian depression.
- Several tectonic structures of the European plate have a very thin crystalline crust. They include deep basins in the North Sea rift system (10 km thick or less), western Black Sea (less than 15 km), southern Caspian Sea, and probably the eastern basin of the Black Sea where ca. 7 km thick basement has been reported recently (Minshull et al., 2005); although the latter result remains controversial and it may

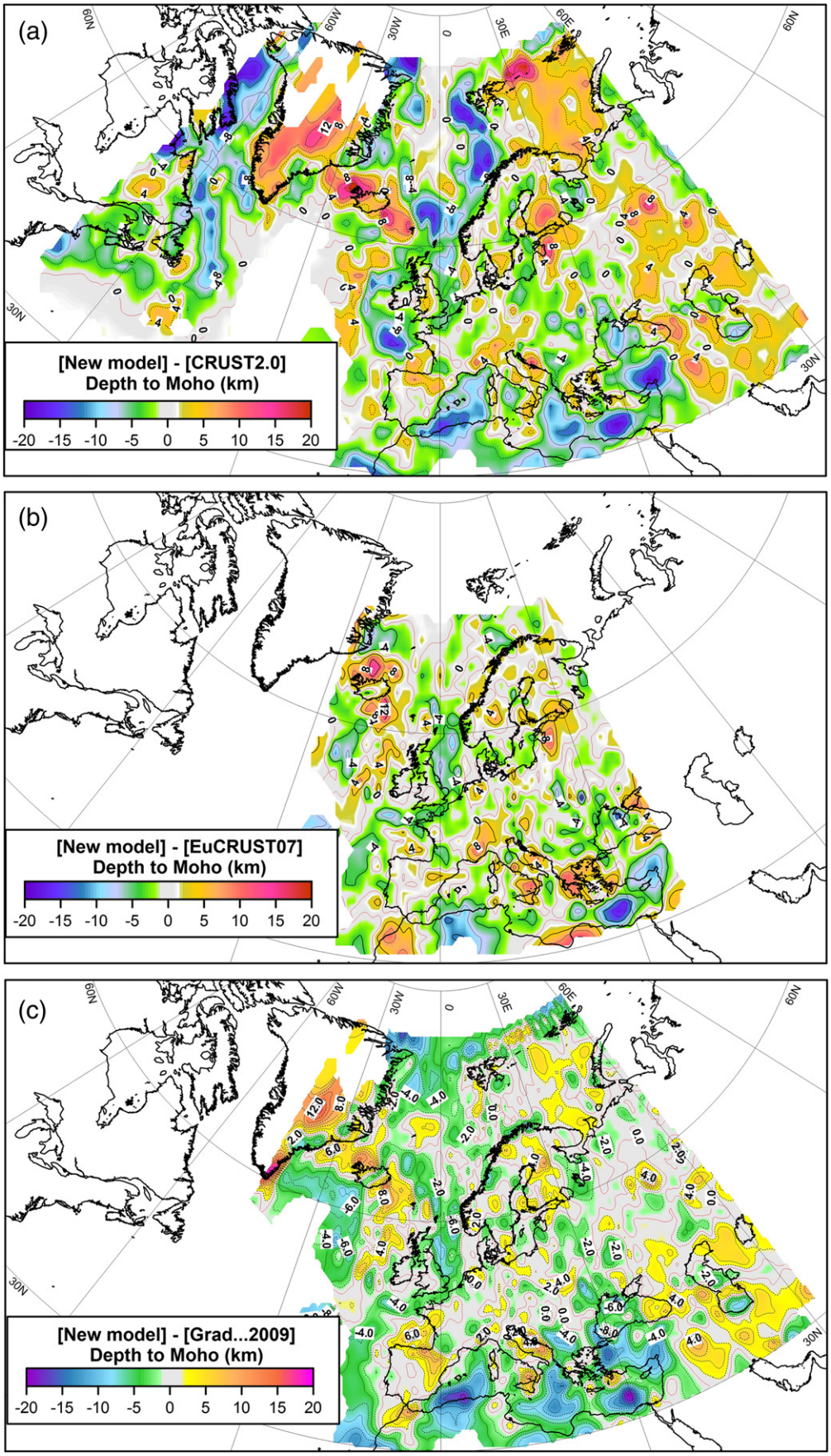

Fig. 12. Differences in depth to Moho between the new regional model EUNAseis and three other crustal models: a global model CRUST 2.0 (Bassin et al., 2000) and two regional models (Grad et al., 2009; Tesauro et al., 2008). In each case, the new model is sampled on the same grid as the one with which it is compared. For comparison with CRUST1.0 model (Laske et al., 2013) see Electronic Supplement 2.

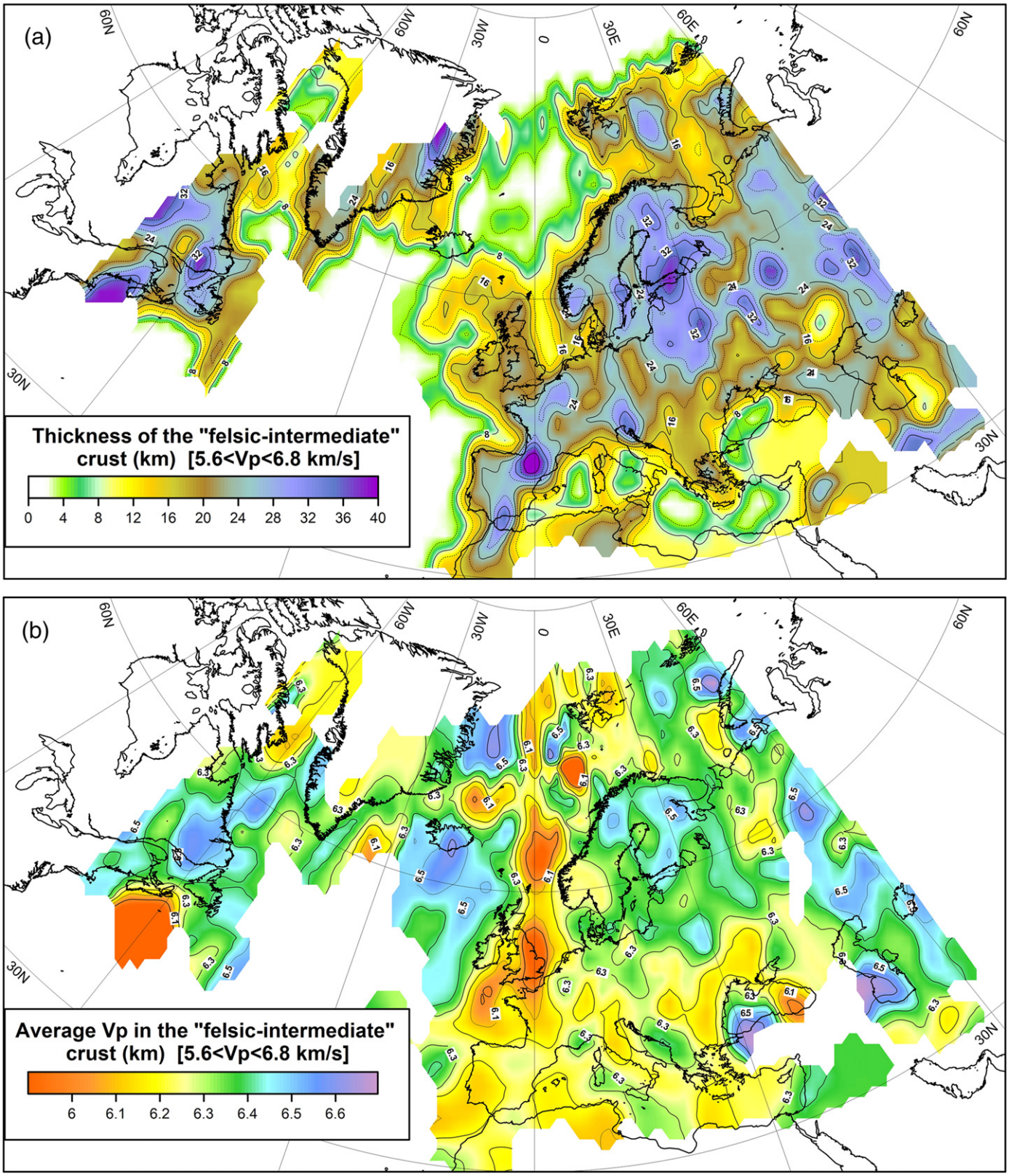

Fig. 13. Thickness of the upper part of the crust (5.6 < Vp < 6.8 km/s) (a) and its average in situ Vp seismic velocity measured in seismic surveys (b). Both maps are constrained with a 3° × 3° interpolation method chosen to preserve the magnitudes (see Fig. 5 for data coverage).

be uncertain if the basement is of oceanic origin.

- Lack of regional correlation between variations in thicknesses of the sedimentary cover and crystalline crust and a greater variability of the latter indicates that some of the deep processes related to crustal formation and modification are not fully reflected in the structure of the sedimentary cover, and that isostatic compensation may not be achieved at Moho in some of the tectonic regions.
- Below the sedimentary cover, the crustal structure of the shelves is

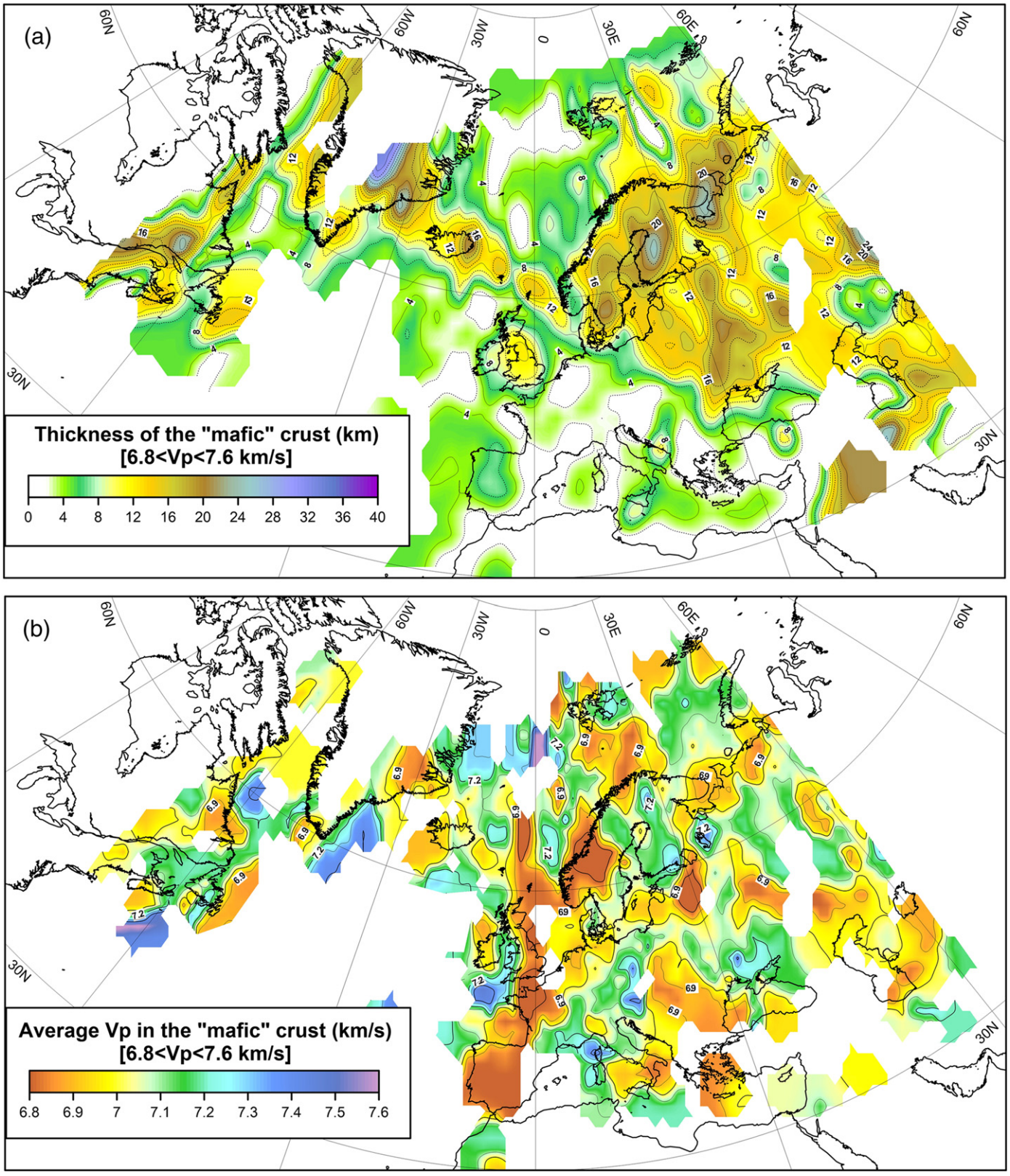

Fig. 14. Thickness of the lower part of the crust (6.8 < Vp < 7.6 km/s) (top) and its average in situ Vp seismic velocity measured in seismic surveys (bottom). Both maps are constrained with a 3° × 3° interpolation method chosen to preserve the magnitudes (see Fig. 5 for data coverage). The color scale for the layer thickness is the same as in Fig. 13.

very heterogeneous. Large variations in thickness of the crystalline crust (from less than 15 km to more than 30 km in the Barents Sea) suggest that the Arctic basins may not be isostatically compensated, probably due to a strong lithosphere.

We have carried out a statistical analysis of the data on crustal properties in our database for the continental crust of the European continent (on-shore regions and shelves) (Table 3 and Fig. 11). Other regions were excluded because of insufficient data coverage for a meaningful

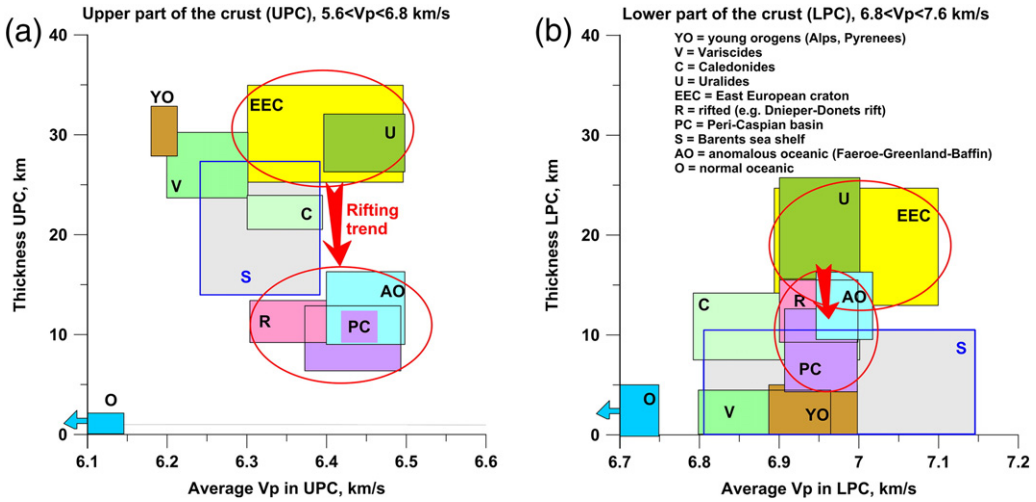

Fig. 15. Seismic properties of the crust showing thicknesses of the upper (a) and lower (b) parts of the crust plotted versus average in situ Vp seismic velocities in these layers. Red arrows show the "rifting trend".

analysis. By the crustal age, the data were analyzed for six age intervals: Archean, Palaeoproterozoic, Mesoproterozoic, Neoproterozoic, Mesozoic–Palaeozoic, and Cenozoic. Crustal tectono-thermal age data on 1° × 1° bins are adopted from the TC1 model (Artemieva, 2006). Cenozoic regions were further subdivided by topography into two groups: lower than 500 m (platforms and basins) and above 500 m (orogens and highlands). We also included the shelves, without specifying their crustal age. The analysis shows systematic, although statistically weak, variations in crustal structure with age. On average, Archean–Palaeoproterozoic crust has similar thickness of ca. 42–44 km, whereas crust younger than 1.7 Ga is only 35–38 km thick and shows no correlation with age (Fig. 11a). The correlation between the thickness of the crystalline crust (which does not include sedimentary sequences) and the crustal age is more pronounced, if young orogens are excluded from the analysis. Statistically, the thickness of the crystalline crust changes from ca. 41 km in the Archean and Paleoproterozoic terranes to ca. 33–35 km in the Meso- and Neoproterozoic terranes, and to ca. 30 km in Meso-Cenozoic crust, given that sedimentary cover is often found above thinned crust and most of the thick sedimentary covers is found in Phanerozoic regions. Thick crustal roots in young orogens have thickened crust as expected, although given their relatively small lateral extent the statistical analysis based on a 1° × 1° grid also includes the adjacent regions (in some cases, foredeep basins with large sedimentary sequences).

6.2.4. Comparison with other crustal models

We present a comparison of our new regional crustal model EUNAseis with other, digitally available, crustal models for the region. These include CRUST 2.0 (Bassin et al., 2000), EuCRUST-07 (Tesauro et al., 2008), and Moho depth in the European plate (Grad et al., 2009) (Fig. 12). To make the comparison adequate, our database is resampled to the same grids as the other crustal models with an interpolation method chosen to preserve the amplitudes. Omitting discussion of particular details, the major observations from the comparison are the following.

We expect that the depth to Moho is one of the best resolved parameters in seismic surveys. However, the amplitude of differences between our model and other crustal models used for the comparison is astonishing large, up to +/−20 km for Moho depth (Fig. 12a, b). The major differences observed in all maps are for the well-constrained belt of anomalous crust between the Faeroe Islands and Greenland (ca. 8–10 km difference) and for the Mediterranean region (15–20 km difference in deep water basins with oceanic crust). However, given the scarcity of seismic data in the latter region and the assumptions behind our model for these basins (see Section 4.2.1), the large difference between the crustal models for parts of the Mediterranean may be insignificant. It is clear that new marine seismic data acquisition is needed there.

Our comparison shows that the CRUST2.0 model (Bassin et al., 2000) has the largest deviation from regional seismic models on Moho depth for significant parts of the region (Fig. 12a). CRUST2.0 has significantly different values for Moho depth for the Alps, the Pyrenees, the region with the thick crust in Central Finland, the North Sea, and the Carpathian–Pannonian region. It underestimates the depth to Moho in most of the East European craton and the Barents Sea shelf by ca. 5 km. In contrast, the crustal thickness along the rifted margins of the North Atlantic ocean is significantly (by 10–15 km) overestimated. Fig. 5 shows that a large amount of new high-resolution seismic data became available for the region of study since that model was constrained, particularly along the North Atlantic margins, while for regions without seismic coverage the CRUST 2.0 model has been constrained by tectonic similarity.

On the whole, comparison between our model and CRUST 2.0 in areas with dense coverage by high-quality data (Fig. 12a) shows that global models constrained by statistical tectonic similarity are reasonable as a low-resolution tectonic generalization, but are erroneous at high-resolution and the approach obviously fails in those large areas where the crust has anomalous structure, like the Greenland–Iceland–Faeroe and Baffin Ridges, deep basins, margins, and cratons with thick crustal roots. The significant discrepancy between the CRUST2.0 model and the seismic structure of the crust reduces the value of regional crustal models which put high weight to the CRUST2.0 values (e.g. Molinari and Morelli, 2011).

There is a significant difference between our model and the regional EuCRUST-07 model (Tesauro et al., 2008). Except for the western Mediterranean (discussed above), the major differences are for the western Alps, the Pyrenees, the Aegean, southern Italy, Morocco, the region with the thick crust in the Baltic States, the North Sea, and the Greenland–Iceland–Faeroe Ridge (Fig. 12b). The discrepancy for the Alps arises from the fact that while EuCRUST-07 considers the depth to the shallow Adriatic plate as depth to Moho, our database adopts the deeper Moho which corresponds to the subducting European plate. For other regions the origin of the differences is less clear, and we attribute them to the fact that for the on-shore part the EuCRUST-07 model is constrained not only by seismic but also by potential field data. For some tectonic provinces, the differences arise due to incomplete information on the crustal structure included in the EuCRUST-07 model. Particularly, for the Aegean, Italy and Morocco, the RF constraints on Moho

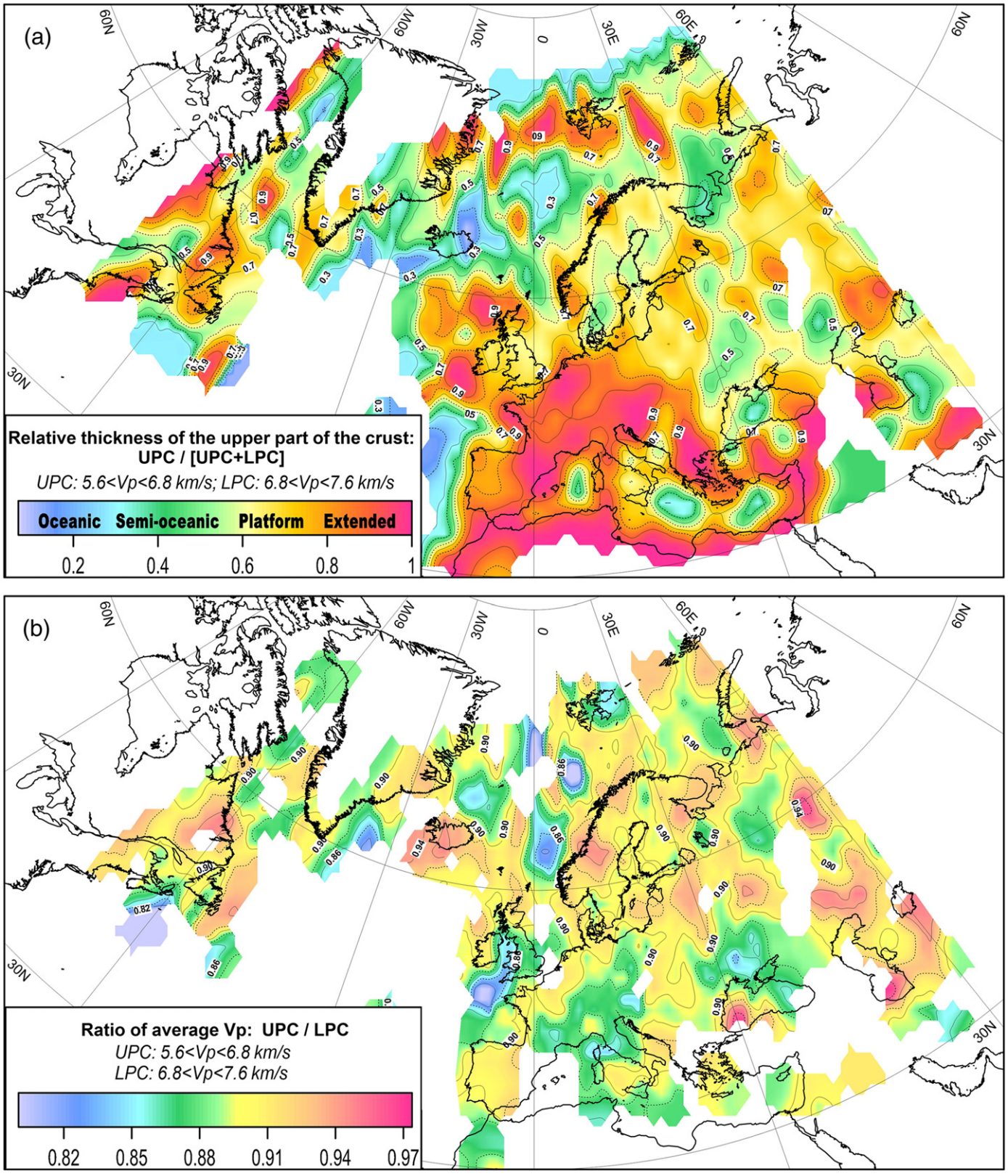

Fig. 16. Relative thicknesses of the upper and lower parts of the crust (a) and ratio of average in situ Vp seismic velocities in the upper and lower parts of the crust (b).

depth became available only recently (Agostinetti and Amato, 2009; de Lis Mancilla et al., 2012; Miller and Agostinetti, 2012; Sodoudi et al., 2013). Similarly, at the time EuCRUST-07 was constructed, seismic data did not exist for significant parts of off-shore regions (compare with Fig. 5). Since most of the North-Atlantic Ocean has anomalous crust, neither assumptions on typical 7–8 km thick oceanic crust, nor constraints by tectonic similarity (EuCRUST-07 model incorporates data from CRUST2.0 for oceans with no seismic data, but clearly for these regions CRUST2.0 also is constrained not by seismic data), nor simple extension of the crustal structure by interpolation (e.g.

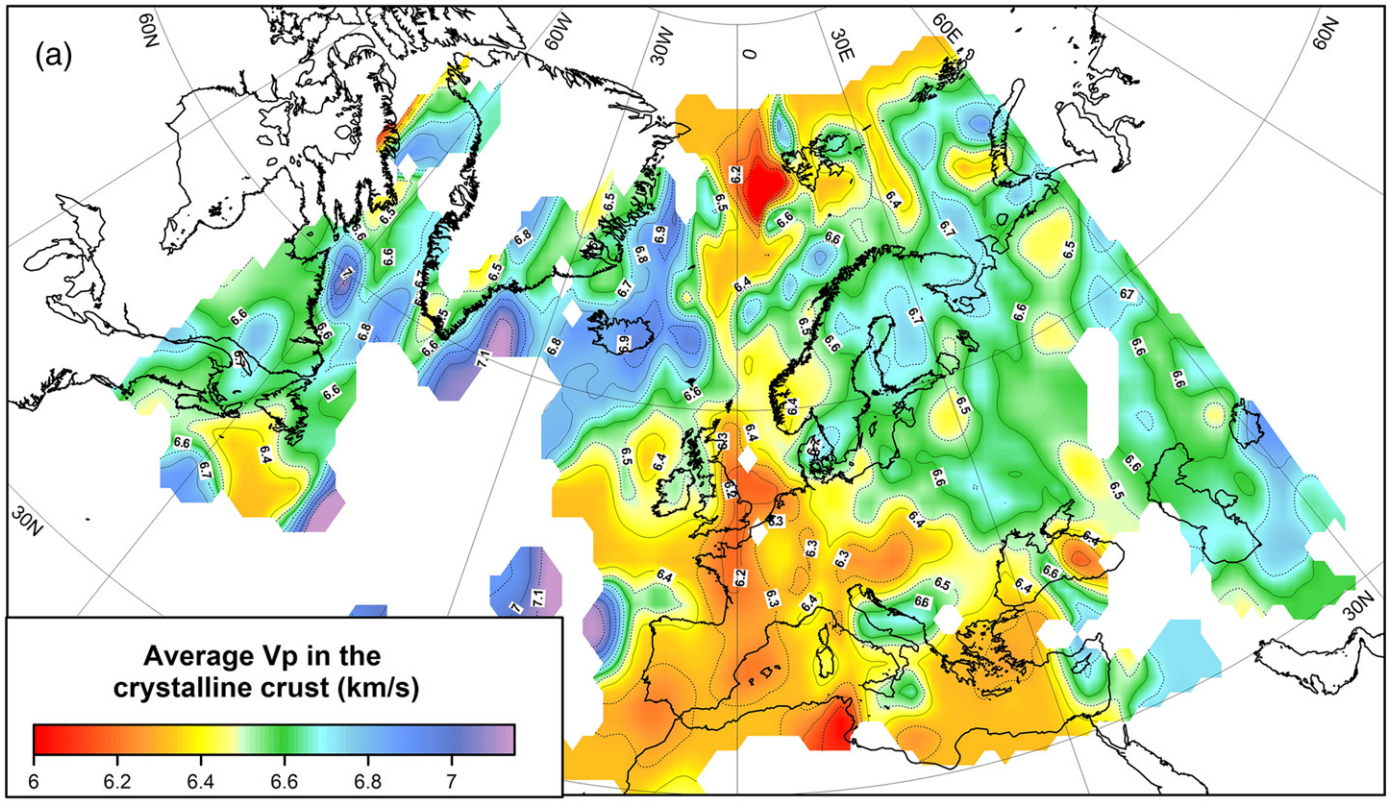

Both maps: Average Vp calculated as Vp in each layer weighted by layer thickness [AA] ("gravity" approach)

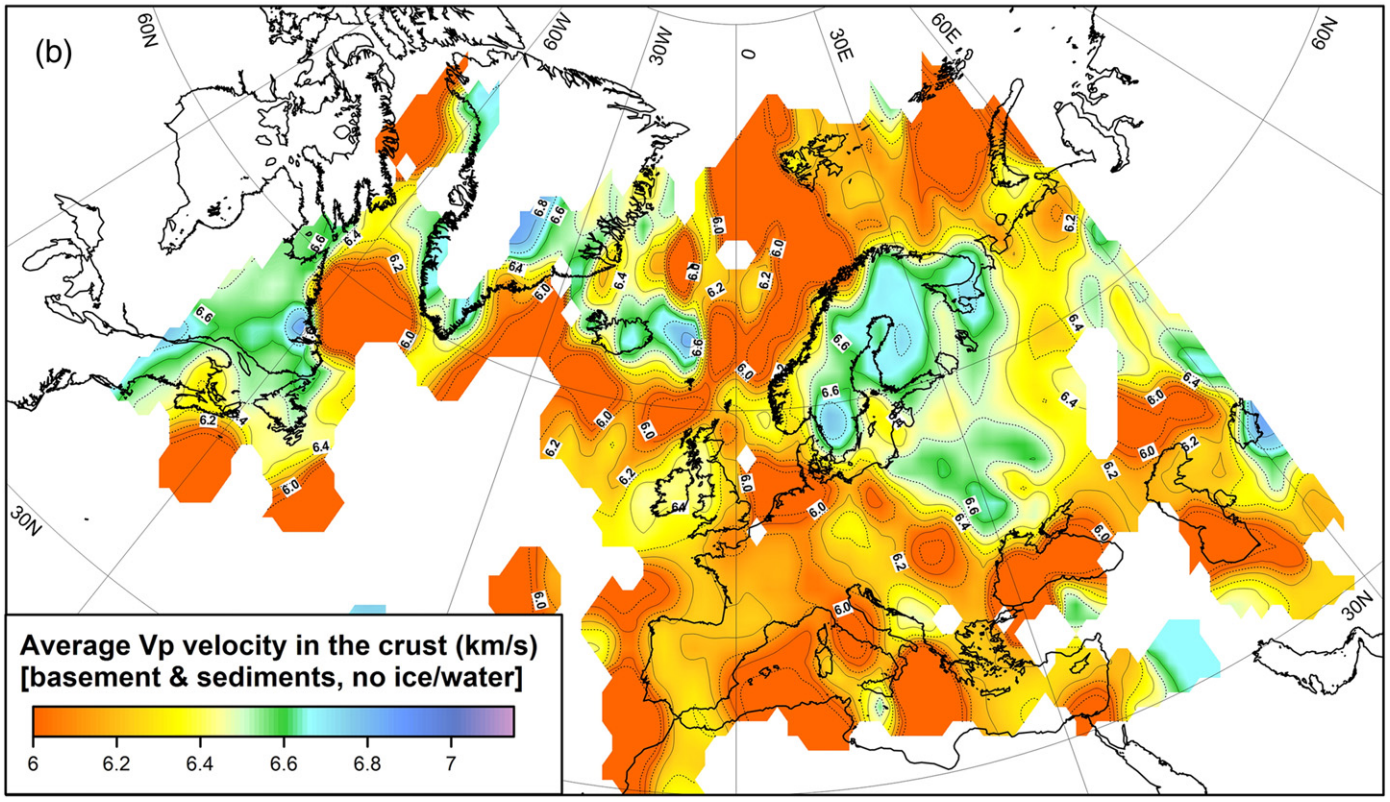

Fig. 17. Average in situ Vp seismic velocity in the crystalline crust (a, c) and in the entire crust (b, d) together with the maps showing the difference between the two applied averaging methods (e, f) (see Fig. 5 for data coverage). Average Vp may be calculated as the average weighted by layer thickness (a, b). This approach directly reflects physical properties of the crust and Vp may be converted to density as is routinely done in gravity studies. Another way to average Vp is by weighing with the travel time required for a seismic wave to pass through each layer (c, d). This calculated average Vp can be used in tomography to introduce crustal correction. The difference between the two approaches is important in areas with thick sedimentary cover. All maps are constrained with a 3° × 3° interpolation method chosen to preserve the magnitudes. White areas in (a–d) — regions without seismic data. Compare with Fig. 10.

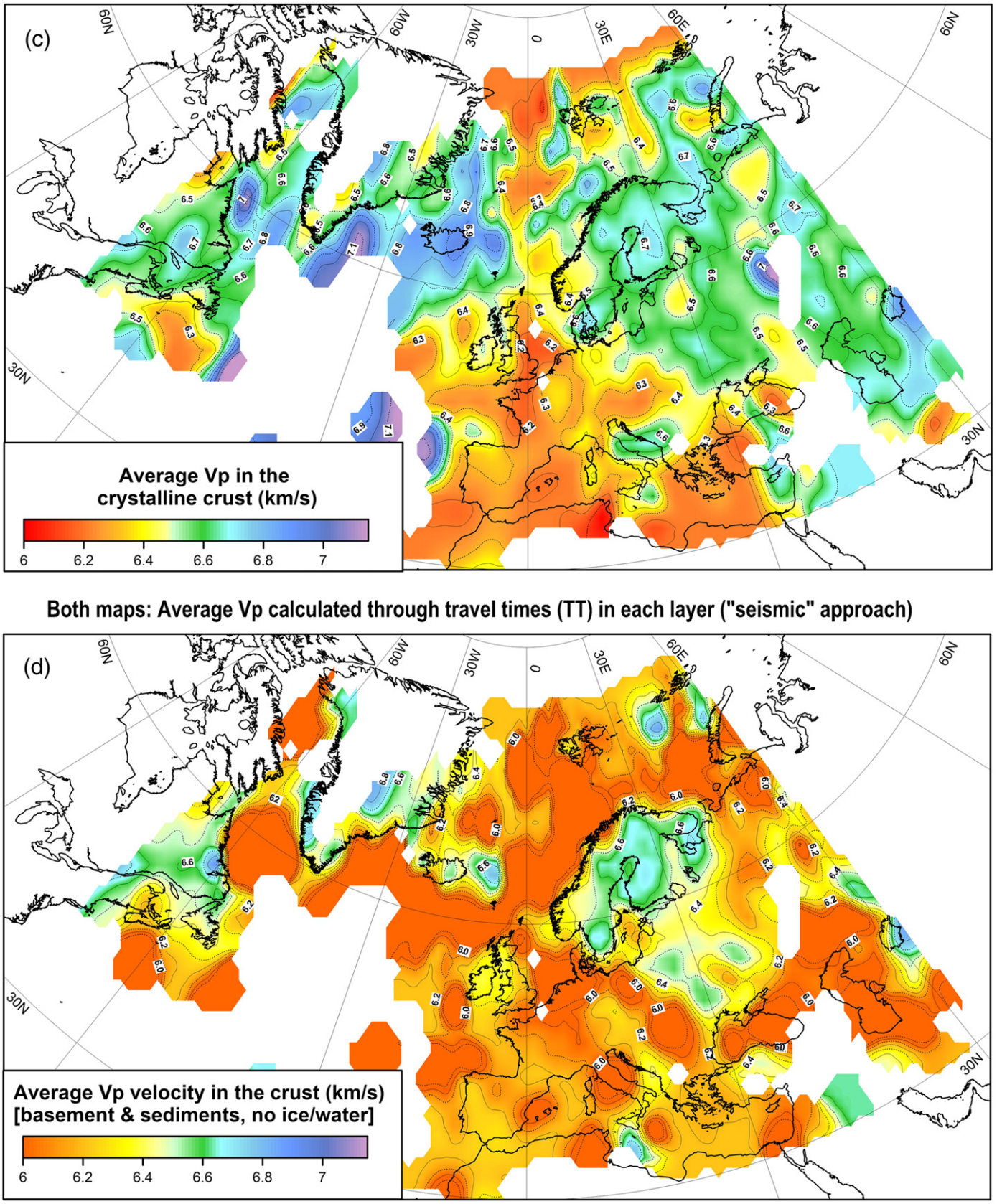

Fig. 17 (*continued*).

to fill-in gaps between different compilations that are included into the EuCRUST-07 model) can provide correct constraints on the anomalous oceanic crustal structure.

For the continental part of Europe, there is a close correspondence between our model and the regional model for the depth to Moho by Grad et al. (2009) (Fig. 12c). The major differences are for Greenland

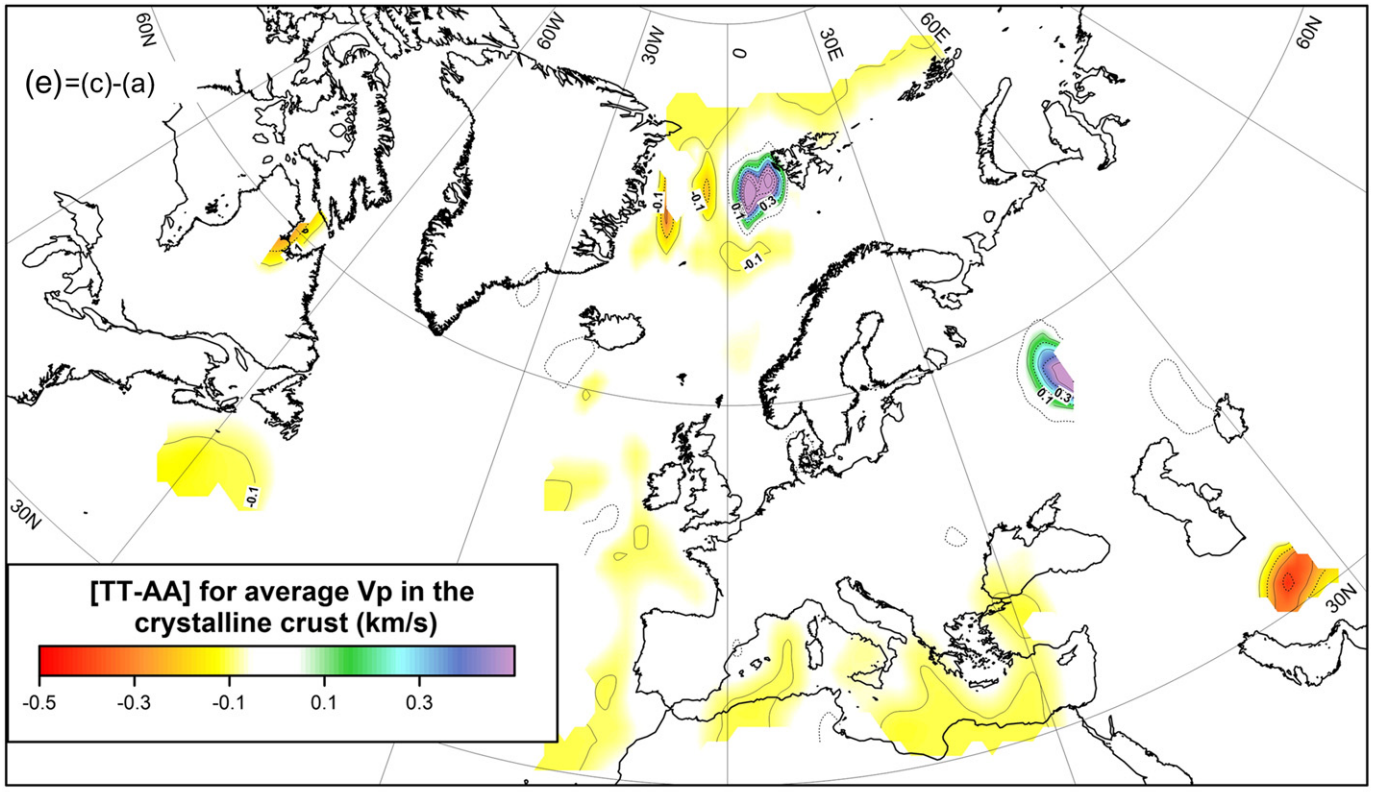

Both maps: Difference between average Vp calculated by travel times [TT] and as layer weighted average [AA]

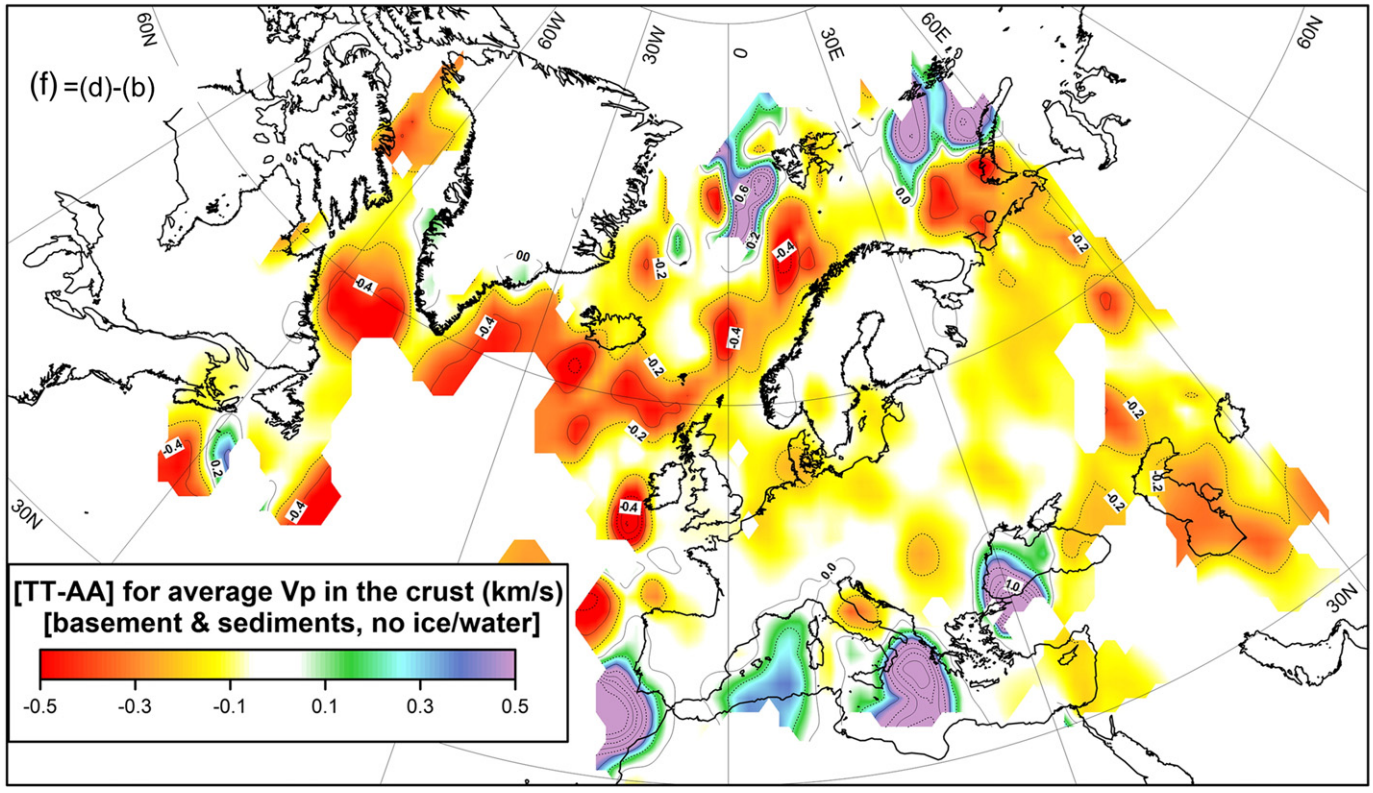

Fig. 17 (*continued*).

where new seismic models are becoming available only now (Shulgin et al., 2012), for the deep water basins of the Mediterranean (note that for the Tyrrhenian Sea our model is based on seismic refraction data, Table 2), for the North Sea which is well covered by seismic profiles (Fig. 5), for the Greenland–Iceland–Faeroe Ridge (covered by several refraction profiles), for the Southern Caspian, and for the western basin of the Black Sea. For the latter two regions only old Soviet profiles exist (plus few RFs for the Southern Caspian (Mangino and

Priestley, 1998)), and new seismic data are needed for high-resolution crustal models.

6.3. Internal structure of the crystalline crust

6.3.1. Preamble

We illustrate the internal structural and compositional heterogeneity of the crystalline crust by showing thicknesses and Vp seismic velocities in two crustal layers (Figs. 13–14). The upper crustal layer is specified by $5.6 < Vp < 6.8$ km/s, whereas the lower crustal layer has Vp velocity above 6.8 km/s. Our presentation does not follow a traditional approach in which 3–4 layers are recognized within typical continental (cratonic) crust, although this approach has been implemented in the EUNAseis database compilation (see Section 4.1.1). In the definition adopted here, the upper part of the crust (UPC) includes both "upper" (felsic, with typical $5.6 < Vp < 6.4$ km/s) and "middle" (with an intermediate composition and typical $6.4 < Vp < 6.8$ km/s) crustal layers, whereas the lower part of the crust (LPC) includes "lower" (mafic) crust with typical $6.8 < Vp < 7.2$ km/s and a high-velocity lower crustal layer with $Vp > 7.2$ km/s.

The reason for such a simplified presentation of the internal crustal structure is the occurrence of significant ambiguity in the recognition of the crustal layers, in particular for seismic profiles with no refraction data. Old interpretations (particularly abundant for the southern parts of the former USSR, Fig. 5) have a large uncertainty in determining both seismic velocities within crustal layers and their thicknesses. In some cases, a significant discrepancy exists between crustal models based on the same data but interpreted by different groups, and in many other cases interpretations of the upper and middle crustal layers remain controversial, often making it essentially arbitrary as to where to put the boundary between them. To add to the complication, reduced velocity layers are often reported for mid-crustal depths, thus allowing to include both the reduced velocity layer and the layer above it into the upper crust, or alternatively to include them both into the middle crust. The situation with the lower and high-velocity lowermost crust is similar, in addition to the fact that many studies do not separate these two layers but show a gradual increase in seismic velocities with depth. However, even with our simplified two-layer crustal model specification, it is often unclear where the boundary between the upper and the lower portions of the crust should be placed.

Our conservative estimate is that the uncertainty in the thickness of each of the two layers can locally be as large as ca. ± 5 km. Yet it is highly variable, and depends on data coverage and quality of the original data and seismic model. The uncertainty in average Vp in each of the two layers is ca. ± 0.1 km/s but can be locally even higher. Similar to all other maps presented here, the maps in Figs. 13–14 are constrained with a $3° \times 3°$ interpolation method chosen to preserve the magnitudes. The additional uncertainty due to interpolation is insignificant as compared to the uncertainty (and ambiguity) in the subdivision of the crust into the top and bottom portions. Note that for the south-eastern parts of Europe, Asia Minor, the Mediterranean, and significant portions of the North Atlantic ocean, the data coverage is too coarse for the analysis to be meaningful, and these regions should be considered with caution.

6.3.2. Upper part of the crust (UPC)

6.3.2.1. Variations in thickness of UPC. In the subdivision adopted here, the upper part of the crust ($5.6 < Vp < 6.8$ km/s) includes the upper, felsic, crust and the middle crust with intermediate composition (Fig. 13). The major regional patterns include:

- In on-shore regions, the UPC is thicker than 20 km almost everywhere with notable exceptions in southern Europe (however, note that the 15–20 km thick UPC in the Dinarides and Balkans is not well constrained by seismic data and may result from interpolation, compare with Fig. 5 for data coverage).
- In much of the craton UPC is ca. 30 km thick. Regions with thick UPC are directly correlated with thick cratonic roots such as observed in the Archean–Paleoproterozoic Karelia and Volga–Uralia. Given that a very similar correlation is observed both in Paleozoic and young orogens (Urals, Alps, Pyrenees), one can speculate that thick UPC in Archean–Paleoproterozoic blocks may result from Precambrian orogenic events.
- Compared to "undisturbed" cratonic crust, cratonic regions with extended crust have thinned UPC (Fig. 15a). This pattern is observed in the Riphean Central Russia rift of the East European platform and is particularly pronounced in the Peri-Caspian and the Timan–Pechora basins. In the Peri-Caspian basin the UPC is thinned to ca. 8–10 km (and the upper, granitic, layer is almost absent), which makes grounds for speculations on a semi-oceanic origin (e.g. Zonenshain and Le Pichon, 1986). In the Central Russia rift system, crustal extension apparently led to thinning of the UPC at the cost of thinning of the rheologically weak middle crustal layer (Artemieva, 2007).
- In agreement with the previous conclusion, thicknesses of UPC and sediments are strongly anticorrelated in the Barents Sea shelf, the North Sea and some other deep basins such as the North and South Caspian Sea basins and the Western Black Sea basin.
- Deep water oceanic regions and the Mediterranean Sea have thin UPC, usually less than 10 km. A similar pattern is observed in the deep parts of the North Atlantic Ocean.
- Surprisingly, the Greenland–Iceland–Faeroe Ridge and the Baffin Ridge have a thickened UPC as compared to adjacent oceanic regions. The difference amounts to 8–10 km and thus is well resolved by the available seismic data. The presence of a thick low-velocity upper crustal portion speaks against an oceanic origin of the crust in these ridges.
- In contrast, the thickness of UPC in other shallow parts of the North Atlantic ocean (the Kolbeinsey Ridge and the Jan Mayen block) is similar to normal oceanic crust. No seismic data is available south of Iceland for the region with anomalous bathymetry along the Reykjanes Ridge.

6.3.2.2. Variations in average Vp of UPC. Before discussing the patterns in regional variations of average Vp seismic velocity in the upper part of the crust, one comment is worth mentioning. Average Vp presented in Fig. 13b is based on seismic surveys and thus refers to in situ conditions. There is, however, a significant difference in temperature regime of the crust in the region and therefore regional variations in average Vp reflect both compositional and thermal heterogeneity. The effect of thermal heterogeneity can be significant and, in general, should be removed to address properly compositional and structural heterogeneity of the crystalline crust (Artemieva and Meissner, 2012). In the present discussion, we do not separate compositional and thermal effects, since it is outside the scope of this paper.

1) The most striking feature in Fig. 13b is a low Vp anomaly (ca. 6.2 km/s) which extends roughly south–north along the zero meridian. It is well constrained by seismic data from the Armorican massif through England and the North Sea into the North Atlantic ocean up to the Voring basin. The origin of the anomaly is unclear, although it may be related to the Central European rift system.
2) There is a strong correlation between the thickness of UPC and its average Vp, which has different patterns for different tectonic structures (see also Figs. 14, 15a).
    a) In regions with thick UPC:
        - low Vp (6.0–6.3 km/s) in UPC is observed in the West European Variscides and young orogens,
        - intermediate Vp (ca. 6.4 km/s) is observed in the Caledonides (note that the transition from the Polish–German Caledonides to Variscides is marked by a change in Vp),
        - high Vp (6.3–6.5 km/s, locally >6.6 km/s) in UPC is observed in the cratons, where a significant part of the high velocities

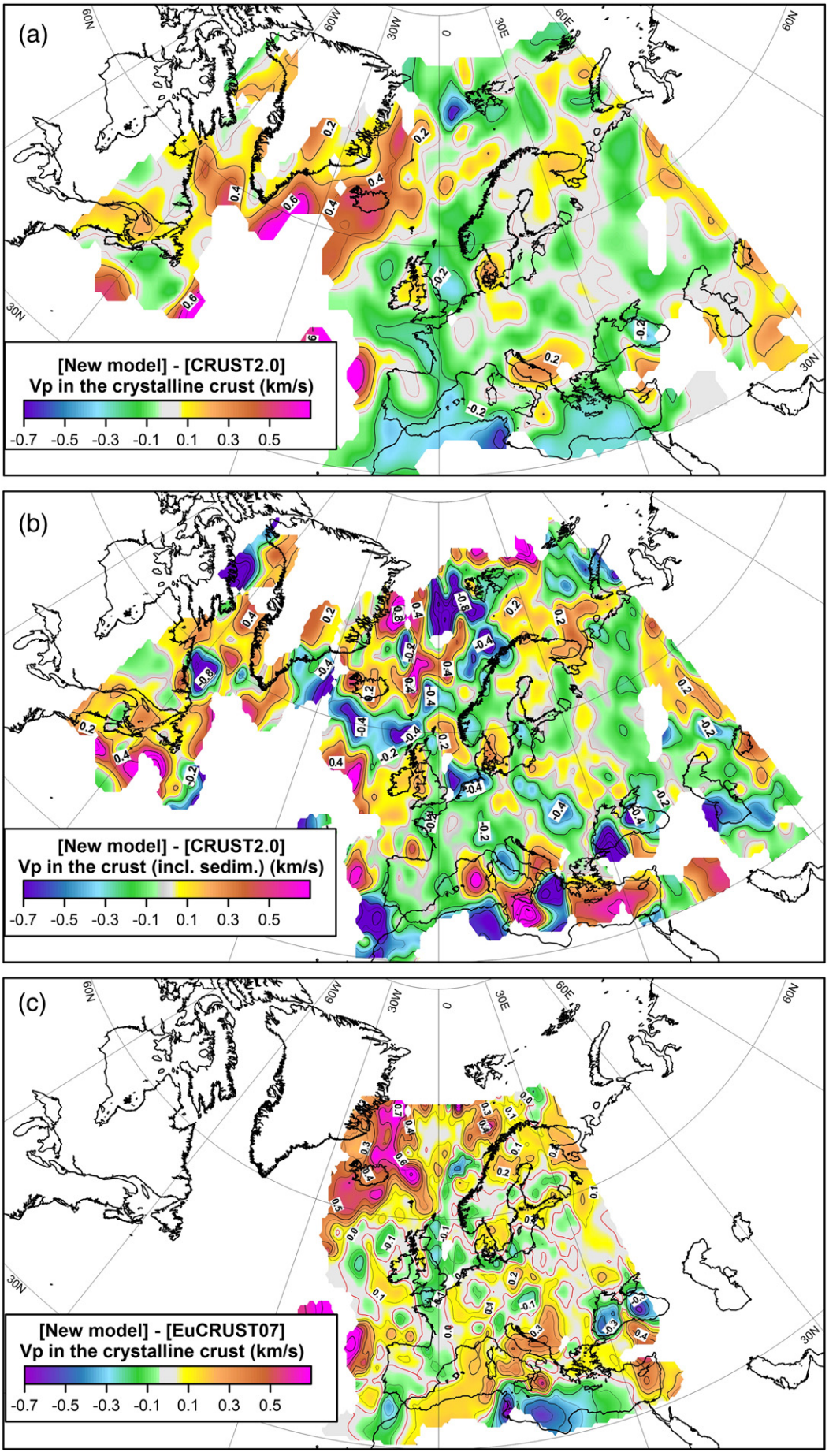
(a)
[New model] - [CRUST2.0]
Vp in the crystalline crust (km/s)
-0.7 -0.5 -0.3 -0.1 0.1 0.3 0.5
(b)
[New model] - [CRUST2.0]
Vp in the crust (incl. sedim.) (km/s)
-0.7 -0.5 -0.3 -0.1 0.1 0.3 0.5
(c)
[New model] - [EuCRUST07]
Vp in the crystalline crust (km/s)
-0.7 -0.5 -0.3 -0.1 0.1 0.3 0.5
60N
60W
30W
0
30E
60E
30N

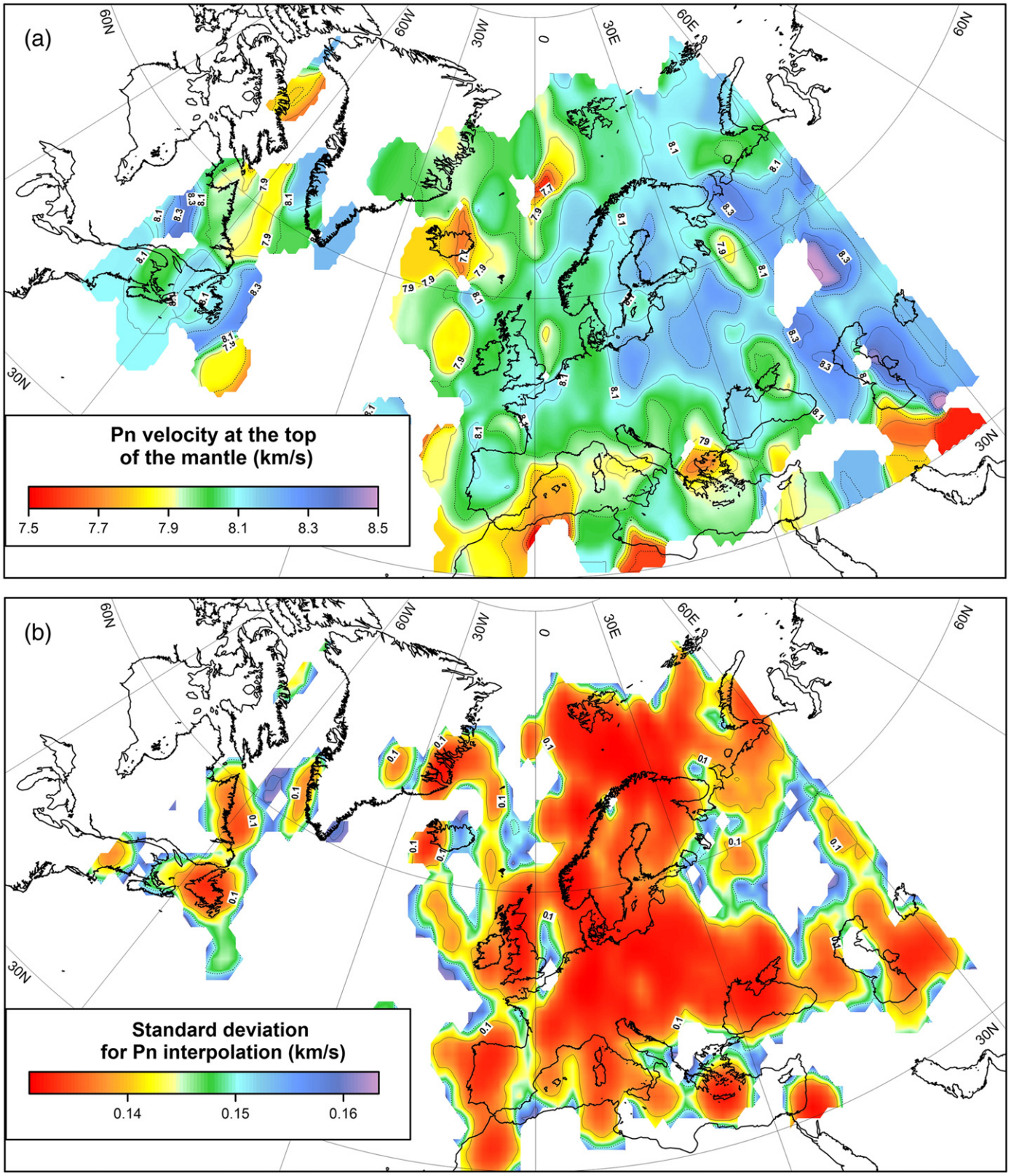

Fig. 19. Pn seismic velocity at the top of the mantle (a), standard deviation of interpolation (b, see comments to Fig. 6), and (c) difference between the new regional model and Pn velocity in the global model CRUST 2.0 (Bassin et al., 2000).

Fig. 18. Differences between the new regional model and two other models (Bassin et al., 2000; Tesauro et al., 2008) in average Vp velocity in the crystalline crust (a, c) and in average Vp velocity in the whole crust (basement and sediments) (b).

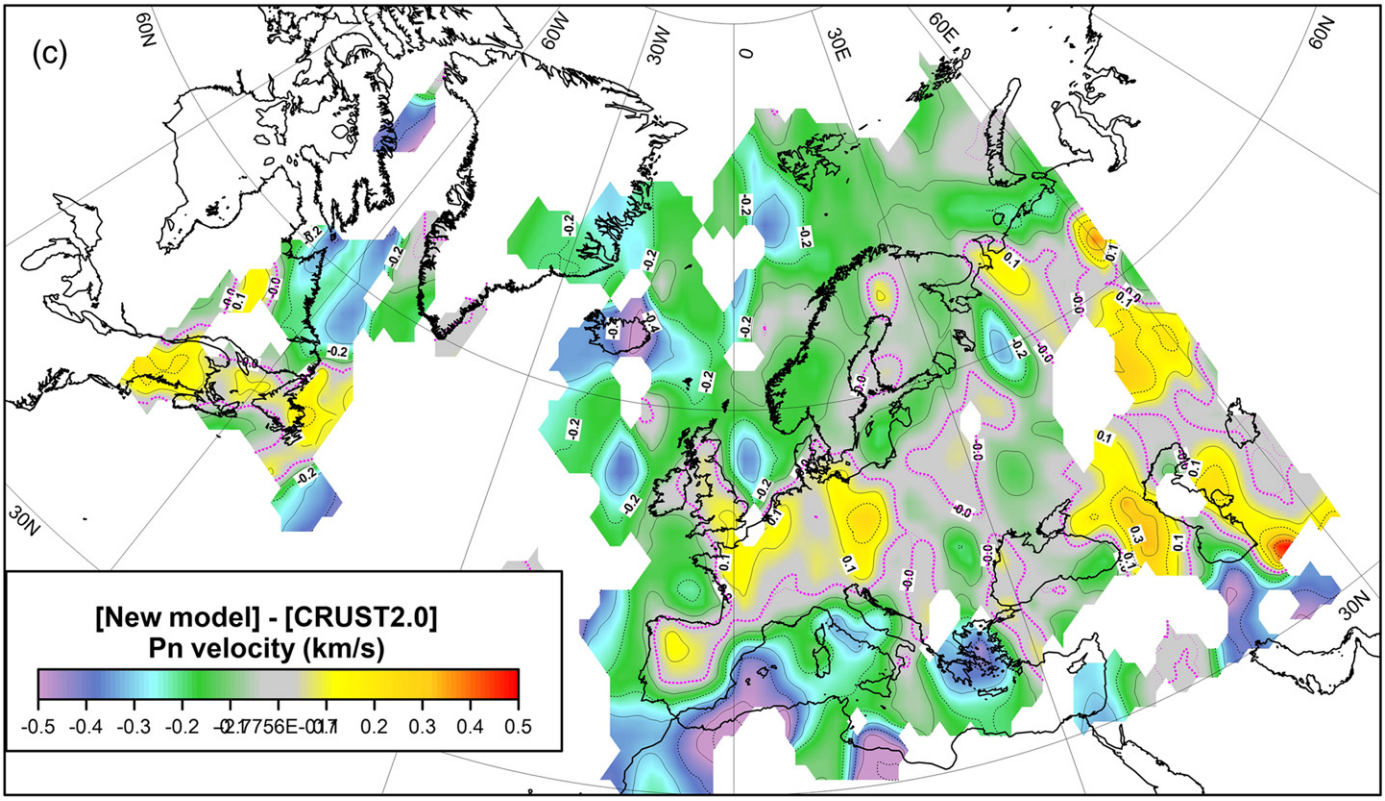

Fig. 19 (*continued*).

results from low crustal temperatures; similar observation holds for the Urals;
- the southern parts of the East European Craton have thinner UPC and lower average Vp (6.2–6.3 km/s) than the other cratonic area; similar pattern exists for the rifted north-eastern part of the craton;
- thickened UPC in the Greenland–Iceland–Faeroe Ridge and the Baffin Ridge has high (6.4–6.5 km/s) average Vp velocities in UPC.

b) In regions with thin (10–15 km) and very thin (<5 km) UPC:

- rifted parts of the craton have average Vp similar to the craton (6.3–6.4 km/s);
- low Vp (<6.3 km/s) in UPC is observed in southern Europe;
- Western Black Sea has high Vp; similar pattern is observed in the South Caspian basin. However, average Vp in UPC of the Eastern Black Sea is low (6.2–6.3 km/s) and suggests different nature of the crust in the two Black Sea basins.

Based on the correlation between the thickness of UPC and its average Vp in different tectonic settings (Fig. 15a), we speculate that rifting of the cratonic crust results in a significant (10–5 km) reduction in the thickness of the upper part of the crust (UPC) without notable change in its average Vp. Such type of crustal modification can be achieved through ductile flow of rheologically weak crustal layers heated during rifting, without any significant additions of magmatic material into UPC.

6.3.3. Lower part of the crust (LPC)

6.3.3.1. Variations in thickness of LPC. In the subdivision adopted here, the lower part of the crust (6.8 < Vp < 7.6 km/s) includes the lower, mafic crust and the bottom part of the crust (where present) with very high Vp velocities (Fig. 14). One may, however, speculate if the existing data guarantees that a possible high-velocity layer at the base of the crust has been detected in all, and particularly, in old regional seismic models. It is well known that detection of high velocity layers at the base of the crust requires high-density, high-quality data, otherwise the lower crustal rocks may form a classic "hidden layer". With this note in mind, the following trends may be recognized in the seismic data for the region.

- Thickness of LPC never exceeds 20–25 km (except for two localized areas in the Baltic Shield and the Urals where LPC is ca. 25 km thick, Figs. 14a, 15b).
- The thickest LPC (15–25 km) is documented for the cratonic regions, with the largest thickness typical for the shield areas (Karelia province of the Baltic Shield, the Voronezh massif, and inner Greenland). Some parts of the Uralides (e.g. the Middle Urals) also have a thick LPC.
- Tectonically young provinces are all missing LPC, except for the Greenland–Iceland–Faeroe Ridge and the Baffin Ridge, where LPC may reach ca. 10 km.
- Paleozoic orogens of Europe have different thickness of LPC: whereas it is basically absent in the Variscides, its thickness is ca. 8–15 km in the Caledonides and ca. 10–25 km in the Uralides.
- LPC is significantly thinned in the Peri-Caspian basin, although the thin-LPC anomaly appears to be shifted to the eastern part of the basin, to the location of the Central rift (compare with Fig. 3). Thin LPC is in line with a mechanism for the Peri-Caspian basin subsidence due to destruction of the lower crust by asthenospheric upwelling (Artyushkov and Baer, 1986). However, thin LPC seems to contradict a hypothesis of basin subsidence due to phase change of gabbro to eclogites (the latter have a chemistry of the continental crust but are denser than the mantle) in a thick lower crustal layer (Artyushkov, 1992). However, Vp seismic velocities in eclogites are nearly the same as mantle velocities and thus crustal eclogites may occur beneath the seismically defined Moho (Mjelde et al., 2012).

6.3.3.2. Variations in average Vp of LPC. Similar to UPC, average Vp in LPC is presented at in situ conditions and its variation reflects both compositional and thermal heterogeneity. As Fig. 14b indicates,

- the fastest (7.1–7.2 km/s) LPC is observed in the shield areas, partly due to low crustal temperatures and partly due to the presence of the high-Vp lowermost crust;
- the platform parts of the craton have slower LPC than shields (6.9–7.0 km/s) since the high-Vp lowermost crust is absent there; there is, however, some Vp increase in the platform parts which have undergone extension and rifting;
- young orogens have slow LPC (6.9–7.0 km/s);
- Paleozoic orogens have significantly different velocity structure of LPC, with slow LPC (6.8–7.0 km/s) in the Variscides and Caledonides, but faster LPC in the Uralides. Fast thick LPC in the Urals may be the remnant of Paleozoic ocean–continent collisional events during which high-velocity island arcs were trapped within the orogen;
- despite the difference in the crustal temperatures between Phanerozoic Europe and the craton, the difference in average Vp in LPC of the two provinces may reflect differences in LPC composition: since in Phanerozoic Europe Moho is 15–25 km shallower than in the craton, temperatures at the LPC depths both in Phanerozoic and in Precambrian Europe can be similar, ca. 500 °C (Artemieva et al., 2006);
- in the Greenland–Iceland–Faeroe Ridge and the Baffin Ridge average Vp in the LPC is ca. 6.9–7.0 km/s; a high-velocity anomaly is documented in the Greenland basin, whereas shelves on the European side have generally lower Vp;
- except for few locations, there is no data on the crustal velocity structure in the Mediterranean; the anomalies shown in Fig. 14b are the result of interpolation of data from the adjacent regions and may not be true.

Similar to the analysis for UPC, we examine correlation between the thickness of LPC (lower part of the crust) and its average Vp in different tectonic settings (Fig. 15b). We conclude that rifting of the cratonic crust reduces thickness of LPC by 5–10 km and, as for UPC, without notable change in its average Vp. This result is unexpected, given that intrusion of mantle-derived melts into rifted crust should increase its average Vp. A possible explanation would include delamination of heavy, intruded portions of the lower crust, producing crustal structure similar to the Variscan (Artemieva and Meissner, 2012).

6.3.4. Thickness ratio of UPC to LPC

The relative contribution of UPC and LPC (see Section 6.2.1 for definitions) to the thickness of the crystalline crust (Fig. 16a) is constrained by interpolated data (Figs. 13a and 14a) and thus has the same uncertainties. Since thicknesses of both UPC and LPC show a strong correlation with tectonic setting, their ratio is a good indicator of crustal tectonic evolution. Oceanic crust, where the upper layer 2 is 1.5–2 km thick and the lower layer 3 is ca. 5 km thick, has the smallest UPC/(UPC + LPC) thickness ratio of ca. 0.25. Highly extended continental crust where the lower crust has been delaminated and is nearly missing (the case of the European Variscides and the Basin and Range Province in western USA) is the other end-member with a ratio close to 1 (Fig. 16a). In stable platforms (e.g. most of the East European platform), the felsic-to-intermediate crust makes 60–70% of the basement thickness. Platform regions which have undergone recent tectonic reworking have thinned UPC; in these regions thicknesses of both crustal layers are nearly equal. Where the ratio becomes less than 0.4, the presence of semi-oceanic crust may be expected as in the Western Black Sea basin. We conclude that the ratio of the UPC thickness to the thickness of the crystalline crust is a critical indicator of crustal tectonic evolution.

Tectonic interpretation of the ratio of average Vp velocity in the upper and lower parts of the basement is less straightforward (Fig. 16b). To some extent, it is less affected by lateral temperature heterogeneity in the crust than average Vp velocities in individual crustal layers and thus is more sensitive to compositional variations in the crust. The transition from the cratonic to Phanerozoic crust is marked by a decrease in the Vp-ratio values, probably due to the general absence of a fast lower crustal layer in tectonically young structures. Increased Vp-ratio values, probably associated with mafic intrusions in the lower crust, are typical for the Riphean rifts within the East European Platform, the European Caledonides, and the belt of anomalous crust which extends from the Faeroe Islands to Iceland and East Greenland and continues at the western coast of Greenland across the Labrador Sea. Strong high Vp-ratio anomalies can also be recognized in the Western Black Sea basin and beneath the Caspian Sea–Turanian plate. Note that seismic data available for the latter are old and may be less reliable.

6.3.5. Average crustal velocities

Based on our new compilation of seismic data we estimate average, in-situ seismic Vp velocity for the Europe–North Atlantic region (Fig. 17). Except for the southern part of the region and old interpretations, the crustal velocity structure is well constrained for most of the region. Similar to the maps in Figs. 13b and 14b, we estimate the uncertainty of average Vp in the crystalline crust as ca. ±0.1 km/s, although it can be higher locally. For the entire crust the velocity uncertainty is highly variable and can be significantly higher in regions where the sedimentary cover (in particular, its thickness) is poorly constrained. Further details related to the sedimentary cover can be found in Section 5.

We present two sets of maps:

- average Vp velocity in the crystalline crust (Fig. 17a, c) since these maps reflect crustal compositional and structural heterogeneity;
- Vp velocity averaged for the entire crust, including the sedimentary cover (Fig. 17b, d), since it is this information that is needed for introducing crustal corrections to seismic tomography models, as well as to gravity and geodynamic models.

We perform two different types of Vp averaging. The first approach is based on simple arithmetic averaging of Vp weighted by thickness of individual crustal layers (Fig. 17a, b). Such simple type of analysis is alike the procedure employed in gravity studies (where direct velocity–density conversion is commonly applied) and is often used in crustal analysis (e.g. Tesauro et al., 2008). The other approach is based on seismic wave travel times and calculates average crustal Vp by weighted averaging of travel time in different crustal layers (Fig. 17c, d). It this type of average crustal VP which should be used to calculate crustal corrections to seismic tomography models. The difference between the two averaging approaches may reach ±0.5 km/s when sedimentary layer is included (Fig. 17e, f). Our discussion of the general patterns is based on the simple averaging method (Fig. 17a, b).

As for the maps in Figs. 13b and 14b, average Vp in the crystalline crust (Fig. 17a) reflects both structural (compositional) and thermal heterogeneity of the crust. Average Vp in the crust (Fig. 16b) includes additionally heterogeneity of the sedimentary cover. This map shows a clear correlation with Fig. 7 and we refer to the discussion of sediment thickness in Section 5. Estimates show that mean crustal temperature varies by up to 400 °C within Europe (Artemieva, 2006). Such strong variation leads to a strong lateral variability of average basement velocities. However, recalculation of average values of in-situ (as measured in the field) Vp seismic velocities to room P–T conditions does not qualitatively modify the overall pattern of variations in Vp velocity but instead sharpens the anomaly pattern (Artemieva and Meissner, 2012).

Our brief discussion of the average basement velocities will focus on large-scale anomalies, while huge deviations exist at small scale in all tectonic provinces. Key observations are the following:

- In on-shore regions, the pattern of average basement Vp velocities closely follows the patterns of (i) average Vp in the UPC (Fig. 13b) and (ii) thickness of the LPC (Fig. 14a). The contribution of the former

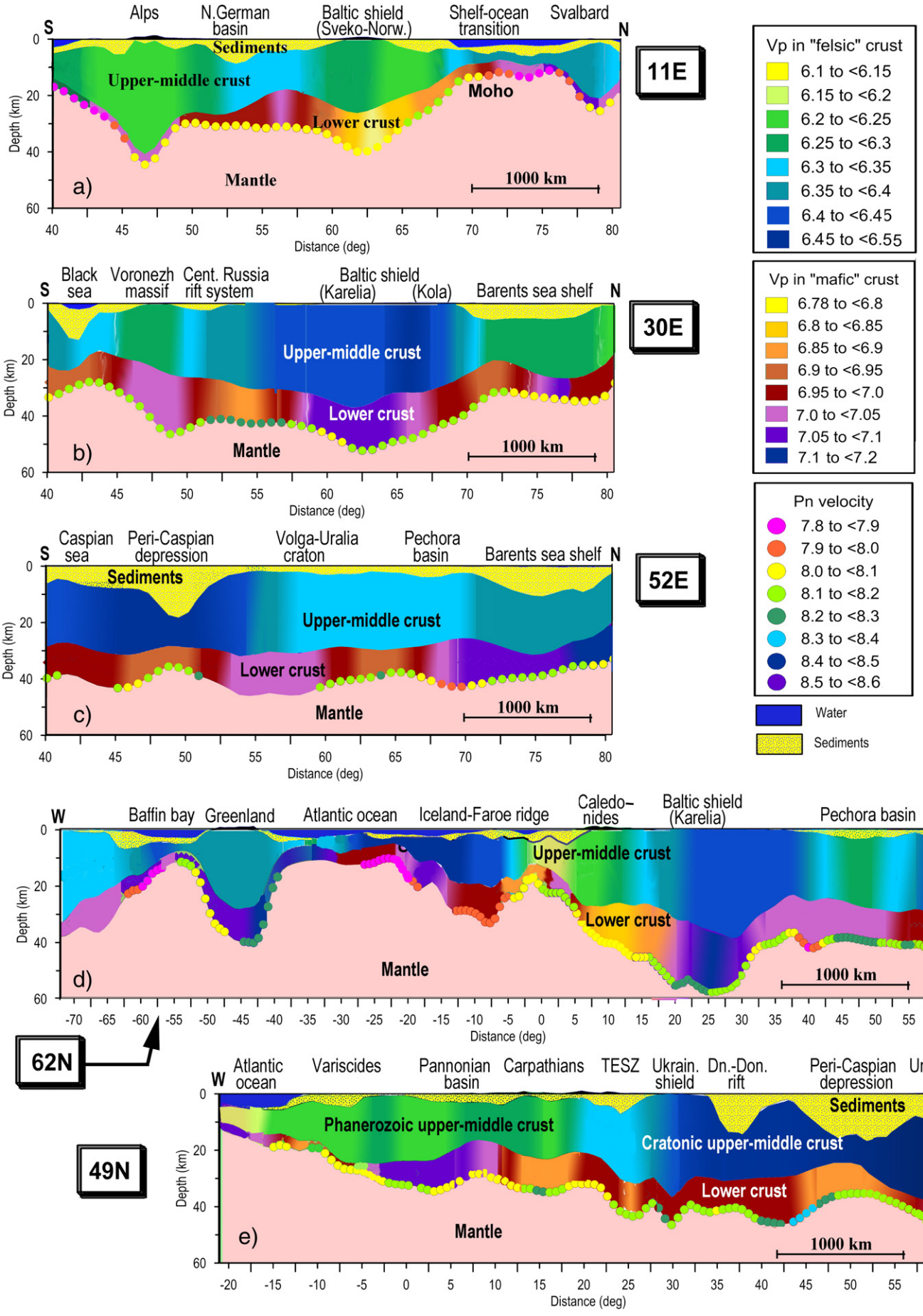
Alps
N.German basin
Baltic shield (Sveko-Norw.)
Shelf-ocean transition
Svalbard
S
N
Sediments
Upper-middle crust
Moho
Lower crust
Mantle
a)
1000 km
11E
Depth (km)
Distance (deg)
Black sea
Voronezh massif
Cent. Russia rift system
Baltic shield (Karelia)
(Kola)
Barents sea shelf
Upper-middle crust
Lower crust
Mantle
b)
1000 km
30E
Caspian sea
Peri-Caspian depression
Volga-Uralia craton
Pechora basin
Barents sea shelf
Sediments
Upper-middle crust
Lower crust
Mantle
c)
1000 km
52E
Vp in "felsic" crust
6.1 to <6.15
6.15 to <6.2
6.2 to <6.25
6.25 to <6.3
6.3 to <6.35
6.35 to <6.4
6.4 to <6.45
6.45 to <6.55
Vp in "mafic" crust
6.78 to <6.8
6.8 to <6.85
6.85 to <6.9
6.9 to <6.95
6.95 to <7.0
7.0 to <7.05
7.05 to <7.1
7.1 to <7.2
Pn velocity
7.8 to <7.9
7.9 to <8.0
8.0 to <8.1
8.1 to <8.2
8.2 to <8.3
8.3 to <8.4
8.4 to <8.5
8.5 to <8.6
Water
Sediments
W
Baffin bay
Greenland
Atlantic ocean
Iceland-Faroe ridge
Caledo–nides
Baltic shield (Karelia)
Pechora basin
E
Upper-middle crust
Lower crust
Mantle
d)
1000 km
62N
Atlantic ocean
Variscides
Pannonian basin
Carpathians
TESZ
Ukrain. shield
Dn.-Don. rift
Peri-Caspian depression
Urals
Sediments
Phanerozoic upper-middle crust
Cratonic upper-middle crust
Lower crust
Mantle
e)
1000 km
49N

Table 3
Statistical properties of the European crust (on-shore and shelves).

Age	Any	0–50 Ma	0–50 Ma	50–550 Ma	560–1000 Ma	1.1–1.6 Ga	1.7–2.5 Ga	>2.5 Ga
Tectonic setting	Shelves[a]	Cenozoic platforms, basins, rifts	Cenozoic orogens and highlands	Mesozoic–Paleozoic platforms, basins, rifts	Neoproterozoic platforms, rifts and shields	Mesoproterozoic platforms and shields	Paleoproterozoic platforms and shields	Archean platforms and shields
Topography (bathymetry) (km)	−0.23 ± 0.09	0.18 ± 0.16	1.20 ± 0.56	0.23 ± 0.32	0.12 ± 0.26	0.24 ± 0.28	0.28 ± 0.34	0.22 ± 0.22
Crustal thickness (km)	30.0 ± 7.1	34.6 ± 5.1	40.1 ± 7.7	36.5 ± 6.5	36.0 ± 7.8	37.9 ± 6.1	43.5 ± 6.4	42.9 ± 6.5
Thickness of crystalline crust (km)	25.4 ± 7.5	30.0 ± 7.5	36.3 ± 8.0	32.5 ± 7.5	32.9 ± 6.7	34.9 ± 7.5	41.6 ± 7.1	40.9 ± 7.8
Thickness of sediments (km)	5.1 ± 3.8	5.1 ± 3.8	4.8 ± 4.5	4.0 ± 4.1	5.3 ± 3.3	2.5 ± 2.5	2.4 ± 3.0	1.3 ± 2.5
Thickness of upper crust (km)	9.5 ± 6.0	15.4 ± 7.8	19.9 ± 11.0	13.8 ± 7.1	16.5 ± 8.2	13.5 ± 6.9	13.2 ± 6.3	12.7 ± 5.3
Thickness of middle crust (km)	7.8 ± 6.2	6.4 ± 5.7	7.2 ± 6.7	9.2 ± 7.3	7.6 ± 7.5	9.8 ± 8.2	13.5 ± 8.8	13.1 ± 9.4
Thickness of lower crust (km)	8.0 ± 6.4	6.5 ± 7.6	3.0 ± 6.5	8.6 ± 6.6	8.6 ± 8.2	12.6 ± 7.9	14.7 ± 7.2	15.1 ± 7.9
Average Vp in crust (incl. seds) (km/s)	6.22 ± 0.41	6.20 ± 0.21	6.21 ± 0.22	6.29 ± 0.27	6.22 ± 0.26	6.42 ± 0.25	6.52 ± 0.20	6.59 ± 0.15
Average Vp in crystalline crust (km/s)	6.56 ± 0.18	6.45 ± 0.21	6.36 ± 0.22	6.49 ± 0.18	6.52 ± 0.18	6.58 ± 0.16	6.63 ± 0.13	6.65 ± 0.11
Pn velocity (km/s)	8.06 ± 0.13	8.04 ± 0.22	7.98 ± 0.22	8.10 ± 0.13	8.03 ± 0.18	8.10 ± 0.14	8.15 ± 0.17	8.14 ± 0.12
Moho temperature[b] (°C)	–	818 ± 140	–	658 ± 146	616 ± 68	545 ± 92	556 ± 90	484 ± 86

Tectono-thermal ages are based on the TC1 model constrained on a 1° × 1° grid (Artemieva, 2006). Crustal parameters are based on point values derived from seismic models and interpolated onto a 1° × 1° grid to bring them to the same grid as the TC1 model.
[a] Shelves, platforms, and orogens are defined as regions with bathymetry/topography of −400 m to 0 m, 0 m to +500 m, and above 500 m, correspondingly.
[b] Data for Moho temperature — from Artemieva (2007).

is important given that, except for the oceanic crust, the UPC typically is thicker than the LPC (Fig. 16a).
- The transition from cratonic to Phanerozoic Europe is marked by a sharp difference in average basement Vp velocity; a significant part of this variation may be caused by differences in the crustal temperatures across the TESZ.
- The cratonic crust has relatively uniform values of average basement Vp velocities, 6.5–6.7 km/s. Within the East European craton the highest average basement velocities are very high (6.6–6.8 km/s) in the Archean blocks with thick lower crust (the Karelian Province of the Baltic Shield, the Ukrainian Shield and the Voronezh Massif, and some blocks of the Volgo–Uralia).
- The Riphean rifts of the East European craton show intermediate (ca. 6.5 km/s) basement velocities because the middle crustal layer is almost absent and the upper "granitic" crustal layer is substantially thickened (Artemieva, 2007). In contrast, the Peri-Caspian Basin, the Southern Caspian Sea and the Western Black Sea basin have higher basement velocities, which may be associated with large amounts of mafic intrusions and a nearly absent felsic crustal layer.
- The Phanerozoic crust of western Europe has average basement Vp velocities of 6.2–6.4 km/s, including the Variscan structures, the British–Irish Caledonides, Cenozoic orogens, and the Central European Rift system (including the Rhine graben and the North Sea rift system). Low average basement velocities (6.2–6.4 km/s) in most parts of Variscan Europe (Abramovitz et al., 1999; Aichroth et al., 1992) may be explained by post-Variscan delamination of the lower crust. In contrast, recent seismic data indicate slightly higher average Vp velocity (6.5 km/s) beneath the Norwegian Caledonides which also lack a high-velocity lower crust (Stratford and Thybo, 2011b). The Massif Central has extremely low average crustal seismic velocity, at least in part due to high crustal temperatures.
- Off-shore regions (including the crust of the North Atlantic ocean and the Barents Sea shelf) have highly variable average crustal velocities. High basement velocities in the Voring Plateau at the Norwegian shelf may be associated with mafic intrusions in the lower crust (Faleide et al., 2008; Mjelde et al., 2009); similar high basement velocities are observed in the Danish–North German area and may also be caused by Palaeozoic mafic intrusions (Thybo et al., 2006). In general, oceanic crust has very high velocity (>6.8 km/s), despite the high temperatures expected for young oceanic floor.
- In the Greenland–Iceland–Faeroe and Baffin Ridges average crustal velocities are high, perhaps reflecting oceanic origin. This observation may contradict expectations at Iceland, where one would expect high crustal temperatures and low Vp due to the presence of the Iceland plume.

Statistical analysis of average crustal Vp shows an overall correlation between average Vp in the crystalline crust and crustal age (Fig. 11c): older crust has higher Vp due to the presense of thick middle and lower crustal layers (Fig. 11b). This trend exists for all on-shore crust, from Archean to Cenozoic. When the sedimentary layer is included, the trend is observed only for the Precambrian crust, although average crustal Vp for crust of any age younger than 1 Ga is very similar: age-dependent variation in average Vp in the crystalline crust is smeared by a significant heterogeneity of the sedimentary layer both in thickness and in Vp (Sections 5.2 and 5.7).

6.3.6. Comparison with other crustal models

Similar to the Moho depth, we present a comparison of average basement Vp velocities and average Vp velocities in the entire crust constrained by our new regional crustal model EUNAseis with the same parameters derived from other crustal models for the region (Fig. 18). Only two models available digitally include information on the inner structure of the crust: CRUST 2.0 (Bassin et al., 2000) and EuCRUST-07 (Tesauro et al., 2008). We do not include the EPcrust model (Molinari and Morelli, 2011) into the comparison since it is based on a completely different methodology (Table 1). In EuCRUST-07, average Vp in the crystalline crust, calculated by simple weighted averaging, Section 6.2.1, is included as part of database. For the sake of comparison, we calculated average Vp for CRUST 2.0 using the same averaging method. To make the comparison adequate, our database has been resampled to the same grid as the other crustal models. We do not discuss the Mediterranean region because it is poorly constrained in the models.

For the crystalline crust, average Vp in CRUST2.0 is systematically 0.1–0.2 km/s higher in most regions with continental crust (except for the Adriatic region), and systematically lower in anomalous oceanic crust around Iceland (by ca. 0.4 km/s) and along the Urals (by 0.1–0.2 km/s) (Fig. 18a). When including sedimentary strata (Fig. 18b), the difference is huge, particularly for deep basins (the Polish Trough along the TESZ, the Barents Sea shelf, the North Sea, the Baffin Bay).

Fig. 20. Five profiles (three meridianal (a–c) and two longitudinal (d, e), coordinates in boxes denote profile locations) showing variations in crustal structure and Pn velocity in different tectonic structures of Europe, Greenland, and the North Atlantics.

We attribute these differences to incorrect velocity structure of the sedimentary cover in CRUST2.0 (cf. Fig. 9a).

Differences of +0.2/−0.1 km/s for Vp in the crystalline crust occur in most of continental Europe between our model and EuCRUST-07 (Fig. 18c), particularly in the Pannonian Basin, the Polish Trough, and the northern Baltic Shield. Much of off-shore crust has significantly lower average Vp in EuCRUST-07 than in our mdoel: up to +0.6 km/s in the belt of anomalous crust between the Faeroe Islands and Greenland and up to +0.5 km/s in western Barents Sea; whereas average Vp is higher in EuCRUST-07 than in our model in the Black Sea (−0.3–0.5 km/s), in the North Sea (−0.2 km/s), and off-shore Norway (up to +0.4 km/s). The origin of these discrepancies is unclear and may be related to a 2-layer crustal parameterization implemented in the EuCRUST-07 model (Table 1), which results in significant distortions of average Vp.

7. Pn velocities

7.1. Preamble

Regional variations in Pn velocities at the top of the mantle are presented in a map (Fig. 19) and are included in the statistical analysis (Fig. 11) and in the five profiles in Fig. 20. The presented Pn velocities are as measured in-situ in seismic experiments. Hence they reflect variation at the top of the mantle regarding:

- temperature (from ca. 400 °C in the cratonic regions to ca. 1000 °C and more in tectonically active parts of the continents and oceans, Artemieva (2006));
- pressure (for a depth range from ca. 10 km in oceans to ca. 60 km in young collisional orogens and in some parts of the craton);
- composition and, in particular, metamorphic state;
- fluid content (in particular, in oceans and subduction zones);
- anisotropy (mainly frozen-in in the lithosphere).

The coverage of the region by seismic refraction profiles is generally too coarse to allow for interpretation of anisotropy, and it is assumed here that the Pn velocity distribution is isotropic to first order. Only a few experiments provide sufficient coverage by crossing profiles to allow inference to be made regarding the degree of anisotropy. Although the results of these experiments are generally consistent with an isotropic Pn velocity distribution, regional earthquake seismological studies often indicate substantial upper mantle seismic velocity anisotropy (Babuska et al., 2002; Plomerova et al., 2002, 2008).

High-density coverage by seismic profiles may resolve Pn velocity amplitude with the uncertainty of ±0.1 km/s, although locally it may reach ±0.2 km/s. Weak amplitude of the Pn phase reported in several studies may add to the uncertainty. Additional uncertainty is associated with data interpolation (Fig. 19b). Although the interpolation procedure has been chosen to preserve the amplitudes of Pn velocity variations in published seismic models, the uncertainty is ca. ±0.1–0.2 km/s due to uneven data coverage (Fig. 19b). Most problematic is the Volga–Uralia craton and the Mediterranean Sea region where the reported Pn values are sparse and, in some places, controversial, and Pn velocity is the least constrained parameter in our compilation.

7.2. General patterns

The compilation generalized in Fig. 19a provides basis for some first order observations:

- Cratonic areas are characterized by very high Pn velocities (8.1–8.3 km/s) (also seen in Fig. 11c). This may not be surprising, considering the low temperature and thick crust of these areas. Note that the highest Pn velocities (8.3–8.5 km/s) are, in general, poorly constrained.
- The Barents Sea shelf has Pn velocities similar to the East European craton (see also Fig. 11c). High upper mantle velocities question the role of active mantle processes in lithosphere modification in the region. However, the crust of the shelf is ca. 10 km thinner than in most of the craton, and therefore similar Pn velocities in the shelf and in the craton indicate either temperature differences at Moho or differences in composition of the uppermost mantle (pressure effect is negligible).
- Some parts of the craton are characterized by relatively low Pn velocities (8.0–8.1 km/s), similar to Phanerozoic Europe. These parts generally include areas that have been modified by Neoproterozoic to Palaeozoic rifting during the formation of the aulacogens of the EEC. A low-Pn anomaly in the Arkhangelsk region is not well constrained.
- Young continental areas are characterized by Pn velocities of ~8.0 km/s (also seen in Fig. 11c). Given the much thinner Variscan crust than in the cratonic part of Europe, these velocities indicate significantly higher lithospheric temperature in western Europe than in the EEC. The Armorican and Iberian massifs have a slightly higher (ca. 8.1 km/s) Pn velocity. Surprisingly, the Pannonian Basin appears to be characterized by "normal" Pn velocity.
- Very low Pn velocity (<7.9 km/s) characterizes tectonically active areas around the Mediterranean Sea and the rifted part of the North Sea. Very low Pn velocity is also observed around Iceland and below some parts of the North Atlantic Ocean.

Comparison of our new crustal model with the global CRUST2.0 model (Fig. 19c) indicates significant difference in Pn velocities in off-shore regions, where most of the seismic models have been developed after CRUST2.0 was released. Note that most of these regions have anomalous crust. This result suggests that "guess" by tectonic similarity, as implemented in the CRUST2.0 model (Bassin et al., 2000) for regions without seismic coverage, does not work for Pn velocity (Fig. 19c). This conclusion is also supported by our analysis of seismic data for Siberia (Cherepanova et al., 2013–this volume).

8. Regional trends

This section discusses the relation between our new crustal seismic model EUNAseis and tectonic setting with focus on the depth to Moho illustrated by five crustal cross-sections (Fig. 20). It complements the discussion in Section 6 based on the various parameters. Given the diversity of tectonic evolution of the region and its highly heterogeneous crustal structure, the amount of available seismic data and the inevitable discrepancies between individual model interpretations, it is impossible to discuss in detail all data and all structures. We thus acknowledge that our discussion is limited to selected tectonic settings and selected publications.

8.1. Precambrian crust

8.1.1. Greenland

Most seismic data from Greenland has been acquired at the rim of the ice sheet, in the fjords and in the surrounding offshore parts. Only one active source seismological investigation has been completed in the interior parts of Greenland in summer 2011 (Thybo and Shulgin, in preparation). This 320 km long profile in the east-central part of Greenland extends EW from about the 2000 m altitude contour close to Scoresbysund Fjord across the top of the ice sheet (Fig. 5). The preliminary model included into our data base shows a gradual increase in crustal thickness from 40 km in the eastern part to around 48 km below the central part of Greenland (Fig. 20d).

The only other existing seismic interpretations of crustal thickness in interior Greenland are based on Receiver Function analysis. There is a significant discrepancy between the P- and S-wave estimates for the same data collected during the GLATIS seismic experiment. While S-wave Receiver Functions show crustal thickness in interior Greenland between 39 and 42 km (Kumar et al., 2007), P-wave Receiver Functions based on the same data provide values of 42–49 km (Dahl-Jensen et al., 2003). However, it is possible that the S-wave Receiver Functions do not detect a lower crustal layer with very high velocity, and that such a layer

mistakenly has been assigned to the upper mantle (cf. the discussion by Artemieva and Thybo, 2008).

The thickest crust in Greenland is apparently associated with the non-reworked Archean block although the resolution is very low due to the very sparse sampling. Close to the coast the crust is generally 30–38 km thick, although a local maximum of 45–48 km is determined at a station in southern West Greenland. Further, very thin crust (24–32 km thick) was determined at three stations in central East Greenland within the Caledonian orogen and at the edge of the onshore exposure of the North Atlantic Igneous Province. This is in the area with the highest (generally 1.5–2.0 km; up to 3.7 km) bedrock elevation in Greenland. The very thin crust may be caused by extreme stretching during continental break-up and formation of the North Atlantic Ocean, and it leaves the high topography enigmatic. However, it is known that velocity determination by the Receiver Functions method is uncertain, not least where small velocity contrasts are involved. Thus, one cannot rule out the possibility that in this extended area a high-velocity crust has been interpreted as mantle, since the transition between the lower crust and the uppermost mantle may be characterized by very small velocity contrast, e.g. due to substantial underplating.

Off-shore seismic refraction profiles determine crustal thicknesses of ca. 40–45 km both in southern West Greenland (Chian and Louden, 1992) and southern East Greenland (Dahl-Jensen et al., 1998) within less than 50 km distance from the coastline. The latter off-shore seismic profile includes a lower crustal layer with very high seismic velocity (7.4–7.6 km/s) below ca. 30 km depth. The location of the profile along the North Atlantic coast indicates that this high-velocity layer may be caused by magmatic underplating (Dahl-Jensen et al., 1998), and the same 10–15 km thick high-velocity layer may extend into the onshore parts (Voss and Jokat, 2007). Nevertheless, Receiver Function estimates in southern East Greenland made at less than 50 km distance from the profile yield a 34 km crustal thickness. Considering the very high velocity of the lower crustal layer, it is likely that the strongest seismic converter observed in RF may be the transition from the middle to the lower crust which then, mistakenly, may be interpreted as the Moho at the base of the high-velocity layer.

A similar situation exists in central Greenland, where the new refraction seismic profile identifies very high seismic velocity within 200 km from the Summit station, in the area where the interpretations of crustal thickness by P- and S-wave Receiver Functions (at the same location) differ by about 11 km. The P-wave Receiver Function estimate is close to the crustal thickness determined by well constrained seismic refraction interpretation. We therefore choose the larger value in this location and elsewhere in the entire study area where the two RF estimates differ.

8.1.2. East European craton

8.1.2.1. Baltic Shield. The deepest Moho (60–65 km) in continental Europe has been interpreted in south-central Finland (Fig. 20d), where crustal thickness in excess of 55 km is documented for the area around the paleo-collision zone (suture) between the Archean and Palaeoproterozoic terranes (Tiira et al., 2006). Away from the suture, the crust in the Archean Karelian province is 37–45 km thick, whereas in the Archean Kola province it is 42–44 km in the northern part and decreases to 36–38 km further south towards the rift systems of the White Sea and the Mezen basin, where it is thinned to 30–35 km (Kostyuchenko and Romanyuk, 1997). In the Archean–Paleoproterozoic Lapland region, the crustal thickness is 42–46 km (Kukkonen and Lahtinen, 2006) (Fig. 20b).

Relatively thick crust (45–50 km) extends across the Baltic Sea from central Finland to eastern Sweden as shown by data from the Bothnian Gulf of the Baltic Sea collected by the international collaborative BABEL deep seismic project in 1990 (BABEL Working Group, 1993b; Korja et al., 2001; Ohlander et al., 1993). The crust in the Bothnian Bay is part of a Mesoproterozoic rift system, it is 45–47 km thick and is largely composed of Mesoproterozoic rapakivi granites (Korja et al., 2001).

Typically, Svecofennian crust is 42–50 km thick and shows very large thickness variation with local anomalies up to 60–65 km in central Finland. In the southern Svecofennian province crustal thickness is 40–45 km and smaller (down to 36–38 km) around intrusions of rapakivi granites at the Baltic coast (BABEL Working Group, 1993a). Old refraction seismic data suggest that crustal thickness in the Sveconorwegian province is variable between 32 and 42 km (EUGENO-S Working Group, 1988; Thybo, 2001). Similar values are found for the crustal thickness of the Gothian province and its accreted terranes, whereas thick crust is observed around local Neoproterozoic suture zones (Abramovitz et al., 1997).

Only one seismic profile (Sovetsk–Riga–Kohtla Jarve) has been recorded in 1984 in the Baltic States. In the absence of any other seismic data, it provides some information on the crustal structure in the region, but its quality is speculative. The results of the only available interpretation (Ankudinov et al., 1991) indicate a crustal thickness of ca. 40 km at the western border of Latvia, increasing to 55–60 km in Proterozoic granulite belts of Latvia and Estonia and decreasing to ca. 50 km towards the Baltic Sea coast. Since almost no other seismic data are available for this entire region (Fig. 5), we have included this profile in our compilation, and it is these data that cause a significant difference in the depth to Moho in our compilation and other existing crustal models (Fig. 12). The only crossing seismic profile is at the western end of the Sovetsk–Riga–Kohtla Jarve profile and shows similar depth to Moho, 40–45 km (EUROBRIDGE, 1999).

8.1.2.2. Sarmatia and Volga–Uralia. The crust of the Archean to Proterozoic East European Craton is, in general, thicker (>45 km) than in many other Precambrian cratons, but similar in thickness to the Siberian craton (Cherepanova et al., 2013–this volume). Very thick crust is observed in the East European (Russian) Platform outside the areas that have been affected by Riphean and Palaeozoic rifting (Fig. 20c). In particular, a recent seismic reflection survey in Tatarstan (north of the Peri-Caspian basin) reveals a complex structure of the Archean basement with evidence for local crustal roots extending down to ca. 60 km depth and apparently related to paleocollisional events (Trofimov, 2006). Similar to the crustal root in Central Finland, the thick crustal root in the Volga–Uralia subcraton could have been formed by Precambrian collisional tectonics.

The crustal structure across the western East European Platform, from the Baltic Sea into the Ukrainian Shield, is well known by interpretations of seismic refraction/wide-angle reflection data from the recent EUROBRIDGE surveys (EUROBRIDGE WG, 1999, 2001). Along the EUROBRIDGE'95 profile, the depth to Moho increases southwards from ca. 45 km in the Baltic Basin to 50–55 km in the Proterozoic Belarus Granulite Belt, and slightly decreases further south (to ca. 50 km) beneath the Osnitsk–Mikashevichi Igneous Belt formed by Andean-type, ca. 2.0 Ga old granodioritic–granitic batholiths. Most of the Belarus High has high Vp velocities (8.3–8.35 km/s) at the top of the mantle, with unusually high (8.6 km/s) Pn velocity in the southern part of the Osnitsk–Mikashevichi Igneous Belt (due to the small size of this area these high Pn velocities are not resolved in the Pn map shown in Fig. 19a). Seismic models for other tectonic structures in Belarus are essentially absent (Garetskii et al., 1990) (Fig. 5).

The EUROBRIDGE'97 profile further south crosses the Pripyat trough (formed at the transition from terranes of Belarus to the Ukrainian shield) and two northern blocks of the Ukrainian shield: the Paleoproterozoic Volyn and the Archean Podolian blocks (Thybo et al., 2003). New seismic interpretations for the region indicate that crustal thickness is generally 45–50 km. The Pripyat trough filled with 3–4 km of young sediments has a similar crustal thickness and is different from the adjacent regions only by lower Pn velocity (8.1 km/s). Seismic velocities at the top of the mantle are 8.35 km/s in the crustal terranes of Belarus and in the north-central parts of the Ukrainian Shield, and

8.2 km/s in the Archean Azov block near the Black Sea coast. The crustal structure of the anorthosite–rapakivi Korosten pluton (1.80–1.75 Ga) of the Volyn block is similar to a typical craton, with some local deepening of the Moho (by ca. 5 km) and the presence of an intrusive body of mafic composition in the upper crust. Seismic models indicate strong heterogeneity in the crustal structure of the Ukrainian shield (Grad and Tripolsky, 1995; Ilchenko, 1990; Sollogub et al., 1980). The depth to Moho is as little as 37–40 km in the southernmost Azov block formed by Archean granulite gneiss complex (Lyngsie et al., 2007), ca. 50 km beneath the Archean Near Dnieper block in the southern part of the shield, and 42 km in the Paleoproterozoic Kirovograd block in the central part of the Shield. Although no obvious correlation between the age of the crust and the depth to Moho can be recognized within the Ukrainian shield, alkaline–ultrabasic formations are mainly found in blocks with thick (ca. 50 km) crust, while gabbro-syenite complexes are more common in blocks with thin (ca. 40 km) crust. The average velocity in the crystalline crust in the Ukrainian Shield is very high (>6.8 km/s), similar to the Karelian Province of the Baltic Shield (Figs. 17a, 20e).

8.1.3. Rifted cratonic crust

Available seismic data on the deep crustal structure are sparse in central Russia, although a dense network of shallow seismic surveys covers the area. Several profiles that image the whole crust were acquired across the Riphean rifts in the East European Platform in the central part of the platform and in the Mezen Province (Kostyuchenko et al., 1999). In the Mezen rift province, crustal thickness reduces to 30–32 km in the axial part of the rifts as compared to 35–37 km thick crust at the flanks. The Central Russia rift (the Belozersk–Semenov profile in the north-eastern part of the Moscow basin, Fig. 20b) has a crustal thickness of 40–42 km along the rift axis, whereas the surrounding crust is ca. 42 km beneath the northern flank and 45–47 km beneath the southern flank according to results obtained along the one seismic DSS profile in this area. Further south, the crust is 45 km thick beneath the Riphean Ryazan–Saratov graben.

The seismic Redkino–Pestovo DSS profile across the 40–50 km wide and 130 km long Valday rift at the north-western edge of the Moscow Basin reveals an unusual crustal structure of this rift. Unlike some of the other aulacogens (Riphean rifts) in the East European Platform, the Valday rift shows no crustal thinning, with an essentially constant crustal thickness (40–43 km) and velocity structure along the profile. There is no high-velocity layer in the lower crust, typical for other Riphean rifts of the East European Platform, and the mantle seismic velocities are high (Vp = 8.2–8.3 km/s; Vs = 4.8–4.85 km/s).

Another Riphean, the 50–100 km wide, Pachelma rift which separates Sarmatia and Volga–Uralia, is clearly outlined by gravity and magnetic anomalies. Crustal thickness is ca. 47–48 km outside the rift and 43 km in the axial zone according to data along two DSS seismic profiles in the northern part. The regional 'GRANIT' transect was recorded across the middle portion of the Pachelma rift in the early 1990s but, so far, no results have been published from this seismic survey.

The largest rift in Europe, the Devonian, 2000 km long, up to 170 km wide, and 22 km deep Dnieper–Donets Rift between the Ukrainian Shield and the Voronezh Massif (Fig. 20e) has been studied by numerous reflection and refraction seismic profiles starting from 1960s (e.g. Chekunov et al., 1992; Ilchenko, 1996; Stovba et al., 1996). Fewer crustal-scale seismic studies are available for its southeastern extension, the Donbas Foldbelt (Ilchenko, 1996; Lobkovsky et al., 1996) and for its northern extension, the Pripyat trough (Grad et al., 2006a,b; Juhlin et al., 1996b; Thybo et al., 2003). A recent high-quality, high-resolution international reflection/refraction seismic survey across the northern part of the Donbas Foldbelt at its transition to the Dnieper–Donets rift (further to the north) shows a constant thickness of the crust at ca. 40 km along the ca. 250 km long part of the profile which goes from the Azov block of the Ukrainian shield in SW to the south-western edge of the Voronezh massif in NE (DOBREfraction'99 WG, 2003; Lyngsie et al., 2007; Maystrenko et al., 2003). Older deep seismic data indicate some thinning of the crust to ca. 38 km under the rift axis in the Dnieper segment further to the northwest, whereas the Moho is at around a depth of 40 km in the Donets segment of the basin. Beneath the Karpinsky Swell (which is the SW extension of the Donbas to the north of the Greater Caucasus towards the Peri-Caspian Basin) the crust is 42–48 km thick (Saintot et al., 2006).

The inner structure of the crust is strongly heterogeneous along the strike of the rift system (Chekunov et al., 1992). A more than 10 km thick high-velocity (>6.9 km/s) lower crustal body has been identified beneath the rift basin itself (DOBREfraction'99 WG, 2003). This crustal feature earlier gave rise to interpretations of a possible "double Moho" (Pavlenkova, 1995). The structure of the sediments is highly variable and increases from ca. 4 km in the Pripyat trough to 20–24 km in the Donbas and in the central part of the Dnieper–Donets Rift, which implies that the crystalline crust is only about 20 km thick in the Donbas Foldbelt and the Dnieper–Donets Rift.

In the Peri-Caspian Basin the Moho depth is 32–36 km in the center and 40–42 km at the basin margins (Fig. 20e). The sediment thickness is anomalous, reaching 20 km (locally 26 km) in the central part and decreasing to 10–12 km at the flanks. As a result, the thickness of the crystalline crust does not exceed 14–16 km in the central part of the depression. Most of the available seismic data for the region are very old; they suggest that felsic crust may be thinned to almost zero in the central part of the Peri-Caspian basin. These data have been used to argue that the crystalline crust may be of oceanic origin or derived from a major magmatic event (Artyushkov and Morner, 1998; Zonenshain and Le Pichon, 1986).

8.2. TESZ

Since the beginning of the 90s, intensive studies have been carried out for the crustal structure of the Trans-European Suture Zone (TESZ) between the Paleo-Mesoproterozoic basement in the east and the Variscan–Caledonian crustal terranes in the west. A series of, often international, collaborative projects have acquired seismic reflection and refraction data that provides a very detailed insight into the crustal structure of this region. The largest projects are the EUGENO-S, BABEL, MONA LISA, DEKORP-BASIN '96, POLONAISE, CELEBRATION'2000, and the ESTRID seismic experiments (e.g. BABEL Working Group, 1993a; EUGENO-S Working Group, 1988; Grad et al., 2003; Guterch et al., 1999; Krawczyk et al., 2002; Malinowski et al., 2005; Meissner et al., 2002; MONA LISA Working Group, 1997a,b; Thybo et al., 2006; Starostenko et al., 2013).

The data provide information, at high lateral resolution, on the abrupt transition from the 43–45 km thick cratonic crust of the Precambrian East European Platform to the 28–32 km thick Variscan–Caledonian crust (Fig. 10a). Notably, the very variable Moho topography within TESZ has up-to 10 km undulations with wavelengths of less than 50 km in the deep basins (Jensen et al., 2002; Thybo, 1997). Crustal thickness of up to 50 km has been observed as a "crustal root" or a 'Moho trough' along the TESZ in southern Sweden, Denmark, Baltic Sea, Poland and Slovakia based on seismic data (BABEL Working Group, 1993a; Giese and Pavlenkova, 1988; Guterch et al., 1986; Thybo, 1990, 2001) and gravity modeling (Yegorova and Starostenko, 1999) (Fig. 20e). The lowermost part of the crustal root has very high seismic velocity, which may be explained by the presence of gabbro-eclogite or basalt–eclogite metamorphic sequences in the transition from lower crust to upper mantle (e.g. Abramovitz and Thybo, 2000).

In the Baltic Shield and into the Baltic Sea, overthickened crust is also observed at the southern extension of the Sorgenfrei–Tornquist Zone, which is a geologic inversion zone within the basin area between Denmark and Sweden. The thickened crust has been interpreted as the result of a "subversion" process, i.e. as a lower crustal root that formed as the deep expression of the tectonic inversion due to compression in the lower crust while the upper crust popped up (BABEL Working

Group, 1993a). In the northern part of this overthickened zone it is likely that crustal intrusions may be related to the root (Thybo, 2001).

Mantle velocities (up to 8.2 km/s) at 35 km depth and a mantle reflector at about 50–55 km depth have been identified by reinterpretation of DSS seismic profiles across the TESZ in Poland. This "double Moho" has been interpreted as a 'crust–mantle' layer in the depth interval 35–55 km (Guterch et al., 1994). However, such a double-Moho is not required by new data with higher resolution and a lowermost crust with slightly elevated velocity around 7.2 km/s may alternatively explain the data (Janik et al., 2002), and new data has demonstrated that several mantle reflectors exist in the Phanerozic side of TESZ (Grad et al., 2002).

8.3. Phanerozoic Europe

8.3.1. Caledonides and Variscides

The Caledonian parts of southern Norway have recently been covered by three crustal refraction seismic profiles during the Magnus Rex project (Stratford et al., 2009; Stratford and Thybo, 2011a,b). The results from this project have largely confirmed old interpretations of the Moho depth in the region, although they also provide significant new details on the crustal structure and add new coverage to the Moho map. The results show that the crustal thicknesses is 36–40 km in the interior of southern Norway, gradually thinning to 30 km or less towards the coast, with substantial, short-wavelength thickening into the Precambrian Baltic Shield proper (Fig. 20a, d), which was not substantially influenced by the Caledonian orogeny (Stratford and Thybo, 2011a). Unexpectedly, beneath the Oslo Rift the crustal thickness is only slightly (by 2 km) shallower than in the surrounding areas (Stratford and Thybo, 2011b). Old refraction data (Fig. 5; e.g. Kinck et al., 1993) suggest that the crust is highly heterogeneous in the Caledonides with its thickness ranging from 33 to 43 km. The new data demonstrates that it is mainly the upper crust that is highly heterogeneous, and that the heterogeneity may be ascribed to deformation structures in the nappe system within the Caledonides (Stratford and Thybo, 2011a).

Beneath the mountains in southern Norway, the Magnus Rex data indicate that the deepest Moho is offset from the highest topography (Stratford and Thybo, 2011a). In contrast, Receiver Function interpretation along two profiles in southern Norway indicates slightly deeper Moho than the coincident refraction data (Svenningsen et al., 2007). Based on the apparent correlation of thicker crust with high topography, these authors suggest the presence of the crustal root beneath the highland plateau. We, however, consider the crust beneath the southern dome of the Norwegian mountains as the "normal" and ascribe lateral variations in crustal thickness to crustal thinning at the Oslo rift and at the passive continental margin, which is also in agreement with newer Receiver Function results (Frassetto and Thybo, 2013). The new refraction seismic data indicate that crustal isostatic compensation may explain up to 2/3 of the topography; thus other mechanisms must be involved in maintaining the high elevation of southern Norway (Stratford et al., 2009; Maupin et al., 2013).

The crust of British–Irish–Danish–German–Polish Caledonides has been studied in great detail in large-scale seismic experiments, such as BIRPS in UK, VARNET-96 in Ireland, DEKORP-BASIN'96 in Germany, MONA LISA and BABEL in Denmark and Germany, POLONAISE'97 and CELEBRATION 2000 in Poland and east-central Europe and the recent ESTRID project in Denmark. The crust in the Danish–German–Polish Caledonides is 28–34 km thick with a regional maximum of 36 km associated with the Ringkobing–Fyn High (in the Danish Tornquist Fan area) and a regional minimum of 24 km in northern Germany (Thybo, 1997, 2001). The Precambrian crust has been significantly thinned (to ca. 25–30 km) in between thicker, more stable blocks during Palaeozoic–Mesozoic rifting and basin formation in the Tornquist Fan area of the North Sea basin (the northern branch of the TESZ that includes the Danish–Norwegian Basin). The thinning has led to significant magmatism probably along transverse faults which today is evidenced by observations of more than 20 km thick mafic batholiths in the area (Sandrin and Thybo, 2008a,b; Sandrin et al., 2008; Thybo, 1997; Thybo et al., 2006). The Caledonian deformed areas have thin crust (26–30 km thick) in the North Sea (Abramovitz and Thybo, 1998, 2000). Crustal thickness is ca. 30–32 km, locally up to 35 km, in the Caledonian regions of the British Isles and Ireland (Chadwick and Pharaoh, 1998; Kelly et al., 2007), comparable to the results of RF interpretation of a crustal thickness of ca. 30–37 km in the Caledonian mountains of East Greenland. Generally, the crust that has experienced the Caledonian deformation is slightly thicker (30–36 km) than the Variscan crust (28–32 km).

The crustal structure of the Variscides (Fig. 20e) has been studied intensively by acquisition of numerous seismic normal incidence and wide-angle reflection profiles, including those in France (ECORS; e.g. Bitri et al., 2001; Bois, 1990; Bois et al., 1989; Brun et al., 1992), Spain (IBERSEIS, ILIHA, NARS; e.g. Carbonell et al., 1998; Flecha et al., 2006; ILIHA DSS Group, 1993; Paulssen et al., 1999; Pulgar et al., 1996), in Germany (DEKORP; e.g. Brun et al., 1992; Meissner et al., 1987a) and across the entire western Europe (EGT; Blundell et al., 1992). Strikingly, the Variscan crust has a sharp subhorizontal Moho across individual sutures of the orogeny and a seismically laminated lower crust (Meissner, 1986). Post-orogenic delamination of the lithosphere (including the lower crust) may explain the presence of the thin crust (ca. 28–32 km) and flat Moho (Aichroth et al., 1992), similar to the modern Basin and Range province (Artemieva and Meissner, 2012; Menard and Molnar, 1988; Mengel and Kern, 1992). Metamorphic transformation of granulite facies lower crustal rocks into eclogite facies rocks provides additional explanation of the specific features of the Variscan crust and the Caledonian deformed crust in the North Sea area (Abramovitz and Thybo, 2000; Mengel and Kern, 1992).

The North German Basin, filled with sedimentary sequences in excess of 10 km thickness (Fig. 20a), was formed as a result of extensive faulting and magmatism which initiated a quick subsidence at ca. 300 Ma followed by formation of Meso-Cenozoic sub-basINS (Ziegler and Dezes, 2006). Seismic data indicate a flat and shallow (possibly new) Moho at a depth of 30–32 km, with massive high-velocity mafic intrusions present in the lower part of the crust (Bayer et al., 1995, 1999; Rabbel et al., 1995; Thybo, 1990, 2001). Since no crustal thinning exists in the North German Basin as compared to the adjacent Variscan terranes, it has been proposed that the basin developed by lithospheric buckling due to compressional stresses from the Alpine collision and ridge push from the North Atlantic spreading ridge (Marotta et al., 2001, 2002).

8.3.2. Uralides

The Uralides orogen has a strongly heterogeneous crustal structure which reflects its complex tectonic evolution (see Section 2.3 for details). Six major tectonic units oriented parallel to the axis of the mountain belt are traditionally recognized within the Uralides orogen from surface geology, potential field data, and seismic modeling. They include two major sectors: paleo-continental in the west, largely formed by deformation of the margin of the East European craton, and paleo-oceanic in the east, although the latter includes not only a large number of Paleozoic oceanic and island arc complexes but some preserved Precambrian basement blocks. The paleo-continental sector includes, from west to east, (i) the Urals Foredeep (a molasse basin), (ii) the West Uralian Zone (a part of the foreland fold-and-thrust belt filled with Palaeozoic sediments), and (iii) the Central Uralian Zone (uplifted Precambrian nucleus). The paleo-oceanic sector includes, from west to east, three accreted complexes: (i) the Tagil–Magnitogorsk volcanic arc complex, (ii) the East Uralian Zone (arc sediments and metamorphic complexes), and (iii) the Trans-Uralian Zone mostly buried beneath the West Siberian sediments (Kashubin et al., 2006; Puchkov, 2010). According to seismic interpretations along the ESRU profile (Friberg et al., 2001; Juhlin et al., 1996a) and the pattern of

magnetic anomalies (Hamilton, 1970), the crust of the Uralides may extend far eastwards below the thick sedimentary successions of the West Siberian Basin, perhaps even to the center of the basin.

The recent international seismic studies of the Ural mountains, ESRU (the Middle Urals) and URSEIS (the Southern Urals), have provided substantial new information on the crustal structure of the orogen, which complements earlier seismic results (Druzhinin et al., 1990; Ryzhiy et al., 1992). Several Russian seismic datasets were jointly interpreted by international teams within EUROPROBE co-operation (Brown et al. (1998, 2002); Carbonell et al. (1996, 2000) for the Southern Urals, Juhlin et al. (1996a) for the northern Middle Urals, and Steer et al. (1995) for the southern Middle Urals).

The ESRU survey consisted of several reflection seismic profiles, ESRU93/95/96/98, ca. 440 km long in total. For example, the survey of 1995 included two profiles, one oriented roughly east–west and the other north–south, with the crossing near the SG-4 deep borehole. According to seismic models of the ESRU surveys, complemented by UWARS and R17 profiles and a segment of the GRANIT profile (Juhlin et al., 1996a; Rybalka and Kashubin, 1992; Thouvenot et al., 1995), the crustal thickness across the Urals changes from west to east from ca. 45 km in the Urals Foredeep to 45–50 km in the West Uralian Zone, and is generally 50 km from the Central to the East Uralian Zone, reaching up-to 60–65 km in the central part (the Tagil island arc complex) (Druzhinin et al., 1990, 1997; Friberg et al., 2001; Juhlin et al., 1998, 2007; Knapp et al., 1998). A similar thick crustal root may be also preserved in the Polar Urals. Gently west-dipping reflections are common in the middle and lower crust along the ESRU profile (Kashubin et al., 2006). Further east, the Moho depth in the Trans-Uralian Zone is ca. 45–40 km shallowing to the east.

A different structure of the crust is revealed by the ca. 400 km long URSEIS combined reflection and refraction profile and a number of short regional profiles in the Southern Urals, ca. 500 km south of the ESRU surveys (Brown et al., 1998; Carbonell et al., 1996, 2000; Steer et al., 1995, 1998a,b; Suleimanov, 2006). Here, from west to east across the Urals, the crustal thickness changes from ca. 38–40 km in the Urals Foredeep to ca. 45 km in the West Uralian Zone. Some Moho deepening (up to 50–55 km) is interpreted towards the Main Uralian Fault (MUF) (Fig. 20e). The crustal root beneath the Magnitogorsk island arc complex to the east of the MUF may extend down ca. 55 km, but generally the crust is ca. 50 km thick from the MUF to the East Uralian Zone. Similar to the ESRU profile, the Moho depth shallows towards the West Siberian basin and is 38–40 km in the Trans-Uralian Zone.

Seismic data for Novaya Zemlya, the northward extension of the Uralides into the Polar region, is limited (Fig. 5). Two regional profiles across the orogen, AR-2 and AR-3, were acquired in 1995–2006 by 'Sevmorgeo' within the framework of the Russian Federal survey (Ivanova et al., 2006, 2011). According to these models, the Moho depth is ca. 40–42 km on both profiles, but the depth to the top of the lower crust (the "Conrad" discontinuity) is at ca. 28–30 km depth in the northern profile and at ca. 25 km in the southern profile.

8.3.3. Alpine fold belt

Meso-Cenozoic tectono-magmatic activity primarily associated with the Europe–Africa plate collision significantly reworked much of the Variscan crust. This reworking affected the Central European Rift system and the tectonic structures of the Cenozoic collisional orogens and associated subduction zones.

The Central European Rift system which extends from the Central Graben in the North Sea to the Mediterranean has shallow Moho, generally 28–30 km deep with a local minimum of ca. 25 km in the Central Graben of the North Sea (Fig. 10a). Similar thickness is reported for the Rhine graben and Massif Central, although with some variations in crustal thickness and structure along strike of the Rhine Graben (Brun et al., 1992). These regions have 2–3 km of sediments, with a significant accumulation of sedimentary deposits in foredeep basins of the Alpine orogen.

Deep Moho, to more than 45 km depth in the eastern Alps and up-to 50–55 km in the western and central Alps is well documented (e.g. Blundell et al., 1992 and references therein; Kissling, 1994; Ye et al., 1995) (Fig. 20a). In the eastern Alps, the new seismic investigations, TRANSALP and ALPS2002, provide detailed images of the crustal structure and the surprisingly complicated topography of the seismic Moho (Behm et al., 2007; Bleibinhaus and Gebrande, 2006; Gebrande et al., 2006; Luschen et al., 2006; Millahn et al., 2006). Together with the distribution of crustal velocity, the Moho geometry indicates that the subduction polarity in the Alps is everywhere southward (Bruckl et al., 2007, 2010), contrary to earlier interpretation of a change in polarity between the eastern and western Alps based on indications from mantle tomography (Lippitsch et al., 2003).

The seismic coverage of the structure and crustal thickness of other Cenozoic orogens in Europe is less than in the Alps. The Pyrenees appear to have a maximal Moho depth of 45–50 km (Díaz and Gallart, 2009; Pedreira et al., 2003) and the eastern Carpathians may have similar Moho depth, in the area close to the Pannonian Basin where the crust is only 25 km thick (Hauser et al., 2001; Horvath et al., 2006; Janik et al., 2011). There is basically no seismic data for other orogens of the southern Europe (e.g. the Balkanides and the Dinarides) (Fig. 5).

Models of the crustal structure and thickness of the Caucasus orogen have mainly appeared in national publications of the countries in the Caucasus region, Russia and Ukraine. Several crustal-scale seismic profiles, acquired largely in the valleys, form the basis for a number of regional compilations (Artemjev et al., 1985; Chekunov, 1994; Krasnopevtseva, 1984). Since the quality of these seismic models is unclear, the crustal thickness in the Caucasus is strongly debated. The crust may be more than 60 km thick below the Greater Caucasus, ca. 40 km thick below the Kura basin and the northern foreland basin. Subduction beneath the Caucasus has not yet been demonstrated by seismic data (mainly because there is no high-resolution regional tomography and the global- and continent-scale tomographic models have very low resolution in the region). Nevertheless northward subduction is indicated by a strong positive free air anomaly parallel to the Main Caucasus Ridge.

8.3.4. Iceland

There is much debate about the crustal thickness in Iceland. There is general consensus that the crust in Iceland is of oceanic type with a Vp velocity of 6.5–7.0 km/s in the "oceanic layer 3" that extends down to depths of 10–20 km (e.g. Foulger et al., 2005; White et al., 1996). The debate focuses on the petrologic nature of layer 4 and the arguments on both sides of the debate are based on the same or similar seismic data. In layer 4, that may extend down to 60 km depth, Vp gradually increases to 7.0–7.6 km/s (Angenheister et al., 1980). The "thin crust" model (Palmason, 1971) explains layer 4 as anomalous peridotite mantle with ca. 2% of melt (Schmeling, 1985), whereas the "thick crust" model (e.g. Menke and Levin, 1994) interprets the same layer as gabbroic "lower crust" with lenses of melt. Note that in both models of the Icelandic crust partial melts are interpreted to exist below 10–20 km depth (Riedel and Ebbing, 2008 and references therein).

An electrical conductor is interpreted at less than 15 km depth below the active rift zones and deeper than 25 km depth in Tertiary areas of Iceland (Bjornsson, 2008). These observations may support the thin-crust model, but 20–40 km deep seismic reflectors may also be interpreted as the Moho (Bjarnason et al., 1993; Gebrande et al., 1980), in accordance with the thick-crust model. The density of layer 4 is probably 3030–3150 kg/m^3 which is in the range between densities for oceanic crust (2970 kg/m^3) and uppermost mantle (3300 kg/m^3), so gravity cannot be used to discriminate between the two models (Darbyshire et al., 2000; Fedorova et al., 2005; Kaban et al., 2002).

The choice between the thin- and thick-crust models has important tectonic implications (Schmeling and Marquart, 2008). In case of the thin-crust model, the onshore spreading rift axis is located directly above the thinnest crust in Iceland with thickness comparable to the offshore rift axes on both sides of Iceland (Stefansson et al., 2008). Further

the temperatures must be very high and layer 4 should contain a high percentage of melts which, however, cannot be confirmed by the seismic studies. In case of the thick-crust model, uppermost mantle temperatures must be low to maintain a 20 km-thick gabbroic layer 4 below the gabbro solidus (Menke and Levin, 1994), in accordance with results of measurements of low regional off-shore heat flow (Stein and Stein, 2003), but in disagreement with on-shore estimations of high temperatures and shallow maximal hypocentre depths of local earthquakes (Bjarnason et al., 1994). The EUNAseis model includes Moho depths according to the "thick crust model" (Figs. 10a, 20d) as more consistent with other data.

8.4. Off-shore regions

8.4.1. Continental shelves

Continental shelves are often thinned off-shore continuations of on-shore crustal structure. The North Atlantic coastal regions have further been affected by oceanic break-up after significant rifting episodes, in particular in the North Sea area (Olsen, 1995 and references therein). The extensional period preceding break-up in the North Atlantic may have lasted about 200 My. Therefore the crust below the North Atlantic shelves are generally thinner than below e.g. the Arctic shelves where the crust may be 30–40 km thick in the Barents Sea and around Svalbard (Clark et al., 2013).

The Barents Sea has continental and subcontinental crust with a typical thickness of ca. 32–39 km and with a generally deeper Moho in the eastern basin (Figs. 10a, 20b, c). The transition from (sub)continental to oceanic crust is very sharp, within a ca. 50 km wide zone (Faleide et al., 2008). The Barents Sea area includes a series of very deep sedimentary basins, in particular in the eastern part where thickness of sediments locally reaches 20 km (Drachev et al., 2010) (Fig. 7a). Given a large thickness of the sedimentary cover, the crystalline crust is relatively thin, locally reducing in thickness to less than 20 km (Fig. 10b) (Ivanova et al., 2006). Although the origin of the basins is debated, there is little doubt that the area was subject to substantial stretching since the late Palaeozoic (Faleide et al., 2008), as reflected by substantial crustal thinning below individual rift basins (Figs. 7, 10). The basins below the Barents Sea may have been significantly influenced by mantle processes, lithospheric buckling and metamorphic processes (Artyushkov, 2005). However, a significant high-velocity anomaly in the upper mantle of the eastern basin of the Barents Sea may indicate that this intracratonic basin developed not by extension but by other processes (Fig. 19a). Similar to the Peri-Caspian Basin, the subsidence of the Barents Sea could have been associated with a local formation of mafic (semi-oceanic) crust (Zonenshain et al., 1990) and/or with magmatic underplating of the crust by high-density material (e.g. Artyushkov, 1993). Likewise the development of several rift basins along the western continental shelf of Norway may have been associated with substantial magmatic addition to the lower crust, in particular where thinning has been extreme, such as at the Vøring graben (Mjelde et al. 2009).

8.4.2. Oceanic crust of the North Atlantic ocean

An important characteristic of the northern North Atlantic ocean is that most of the area has anomalous crustal structure and anomalous bathymetry (Fig. 2b) which generally does not follow the expected square-root of age dependence (Stein and Stein, 1992): the sea bottom usually is observed at shallower depth than predicted by the model. The number of seismic observations in those parts of the North Atlantic Ocean where the bathymetry is normal (i.e. follows the square-root of age dependence) is limited, as most marine seismic experiments were made in areas with anomalous bathymetry. Where seismic data are available, the thickness of the "normal" oceanic crust is 7–10 km and indicates normal melting conditions at the mid-oceanic ridge.

Generally, substantial underplating developed in association with stretching, rifting and break-up at the North Atlantic margins. The underplate was intensively studied in the late 80s in a series of seismic experiments, including OBS seismic and two-ship expanding spread experiments. These experiments indicate that the underplating caused massive uniform bodies of magmatic rocks added to the lower crust below seaward dipping volcanic reflectors near the surface (e.g. Fowler et al., 1989; White et al., 1987). The seaward dipping reflectors are interpreted as volcanic flows associated with break-up which were tilted during the subsequent cooling. They are well resolved in a series of seismic reflection sections, whereas the resolution of the lower crustal underplated material is low. Subsequent acquisition of high-resolution refraction and reflection seismic data has, on the contrary, imaged layered sequences of magmatic additions to the lower crust instead of homogenous large magmatic bodies (White et al., 2008), similar to recent observation of layered sequences of magmatic addition to the lower crust at active rift zones (Thybo et al., 2000; Thybo and Nielsen, 2009).

A remarkable anomaly in the crustal structure is observed along the Faroe–Iceland–Greenland Ridge where anomalously thick, 30–35 km, crust (Fig. 20d) is interpreted to be of oceanic origin (Bott and Gunnarsson, 1980; Holbrook et al., 2001; Staples et al., 1997) and bathymetry does not follow the "square root of age" law (Fig. 2b). There is strong debate on the origin of the thick crust which is usually linked to the effect of unusually high temperatures below Iceland (Mihalffy et al., 2008; Parkin and White, 2008). According to one of the hypotheses, thick crust marks the plume track. However, the symmetry requires that this plume has been semi-stationary with respect to the boundary between the American and European plates for the last ca. 55 My (Lundin and Dore, 2005). Another explanation suggests the presence of a major melting anomaly with persistent volcanism centered at ca. 65N at the Mid-Atlantic Ridge and associated with small-scale convection at the divergent plate boundary (Boutilier and Keen, 1999; Parkin and White, 2008). There is little doubt that the mantle temperatures around Iceland are substantially higher than in the surrounding parts of the North Atlantic ocean, and it is challenging to find an alternative (to a mantle plume) explanation for the cause of excess magmatism during most of the time since the spreading began or a mechanism that has fed magma from Iceland to the distal portion of the ocean (e.g. Holbrook et al., 2001). Importantly, our study indicates the presence of a similar crustal anomaly on the western side of Greenland, the "Baffin Ridge" with thick crust across the Baffin Bay (Fig. 10). One may speculate if this structure might have similar origin or even represent a westward continuation of the Faeroe–Iceland–Greenland Ridge.

9. Conclusions

This study presents a new compilation EUNAseis of the available seismic data on the structure of the crust in an area which encompasses Europe, the North Atlantic Ocean, Iceland, and Greenland. This data has been used to review and analyze the seismic structure of the crust, including depth to the basement, crustal thickness, average Vp basement velocities, and Pn velocity in the uppermost mantle. The present compilation is based solely on seismic information and thus provides a tool for potential data modeling. Compared to earlier models of crustal structure, the present compilation also demonstrates a significant improvement in the coverage and spatial resolution, which has led to the identification of a much more heterogeneous crustal structure than previously presented.

The analysis of the crustal structure based on the new database EUNAseis and illustrated in this paper indicates the following:

i) The depth to Moho is highly variable throughout the region:
   - Moho is 40–60 km deep in the Precambrian crust of the cratons. For central Greenland, where the bedrock surface is below sea level, the existing, limited seismic data indicate crustal thickness values typical for the cratonic regions. Thick crustal roots (50–60 km) in some Archean–Paleoproterozoic terranes may represent ancient sutures (subduction zones); thinned cratonic crust (30–38 km) is typical for intracratonic

rifts and aulacogens.
- The craton to noncraton transition across the TESZ is marked by a sharp (ca. 10 km) decrease in the Moho depth over a short lateral distance of less than 100 km width.
- Young (Phanerozoic) crust has variable thickness similar to ancient crust, ranging from ca. 30 km in the Variscides (where the lower lithosphere including the lower crust may have been delaminated) to more than 50 km in the young orogens of the Alpine fold belt.
- The shelves appear to have a rather uniform depth to Moho: ca. 32–39 km in the Arctic shelf and ca. 20–24 km in the North Atlantic Ocean. The shelf to ocean transition is very narrow and commonly occurs within a 50 km wide zone.
- The Iceland–Faeroe, the Greenland–Iceland, and the Baffin Bay Ridges have anomalous crustal thickness (25–30 km), interpreted as being of oceanic origin.

ii) The thickness of the crystalline crust shows greater variations than depth to Moho:
- In the East European Craton it spans from ca. 60 km in the Baltic Shield to less than 20 km in the Peri-Caspian depression and the Dnieper–Donets rift. Anomalously thin crystalline crust of the Peri-Caspian depression, the South Caspian Sea, the western Black Sea (less than 15 km), and probably the eastern basin of the Black Sea (7 km), might have transitional, or even oceanic, origin which is also supported by the absence of an upper granitic layer in some of these regions. A very thin crystalline crust (10 km thick or less) is observed also locally in the North Sea rift system.
- An overall lack of correlation between variations in thicknesses of the sedimentary cover and crystalline crust in much of the region indicates that some deep processes are not fully reflected in the sedimentary cover, and that isostatic compensation may not be achieved at Moho in some tectonic areas.
- The crustal structure of the shelves is very heterogeneous with variations in thickness of crystalline crust from less than 15 km to more than 30 km; this also may imply that the Arctic basins may not be isostatically compensated by the crust, probably due to the presence of a mechanically strong cratonic lithosphere.

iii) The Vp velocity structure is highly variable both in the sedimentary layer and in the crystalline crust:
- In the sedimentary layer, average Vp shows a mosaic pattern, with no correlation between this parameter and basin depth. Weak correlation between average Vp and crustal age is significantly smeared by variations in composition and metamorphic state of the sediments, related to the burial history.
- In the crystalline crust, the highest average basement Vp velocities (6.5–6.8 km/s) are typical of the cratons with the highest values in the Archean blocks with thick lower crust. Intermediate (ca. 6.5 km/s) basement velocities in the Riphean rifts of the East European Craton may be due to a near absence of the middle crustal layer and a substantial thickening of the upper crustal layer.
- The transition from cratonic to Phanerozoic Europe is marked by a sharp difference in average basement Vp velocity reducing to 6.2–6.4 km/s in most Phanerozoic structures of western Europe; this variation is partially caused by differences in crustal temperatures across the TESZ.
- High basement Vp in the Peri-Caspian Basin, the Southern Caspian Sea and the western Black Sea basin may be associated with large amounts of mafic intrusions and a nearly absent felsic crustal layer. Off-shore regions have highly variable average crustal Vp with high basement velocities in the Voring Plateau which may also be associated with mafic intrusions in the lower crust.

iv) Strong variation in in-situ Pn velocity in the uppermost mantle reflects variations in regional geotherms, depth to Moho, seismic anisotropy, metamorphic state, and fluid regime.
- Cratonic areas are generally characterized by very high Pn velocities (>8.2 km/s) with some reduction in the Riphean and Paleozoic rifts. Relatively high Pn velocities are also observed in the Barents Sea shelf.
- Phanerozoic continental areas are characterized by Pn velocities of ~8.0 km/s; very low Pn velocity (<7.9 km/s) characterizes tectonically active areas around the Mediterranean Sea and the rifted part of the North Sea.
- Very low Pn velocity is observed around Iceland and some parts of the Atlantic Ocean, but data are mostly available for regions with anomalous bathymetry.

Based on our study, we further draw some general conclusions:

1. For each tectonic setting, there are significant variations in crustal thickness between structures of different tectono-thermal ages. The global averages (Christensen and Mooney, 1995) do not correspond to the crustal structure of any particular European collisional orogen, extensional and plume-related structure. The crust of cratonic areas in Europe also differs from the global averages: it is generally 5–10 km thicker and has higher average basement velocity.
2. The relative thickness of the upper-middle (Vp < 6.8 km/s) and lower (Vp > 6.8 km/s) parts of the crystalline crust may be indicative for the tectonic origin of an area. The ratio (UPC/UPC + LPC) increases from <0.4 in the oceanic crust to ca. 0.6–0.7 in the cratonic crust. Extended continental crust where the lower crust has been delaminated has an extreme ratio of >0.8.
3. Rifting, in general, leads mainly to thinning of the upper-middle crust (by ca. 15 km) without change in the Vp in this crustal layer. The lower crust is also thinned during rifting but to a lesser extent (by 5–10 km). The latter conclusion is unexpected as magmatic addition to the crust mainly happens to the lower crust (Thybo and Nielsen, 2009). Since no general increase in the lower crustal Vp is observed in rifted regions, the gabbro-eclogite phase transition may play an important role and lead to lower crustal delamination, effectively reducing average crustal Vp.
4. On continental shelves, thicknesses of the upper-middle (Vp < 6.8 km/s) and lower (Vp > 6.8 km/s) parts of the crystalline crust and average Vp velocities in these crustal layers differ from the values typical for rifted continental crust, indicating an importance of other processes in shelf evolution.
5. Most of the North Atlantic Ocean north of 55N does not follow the predictions of the cooling half-space model for bathymetric change with ocean age. The exceptionally thick crust of probable oceanic origin underlies the Greenland–Iceland–Faeroe Ridge; a similar "Baffin Ridge" feature is observed in the Baffin Bay and may be its continuation.

Supplementary data to this article can be found online at http://dx.doi.org/10.1016/j.tecto.2013.08.004.

Acknowledgments

The authors are grateful to a large number of European seismologists for discussions of their regional crustal models. Research grant FNU-10-083081 (Denmark) to IMA is gratefully acknowledged. We acknowledge the extensive comments to the paper from three anonymous reviewers and the guest Editor, Brian Kennett. The handling Editor for this paper was Laurent Jolivet. The electronic version of the crustal database is available for free download from the authors' website, www.lithosphere.info.

References

Abramovitz, T., Landes, M., Thybo, H., Jacob, A.W.B., Prodehl, C., 1999. Crustal velocity structure across the Tornquist and Iapetus Suture Zones — a comparison based on MONA LISA and VARNET data. Tectonophysics 314 (1–3), 69–82.

Abramovitz, T., Thybo, H., and MONA LISA Working Group, 1998. Seismic structure across the Caledonian Deformation Front along MONA LISA profile 1 in the southeastern North Sea. Tectonophysics 288 (1–4), 153–176.

Abramovitz, T., Thybo, H., 2000. Seismic images of Caledonian, lithosphere-scale collisional structures in the southeastern North Sea along Mona Lisa Profile 2. Tectonophysics 317, 27–54.

Abramovitz, T., Thybo, H., Berthelsen, A., 1997. Proterozoic sutures and terranes in the southeastern Baltic Shield interpreted from BABEL deep seismic data. Tectonophysics 270, 259–277.

Afanasenkov, A.P., Nikishin, A.M., Obukhov, A.N., 2007. Eastern Black Sea Basin: Geologic Structure and Hydrocarbon Potential. Nauchnyi Mir, Moscow (in Russian).

Agostinetti, N.P., Amato, A., 2009. Moho depth and Vp/Vs ratio in Peninsular Italy from teleseismic receiver functions. J. Geophys. Res. 114, 17.

Agostinetti, N.P., Levin, V., Park, J., 2008. Crustal structure above a retreating trench: receiver function study of the northern Apennines orogen. Earth Planet. Sci. Lett. 275, 211–220.

Aichroth, B., 1990. The European Geotraverse seismic refraction experiment of 1986 from Genoa, Italy, to Kiel, Germany. Tectonophysics 176, 43–57.

Aichroth, B., Prodehl, C., Thybo, H., 1992. Crustal structure along the central segment of the EGT from seismic-refraction studies. Tectonophysics 207, 43–64.

Alvarez-Marron, J., et al., 1996. Seismic structure of the northern continental margin of Spain from ESCIN deep seismic profiles. Tectonophysics 264 (1–4), 153–174.

Amundsen, H., Evdokimov, A., Dibner, V., Andresen, A., 1998. Petrogenetic significance and evolution of Mesozoic magmatism, Franz Josef Land and the Barents Sea. In: Solheim, A., Musatov, E., Heintz, N. (Eds.), Geological Aspects of Franz Josef Land and the Northernmost Barents Sea (the Northern Barents Sea Geotraverse). Norsk Polarinstitutt, Meddelelser, p. 151.

Anell, I., Thybo, H., Artemieva, I., 2009. Cenozoic uplift and subsidence in the North Atlantic region: geological evidence revisited. Tectonophysics 474, 78–105.

Angenheister, G., et al., 1980. Reykjanes Ridge Iceland seismic experiment (RRISP 77). J. Geophys. 47, 228–238.

Angus, D.A., Wilson, D.C., Sandvol, E., Ni, J.F., 2006. Lithospheric structure of the Arabian and Eurasian collision zone in eastern Turkey from S-wave receiver functions. Geophys. J. Int. 166 (3), 1335–1346.

Ankudinov, S.A., Brio, H.S., Sadov, A.S., 1991. Deep structure of the crust in the Baltic republics based on DSS seismic studies. Seismol. Bul. Belorussia 1, 111–117.

Artemieva, I.M., 2003. Lithospheric structure, composition, and thermal regime of the East European craton: implications for the subsidence of the Russian Platform. Earth Planet. Sci. Lett. 213, 429–444.

Artemieva, I.M., 2006. Global 1° × 1° thermal model TC1 for the continental lithosphere: implications for lithosphere secular evolution. Tectonophysics 416, 245–277 (See also: www.lithosphere.info).

Artemieva, I.M., 2007. Dynamic topography of the East European Craton: shedding light upon the lithospheric structure, composition and mantle dynamics. Glob. Planet. Chang. 58, 411–434.

Artemieva, I.M., Meissner, R., 2012. Crustal thickness controlled by plate tectonics: a review of crust–mantle interaction processes illustrated by European examples. Tectonophysics 519, 3–34.

Artemieva, I.M., Thybo, H., 2008. Deep Norden: highlights of the lithospheric structure of Northern Europe, Iceland, and Greenland. Episodes 31 (1), 98–106.

Artemieva, I.M., Thybo, H., Kaban, M.K., 2006. Deep Europe today: geophysical synthesis of the upper mantle structure and lithospheric processes over 3.5 Ga. European Lithosphere Dynamics. In: Gee, D., Stephenson, R. (Eds.), Geol. Soc. London Memoirs, 32, pp. 11–41.

Artemjev, M.E., Golland, V.E., Niauri, G.A., 1985. New data on the isostasy of the Caucasus. Phys. Solid Earth 21 (2), 85–93.

Artemjev, M.E., Kaban, M.K., 1994. Density inhomogeneities, isostasy and flexural rigidity of the lithosphere in the Transcaspian region. Tectonophysics 240, 281–297.

Artyushkov, E.V., 1992. Role of crustal stretching on subsidence of the continental crust. Tectonophysics 215, 187–207.

Artyushkov, E.V., 1993. Physical Tectonics. Nauka, Moscow (456 pp.).

Artyushkov, E.V., 2005. The formation mechanism of the Barents Basin. Russ. Geol. Geophys. 46 (7), 700–713.

Artyushkov, E.V., Baer, M.A., 1986. Mechanism of formation of hydrocarbon basins: the west Siberia, Volga–Urals, Timan–Pechora basins and the Permian Basin of Texas. Tectonophysics 122, 247–281.

Artyushkov, E.V., Morner, N.A., 1998. Steep bending of continental lithosphere without its stretching or plate collision: an indication for lithospheric failure and phase transitions. Terra Nova 10 (2), 101–105.

Avchan, G.M., Oserskaya, M.L., 1985. The Petrophysical Characteristics of the Sedimentary Cover of the USSR Oil and Gas Provinces. Nedra, Moscow (192 pp. (in Russian)).

Avedik, F., Berendsen, D., Fucke, H., et al., 1984. Seismic investigations along the Scandinavian "Blue Norma" profile. Ann. Geophys. 2 (5), 571–578.

Azbel, I. Ya, Korhonen, H., Kosminstaya, I.P., et al., 1993a. Velocity cross-section of the crust along the BALTIC seismic profile. Structure of the Lithosphere of the Baltic Shield. Nat. Geophys. Comm., Russian Acad. Sci., Moscow, pp. 37–42.

Azbel, I. Ya, Yegorkin, A.V., Ionkins, V.T., 1993b. Velocity cross-section of the crust along the Pechenga–Umbozero–Rybachiy seismic profile. Structure of the Lithosphere of the Baltic Shield. Nat. Geophys. Comm., Russian Acad. Sci., Moscow, pp. 33–37.

Babadzhanov, T.L., Kunin, N.Ya. (Editors), 1991. The maps of the basement surface and intermediate structural horizons for Mid-Asia. Scale: 1:1,000,000. Tashkent.

BABEL Working Group, 1990. Evidence for early Proterozoic plate tectonics from seismic reflection profiles in the Baltic Shield. Nature 348, 34–38.

BABEL Working Group, 1993a. Deep seismic reflection/refraction interpretation of crustal structure along BABEL profiles A and B in the southern Baltic Sea. Geophys. J. Int. 112, 325–343.

BABEL Working Group, 1993b. Integrated seismic studies of the Baltic Shield using data in the Gulf of Bothnia region. Geophys. J. Int. 112 (3), 305–324.

Babuska, V., Plomerova, J., Vecsey, L., Granet, M., Achauer, U., 2002. Seismic anisotropy of the French Massif Central and predisposition of Cenozoic rifting and volcanism by Variscan suture hidden in the mantle lithosphere. Tectonics 21 (4), 11-1/11-20 http://dx.doi.org/10.1029/2001TC901035.

Bamber, J.L., Layberry, R.L., Gogineni, S., 2001. A new ice thickness and bed data set for the Greenland ice sheet 1. Measurement, data reduction, and errors. J. Geophys. Res. 106, 33773–33780.

Bamford, D., et al., 1976. Lithospheric seismic profile in Britain. 1. Preliminary results. Geophys. J. Roy. Astron. Soc. 44 (1), 145–158.

Banda, E., 1988. Crustal parameters in the Iberian peninsula. Phys. Earth Planet. Inter. 51, 222–225.

Banda, E., Gallart, J., Garciaduenas, V., Danobeitia, J.J., Makris, J., 1993. Lateral variation of the crust in the Iberian peninsula — new evidence from the Betic Cordillera. Tectonophysics 221, 53–66.

Barton, P.J., 1992. LISPB revisited — a new look under the Caledonides of northern Britain. Geophys. J. Int. 110 (2), 371–391.

Barton, A.J., White, R.S., 1997. Crustal structure of Edoras Bank continental margin and mantle thermal anomalies beneath the North Atlantic. J. Geophys. Res. Solid Earth 102 (B2), 3109–3129.

Barton, P., Wood, R., 1984. Tectonic evolution of the North-Sea basin — crustal stretching and subsidence. Geophys. J. Roy. Astron. Soc. 79 (3), 987.

Bassin, C., Laske, G., Masters, G., 2000. The current limits of resolution for surface wave tomography in North America. EOS Trans. Am. Geophys. Union 81, F897.

Baturin, D., Fedukhina, T., Savostin, L., Yunov, A., 1994. A geophysical survey of the Spitsbergen margin and surrounding areas. Mar. Geophys. Res. 16, 463–484.

Bayer, U., Grad, M., Pharaoh, T.C., Thybo, H., Guterch, A., Banka, D., Lamarche, J., Lassen, A., Lewerenz, B., Scheck, M., Marotta, A.-M., 2002. The southern margin of the East European Craton: new results from seismic sounding and potential field between the North Sea and Poland. Tectonophysics 360, 301–314.

Bayer, U., Scheck, M., Hauf, Y., 1995. Structural evolution of the Northeast German Basin during Early Permian to Keuper — volumetric analysis of sediment accumulation. Terra Nostra 95, 80–89.

Bayer, U., Scheck, M., Rabbel, W., Krawczyk, C.M., Götze, H.-J., Stiller, M., Beilecke, Th., Marotta, A.-M., Barrio-Alvers, L., Kuder, J., 1999. An integrated study of the NE German Basin. Tectonophysics 314, 285–307.

Behm, M., Bruckl, E., Chwatal, W., Thybo, H., 2007. Application of stacking and inversion techniques to three-dimensional wide-angle reflection and refraction seismic data of the Eastern Alps. Geophys. J. Int. 170 (1), 275–298.

Behrens, K., Goldflat, S., Heikkinen, P., et al., 1989. Reflection seismic measurements across the Granulite Belt of the POLAR Profile in the northern Baltic Shield, Northern Finland. Tectonophysics 162, 101–111.

Beloussov, V.V., Pavlenkova, N.I., Kvyatkovskaya, G.I. (Eds.), 1991. Deep Structure of the USSR Territory. Moscow, Nauka.

Beloussov, V.G., Volvovski, B.S., Volvovski, I.S., Ryaboi, V.Z., 1962. Experimental recording of deep reflected waves. Bull. (Izvestiya) Acad. Sci., U.S.S.R., Geophys. Ser. English translation 8 (1962), 662–669.

Beloussov, V.V., et al., 1988. Structure and evolution of the Earth's crust and upper mantle of the Black Sea. Boll. Geof.Teor.Appl. 30, 109–196.

Ben-Avraham, Z., Ginzburg, A., Makris, J., Eppelbaum, L., 2002. Crustal structure of the Levant Basin, eastern Mediterranean. Tectonophysics 346, 23–43.

Bertrand, E., Deschamps, A., 2000. Lithospheric structure of the southern French Alps inferred from broadband analysis. Phys. Earth Planet. Inter. 122, 79–102.

Bibikova, E.V., Bogdanova, S.V., Larionov, A.N., Fedotova, A.A., Postnikov, A.V., Popova, L.P., Kirnozova, T.I., Fugzan, M.M., 2008. New data on the early Archean age of granitoids in the Volga–Ural segment of the East European Craton. Dokl. Earth Sci. 419 (2), 219–223 http://dx.doi.org/10.1007/s11471-008-2012-9.

Bijwaard, H.W., Spakman, W., Engdahl, E.R., 1998. Closing the gap between regional and global travel time tomography. J. Geophys. Res. 103, 30055–30078.

Bitri, A., Brun, J.P., Truffert, C., Guennoc, P., 2001. Deep seismic imaging of the Cadomian thrust wedge of Northern Brittany. Tectonophysics 331 (1–2), 65–80.

Bitri, A., et al., 1997. Crustal structure of the Cadomian block in the north Brittany (France): seismic reflection and magnetotelluric sounding (Geofrance 3D Armor project). C. R. Acad. Sci. Sci. Terre Planets 325 (3), 171–177.

Bjarnason, I.T., Menke, W., Flovenz, O.G., 1994. Tomographic image of the Mid-Atlantic plate boundary in southwestern Ireland — reply. J. Geophys. Res. Solid Earth 99, 17915–17917.

Bjarnason, I.T., Menke, W., Flovenz, O.G., Caress, D., 1993. Tomographic image of the Mid-Atlantic Plate Boundary in southwestern Iceland. J. Geophys. Res. Solid Earth 98, 6607–6622.

Bjornsson, A., 2008. Temperature of the Icelandic crust: inferred from electrical conductivity, temperature surface gradient, and maximum depth of earthquakes. Tectonophysics 447, 136–141.

Björnsson, A., Eysteinsson, H., Beblo, M., 2005. Crustal formation and magma genesis beneath Iceland: magnetotelluric constraints. GSA Spec. Pap. 388, 665–686 http://dx.doi.org/10.1130/1130-8137-2388-1134.1665.

Bleibinhaus, F., Beilecke, T., Bram, K., Gebrande, H., 1999. A seismic velocity model for the SW Baltic Sea derived from BASIN'96 refraction seismic data. Tectonophysics 314 (1–3), 269–283.

Bleibinhaus, F., Gebrande, H., 2006. Crustal structure of the Eastern Alps along the TRANSALP profile from wide-angle seismic tomography. Tectonophysics 414 (1–4), 51–69.

Blundell, D., Freeman, R., Mueller, S. (Eds.), 1992. A Continent Revealed. The European Geotraverse. Cambridge University Press (275 pp.).

Bogdanova, S.V., De Waele, B., Bibikova, E.V., et al., 2010. Volgo–Uralia: the first U–Pb, Lu–Hf and Sm–Nd isotopic evidence of preserved Paleoarchean crust. Am. J. Sci. 310, 1345–1383 http://dx.doi.org/10.2475/10.2010.06.

Bohnhoff, M., Makris, J., Papanikolaou, D., Stavrakakis, G., 2001. Crustal investigation of the Hellenic subduction zone using wide aperture seismic data. Tectonophysics 343 (3–4), 239–262.

Bois, C., 1990. Major geodynamic processes studied from the ECORS deep seismic profiles in France and adjacent areas. Tectonophysics 173 (1–4), 397–410.

Bois, C., et al., 1989. Contribution of deep seismic profiling to the knowledge of the lower crust in France and neighbouring areas. Tectonophysics 145 (3–4), 253–275.

Bosse, V., Feraud, G., Ballevre, M., et al., 2005. Rb–Sr and $^{40}Ar/^{39}Ar$ ages in blueschists from the Ile de Groix (Armorican Massif, France): implications for closure mechanisms in isotopic systems. Chem. Geol. 220, 21–45.

Bott, M.H.P., Gunnarsson, K., 1980. Crustal structure of the Iceland–Faeroe ridge. J. Geophys. 47, 221–227.

Boutilier, R.R., Keen, C.E., 1999. Small-scale convection and divergent plate boundaries. J. Geophys. Res. 104, 7389–7403.

Breivik, A.J., Mjelde, R., Faleide, J.I., Murai, Y., 2012. The eastern JanMayen microcontinent volcanic margin. Geophys. J. Int. 188, 798–818.

Breivik, A.J., Mjelde, R., Grogan, P., Shimamura, H., Murai, Y., Nishimura, Y., 2003. Crustal structure and transform margin development south of Svalbard based on ocean bottom seismometer data. Tectonophysics 369, 37–70.

Breivik, A.J., Mjelde, R., Grogan, P., Shimamura, H., Murai, Y., Nishimura, Y., 2005. Caledonide development offshore–onshore Svalbard based on ocean bottom seismometer, conventional seismic, and potential field data. Tectonophysics 401, 79–117.

Breivik, A.J., Mjelde, R., Raum, T., Faleide, J.I., Murai, Y., Flueh, E.R., 2011. Crustal structure beneath the Trøndelag Platform and adjacent areas of the Mid-Norwegian margin, as derived from wide-angle seismic and potential field data. Nor. J. Geol. 90, 141–161.

Brodsky, A.Ya., Voronin, N.I., 1994. The model of deep structure of transition zone between Karpinsky Swell and Astrakhan Dome. Otecestvennaa Geol. 4, 50–53 (in Russian).

Bronguleev, V.V., et al. (Ed.), 1975. Map of topography for sedimentary layers of different ages within the East European Platform. M 1:2,500,000. Maps for six sedimentary layers.

Brooks, C.K., 2011. The East Greenland rifted volcanic margin. Geological Survey of Denmark and Greenland Bulletin, 24 (96 pp.).

Brown, D., Juhlin, C., Alvarez-Marro N, J., Pe Rez-Estaun, A., Oslianski, A., 1998. The crustal-scale structure and geodynamic evolution of an arc–continent collision zone in the Southern Urals, Russia. Tectonics 2, 158–170.

Brown, D., Juhlin, C., Tryggvason, A., et al., 2002. The crustal architecture of the Southern and Middle Urals from the URSEIS, ESRU, and Alapaev reflection seismic profiles. Mountain Building in the Uralides: Pangea to Present. In: Brown, D., Juhlin, C., Puchkov, V. (Eds.), Geophys. Monogr. Am. Geophys. Union, 132, pp. 33–48.

Bruckl, E., et al., 2003. ALP 2002 seismic experiment. Stud. Geophys. Geod. 47 (3), 671–679.

Bruckl, E., Bleibinhaus, F., Gosar, A., et al., 2007. Crustal structure due to collisional and escape tectonics in the Eastern Alps region based on profiles Alp01 and Alp02 from the ALP 2002 seismic experiment. J. Geophys. Res. Solid Earth 112 (B6) http://dx.doi.org/10.1029/2006JB004687.

Brückl, E., Behm, M., Decker, K., Grad, M., Guterch, A., Keller, G.R., Thybo, H., 2010. Crustal structure and active tectonics in the Eastern Alps. Tectonics 29 http://dx.doi.org/10.1029/2009TC002491.

Brun, J.P., et al., 1992. Deep crustal structure of the Rhine Graben from DEKORP ECORS seismic-reflection data — a summary. Tectonophysics 208 (1–3), 139–147.

Bullock, A.D., Minshull, T.A., 2005. From continental extension to seafloor spreading: crustal structure of the Goban Spur rifted margin, southwest of the UK. Geophys. J. Int. 163 (2), 527–546.

Burchfiel, C., Nakov, R., Tzankov, Z., Royden, L.H., 2000. Cenozoic extension in Bulgaria and northern Greece: the northern part of the Aegean extensional regime. Tectonics and Magmatism in Turkey and the Surrounding Area. In: Bozkurt, E., Winchester, J.A., Piper, J.D.A. (Eds.), Geological Society, London, Special Publications, 173, pp. 325–352.

Burianov, V.B., Gordienko, V.V., Zavgorodnyaya, O.V., 1985. A Geophysical Model of the Tectonosphere of the Ukraine. Naukova Dumka, Kiev (in Russian).

Burollet, P.F., 1986. Deep Mediterranean basins and their oil potential. In: Halbouty, M.T. (Ed.), Future Petroleum Provinces of the World. AAPG Mem, 40, pp. 545–557.

Bush, V.A., Kaz'min, V.G., 2008. Crystalline basement and fold complex of the Volga–Ural, Pericaspian, and Fore-Caucasus petroliferous basins. Geotektonika 5, 79–94 http://dx.doi.org/10.1134/S001685 (English translation: Geotectonics (Springer) 42(5), 396–409).

Calvert, A., et al., 2000. Geodynamic evolution of the lithosphere and upper mantle beneath the Alboran region of the western Mediterranean: constraints from travel time tomography. J. Geophys. Res. 105 (B5), 10871–10898.

Canales, J.P., Detrick, R.S., Lin, J., Collins, J.A., Toomey, D.R., 2000. Crustal and upper mantle seismic structure beneath the rift mountains and across a nontransform offset at the Mid-Atlantic Ridge (35° N). J. Geophys. Res. 105 (B2), 2699–2719.

Carbonell, R., Gallart, J., Perez-Estaun, A., Diaz, J., Kashubin, S., Mechie, J., Wenzel, F., Knapp, J., 2000. Seismic wide-angle constraints on the crust of the southern Urals. J. Geophys. Res. (ISSN: 0148-0227) 105 (B6) http://dx.doi.org/10.1029/2000JB900048.

Carbonell, R., Perez-Estaun, A., Gallart, J., Diaz, J., Kashubin, S., Mechie, J., Stadtlander, R., Schulze, A., Knapp, J.H., Morozov, A., 1996. A crustal root beneath the Urals: wide-angle seismic evidence. Science 274, 222–224.

Carbonell, R., et al., 1998. A multidisciplinary geophysical study in the Betic chain (southern Iberia Peninsula). Tectonophysics 288 (1–4), 137–152.

Cassinis, R., 2006. Reviewing pre-TRANSALP DSS models. Tectonophysics 414, 79–86.

Castellarin, A., Cantelli, L., 2000. Neo-Alpine evolution of the Southern Eastern Alps. J. Geodyn. 30, 251–274.

Cavazza, W., Roure, F., Spakman, W., Stampfli, G.M., Ziegler, P.A. (Eds.), 2004. The TRANSMED Atlas — The Mediterranean Region from Crust to Mantle. Springer, Berlin, Heidelberg (141 pp. and CD-ROM).

Cernobori, L., et al., 1996. Crustal image of the Ionian basin and its Calabrian margins. Tectonophysics 254, 175–189.

Cerveny, V., Popov, M.M., Psencik, I., 1982. Computation of wave fields in inhomogeneous-media Gaussian-beam approach. Geophys. J. Roy. Astron. Soc. 70 (1), 109–128.

Chadwick, R.A., Pharaoh, T.C., 1998. The seismic reflection Moho beneath the United Kingdom and adjacent areas. Tectonophysics 299 (4), 255–279.

Chauvel, C., Hemond, C., 2002. Melting of a complete section of recycled oceanic crust: trace element and Pb isotopic evidence from Iceland. Geochem. Geophys. Geosyst. 1 http://dx.doi.org/10.1029/1999GC000002.

Chekunov, A.V. (Ed.), 1994. The Lithosphere of the Central and Eastern Europe—Young Platforms and the Alpine Fold Belt. Naukova Dumka, Kiev (in Russian).

Chekunov, A.V., Garvish, V.K., Kutas, R.I., Ryabchun, L.I., 1992. Dnepr–Donets palaeorift. Tectonophysics 208, 257–272.

Chekunov, A.V., Kaluzhnaya, L.T., Ryabchun, L.I., 1993. The Dnieper–Donets paleorift, Ukraine—deep structures and hydrocarbon accumulations. J. Pet. Geol. 16, 183–196.

Cherepanova, Yu., Artemieva, I.M., Thybo, H., Chemia, Z., 2013. Crustal structure of the Siberian Craton and the West Siberian Basin: an appraisal of existing seismic data. Tectonophysics 609, 154–183 (in this volume).

Chian, D.P., Keen, C., Reid, I., Louden, K.E., 1995a. Evolution of nonvolcanic rifted margins — new results from the conjugate margins of the Labrador Sea. Geology 23 (7), 589–592.

Chian, D.P., Louden, K., 1992. The structure of Archean–Ketilidian crust along the continental-shelf of southwestern Greenland from a seismic refraction profile. Can. J. Earth Sci. 29, 301–313.

Chian, D.P., Louden, K., 1994. The continent–ocean crustal transition across the southwest Greenland margin. J. Geophys. Res. 99 (B5), 9117–9135.

Chian, D.P., Louden, K.E., Minshull, T.A., Whitmarsh, R.B., 1999. Deep structure of the ocean–continent transition in the southern Iberia Abyssal Plain from seismic refraction profiles: Ocean Drilling Program (Legs 149 and 173) transect. J. Geophys. Res. 104 (B4), 7443–7462.

Chian, D.P., Louden, K.E., Reid, I., 1995b. Crustal structure of the Labrador Sea conjugate margin and implications for the formation of nonvolcanic continental margins. J. Geophys. Res. Solid Earth 100 (B12), 24239–24253.

Christensen, N.I., Mooney, W.D., 1995. Seismic velocity structure and composition of the continental crust: a global view. J. Geophys. Res. 100, 9761–9788.

Christie, P.A., 1982. Interpretation of refraction experiments in the North Sea. Philos. Trans. R. Soc. Lond. 305, 101–112.

Clark, S.A., Faleide, J.I., Hauser, J., et al., 2013. Stochastic velocity inversion of seismic reflection/refraction traveltime data for rift structure of the southwest Barents Sea. Tectonophysics 593, 135–150 http://dx.doi.org/10.1016/j.tecto.2013.1002.1033.

Clement, C., Hirn, A., Charvis, P., Sachpazi, M., Marnelis, F., 2000. Seismic structure and the active Hellenic subduction in the Ionian islands. Tectonophysics 329, 141–156.

Clement, C., et al., 2004. Reflection-refraction seismics in the Gulf of Corinth: hints at deep structure and control of the deep marine basin. Tectonophysics 391 (1–4), 97–108.

Cloetingh, S.A.P.L., Burov, E., Matenco, L., 2004. Thermo-mechanical controls on the mode of continental collision in the SE Carpathians (Romania). Earth Planet. Sci. Lett. 218, 57–76.

Clowes, R.M., Kanasewi, E.R., Cumming, G.L., 1968. Deep crustal seismic reflections at near-vertical incidence. Geophysics 33 http://dx.doi.org/10.1190/1191.1439942.

Contrucci, I., et al., 2005. Deep structure of the North Tyrrhenian Sea from multi-channel seismic profiles and on land wide angle reflection/refraction seismic recording (LISA cruise): geodynamical implications. Tectonophysics 406 (3–4), 141–163.

Coward, M.P., Dietrich, D., Park, R.G., 1987. Alpine Tectonics. Geol. Soc. Spec. Publ. No. 45.

Cowie, L., Kusznir, N., 2012. Gravity inversion mapping of crustal thickness and lithosphere thinning for the eastern Mediterranean. Lead. Edge 31, 810–814 http://dx.doi.org/10.1190/tle31070810.1.

Czuba, W., 2007. 2.5-D seismic tomographic modelling of the crustal structure of north-western Spitsbergen based on deep seismic soundings. Mar. Geophys. Res. 28, 213–233.

Czuba, W., Grad, M., Guterch, A., et al., 2008. Seismic crustal structure along the deep transect Horsted'05, Svalbard. Pol. Polar Res. 29 (3), 279–290.

Czuba, W., Grad, M., Mjelde, R., et al., 2011. Continent–ocean-transition across a trans-tensional margin segment: off Bear Island, Barents Sea. Geophys. J. Int. 184, 541–554.

Czuba, W., et al., 2005. Crustal structure of northern Spitsbergen along the deep seismic transect between the Molloy Deep and Nordaustlandet. Geophys. J. Int. 161 (2), 347–364.

Dahl-Jensen, T., Dyrelius, D., Juhlin, C., Palm, H., Pedersen, L.B., 1987. Deep reflection seismics in the Precambrian of Sweden. Geophys. J. Roy. Astron. Soc. 89, 371–378.

Dahl-Jensen, T., Larsen, T.B., Voss, P., 2012. Sedimentary thickness from Receiver Function analysis — a simple approach. Case study from North Greenland. Geophys. Res. Abstr. 14 EGU2012-1649-1.

Dahl-Jensen, T., Larsen, T.B., Woelbern, I., et al., 2003. Depth to Moho in Greenland: receiver-function analysis suggests two Proterozoic blocks in Greenland. EPSL 205, 379–393.

Dahl-Jensen, T., Thybo, H., Hopper, J., Rosing, M., 1998. Crustal structure at the SE Greenland margin from wide-angle and normal incidence seismic data. Tectonophysics 288, 191–198.

Dallmeyer, R.D., Tucker, R.D., 1993. U–Pb zircon age for the Lagoa–Augen-gneiss, Morais complex, Portugal — tectonic implications. J. Geol. Soc. 150, 405–408.

Darbyshire, F.A., White, R.S., Priestley, K.F., 2000. Structure of the crust and uppermost mantle of Iceland from a combined seismic and gravity study. EPSL 181, 409–428.

de Lis Mancilla, F., Stich, D., Morales, J., et al., 2012. Crustal thickness variations in northern Morocco. J. Geophys. Res. 117 http://dx.doi.org/10.1029/2011JB008608 (Article Number: B02312).

Dentith, M.C., Hall, J., 1989. Mavis — an upper crustal seismic refraction experiment in the midland valley of Scotland. Geophys. J. Int. 99 (3), 627–643.
Dewey, J.F., 1982. Plate-tectonics and the evolution of the British-Isles. J. Geol. Soc. 139, 371–412.
Dezes, P., Schmid, S.M., Ziegler, P.A., 2004. Evolution of the European Cenozoic Rift System: interaction of the Alpine and Pyrenean orogens with their foreland lithosphere. Tectonophysics 389 (1–2), 1–33.
Di Bona, M., Lucente, F.P., Agostinetti, N.P., 2008. Crustal structure and Moho depth profile crossing the central Apennines (Italy) along the N42° parallel. J. Geophys. Res. 113 http://dx.doi.org/10.1029/2008JB005625.
Díaz, J., Gallart, J., 2009. Crustal structure beneath the Iberian Peninsula and surrounding waters: a new compilation of deep seismic sounding results. Phys. Earth Planet. Inter. 173, 181–190 http://dx.doi.org/10.1016/j.pepi.2008.11.008.
Díaz, J., Gallart, J., Pulgar, J.A., Ruiz, M., Pedreira, D., 2009. Crustal structure beneath North-West Iberia imaged using receiver functions. Tectonophysics 478, 175–183.
Díaz, J., Hirn, A., Gallart, J., Abalos, B., 1996. Upper-mantle anisotropy in SW Iberia from long-range seismic profiles and teleseismic shear-wave data. Phys. Earth Planet. Inter. 95 (3–4), 153–166.
Díaz, J., Pedreira, D., Ruiz, M., Pulgar, J.A., Gallart, J., 2012. Mapping the indentation between the Iberian and Eurasian plates beneath the Western Pyrenees/Eastern Cantabrian Mountains from receiver function analysis. Tectonophysics http://dx.doi.org/10.1016/j.tecto.2012.1007.1005.
Divins, D.L., 2008. NGDC total sediment thickness of the world's oceans & marginal seas. http://www.ngdc.noaa.gov/mgg/sedthick/sedthick.html.
DOBREfraction'99 Working Group, 2003. "DOBREfraction'99"-velocity model of the crust and upper mantle beneath the Donbas Foldbelt (East Ukraine). Tectonophysics 371, 81–110.
Dohr, G., Fuchs, K., 1967. Statistical evaluation of deep crustal reflections in Germany. Geophysics 32, 951–967.
Doloei, J., Roberts, R., 2003. Crust and uppermost mantle structure of Tehran region from analysis of teleseismic P-waveform receiver functions. Tectonophysics 364 (3–4), 115–133.
Døssing, A., Dahl-Jensen, T., Thybo, H., Mjelde, R., Nishimura, Y., 2008. The East Greenland Ridge in the North Atlantic Ocean: an integrated geophysical study of a continental sliver in a boundary transform fault setting. J. Geophys. Res. 113 http://dx.doi.org/10.1029/2007JB005536.
Drachev, S.S., Malyshev, N.A., Nikishin, A.M., 2010. Tectonic history and petroleum geology of the Russian Arctic Shelves: an overview. Pet. Geol. Conf. Ser. 7, 591–619.
Drakatos, G., Karastathis, V., Makris, J., Papoulia, J., Stavrakakis, G., 2005. 3D crustal structure in the neotectonic basin of the Gulf of Saronikos (Greece). Tectonophysics 400 (1–4), 55–65.
Druzhinin, V.S., Egorkin, A.V., Kashubin, S.N., 1990. New data on the deep structure of the Urals and adjacent regions from DSS studies. Dokl. Akad. Nauk SSSR 315 (5), 1086–1090 (in Russian).
Druzhinin, V.S., Kashubin, S.N., Kashubina, T.V., Kolmogorova, V.A., Parygin, G.V., Rybalka, A.V., Tiunova, A.M., 1997. The main features of the interface between the crust and the upper mantle in the Middle Urals (in the vicinity of the deep drillhole SG-4). Tectonophysics 269, 259–267.
Du, Z.J., Foulger, G.R., Julian, B.R., et al., 2002. Crustal structure beneath western and eastern Iceland from surface waves and receiver functions. Geophys. J. Int. 149, 349–363.
Dubuisson, G., Mercier, J.C.C., Girardeau, J., et al., 1989. Evidence for a lost ocean in Variscan terranes of the western Massif Central, France. Nature 337, 729–732.
Duin, E.J.T., Doornenbal, J.C., Rijkers, R.H.B., Verbeek, J.W., Wong, T.E., 2006. Subsurface structure of the Netherlands — results of recent onshore and offshore mapping. Geol. Mijnb. 85 (4), 245–276.
Duin, E., Rijkers, R., Remmelts, G., 1995. Deep seismic reflections in the Netherlands, an overview. Geol. Mijnb. 74 (3), 191–197.
Duschenes, J., Sinha, M.C., Louden, K.E., 1986. A seismic refraction experiment in the Tyrrhenian Sea. Geophys. J. Roy. Astron. Soc. 85, 139–160.
ECORS Pyrenees Team, 1988. The ECORS deep reflection seismic survey across the Pyrenees. Nature 331, 508–510.
Effimoff, I., 2002. Future hydrocarbon potential of Kazakhstan. Pet. Provinces of the Twenty-First Century 74, 243–258.
Egger, A., Demartin, M., Ansorge, J., Banda, E., Maistrello, M., 1988. The gross structure of the crust under Corsica and Sardinia. Tectonophysics 150 (3), 363–389.
Egorkin, A.V., 1991. Crustal structure from seismic long-range profiles. In: Beloussov, V.V. (Ed.), Deep Structure of the Territory of the USSR. Nauka, Moskva, pp. 118–134.
Egorkin, A.V., 1999. Velocity structure, composition and discrimination of crustal provinces in the former Soviet Union. Tectonophysics 298 (198), 395–404.
Eldholm, O., Grue, K., 1994. North-Atlantic volcanic margins — dimensions and production-rates. J. Geophys. Res. 99, 2955–2968.
Eldholm, O., Tsikalas, F., Faleide, J.I., 2002. The continental margin off Norway 62–75°N: Palaeogene tectono-magmatic segmentation and sedimentation. The North Atlantic Igneous Province: Stratigraphy, Tectonics, Volcanic and Magmatic Processes. In: Jolley, D.W., Bell, B.R. (Eds.), Geol. Soc., London, Spec. Pub. pp. 39–68.
Engen, O., Faleide, J.I., Dyreng, T.K., 2008. Opening of the Fram Strait gateway: a review of plate tectonic constraints. Tectonophysics 450 (1–4), 51–69.
England, R.W., Hobbs, R.W., 1997. The structure of the Rockall Trough imaged by deep seismic reflection profiling. J. Geol. Soc. 154, 497–502.
Erinchek, Yu.M., Milstein, E.D., 2006. Crustal structure in Russia from national seismic surveys. VSEGEI, St. Petersburg. Ministry of Natural, Resources, Russia (unpublished).
EUGENO-S Working Group, 1988. Crustal structure and tectonic evolution of the transition between the Baltic Shield and the North German Caledonides (the EUGENO-S project). Tectonophysics 150 (3), 253–348.
EUROBRIDGE Seismic WG, 2001. EUROBRIDGE'95: deep seismic profiling within the East European Craton. Tectonophysics 339, 153–175.
EUROBRIDGE Seismic Working Group, 1999. Seismic velocity structure across the Fennoscandia–Sarmatia suture of the East European Craton beneath the EUROBRIDGE profile through Lithuania and Belarus. Tectonophysics 314, 193–217.
EUROBRIDGE Seismic Working Group, 2000. EUROBRIDGE'97: modelling of S-waves field on the EB'97 seismic profile. Geophys. J. (Kiev) 22, 87–88.
EXXON, 1985. Tectonic map of the world. Scale 1:10,000,000. Exxon Prod. Research Co., AAPGF, Tulsa, OK, USA.
Faccenna, C., Funiciello, F., Giardini, D., Lucente, P., 2001. Episodic back-arc extension during restricted mantle convection in the central Mediterranean. Earth Planet. Sci. Lett. 187, 105–116.
Faleide, J.I., Tsikalas, F., Breivik, A.J., Mjelde, R., Ritzmann, O., Engen, O., Wilson, J., Eldholm, O., 2008. Structure and evolution of the continental margin off Norway and Barents Sea. Episodes 31, 82–91.
Fedorova, T., Jacoby, W.R., Wallner, H., 2005. Crust–mantle transition and Moho model for Iceland and surroundings from seismic, topography, and gravity data. Tectonophysics 396, 119–140.
Fernandez-Suarez, J., Alonso, G.G., Cox, R., et al., 2002. Assembly of the Armorica microplate: a strike-slip terrane delivery? Evidence from U–Pb ages of detrital zircons. J. Geol. 110, 619–626.
Fernandez-Viejo, G., Gallart, J., Pulgar, J.A., Gallastegui, J., Danobeitia, J.J., Cordoba, D., 1998. Crustal transition between continental and oceanic domains along the North Iberian margin from wide angle seismic and gravity data. Geophys. Res. Lett. 25, 4249–4252.
Ferrer, O., Roca, E., Benjumea, B., Muñoz, J.A., Ellouz, N., the MARCONI Team, 2008. The deep seismic reflection MARCONI-3 profile: role of extensional Mesozoic structure during the Pyrenean contractional deformation at the eastern part of the Bay of Biscay. Mar. Pet. Geol. 25, 714–730 http://dx.doi.org/10.1016/j.marpetgeo.2008.06.002.
FIRE Working Group, 1996. Seismic images of crust beneath Iceland contribute to long-standing debate. Eos 77 (21), 197 (199).
Flecha, I., et al., 2006. Imaging granitic plutons along the IBERSEIS profile. Tectonophysics 420 (1–2), 37–47.
Foulger, G.R., Anderson, D.L., 2005. A cool model for the Iceland hotspot. J. Volcanol. Geotherm. Res. 141 (1–2), 1–22.
Foulger, G.R., Natland, J.H., Anderson, D.L., 2005. Genesis of the Iceland melt anomaly by plate tectonic processes. Plates, plumes, and paradigms. In: Foulger, G.R., Natland, J.H., Presnall, D.C., Anderson, D.L. (Eds.), Geological Society of America, Special Paper, 388, pp. 595–626 (Boulder, CO, USA).
Fowler, S.R., White, R.S., Westbrook, G.K., Spence, G.D., 1989. The Hatton Bank continental margin, II. Deep structure from two-ship expanding spread seismic profiles. Geophys. J. 96, 295–309.
Frassetto, A., Thybo, H., 2013. Receiver function analysis of the crust and upper mantle in Fennoscandia — isostatic implications. Earth Planet. Sci. Lett. http://dx.doi.org/10.1016/j.epsl.2013.07.001 (in press).
Friberg, M., Juhlin, C., Roth, J., Horstmeyer, H., Rybalka, A., Bliznetsov, M., 2001. Europrobe seismic reflection profiling across the eastern Middle Urals and West Siberian Basin. Terra Nova 14, 7–13.
Fuchs, K., Muller, G., 1971. Computation of synthetic seismograms with reflectivity method and comparison with observations. Geophys. J. Roy. Astron. Soc. 23, 417–443.
Fuchs, K., et al., 1987. Crustal evolution of the Rhinegraben area. 1. Exploring the lower crust in the Rhinegraben rift by unified geophysical experiments. Tectonophysics 141 (1–3), 261–275.
Funck, T., Gohl, K., Damm, V., Heyde, I., 2012. Tectonic evolution of southern Baffin Bay and Davis Strait: Results from a seismic refraction transect between Canada and Greenland. J. Geophys. Res. 117 (B04107).
Gaal, R., Gorbatschev, R., 1987. An outline of the Precambrian evolution of the Baltic shield. Precambrian Res. 35, 15–52.
Gajewski, D., Holbrook, W.S., Prodehl, C., 1987. A 3-dimensional crustal model of southwest Germany derived from seismic refraction data. Tectonophysics 142 (1), 49–70.
Gallart, J., Daignieres, M., Gagnepainbeyneix, J., Hirn, A., 1985. Relationship between deep-structure and seismicity in the Western Pyrenees. Ann. Geophys. 3 (2), 239–248.
Garcia-Duenas, V., et al., 1992. A deep seismic-reflection survey across the Betic chain (southern Spain) — first results. Tectonophysics 232, 77–89.
Garetskii, R.G., Boborykin, A.M., Bogino, V.A., German, V.A., Veres, S.A., Klushin, S.V., Shafaruk, V.G., 1990. Deep seismic sounding on the territory of Belorussia. Geophys. J. Int. 8, 439–448.
Garkalenko, I.A., 1970. The deep-seated crustal structure in the western part of the Black sea and adjacent areas: seismic reflection measurement. Tectonophysics 10, 539–547.
Gebrande, H., Miller, H., Einarsson, P., 1980. Seismic structure of Iceland along RRISP-Profile I. J. Geophys. 47, 239–249.
Gebrande, H., et al., 2006. TRANSALP — a transect through a young collisional orogen: Introduction. Tectonophysics 414 (1–4), 1–7.
Geissler, W.H., Kampf, H., Skacelova, Z., Plomerova, J., Babuska, V., Kind, R., 2012. Lithosphere structure of the NE Bohemian Massif (Sudetes) — a teleseismic receiver function study. Tectonophysics 564, 12–37.
GEON — Reports of DSS Profiles in the Soviet Union. Centre of Regional Geophysical and Geoecological Research (Russian Ministry of Geology), 1979–1994. Moscow.
Gernigon, L., Olesen, O., Ebbing, J., et al., 2009. Geophysical insights and early spreading history in the vicinity of the Jan Mayen Fracture Zone, Norwegian–Greenland Sea. Tectonophysics 468, 185–205.
Giese, P., Makris, J., Akashe, B., Rower, P., Letz, H., Mostaanpour, M., 1984. The crustal structure in Southern Iran derived from seismic explosion data. N. Jb. Geol. Paläeont. (Abh.) 168, 230–243.
Giese, P., Pavlenkova, N.I., 1988. Structural maps of the Earth's crust in Europe. Izv. Akad. Nauk SSSR Fiz. Zemli 10, 3–14 (in Russian).
Ginzburg, A., Makris, J., Fuchs, K., Prodehl, C., 1981. The structure of the crust and upper mantle in the Dead-Sea rift. Tectonophysics 80 (1–4), 109–119.

Ginzburg, A., Makris, J., Nicolich, R., 1986. European Geotraverse — a seismic refraction profile across the Ligurian Sea. Tectonophysics 126 (1), 85–97.
Ginzburg, A., et al., 1985. The deep seismic structure of the northern continental-margin of the Bay of Biscay. Ann. Geophys. 3 (4), 499–510.
Godin, Yu.N., 1969. Deep Structure of the Turkmenian Territory Based on Geophysical Data. Nauka, Moscow (252 pp. (in Russian).
Gohl, K., Smithson, S.B., 1993. Structure of Archean crust and passive margin of Southwest Greenland from seismic wide-angle data. J. Geophys. Res. Solid Earth 98 (B4), 6623–6638.
Gök, R., Mahdi, H., Al-Shukri, H., Rodgers, A., 2008. Crustal structure of Iraq from receiver functions and surface wave dispersion: implications for understanding the deformation history of the Arabian–Eurasian collision. Geophys. J. Int. 172, 1179–1187.
Gok, R., Pasyanos, M.E., Zor, E., 2007. Lithospheric structure of the continent–continent collision zone: eastern Turkey. Geophys. J. Int. 169 (3), 1079–1088.
Gomez, M., et al., 2004. Extensional geometry of the mid Norwegian Margin before Early Tertiary continental breakup. Mar. Pet. Geol. 21 (2), 177–194.
Gonzalez-Fernandez, A., Cordoba, D., Matias, L.M., Torne, M., 2001. Seismic crustal structure in the Gulf of Cadiz (SW Iberian Peninsula). Mar. Geophys. Res. 22 (3), 207–223.
Gorbatschev, R., Bogdanova, S., 1993. Frontiers in the Baltic Shield. Precambrian Res. 64, 3–22.
Grad, M., Guterch, A., Lund, C.E., 1991. Seismic models of the lower lithosphere beneath the southern Baltic Sea between Sweden and Poland. Tectonophysics 189 (1–4), 219–227.
Grad, M., Guterch, A., Polkowska-Purys, A., 2005. Crustal structure of the Trans-European suture zone in Central Poland — reinterpretation of the LT-2, LT-4 and LT-5 deep seismic sounding profiles. Geol. Q. 49, 243–252.
Grad, M., Jensen, S.L., Keller, G.R., et al., 2003. Crustal structure of the Trans-European suture zone region along POLONAISE'97 seismic profile P4. J. Geophys. Res. 108 (B11) (Article Number: 2541).
Grad, M., Keller, G.R., Thybo, H., Guterch, A., 2002. Lower lithospheric structure beneath the Trans-European suture zone from POLONAISE'97 seismic profiles. Tectonophysics 360, 153–168.
Grad, M., Luosto, U., 1987. Seismic models of the crust of the Baltic shield along the SVEKA profile in Finland. Ann. Geophys. 5B, 639–650.
Grad, M., Tiira, T., ESC Moho Working Group, 2009. The Moho depth of the European plate. Geophys. J. Int. 176, 279–292.
Grad, M., Tripolsky, A.A., 1995. Crustal structure from P-seismic-wave and S-seismic-wave and petrological models of the Ukrainian shield. Tectonophysics 250 (1–3), 89–112.
Grad, M., et al., 1999. Crustal structure of the Mid-Polish Trough beneath the Teisseyre–Tornquist Zone seismic profile. Tectonophysics 314 (1–3), 145–160.
Grad, M., Guterch, A., Keller, G.R., et al., 2006a. Lithospheric structure beneath trans-Carpathian transect from Precambrian platform to Pannonian basin: CELEBRATION 2000 seismic profile CEL05. J. Geophys. Res. Solid Earth 111 http://dx.doi.org/10.1029/2005jb003647.
Grad, M., et al., 2006b. Lithospheric structure of the western part of the East European Craton investigated by deep seismic profiles. Geol. Q. 50 (1), 9–22.
Gradstein, F.M., Ogg, J.G., Schmitz, M.D., Ogg, G.M., 2012. The Geologic Time Scale 2012. Elsevier (1176 pp.).
Grandjean, G., Guennoc, P., Recq, M., Andreo, P., 2001. Refraction/wide-angle reflection investigation of the Cadomian crust between northern Brittany and the Channel Islands. Tectonophysics 331 (1–2), 45–64.
Grauert, B., Hanny, R., Soptraja, G., 1973. Age and origin of detrital zircons from pre-Permian basements of Bohemian-Massif and Alps. Contrib. Mineral. Petrol. 40, 105–130.
Gregersen, S., 1991. Crustal structure across the Tornquist Zone (southwestern edge of the Baltic Shield): a review of the Eugeno-S geophysical results. Tectonophysics 189, 165–182.
Grevemeyer, I., Weigel, W., Whitmarsh, R.B., Avedik, F., Dehghani, G.A., 1997. The Aegir Rift: crustal structure of an extinct spreading axis. Mar. Geophys. Res. 19 (1), 1–23.
Guerrot, C., 1989. Archean protoliths within early Proterozoic granulitic crust of the west European Hercynian belt — possible relics of the West-African craton. Geology 17, 241–244.
Guggisberg, B., Kaminski, W., Prodehl, C., 1991. Crustal structure of the Fennoscandian Shield: a traveltime interpretation of the long-range FENNOLORA seismic refraction profile. Tectonophysics 195, 105–137.
Gurbuz, C., Evans, J.R., 1991. A seismic refraction study of the western Tuz Golu basin, central Turkey. Geophys. J. Int. 106 (1), 239–251.
Guterch, A., Grad, M., Janik, T., Materzok, R., Luosto, U., Yliniemi, J., Luck, E., Schulze, A., Forster, K., 1994. Crustal structure of the transition zone between Precambrian and Variscan Europe from new seismic data along LT-7 profile (NW Poland and eastern Germany). C. R. Acad. Sci. (Paris) II 319, 1489–1494.
Guterch, A., Grad, M., Materzok, R., Perchuc, E., 1986. Deep structure of the Earth's crust in the contact zone of the Palaeozoic and Precambrian platforms in Poland (Tornquist–Teisseyre Zone). Tectonophysics 128 (3–4), 251–279.
Guterch, A., Grad, M., Spicak, A., et al., 2003. An overview of recent seismic refraction experiments in Central Europe. Stud. Geophys. Geod. 47 (3), 651–657.
Guterch, A., Grad, M., Thybo, H., Keller, G.R., 1999. POLONAISE '97 — an international seismic experiment between Precambrian and Variscan Europe in Poland. Tectonophysics 314 (1–3), 101–121.
Gutierrez-Alonso, G., Fernandez-Suarez, J., Collins, A.S., et al., 2005. Amazonian Mesoproterozoic basement in the core of the Ibero-Armorican Arc: $^{40}Ar/^{39}Ar$ detrital mica ages complement the zircon's tale. Geology 33, 637–640.
Haan, E.A., Arnott, R.J., 1991. The late Tertiary evolution of the Alpine system of the Mediterranean area. In: Spencer, A.M. (Ed.), Generation, Accumulation and Production of Europe's Hydrocarbons. Sp. Publ. EAPG No. 1. Oxford University Press, pp. 341–354.
Hamilton, W., 1970. The Uralides and the motion of the Russian and Siberian platforms. Geol. Soc. Am. Bull. 81, 2553–2576.
Harland, W.B. (Ed.), 1997. The Geology of Svalbard. Geol. Soc. Mem., vol. 17. Geological Society, London.
Hatzfeld, D., Tatar, M., Priestley, K., et al., 2003. Seismological constraints on the crustal structure beneath the Zagros Mountain belt (Iran). Geophys. J. Int. 155, 403–410.
Hauser, F., Raileanu, V., Fielitz, W., Bala, A., Prodehl, C., Polonic, G., Schulze, A., 2001. VRANCEA99—the crustal structure beneath the southeastern Carpathians and the Moesian Platform from a seismic refraction profile in Romania. Tectonophysics 340, 233–256.
Hauser, F., et al., 2007. Seismic crustal structure between the Transylvanian basin and the Black Sea, Romania. Tectonophysics 430 (1–4), 1–25.
Hirn, A., et al., 1996. A traverse of the Ionian islands front with coincident normal incidence and wide-angle seismics. Tectonophysics 264 (1–4), 35–49.
Hirschlebar, H.B., et al., 1975. Seismic investigations along the Scandinavian "Blue Road" traverse. J. Geophys. 41, 135–148.
Holbrook, W.S., et al., 2001. Mantle thermal structure and active upwelling during continental breakup in the North Atlantic. Earth Planet. Sci. Lett. 190, 251–266.
Holder, A.P., Bott, M.H.P., 1971. Crustal structure in vicinity of south-west England. Geophys. J. Roy. Astron. Soc. 23 (5), 465.
Horvath, F., Bada, G., Szafian, P., et al., 2006. Formation and deformation of the Pannonian Basin: constraints from observational data. European Lithosphere Dynamics. In: Gee, D., Stephenson, R. (Eds.), Geol. Soc. London Sp. Publ., 32, pp. 191–206.
Hrubcova, P., et al., 2005. Crustal and uppermost mantle structure of the Bohemian Massif based on CELEBRATION 2000 data. J. Geophys. Res. 110 (B11).
Ilchenko, T.V., 1990. Velocity model of the earth's crust in the Ukrainian shield along the Geotraverse VIII (Reni-Krivoi Rog). Geophys. J. Int. 9, 55–62.
Ilchenko, T., 1996. Dniepr–Donets Rift: deep structure and evolution from DSS profiling. Tectonophysics 268, 83–98.
ILIHA DSS Group, 1993. A deep seismic sounding investigation of lithospheric heterogeneity and anisotropy beneath the Iberian Peninsula. Tectonophysics 221, 35–51.
Ismail-Zadeh, A.T., Kostyuchenko, S.L., Naimark, B.M., 1997. The Timan–Pechora Basin (northeastern European Russia): tectonic subsidence analysis and a model of formation mechanism. Tectonophysics 283 (1–4), 205–218.
Ivan, M., 2011. Crustal thickness in Vrancea area, Romania from S to P converted waves. J. Seismol. 15, 317–328.
Ivanova, N.M., Sakoulina, T.S., Roslov, Y.V., 2006. Deep seismic investigation across the Barents–Kara region and Novozemelskiy Fold Belt (Arctic Shelf). Tectonophysics 420, 123–140.
Ivanova, N.M., Sakulina, T.S., Belyaev, I.V., et al., 2011. Depth model of the Barents and Kara seas according to geophysical surveys results. Arctic Petroleum Geology. In: Spencer, A.M., Embry, A.F., Gautier, D.L., Stoupakova, A.V., Sørensen, K. (Eds.), Geological Society, London, Memoirs, 35, pp. 209–221 http://dx.doi.org/10.1144/M35.12 (Chapter 12).
Ivanovsky, I.K., 1896. Krasnovodsk earthquake of 27.06.1895. Zheleznodorozhnoe delo, 40.
Janik, T., Grad, M., Guterch, A., et al., 2011. Crustal structure of the Western Carpathians and Pannonian Basin: seismic models from CELEBRATION 2000 data and geological implications. J. Geodyn. 52, 97–113.
Janik, T., Kozlovskaya, E., Heikkinen, P., et al., 2009. Evidence for preservation of crustal root beneath the Proterozoic Lapland–Kola orogen (northern Fennoscandian shield) derived from P and S wave velocity models of POLAR and HUKKA wide-angle reflection and refraction profiles and FIRE4 reflection transect. J. Geophys. Res. 114, B06308.
Janik, T., Yliniemi, J., Grad, M., Thybo, H., Tiira, T., 2002. Crustal structure across the TESZ along POLONAISE'97 seismic profile P2 in NW Poland. Tectonophysics 360 (1–4), 129–152.
Janik, T., et al., 2005. Lithospheric structure of the Trans-European suture zone along the TTZ-CEL03 seismic transect (from NW to SE Poland). Tectonophysics 411 (1–4), 129–156.
Japsen, P., 1998. Regional velocity–depth anomalies, North Sea Chalk; a record of overpressure and Neogene uplift and erosion. AAPG Bull. 82, 2031–2074.
Japsen, P., Chalmers, J.A., 2000. Neogene uplift and tectonics around the North Atlantic: overview. Glob. Planet. Chang. 24, 165–173.
Jensen, S.L., Janik, T., Thybo, H., 1999. Seismic structure of the Palaeozoic Platform along POLONAISE'97 profile P1 in northwestern Poland. Tectonophysics 314 (1–3), 123–143.
Jensen, S.L., Thybo, H., Polonaise'97 Working Group., 2002. Moho topography and lower crustal wide-angle reflectivity around the TESZ in southern Scandinavia and northeastern Europe. Tectonophysics 360 (1–4), 187–213.
Jokat, W., Schmidt-Aursch, M.C., 2007. Geophysical characteristics of the ultraslow spreading Gakkel Ridge, Arctic Ocean. Geophys. J. Int. 168, 983–998.
Jones, E.J.W., White, R.S., Hughes, V.J., Matthews, D.H., Clayton, B.R., 1984. Crustal structure of the continental-shelf off northwest Britain from 2-ship seismic experiments. Geophysics 49 (10), 1605–1621.
Juhlin, C., Brown, D., Rybalka, A., Petrov, G., 2007. Moho imbrication in the Middle Urals. Terra Nova 19 (3), 189–194.
Juhlin, C., Friberg, M., Echtler, H.P., Hismatulin, T., Rybalka, A., Green, A.G., Ansorge, J., 1998. Crustal structure of the Middle Urals: results from the (ESRU) Europrobe seismic reflection profiling in the Urals experiments. Tectonics 17 http://dx.doi.org/10.1029/98TC02762.
Juhlin, C., Knapp, J.H., Kashubin, S., Bliznetsov, M., 1996a. Crustal evolution of the Middle Urals based on seismic reflection and refraction data. Tectonophysics 264 (1–4), 21–34.
Juhlin, C., Stephenson, R.A., Klushin, S., 1996b. Reappraisal of deep seismic reflection profile VIII across the Pripyat Trough. Tectonophysics 268, 99–108.
Kaban, M.K., Flovenz, O.G., Palmason, G., 2002. Nature of the crust–mantle transition zone and the thermal state of the upper mantle beneath Iceland from gravity modeling. Geophys. J. Int. 149, 281–299.

Kalsbeek, F., 1993. Geochronology of Archean and Proterozoic events in the Ammassalik area, south-east Greenland, and comparisons with the Lewisian of Scotland and the Nagssugtoqidian of West Greenland. Precambrian Res. 62, 239–270.
Kandilarov, A., Mjelde, R., Okino, K., Murai, Y., 2008. Crustal structure of the ultra-slow spreading Knipovich Ridge, North Atlantic, along a presumed amagmatic portion of oceanic crustal formation. Mar. Geophys. Res. 29 (2), 109–134.
Karagianni, E.E., et al., 2002. Rayleigh wave group velocity tomography in the Aegean area. Tectonophysics 358 (1–4), 187–209.
Kashubin, S., Juhlin, C., Friberg, M., et al., 2006. Crustal structure of the Middle Urals based on seismic reflection data. European Lithosphere Dynamics. In: Gee, D.G., Stephenson, R.A. (Eds.), Geological Society, London, Memoirs, 32, pp. 427–442.
Kelly, A., England, R.W., Maguire, P.K.H., 2007. A crustal seismic velocity model for the UK, Ireland and surrounding seas. Geophys. J. Int. 171, 1172–1184.
Khais, K., Tsokas, G.N., 1999. Nature of the Levantine (eastern Mediterranean) crust from multiple-source Werner deconvolution of Bouguer gravity anomalies. J. Geophys. Res. 104, 25469–25478.
Kinck, J.J., Husebye, E.S., Larsson, F.R., 1993. The Moho depth distribution in Fennoscandia and the regional tectonic evolution from Archean to Permian times. Tectonophysics 64 (1–4), 23–51.
Kissling, E., 1994. Deep structure of the Alps; what do we really know? Phys. Earth Planet. Inter. 11 (1–2), 87–112.
Klingelhofer, F., Edwards, R.A., Hobbs, R.W., et al., 2005. Crustal structure of the NE Rockall Trough from wide-angle seismic data modeling. J. Geophys. Res. 110, B11105 http://dx.doi.org/10.1029/2005JB003763.
Knapp, J.H., et al., 1998. Seismic reflection fabrics of continental collision and post-orogenic extension in the Middle Urals, central Russia. Tectonophysics 288 (1–4), 115–126.
Knapp, J.H., et al., 2005. Crustal constraints on the origin of mantle seismicity in the Vrancea zone, Romania: the case for active continental lithospheric delamination. Tectonophysics 410 (1–4), 311–323.
Kodaira, S., Goldschmidt-Rokita, A., Hartmann, J.M., Hirschleber, H.B., Iwasaki, T., Kanazawa, T., Krahn, H., Tomita, S., Shimamura, H., 1995. Crustal structure of the Lofoten continental margin, off northern Norway, from ocean-bottom seismographic studies. Geophys. J. Int. 121, 907–924.
Kodaira, S., Mjelde, R., Gunnarsson, K., Shiobara, H., Shimamura, H., 1997. Crustal structure of the Kolbeinsey Ridge, North Atlantic, obtained by the use of ocean bottom seismographs. JGR 102 (B2), 3131–3151.
Kodaira, S., Mjelde, R., Gunnarsson, K., Shiobara, H., Shimamura, H., 1998. Structure of the Jan Mayen microcontinent and implications for its evolution. Geophys. J. Int. 132, 383–400.
Kondorskaya, N., Shebalin, N., 1977. New Catalog of Strong Earthquakes in the Territory of the USSR from Ancient Times to 1975, Academy of Sciences, Moscow, English translation, updated through 1977, available as Report SE-31. World Data Center A for Solid Earth Geophysics, Boulder, CO 606 pp.
Konert, G., Afifi, A.M., Al-Harjri, S.A., Droste, H.J., 2001. Paleozoic stratigraphic and hydrocarbon habitat of the Arabian Plate. GeoArabia 6, 407–442.
Korenaga, J., Kelemen, P.B., 2000. Major element heterogeneity in the mantle source of the North Atlantic igneous province. Earth Planet. Sci. Lett. 184, 251–268.
Korja, A., Heikkinen, P., Aaro, S., 2001. Crustal structure of the northern Baltic Sea palaeorift. Tectonophysics 331, 341–358.
Korsman, K., Korja, T., Pajunen, M., Virransalo, P., GGT/SVEKA WG, 1999. The GGT/SVEKA transect: structure and evolution of the continental crust in the Palaeoproterozoic Svecofennian orogen in Finland. Int. Geol. Rev. 41, 287–333.
Kosminskaya, I.P., Riznichenko, Y.V., 1964. Seismic studies of the earth's crust in Eurasia. In: Odishaw, H. (Ed.), Solid Earth and Interface Phenomena. Research in Geophysics, vol. 2. MIT Press, Cambridge, pp. 81–122.
Kostyuchenko, S.L., 1999. Structure of the Crust in Russia. (Dr. Sci. Thesis) GEON, Ministry of Natural Resources, Moscow, Russia (386 pp. (in Russian)).
Kostyuchenko, S.L., Egorkin, A.V., Solodilov, L.N., 1999. Structure and genetic mechanisms of the Precambrian rifts of the East-European Platform in Russia by integrated study of seismic, gravity and magnetic data. Tectonophysics 313, 9–28.
Kostyuchenko, S.L., Morozov, A.F., Stephenson, R.A., et al., 2004. The evolution of the southern margin of the East European Craton based on seismic and potential field data. Tectonophysics 381, 101–118.
Kostyuchenko, S.L., Romanyuk, T.V., 1997. Nature of the Mezen gravity maximum. Izvestya (translated from Fizika Zemli 1997, 12, 3–22) Phys. Solid Earth 33 (12), 961–980.
Kozlovskaya, E., Kosarev, G., Aleshin, I., et al., 2008. Structure and composition of the crust and upper mantle of the Archean–Proterozoic boundary in the Fennoscandian shield obtained by joint inversion of receiver function and surface wave phase velocity of recording of the SVEKALAPKO array. Geophys. J. Int. 175, 135–152.
Krasnopevtseva, U.V., 1984. Deep Structure of the Caucasus Seismic Region (in Russian). Nauka, Moscow (109 pp.).
Krawczyk, C.M., Eilts, F., Lassen, A., Thybo, H., 2002. Seismic evidence of Caledonian deformed crust and uppermost mantle structures in the northern part of the Trans-European Suture Zone, SW Baltic Sea. Tectonophysics 360 (1–4), 215–244.
Kukkonen, I.T., Lahtinen, R. (Eds.), 2006. Finish Reflection Experiment FIRE 2001–2005. Geol. Survey of Finland, Espoo (247 pp.).
Kumar, P., Kind, R., Priestley, K., Dahl-Jensen, T., 2007. Crustal structure of Iceland and Greenland from receiver function studies. JGR 112, B03301 http://dx.doi.org/10.1029/2005JB003991.
Kunin, N.Ya., Odekov, O.A., Semenova, G.I., 1973. Deep structure of the Southern Caspian. Izv. Akad. Nauk Turk. SSR, Ashkhabad, No. 5, pp. 19–26 (in Russian).
Kunin, N.Ya., Sheikh-Zade, E.R., Semenova, G.I., 1992. Structure of the Eurasian Lithosphere. MGC RAS, Moscow, Nauka (266 pp.).
Landes, M., O'Reilly, B.M., Readman, P.W., Shannon, P.M., Prodehl, C., 2003. VARNET-96: three-dimensional upper crustal velocity structure of SW Ireland. Geophys. J. Int. 153 (2), 424–442.
Lardeaux, J.M., et al., 2006. A crustal-scale cross-section of the south-western Alps combining geophysical and geological imagery. Terra Nova 18 (6), 412–422.
Laske, G., Masters, G., 1997. A global digital map of sediment thickness. EOS Trans. Am. Geophys. Union 78, F483.
Laske, G., Masters, G., Ma, Z., Pasyanos, M., 2013. Update on CRUST1.0 - A 1-degree Global Model of Earth's Crust. Geophys. Res. Abstracts, 15, Abstract EGU2013–2658 http://igppweb.ucsd.edu/~gabi/rem.html.
Lassen, A., Thybo, H., 2004. Seismic evidence for Late Proterozoic orogenic structures below the Phanerozoic sedimentary cover in the Kattegat area, SW Scandinavia. Tectonics 23 http://dx.doi.org/10.1029/2003TC001499.
Lassen, A., Thybo, H., 2012. Neoproterozoic and Palaeozoic evolution of SW Scandinavia based on integrated seismic interpretation. Precambrian Res. 204–205, 75–104.
Lassen, A., Thybo, H., Berthelsen, A., 2001. Reflection seismic evidence for Caledonian deformed sediments above Sveconorwegian basement in the southwestern Baltic Sea. Tectonics 20 (2), 268–276.
Lawver, L.A., Muller, R.D., 1994. Iceland hotspot track. Geology 22, 311–314.
Lefort, J.P., Agarwal, B.N.P., 2000. Gravity and geomorphological evidence for a large crustal bulge cutting across Brittany (France): a tectonic response to the closure of the Bay of Biscay. Tectonophysics 323 (3–4), 149–162.
Leonov, Yu.G., Volozh, Yu.A., 2004. Sedimentary Basins. Methods of Study, Structure and Evolution. Nauchny Mir, Moscow (570 pp.).
Li, X., et al., 2003. Receiver function study of the Hellenic subduction zone: imaging crustal thickness variations and the oceanic Moho of the descending African lithosphere. Geophys. J. Int. 155 (2), 733–748.
Lider, V.A., 1976. Quaternary Deposits of the Urals. Nedra, Moscow (144 pp. (in Russian)).
Lie, J.E., Andersson, M., 1998. The deep-seismic image of the crustal structure of the Tornquist Zone beneath the Skagerrak Sea, northwestern Europe. Tectonophysics 287 (1–4), 139–155.
Lie, J.E., Pedersen, T., Husebye, E.S., 1990. Observations of seismic reflectors in the lower lithosphere beneath the Skagerrak. Nature 346 (6280), 165–168.
Liebscher, H.J., 1964. Deutungsversuche für die Struktur der tieferen Erdkruste nach reflexionsseismischen und gravimetrischen Messungen im deutschen Alpenvorland. Z. Geophys. 30, 51–96 115–126.
Lippitsch, R., Kissling, E., Ansorge, J., 2003. Upper mantle structure beneath the Alpine orogen from high-resolution teleseismic tomography. J. Geophys. Res. 108 (B8), 2376 http://dx.doi.org/10.1029/2002JB002016.
Lizarralde, D., Holbrook, W.S., 1997. US mid-Atlantic margin structure and early thermal evolution. J. Geophys. Res. 102 (B10), 22855–22875.
Ljones, F., et al., 2004. Crustal transect from the North Atlantic Knipovich Ridge to the Svalbard margin west of hornsund. Tectonophysics 378 (1–2), 17–41.
Lobach-Zhuchenko, S.B. (Ed.), 1988. Greenstone Belts in the Basement of the East European Platform. Nauka, Leningrad (212 pp.).
Lobkovsky, L.I., et al., 1996. Extensional basins of the former Soviet Union—structure, basin formation mechanisms and subsidence history. Tectonophysics 266, 251–285.
Lundin, E.R., Dore, A.G., 2005. Fixity of the Iceland "hotspot" on the Mid-Atlantic Ridge: observational evidence, mechanisms, and implications for Atlantic volcanic margins. Plates, plumes, and paradigms. In: Foulger, G.R., Natland, J.H., Presnall, D.C., Anderson, D.L. (Eds.), Geological Society of America, Special Paper, 388, pp. 627–652 (Boulder, CO, USA).
Luosto, U., Tiira, T., Korhonen, H., Azbel, I., Burmin, V., Buyanov, A., Kosminskaya, I.P., Ionkis, V., Sharov, N., 1990. Crust and upper mantle structure along the DSS Baltic profile in SE Finland. Geophys. J. Int. 101, 89–110.
Luosto, U., Flueh, E.R., Lund, C.-E., working group, 1989. The crustal structure along the POLAR profile from seismic refraction investigation. Tectonophysics 162, 51–85 http://dx.doi.org/10.1016/0040-1951(89)90356-9.
Luschen, E., Lammerer, B., Gebrande, H., Millahn, K., Nicolich, R., 2004. Orogenic structure of the Eastern Alps, Europe, from TRANSALP deep seismic reflection profiling. Tectonophysics 388 (1–4), 85–102.
Luschen, E., et al., 2006. TRANSALP — deep crustal Vibrosels and explosive seismic profiling in the Eastern Alps. Tectonophysics 414 (1–4), 9–38.
Lyngsie, S.B., Thybo, H., 2007. A new tectonic model for the Laurentia–Avalonia–Baltica sutures in the North Sea: a case study along MONA LISA profile 3. Tectonophysics 429, 201–227.
Lyngsie, S.B., Thybo, H., Lang, R., 2007. Rifting and lower crustal reflectivity: a case study of the intracratonic Dnieper–Donets rift zone, Ukraine. J. Geophys. Res. 112, B12402 http://dx.doi.org/10.1029/2006JB004795.
Macdonald, R., Fettes, D.J., 2006. The tectonomagmatic evolution of Scotland. Trans. R. Soc. Edinb. Earth Sci. 97, 213–295.
Maguire, P., England, R., Hardwick, A., 2011. LISPB DELTA, a lithospheric seismic profile in Britain: analysis and interpretation of the Wales and southern England section. J. Geol. Soc. 168, 61–82.
Maillard, A., Malod, J., Thiebot, E., Klingelhoefer, F., Rehault, J.P., 2006. Imaging a lithospheric detachment at the continent–ocean crustal transition off Morocco. Earth Planet. Sci. Lett. 241 (3–4), 686–698.
Maillard, A., Mauffret, A., 2011. Structure and present-day compression in the offshore area between Alicante and Ibiza Island (Eastern Iberian Margin). Tectonophysics http://dx.doi.org/10.1016/j.tecto.2011.07.007.
Makris, J., Egloff, F., Nicolich, R., Rihm, R., 1999. Crustal structure from the Ligurian Sea to the Northern Apennines — a wide angle seismic transect. Tectonophysics 301 (3–4), 305–319.
Makris, J., Nicolich, R., Weigel, W., 1986. A seismic study in the western Ionian Sea. Ann. Geophys. B4, 665–678.
Makris, J., et al., 1983. Seismic refraction profiles between Cyprus and Israel and their interpretation. Geophys. J. Roy. Astron. Soc. 75 (3), 575–591.
Makris, J., et al., 1988. Continental-crust under the southern Porcupine Sea right west of Ireland. Earth Planet. Sci. Lett. 89 (3–4), 387–397.

Malinowski, M., Zelazniewicz, A., Grad, M., et al., 2005. Seismic and geological structure of the crust in the transition from Baltica to Palaeozoic Europe in SE Poland — CELEBRATION 2000 experiment, profile CEL02. Tectonophysics 401, 55–77.
Mallet, R., 1852. Second report on the facts of earthquake phenomena. Report of the Twenty-first Meeting of the British Association for the Advancement of Science. 272–320.
Mangino, S., Priestley, K., 1998. The crustal structure of the southern Caspian region. Geophys. J. Int. 133 (3), 630–648.
Marone, F., van der Meijde, M., van der Lee, S., Giardini, D., 2003. Joint inversion of local, regional and teleseismic data for crustal thickness in the Eurasia–Africa plate boundary region. Geophys. J. Int. 154 (2), 499–514.
Marotta, A.M., Bayer, U., Scheck, M., Thybo, H., 2001. The stress field below the NE German Basin; effects induced by the Alpine collision. Geophys. J. Int. 144 (2), F8–F12.
Marotta, A.M., Bayer, U., Thybo, H., Scheck, M., 2002. Origin of the regional stress in the North German basin: results from numerical modelling. Tectonophysics 360, 245–264.
Mart, Y., Ryan, W.B.F., Lunina, O.V., 2005. Review of the tectonics of the Levant Rift system: the structural significance of oblique continental breakup. Tectonophysics 395, 209–232.
Masson, F., Hauser, F., Jacob, A.W.B., 1999. The lithospheric trace of the Iapetus Suture in SW Ireland from teleseismic data. Tectonophysics 302, 83–98.
Mattavelli, L., Novelli, L., Anelli, L., 1991. Occurrence of hydrocarbons in the Adriatic basin. Generation, Accumulation and Production of Europe's Hydrocarbons. In: Spencer, A.M. (Ed.), Sp. Publ. EAPG No. 1. Oxford University Press, pp. 369–380.
Matte, P., 1986. Tectonics and plate tectonics model for the Variscan Belt of Europe. Tectonophysics 126, 329–374.
Matte, P., Hirn, A., 1988. Seismic signature and tectonic cross-section of the Variscan crust in western France. Tectonics 7 (2), 141.
Mauffret, A., Pascal, G., Maillard, A., Gorini, C., 1995. Tectonics and deep-structure of the north-western Mediterranean basin. Mar. Pet. Geol. 12 (6), 645–666.
Maupin, V., Agostini, A., Artemieva, I., et al., 2013. The deep structure of the Scandes and its relation to tectonic history and present-day topography. Tectonophysics http://dx.doi.org/10.1016/j.tecto.2013.03.010.
Maystrenko, Yu., Stovba, S.M., Stephenson, R.A., et al., 2003. Crustal-scale pop-up structure in cratonic lithosphere: DOBRE deep seismic reflection study of the Donbas Foldbelt, Ukraine. Geology 31 (8), 733–736.
McCaughey, M., Barton, P.J., Singh, S.C., 2000. Joint traveltime inversion of wide-angle seismic data and a deep reflection profile from the central North Sea. Geophys. J. Int. 141 (1), 100–114.
McKenzie, D., Stracke, A., et al., 2004. Source enrichment process responsible for isotopic anomalies in oceanic island basalts. Geochim. Cosmochim. Acta 68, 2699–2724.
Mechie, J., Egorkin, A.V., Fuchs, K., Ryberg, T., Solodilov, L., Wenzel, F., 1993. P-wave mantle velocity structure beneath northern Eurasia from long-range recordings along the profile Quartz. Phys. Earth Planet. Inter. 79, 269–286.
Mechie, J., et al., 2005. Crustal shear velocity structure across the Dead Sea transform from two-dimensional modelling of DESERT project explosion seismic data. Geophys. J. Int. 160 (3), 910–924.
Medialdea, T., Surinach, E., Vegas, R., Banda, E., Ansorge, J., 1986. Crustal structure under the western end of the Betic-Cordillera (Spain). Ann. Geophys. Series B—Terr. Planet. Phys. 4 (4), 457–464.
Meissner, R., 1967. Exploring deep interfaces by seismic wide angle measurements. Geophys. Prospect. 15, 598–617.
Meissner, R., 1986. The Continental Crust: A Geophysical Approach. Acad. Press, Orlando, Florida (426 pp.).
Meissner, R., Bortfeld, R.K., 1990. DEKORP — Atlas. Springer-Verlag, Berlin.
Meissner, R., Thybo, H., Abramovitz, T., 2002. Interwedging and inversion structures around the trans-European suture zone in the Baltic Sea, a manifestation of compressive tectonic phases. Tectonophysics 360 (1–4), 265–280.
Meissner, R., Wever, T., Bittner, R., 1987a. Results of DEKORP 2-s and other reflection profiles through the Variscides. Geophys. J. Roy. Astron. Soc. 89, 319–324.
Meissner, R., Wever, T., Flueh, E.R., 1987b. The Moho in Europe; implications for crustal development. In: Blundell, D.J., Brown, L.D. (Eds.), The Lower Continental Crust. Gauthier-Villars, Paris, France, pp. 357–364.
Mele, G., Sandvol, E., 2003. Deep crustal roots beneath the northern Apennines inferred from teleseismic receiver functions. Earth Planet. Sci. Lett. 211 (1–2), 69–78.
Mele, G., Sandvol, E., Cavinato, G.P., 2006. Evidence of crustal thickening beneath the central Apennines (Italy) from teleseismic receiver functions. Earth Planet. Sci. Lett. 249 (3–4), 425–435.
Menard, G., Molnar, P., 1988. Collapse of a Hercynian Tibetan Plateau into a late Palaeozoic European Basin and Range Province. Nature 334, 235–237.
Mengel, K., Kern, H., 1992. Evolution of the petrological and seismic Moho; implications for the continental crust–mantle boundary. Terra Nova 4 (1), 109–116.
Menke, W., Levin, V., 1994. Cold crust in a hot spot. Geophys. Res. Lett. 21, 1967–1970.
Merle, O., Michon, L., 2001. The formation of the West European rift: a new model as exemplified by the Massif Central area. Bull. Soc. Geol. Fr. 172, 81–89.
Mickus, K., Jallouli, C., 1999. Crustal structure beneath the Tell and Atlas Mountains (Algeria and Tunisia) through the analysis of gravity data. Tectonophysics 314 (4), 373–385.
Mihalffy, P., Steinberger, B., Schmeling, H., 2008. The effect of the large-scale mantle flow field on the Iceland hotspot track. Tectonophysics 447 (1–4), 5–18.
Millahn, K., Luschen, E., Gebrande, H., 2006. TRANSALP — cross-line recording during the seismic reflection transect in the Eastern Alps. Tectonophysics 414 (1–4), 39–49.
Miller, M.S., Agostinetti, N.P., 2012. Insights into the evolution of the Italian lithospheric structure from S receiver function analysis. Earth Planet. Sci. Lett. 345, 49–59.
Minakov, A., Mjelde, R., Faleide, J.I., et al., 2012. Mafic intrusions east of Svalbard imaged by active-source seismic tomography. Tectonophysics 518–521, 106–118.
Minshull, T.A., White, N.J., Edwards, R.A., et al., 2005. New seismic data reveal the deep structure of the Eastern Black Sea Basin. Eos 86, 413,419.
Minshull, T.A., et al., 1998. Deep structure in the vicinity of the ocean–continent transition zone under the southern Iberia abyssal plain. Geology 26 (8), 743–746.
Mints, M.V., et al., 2007. Crust and upper mantle along profiles 1-EB, 4B, FIRE-1. Models of the Earth's Crust and Upper Mantle by Deep Seismic Profiling. Proc. Intern. Symp., 18–20 September, 2007. Rosnedra. VSEGEI, St. Petersburg. ISBN: 978-5-93761-101-7 (pp. 110–114, 115–119, 120–125).
Mitrovica, J.X., Pysklywec, R.N., Beaumont, C., Rutty, A., 1996. The Devonian to Permian sedimentation of the Russian platform; an example of subduction-controlled long-wavelength tilting of continents. J. Geodyn. 22, 79–96.
Mjelde, R., Faleide, J.I., Breivik, A.J., Rauma, T., 2008a. Lower crustal composition and crustal lineaments on the Vøring Margin, NE Atlantic: a review. Tectonophysics http://dx.doi.org/10.1016/j.tecto.2008.04.018.
Mjelde, R., Faleide, J.I., Breivik, A.J., Raum, T., 2009. Lower crustal composition and crustal lineaments on the Vøring Margin, NE Atlantic: A review. Tectonophysics 472, 183–193.
Mjelde, R., Goncharov, A., Muller, R.D., 2012. The Moho: Boundary above upper mantle peridotites or lower crustal eclogites? A global review and new interpretations for passive margins. Tectonophysics http://dx.doi.org/10.1016/j.tecto.2012.03001.
Mjelde, R., Raum, T., Breivik, A.J., Faleide, J.I., 2008b. Crustal transect across the North Atlantic. Mar. Geophys. Res. 29 (2), 73–87.
Mjelde, R., Raum, T., Kandilarov, A., Murai, Y., Takanami, T., 2008c. Crustal structure and evolution of the outer Møre Margin, NE Atlantic. Tectonophysics http://dx.doi.org/10.1016/j.tecto.2008.06.003.
Mjelde, R., Sellevoll, M.A., Shimamura, H., Iwasaki, T., Kanazawa, T., 1992. A crustal study off Lofoten, N. Norway, by use of 3-component Ocean Bottom Seismographs. Tectonophysics 212, 269–288.
Mjelde, R., Shimamura, H., Kanazawa, T., et al., 2003. Crustal lineaments, distribution of lower crustal intrusives and structural evolution of the Voring Margin, NE Atlantic; new insight from wide-angle seismic models. Tectonophysics 369, 199–218.
Mjelde, R., et al., 1998. Crustal structure of the northern part of the Voring Basin, mid-Norway margin, from wide-angle seismic and gravity data. Tectonophysics 293 (3–4), 175–205.
Mjelde, R., et al., 2001. Crustal structure of the outer Voring Plateau, offshore Norway, from ocean bottom seismic and gravity data. J. Geophys. Res. Solid Earth 106 (B4), 6769–6791.
Mjelde, R., et al., 2002. Geological development of the Sorvestsnaget Basin, SW Barents Sea, from ocean bottom seismic, surface seismic and gravity data. Nor. J. Geol. 82 (3), 183–202.
Mjelde, R., et al., 2005. Continent–ocean transition on the Voring Plateau, NE Atlantic, derived from densely sampled ocean bottom seismometer data. J. Geophys. Res. Solid Earth 110 (B5).
Mohsen, A., et al., 2005. A receiver function study across the Dead Sea Transform. Geophys. J. Int. 160 (3), 948–960.
Molinari, I., Morelli, A., 2011. EPcrust: a reference crustal model for the European Plate. Geophys. J. Int. 185, 352–364.
MONA LISA Working Group, 1997a. Deep seismic investigations of the lithosphere in the southeastern North Sea. Tectonophysics 269, 1–19.
MONA LISA Working Group, 1997b. Closure of the Tornquist Sea: constraints from MONA LISA deep seismic reflection data. Geology 25, 1071–1074.
Mooney, W.D., Brocher, T.M., 1987. Coincident seismic reflection/refraction studies of the continental lithosphere; a global review. Rev. Geophys. 25, 723–742.
Morgan, J.V., Barton, P.J., White, R.S., 1989. The Hatton Bank continental-margin. 3. Structure from wide-angle OBS and multichannel seismic refraction profiles. Geophys. J. Int. 98 (2), 367–384.
Morozova, E.A., Morozov, I.B., Smithson, S.B., Solodilov, L., 2000. Lithospheric boundaries and upper mantle heterogeneity beneath Russian Eurasia: evidence from the DSS profile QUARTZ. Tectonophysics 329, 333–344.
Mosar, J., Torsvik, T.H., team, B., 2002. Opening the Norwegian and Greenland Seas: plate tectonics in Mid Norway since the Late Permian. In: Eide, E.A. (Ed.), BATLAS — Mid Norway Plate Reconstruction Atlas with Global and Atlantic Perspectives. Geological Survey of Norway, pp. 18–39.
Mucuta, D.M., Knapp, C.C., Knapp, J.H., 2006. Constraints from Moho geometry and crustal thickness on the geodynamic origin of the Vrancea Seismogenic Zone (Romania). Tectonophysics 420 (1–2), 23–36.
Müller, D., 2002. The age of the ocean floor. http://www.ngdc.noaa.gov/mgg/mggd.html.
Müller, R.D., Sdrolias, M., Gaina, C., Roest, W.R., 2008. Age, spreading rates and spreading symmetry of the world's ocean crust. Geochem. Geophys. Geosyst. 9 http://dx.doi.org/10.1029/2007GC001743.
Nalivkin, V.D., 1976. Dynamics of the development of the Russian platform structures. Tectonophysics 36, 247–262.
Neprochnov, Y.P., Kosminskaya, I.P., Malovitsky, Ya.P., 1970. Structure of the crust and upper mantle of the Black and Caspian seas. Tectonophysics 10, 517–538.
Neprochnov, Yu.P., Malovitsky, Ya.P., Belokurov, V.S., Garkalenko, I.A., 1975. Profile sections of the crust based on DSS. In: Boulanger, Yu.D. (Ed.), The Earth's Crust and the History of the Black Sea Evolution. Nauka, Moscow, pp. 284–289 (in Russian).
Netzeband, G.L., et al., 2006. The Levantine Basin — crustal structure and origin. Tectonophysics 418 (3–4), 167–188.
Nicolich, R., Laigle, M., Hirn, A., Cernobori, L., Gallart, J., 2000. Crustal structure of the Ionian margin of Sicily: Etna volcano in the frame of regional evolution. Tectonophysics 329, 121–139.
Nielsen, L., Balling, N., Jacobsen, B.H., 2000. Seismic and gravity modelling of crustal structure in the Central Graben, North Sea; observations along MONA LISA Profile 3. Tectonophysics 328 (3–4), 229–244.
Nielsen, L., Boldreel, L.O., Hansen, T.M., Lykke-Andersen, H., Stemmerik, L., Surlyk, F., Thybo, H., 2011. Integrated seismic analysis of the Chalk Group in eastern Denmark—

implications for estimates of maximum palaeo-burial in southwest Scandinavia. Tectonophysics 511, 14–26.
Nielsen, L., Thybo, H., 2006. Identification of crustal and upper mantle heterogeneity by modelling of controlled-source seismic data. Tectonophysics 416 (1–4), 209–228.
Nielsen, L., Thybo, H., Solodilov, L., 1999. Seismic tomographic inversion of Russian PNE data along profile Kraton. Geophys. Res. Lett. 26 (22), 3413–3416.
Nikishin, A.M., Ziegler, P.A., Panov, D.I., et al., 2001. Mesozoic and Cainozoic evolution of the Scythian Platform-Black Sea–Caucasus domain. In: Ziegler, P.A., Cavazza, W., Robertson, A.H.F., Crasquin-Soleau, S. (Eds.), Peri-Tethys Memoir 6: Peri-Tethyan Rift/Wrench Basins and Passive Margins, 186, pp. 295–346.
NOAA National Geophysical Data Center, 2001. 2 Minute Gridded Global Relief Data (ETOPO2). NGDC, Boulder, Colorado (www.ngdc.noaa.gov/mgg/fliers/01mgg04.html).
Nutman, A.P., McGregor, V.R., Friend, C.R.L., Bennett, V.S., Kinny, P.R., 1993. The Itsaq Gneiss Complex of southern west Greenland; the world's most extensive record of early crustal evolution (3900–3600 Ma). Precambrian Res. 78, 1–39.
O'Reilly, B.M., Hauser, F., Jacob, A.W.B., Shannon, P.M., 1996. The lithosphere below the Rockall Trough: wide-angle seismic evidence for extensive serpentinisation. Tectonophysics 255 (1–2), 1–23.
O'Reilly, B.M., et al., 1995. The transition between the Erris and the Rockall basins — new evidence from wide-angle seismic data. Tectonophysics 241 (1–2), 143–163.
Ohlander, B., et al., 1993. Delineation and character of the Archean–Proterozoic boundary in northern Sweden. Precambrian Res. 64 (1–4), 67–84.
Okay, A.I., Tüysüz, O., 1999. Tethyan sutures of Turkey. The Mediterranean Basins: Tertiary Extension Within the Alpine Orogen. In: Durand, B., Jolivet, L., Horvàth, F., Séranne, M. (Eds.), Geological Society, London, Special Publications, 156, pp. 475–515.
Olesen, O., et al., 2002. Bridging the gap between the onshore and offshore geology in Nordland, northern Norway. Nor. J. Geol. 82, 243–262.
Olsen, K.H. (Ed.), 1995. Continental rifts: evolution, structure, tectonics. Developments in Geotectonics, 25. Elsevier, Amsterdam.
Olsson, S., Roberts, R.G., Bothvarsson, R., 2007. Analysis of waves converted from S to P in the upper mantle beneath the Baltic Shield. Earth Planet. Sci. Lett. 257, 37–46.
O'Reilly, B.M., et al., 2006. Crustal thinning, mantle exhumation and serpentinization in the Porcupine Basin, offshore Ireland: evidence from wide-angle seismic data. J. Geol. Soc. 163, 775–787.
Oserskaya, M.L., Podoba, N.V. (Eds.), 1967. Physical Properties of Sediment Cover of USSR Territory. Nedra, Moscow (772 pp. (in Russian)).
Ottemoller, L., Midzi, V., 2003. The crustal structure of Norway from inversion of teleseismic receiver functions. J. Seismol. 7 (1), 35–48.
Palmason, G., 1971. Crustal structure of Iceland from explosion seismology. Societas Sci. Islandica 40, 187.
Palmason, G., 1986. Model of crustal formation in Iceland, and application to submarine mid-ocean ridges. The Western North Atlantic Region. In: Vogt, P.R., Tucholke, B.E. (Eds.), The Geology of North America, vol. M. Geological Society of America, pp. 87–97.
Papanikolaou, D., Barghati, H., Dabovski, C., et al., 2004. Transect VII: East European Craton–Scythian Platform–Dobrogea–Balkanides–Rhodope Massif–Hellenides–East Mediterranean–Cyrenaica. In: Cavvaza, W., Roure, F., Spakman, W., Stampfli, G.M., Ziegler, P.A. (Eds.), The TRANSMED Atlas — The Mediterranean Region from Crust to Mantle. Springer, Berlin Heidelberg (CD-ROM).
Parkin, C.J., White, R.S., 2008. Influence of the Iceland mantle plume on oceanic crust generation in the North Atlantic. Geophys. J. Int. 173 (1), 168–188.
Paul, A., Hatzfeld, D., Kaviani, A., Tatar, M., Pequegnat, C., 2010. Seismic imaging of the lithospheric structure of the Zagros mountain belt (Iran). In: Leturmy, P., Robin, C. (Eds.), Tectonic and Stratigraphic Evolution of Zagros and Makran during the Mesozoic-Cenozoic, Geol. Soc. London Spec. Publ., 330, pp. 5–18.
Paulssen, H., et al., 1999. The NARS-DEEP Project. EUROPROBE GeoRift; Volume 2, Intraplate Tectonics and Basin Dynamics of the Eastern European Craton and Its Margins. In: Stephenson, R.A., Wilson, M., Starostenko, V.I. (Eds.), Tectonophysics. Elsevier, Amsterdam, Netherlands, pp. 1–8.
Pavlenkova, N.I., 1995. Double Moho in the Dnieper–Donets basin. C. R. Acad. Sci. Paris IIa 321, 85–93.
Pavlenkova, N.I., 1996. Crust and upper mantle structure in Northern Eurasia from seismic data. Adv. Geophys. 37, 1–133.
Pavlenkova, N., Yegorkin, A., 1983. Upper mantle heterogeneity in the northern part of Eurasia. Phys. Earth Planet. Inter. 33, 180–193.
Pedreira, D., Pulgar, J.A., Gallart, J., Díaz, J., 2003. Seismic evidence of Alpine crustal thickening and wedging from the western Pyrenees to the Cantabrian Mountains (north Iberia). J. Geophys. Res. 108 (B4), 2204 http://dx.doi.org/10.1029/2001JB001667.
Perchuc, E., Thybo, H., 1996. A new model of upper mantle P-wave velocity below the Baltic Shield. Tectonophysics 253, 227–245.
Pfiffner, O.A., Lehner, P., Heitzmann, P., Mueller, St, Steck, A. (Eds.), 1997. Deep Structure of the Swiss Alps. In: Results of NRP, vol. 20. Birkhauser Verlag, Basel (448 pp.).
Pharaoh, T.C., 1999. Palaeozoic terranes and their lithospheric boundaries within the Trans-European Suture Zone (TESZ): a review. Tectonophysics 314, 17–41.
Planke, S., Skogseid, J., Eldholm, O., 1991. Crustal structure off Norway, 62° to 70° north. Tectonophysics 182, 91–107.
Plomerova, J., Babuska, V., Vecsey, L., Kouba, D., 2002. Seismic anisotropy of the lithosphere around the Trans-European Suture Zone (TESZ) based on teleseismic body-wave data of the TOR experiment. Tectonophysics 360 (1–4), 89–114.
Plomerova, J., Babuska, V., Kozlovskaya, E., Vecsey, L., Hyvönen, L.T., 2008. Seismic anisotropy - A key to resolve fabrics of mantle lithosphere of Fennoscandia. Tectonophysics 462, 125.
Posgay, K., Bodogy, T., Hegedüs, E., Kovácsvölgyi, S., Lenkey, L., Szafián, P., Takács, E., Tımár, Z., Varga, G., 1995. Asthenospheric structure beneath a Neogene basin in SE Hungary. Tectonophysics 252, 467–484.
Powell, C.M.R., Sinha, M.C., 1987. The PUMA experiment west of Lewis, UK. Geophys. J. Roy. Astron. Soc. 89 (1), 259–264.
Prodehl, C., Mueller, S., Glahn, A., Gutscher, M., Haak, V., 1992. Lithospheric cross-sections of the European Cenozoic rift system. Tectonophysics 208 (1–3), 113–138.
Prodehl, C., Kennett, B., Artemieva, I.M., Thybo, H., 2013. 100 years of seismic research on the Moho. Tectonophysics 609, 9–44 (this volume).
Prodehl, C., Mueller, St, Haak, V., 1995. The European Cenozoic rift system. Continental Rifts: Evolution, Structure, Tectonics. In: Olsen, K.H. (Ed.), Developm. Geotecton., 25. Elsevier, pp. 133–212.
Puchkov, V.N., 1997. Structure and geodynamics of the Uralide orogen. Orogeny Through Time. In: Burg, J.P., Ford, M. (Eds.), Geological Society, London, Special Publications, 121, pp. 201–236.
Puchkov, V.N., 2010. Geology of the Urals and Cis-Urals: Actual Problems of Stratigraphy, Tectonics, Geodynamics and Metallogeny. DesignPoligraphService Press, Ufa (280 pp. (in Russian with English annotations)).
Pulgar, J.A., et al., 1996. Seismic image of the Cantabrian Mountains in the western extension of the Pyrenees from integrated ESCIN reflection and refraction data. Tectonophysics 264 (1–4), 1–19.
Rabbel, W., Forste, K., Schulze, A., et al., 1995. A high-velocity layer in the lower crust of the North German Basin. Terra Nova 7, 327–337.
Raum, T., et al., 2002. Crustal structure of the southern part of the Voring Basin, mid-Norway margin, from wide-angle seismic and gravity data. Tectonophysics 355 (1–4), 99–126.
Raum, T., et al., 2006. Crustal structure and evolution of the southern Voring basin and Voring transform margin, NE Atlantic. Tectonophysics 415, 167–202.
Reid, I., Jackson, H.R., 1997. Crustal structure of northern Baffin Bay: seismic refraction results and tectonic implications. JGR 102 (B1), 523–542.
Reid, I.D., Keen, C.E., 1990. High seismic velocities associated with reflections from within the lower oceanic-crust near the continental-margin of eastern Canada. Earth Planet. Sci. Lett. 99 (1–2), 118–126.
Richardson, K.R., Smallwood, J.R., White, R.S., Snyder, D.B., Maguire, P.K.H., 1998. Crustal structure beneath the Faroe Islands and the Faroe–Iceland Ridge. Tectonophysics 300 (1–4), 159–180.
Riedel, C., Ebbing, J., 2008. Hotspot–ridge interaction and its influence on Icelandic crust formation and dynamics. Tectonophysics 447 (1–4), 1–4.
Rijkers, R.H.B., Duin, E.J.T., 1994. Crustal observations beneath the southern North-Sea and their tectonic and geological implications. Tectonophysics 240, 215–224.
Rijkers, R., Duin, E.D., Dusar, M., Langenaeker, V., 1993. Crustal structure of the London–Brabant massif, southern North-Sea. Geol. Mag. 130 (5), 569–574.
Ritzmann, O., Maercklin, N., Faleide, J.I., Bungum, H., Mooney, W.D., Detweiler, S.T., 2007. A three-dimensional geophysical model of the crust in the Barents Sea region: model construction and basement characterization. Geophys. J. Int. 170, 417–435.
Ritzmann, O., et al., 2004. A deep seismic transect from Hovgard Ridge to northwestern Svalbard across the continental–ocean transition: a sheared margin study. Geophys. J. Int. 157 (2), 683–702.
Roberts, D.G., Ginzburg, A., 1984. Deep crustal structure of southwest Rockall Plateau. Nature 308 (5958), 435–439.
Roslov, Yu.V., Sakoulina, T.S., Pavlenkova, N.I., 2009. Deep seismic investigations in the Barents and Kara Seas. Tectonophysics 472, 301–308.
Ruzek, B., et al., 2006. Crustal anisotropy in the Bohemian Massif, Czech Republic: observations based on Central European Lithospheric Experiment Based on Refraction (CELEBRATION) 2000 (vol 108, pg 2392, 2003). J. Geophys. Res. 111 (B5).
Ryaboy, V.Z., 1966. Structure of the earth crust and the upper mantle along the DSS profile Kopet-Dag-Aral Sea. Sov. Geol. 5, 159–162 (in Russian).
Ryaboy, 1990. Upper mantle structure along a profile from Oslo (NORESS) to Helsinki to Leningrad, based on explosion seismology. Bull. Seismol. Soc. Am. 80, 2194–2213.
Rybalka, V., Kashubin, S. (Eds.), 1992. GRANIT Transect: Methods and results of investigations. Ekaterinburg, URGK I UTP VNTGeo. 113 pp. (in Russian).
Ryberg, T., et al., 1996. Two-dimensional velocity structure beneath northern Eurasia derived from the super long-range seismic profile Quartz. Bull. Seismol. Soc. Am. 86 (3), 857–867.
Ryzhiy, B.P., Druzhinin, V.S., Yunsov, F.F., Ananyin, I.V., 1992. Deep structure of the Urals region and its seismicity. Phys. Earth Planet. Inter. 75, 185–191.
Saintot, A., Brunet, M.-F., Yakovlev, F., et al., 2006. The Mesozoic–Cenozoic tectonic evolution of the Greater Caucasus. European Lithosphere Dynamics. In: Gee, D., Stephenson, R. (Eds.), Geol. Soc. London Sp. Publ., 32, pp. 277–289.
Sandrin, A., Nielsen, L., Thybo, H., 2008. Layered crust–mantle transition zone below a large crustal intrusion in the Norwegian–Danish Basin. Tectonophysics http://dx.doi.org/10.1016/j.tecto.2008.05.039.
Sandrin, A., Thybo, H., 2008a. Deep seismic investigation of crustal extensional structures in the Danish Basin along the ESTRID-2 profile. Geophys. J. Int. 173, 623–641.
Sandrin, A., Thybo, H., 2008b. Seismic constraints on a large mafic intrusion with implications for the subsidence history of the Danish Basin. J. Geophys. Res. 113 http://dx.doi.org/10.1029/2007JB005067.
Sapin, M., Prodehl, C., 1973. Long-range profiles in western Europe. 1. Crustal structure between Bretagne and Central Massif of France. Ann. Geophys. 29 (1), 127–145.
Sartori, R., et al., 2004. Crustal features along a W–E tyrrhenian transect from Sardinia to Campania margins (Central mediterranean). Tectonophysics 383 (3–4), 171–192.
Saunders, A.D., Fitton, J.G., Kerr, A.C., Norry, M.J., Kent, R.W., 1997. The North Atlantic igneous province, geophysical monograph. Geophys. Monogr. Am. Geophys. Union 45–93.
Saunders, P., Priestley, K., Taymaz, T., 1998. Variations in the crustal structure beneath western Turkey. Geophys. J. Int. 134, 373–389.
Sayil, N., Osmansahin, I., 2000. Investigation of crust and upper-mantle structure in the Black Sea with group-velocity data. Bull. Seismol. Soc. Am. 90, 870–875.
Scarascia, S., Cassinis, R., 1997. Crustal structures in the central-eastern Alpine sector: a revision of the available DSS data. Tectonophysics 271 (1–2), 157–188.

Scarascia, S., Lozej, A., Cassinis, R., 1994. Crustal structures of the Ligurian, Tyrrhenian and Ionian Seas and adjacent onshore areas interpreted from wide-angle seismic profiles. Boll. Geofis. Teor. Appl. 36 (5–19).
Schmeling, H., 1985. Partial melt below Iceland: a combined interpretation of seismic and conductivity data. J. Geophys. Res. 90, 10105–10116.
Schmeling, H., Marquart, G., 2008. Crustal accretion and dynamic feedback on mantle melting of a ridge centred plume: the Iceland case. Tectonophysics 447 (1–4), 31–52.
Schmelzbach, C., Zelt, C.A., Juhlin, C., Carbonell, R., 2008. P- and S–V-velocity structure of the South Portuguese Zone fold-and-thrust belt, SW Iberia, from traveltime tomography. Geophys. J. Int. 175 (2), 689–712.
Schmid, S.M., Pfiffner, O.A., Froitzheim, N., Schonborn, G., Kissling, E., 1996. Geophysical–geological transect and tectonic evolution of the Swiss–Italian Alps. Tectonics 15 (5), 1036–1064.
Schmidt-Aursch, M., Jokat, W., 2005a. The crustal structure of central East Greenland — I: from the Caledonian orogen to the tertiary igneous province. Geophys. J. Int. 160 (2), 736–752.
Schmidt-Aursch, M.C., Jokat, W., 2005b. The crustal structure of central East Greenland — II: from the Precambrian shield to the recent mid-oceanic ridges. Geophys. J. Int. 160 (2), 753–760.
Schroeder, W., 1984. The empirical age–depth relation and depth anomalies in the Pacific ocean basin. J. Geophys. Res. 89, 9873–9883.
Scrocca, D., et al., 2004. CROP ATLAS — deep seismic reflection profiles of the Italian crust. Mem. Descrittive della Carta Geologica d'Italia 62 (Publication sponsored by Servizio Geologico Nazionale (now APAT)).
Segalovich, V.I., Volozh, Yu.A., Antipov, M.P., Vasil'ev, O.A., 2007. Nature of the North Caspian gravity anomaly. Geotektonika, 2007, No. 3, 30–45 (English translation. Geotectonics (Springer) 41 (3), 195–209 http://dx.doi.org/10.1134/S0016852107030028).
Sellevol, M.A., 1973. Mohorovicic discontinuity beneath Fennoscandia and adjacent parts of Norwegian Sea and North-Sea. Tectonophysics 20 (1–4), 359–366.
Sellevoll, M.A., Warrick, R.E., 1971. A refraction study of the crustal structure in southern Norway. Bull. Seismol. Soc. Am. 61, 457–471.
Semikhatov, M.A., 1991. General problems of Proterozoic stratigraphy in the USSR: Soviet Scientific Review, Section B. Geology Reviews. Harwood Acad. Publ.(189 pp.).
Sengör, A.M.C., 1990. Plate-tectonics and orogenic research after 25 years — a Tethyan perspective. Earth Sci. Rev. 27, 1–201.
Sengör, A.M.C., Natal'in, B.A., Burtman, V.S., 1993. Evolution of the Altaid tectonic collage and Palaeozoic crustal growth in Eurasia. Nature 364, 299–307.
Sharov, N.V., Kosminskaya, I.P., Azbel, I., Zagorodny, V., Korhonen, H., Luosto, U., 1990. Compiling DSS profiles in the southeast of the Baltic Shield. Geotectonics 24 (1), 35–42.
Sharov, N.V., Slabunov, A.I., Isanina, E.V., et al., 2010. Seismo-geological cross-section of the crust along the DSS-CDP profile "Land-Sea" Kalevala-Kem-Western White Sea. Geophysical J. (Ukraine) 5 (32), 21–34.
Shulgin, A., Thybo, H., TopoGreenland Refraction Seismic Field Team (S. Reiche, G. Kaip, B. Greschke, Z. Chemia, A. S. Bruun, and H. Thybo), 2012. Crustal structure in central-eastern Greenland. Abstr. 34th Int. Geol. Congress, Brisbane, Aug. 2012.
Sichien, E., Henriet, J.-P., Camelbeeck, T., De Baets, B., 2012. Estimating crustal thickness in Belgium and surrounding regions from Moho-reflected waves. Tectonophysics 560–561, 105–119.
Sigmundsson, F., Schmundsson, K., 2008. Iceland: a window on North-Atlantic divergent plate tectonics and geologic processes. Episodes 31, 92–97.
Skaarup, N., Jackson, H.R., Oakey, G.N., 2006. Margin segmentation of Baffin Bay/Davis Strait, eastern Canada based on seismic reflection and potential field data. Mar. Pet. Geol. 23, 127–144.
Smith, P.J., Bott, M.H.P., 1975. Structure of crust beneath Caledonian Foreland and Caledonian Belt of North Scottish Shelf region. Geophys. J. Roy. Astron. Soc. 40 (2), 187–205.
Snyder, D.B., Hobbs, R.W., 1999. BIRPS Atlas II: A Second Decade of Deep Seismic Reflection Profiling. Geol. Soc. London, London.
Sodoudi, F., Bruestle, A., Meier, T., Kind, R., Friederich, W., EGELADOS working group, 2013. New constraints on the geometry of the subducting African plate and the overriding Aegean plate obtained from P receiver functions and seismicity. Solid Earth Discuss. 5, 427–461 http://dx.doi.org/10.5194/sed-5-427-2013 (www.solid-earth-discuss.net/5/427/2013/).
Sollogub, V.B., 1970. On certain regularities of crustal structure associated with the major geologic features of southeastern Europe. Tectonophysics 10, 549–559.
Sollogub, V.B., et al., 1980. Crustal Structure of Central and Eastern Europe Based on Geophysical Data. Naukova Dumka, Kiev (in Russian).
Souriau, A., Chevrot, S., Olivera, C., 2008. A new tomographic image of the Pyrenean lithosphere from teleseismic data. Tectonophysics 460, 206–214 http://dx.doi.org/10.1016/j.tecto.2008.08.014.
Sroda, P., Czuba, W., Grad, M., Guterch, A., Gaczynski, E., 2002. Three-dimensional seismic modelling of crustal structure in the TESZ region based on POLONAISE'97 data. Tectonophysics 360, 169–185.
Sroda, P., Czuba, W., Guterch, A., et al., 1999. P- and S-wave velocity model of the southwestern margin of the Precambrian East European Craton; POLONAISE '97, Profile P3. Tectonophysics 314, 175–192.
Sroda, P., et al., 2006. Crustal and upper mantle structure of the Western Carpathians from CELEBRATION 2000 profiles CEL01 and CEL04: seismic models and geological implications. Geophys. J. Int. 167 (2), 737–760.
Stampfli, G.M., Borel, G.D., 2004. The TRANSMED transects in space and time; constraints on the palaeotectonic evolution of the Mediterranean Domain. In: Cavvaza, W., Roure, F., Spakman, W., Stampfli, G.M., Ziegler, P.A. (Eds.), The TRANSMED Atlas — The Mediterranean Region from Crust to Mantle. Springer-Verlag, Berlin, Heidelberg, pp. 53–80.
Stangl, R., 1990. Die Struktur der Lithosphäire in Schweden, abgeleitet aus einer gemeinsamen Interpretation der P- und S-Wellen Registrierungen auf dem FENNOLORA-Profil. University of Karlsruhe (187 pp.).
Staples, R.K., et al., 1997. Faeroe–Iceland ridge experiment 1. Crustal structure of northeastern Iceland. J. Geophys. Res. 102, 7849–7866.
Starostenko, V., Janik, T., Kolomiyets, K., et al., 2013. Seismic velocity model of the crust and upper mantle along profile PANCAKE across the Carpathians between the Pannonian Basin and the East European Craton. Tectonophysics http://dx.doi.org/10.1016/j.tecto.2013.07.008.
Starostenko, V., et al., 2004. Topography of the crust–mantle boundary beneath the Black Sea Basin. Tectonophysics 381, 211–233.
Steer, D.N., Knapp, J.H., Brown, L.D., 1998a. Super-deep reflection profiling: exploring the continental mantle lid. Tectonophysics 286 (1–4), 111–121.
Steer, D.N., Knapp, J.H., Brown, L.D., Echtler, H.P., Péréz-Estaun, A., Berzin, R., 1998b. Deep structure of the continental lithosphere in an unextended orogen: an explosive source seismic reflection profile in the Urals (Urals Seismic Experiment and Integrated Studies (URSEIS 1995). Tectonics 17, 143–157.
Steer, D.N., Knapp, J.H., Brown, L.D., Rybalka, A.V., Sokolov, V.B., 1995. Crustal structure of the Middle Urals based on reporocessing of Russian seismic reflection data. Geophys. J. Int. 123, 673–682.
Stefansson, R., Gudmundsson, G.B., Halldorsson, P., 2008. Tjornes fracture zone. New and old seismic evidences for the link between the North Iceland rift zone and the Mid-Atlantic ridge. Tectonophysics 447 (1–4), 117–126.
Stein, C.A., Stein, S., 1992. A model for the global variation in oceanic depth and heat flow with lithospheric age. Nature 359, 123–129.
Stein, C.A., Stein, S., 2003. Mantle plumes: heat-flow near Iceland. Astron. Geophys. 44, 8-U1.
Stepanyuk, L., Claesson, S., Bibikova, E., Bogdanova, S., 1998. Sm–Nd crustal ages along the EUROBRIDGE transect in the Western Ukrainian Shield. Geophys. J. (Kiev, Ukraine) 20 (4), 118–120.
Stipcevic, J., Tkalcic, H., Herak, M., Markusic, S., Herak, D., 2011. Crustal and uppermost mantle structure beneath the External Dinarides, Croatia, determined from teleseismic receiver functions. Geophys. J. Int. 185, 1103–1119.
Stovba, S., Stephenson, R., Dvoryanin, E., 1995. Dnieper–Donets basin, Ukraine: main observations from regional seismic reflection profiles. C. R. Aca. Sc — Series IIA t. 321, 1103–1110.
Stovba, S., Stephenson, R.A., Kivshik, M., 1996. Structural features and evolution of the Dniepr–Donets Basin, Ukraine, from regional seismic reflection profiles. Tectonophysics 268, 127–147.
Stratford, W., Thybo, H., 2011a. Crustal structure and composition of the Oslo Graben, Norway. Earth Planet. Sci. Lett. 304, 431–442.
Stratford, W., Thybo, H., 2011b. Seismic structure and composition of the crust beneath the southern Scandes, Norway. Tectonophysics 502, 364–382.
Stratford, W., Thybo, H., Faleide, J.I., Olesen, O., Tryggvason, A., 2009. New Moho Map for onshore southern Norway. Geophys. J. Int. 178, 1755–1765.
Suckro, S., Gohl, K., Funck, T., et al., 2012. The crustal structure of southern Baffin Bay: implications from a seismic refraction experiment. Geophys. J. Int. 190, 37–58.
Suleimanov, A.K., 2006. CDP studies for the URSEIS profile. Structure and Dynamics of the East European Lithosphere. GEOS, 2. Geokart, Moscow, pp. 363–373 (in Russian).
Surinach, E., Vegas, R., 1988. Lateral inhomogeneities of the Hercynian crust in central Spain. Phys. Earth Planet. Inter. 51 (1–3), 226–234.
Svenningsen, L., Balling, N., Jacobsen, B.H., Kind, R., Wylegalla, K., Schweitzer, J., 2007. Crustal root beneath the highlands of southern Norway resolved by teleseismic receiver functions. Geophys. J. Int. 170, 1129–1138.
Taghizadeh-Farahmand, F., Sodoudi, F., Afsari, N., Ghassemi, M., 2010. Lithospheric structure of NW Iran from P and S receiver functions. J. Seismol. 14, 823–836 http://dx.doi.org/10.1007/s10950-010-9199-2.
Tellez, J., Cordoba, D., 1996. Observation of converted Moho reflections in the north-west of the Iberian Peninsula. Geophys. J. Int. 124 (1), 7–17.
Tesauro, M., Kaban, M.K., Cloetingh, S.A.P.L., 2008. EuCRUST-07: a new reference model for the European crust. Geophys. Res. Lett. 35 (5) (Article Number: L05313).
Thinon, I., et al., 2003. Deep structure of the Armorican Basin (Bay of Biscay): a review of Norgasis seismic reflection and refraction data. J. Geol. Soc. 160, 99–116.
Thouvenot, F., Kashubin, S.N., Poupinet, G., Makovsky, V.V., Kashubina, T.V., Matte, P., Jenatton, L., 1995. The root of the Urals: evidence from wide-angle reflection seismics. Tectonophysics 250, 1–13.
Thouvenot, F., et al., 2007. Are there really superposed Mohos in the southwestern Alps? New seismic data from fan-profiling reflections. Geophys. J. Int. 170 (3), 1180–1194.
Thybo, H., 1990. A seismic velocity model along the EGT profile — from the North German Basin into the Baltic Shield. In: Freeman, R., Giese, P., Muller, S.T. (Eds.), The European Geotraverse. Integrative Studies. European Science Foundation, Strasbourg, pp. 99–108.
Thybo, H., 1997. Geophysical characteristics of the Tornquist Fan area, northwest TESZ: indication of Late Carboniferous to Early Permian dextral transtension. Geol. Mag. 134, 597–606.
Thybo, H., 2000. Crustal structure and tectonic evolution of the Tornquist Fan region as revealed by geophysical methods. Bull. Geol. Soc. Den. 46, 145–160.
Thybo, H., 2001. Crustal structure along the EGT profile across the Tornquist Fan interpreted from seismic, gravity and magnetic data. Tectonophysics 334, 155–190.
Thybo, H., Artemieva, I.M., 2013. Moho and magmatic underplating in continental lithosphere. Tectonophysics 609, 605–619 (in this volume).
Thybo, H., Nielsen, C.A., 2009. Magma-compensated crustal thinning in continental rift zones. Nature 457, 873–876.
Thybo, H., Perchuc, E., Gregersen, S., 1998. Interpretation in statu nascendi of seismic wide-angle reflections based on EUGENO-S data. Tectonophysics 289 (4), 281–294.
Thybo, H., Maguire, P.K.H., Birt, C., Perchuc, E., 2000. Seismic reflectivity and magmatic underplating beneath the Kenya Rift. Geophys. Res. Lett. 27, 2745–2748.
Thybo, H., Pharaoh, T., Guterch, A. (Eds.), 1999. Geophysical Investigations of the Trans-European Suture Zone. Tectonophysics, 314 (350 pp.).

Thybo, H., Pharaoh, T., Guterch, A. (Eds.), 2002. The Trans European Suture Zone II, Tectonophysics, 360 (314 pp.).
Thybo, H., Sandrin, A., Nielsen, L., Lykke-Andersen, H., Keller, G.R., 2006. Seismic velocity structure of a large mafic intrusion in the crust of central Denmark from project ESTRID. Tectonophysics 420, 105–122.
Thybo, H., Schonharting, G., 1991. Geophysical evidence for Early Permian igneous activity in a transtensional environment, Denmark. Tectonophysics 189 (1–4), 193–208.
Thybo, H., Shulgin, A.A., 2013. Crustal structure in east-central Greenland. J. Geophys. Res. (in preparation).
Thybo, H., et al., 2003. Upper lithospheric seismic velocity structure across the Pripyat Trough and the Ukrainian Shield along the EUROBRIDGE'97 profile. Tectonophysics 371 (1–4), 41–79.
Tichomirowa, M., Whitehouse, M.J., Nasdala, L., 2005. Resorption, growth, solid state recrystallisation, and annealing of granulite facies zircon — a case study from the Central Erzgebirge, Bohemian Massif. Lithos 82, 25–50.
Tiira, T., Hyvonen, T., Komminaho, K., Korja, A., Heikkinen, P., 2006. 3-D inversion of Moho discontinuity using wide-angle reflections in the Baltic Shield. EGU abstracts, Vienna, April 2006, EGU06-A-06893.
Tilmann, F.J., Dahm, T., 2008. Constraints on crustal and mantle structure of the oceanic plate south of Iceland from ocean bottom recorded Rayleigh waves. Tectonophysics 447 (1–4), 66–79.
Torsvik, T.H., Müller, R.D., Van der Voo, R., Steinberger, B., Gaina, C., 2008. Global plate motion frames: Toward a unified model. Rev. Geophys. 46 Article Number: RG3004, http://dx.doi.org/10.1029/2007RG000227.
TRANSALP Working Group, 2002. First deep seismic reflection images of the Eastern Alps reveal giant crustal wedges and transcrustal ramps. Geophys. Res. Lett. 29 (10), 92-1/92-4 http://dx.doi.org/10.1029/2002GRL014911.
Trofimov, V.A., 2006. Deep CMP seismic surveying along the Tatseis-2003 geotraverse across the Volga–Ural petroliferous province. Geotektonika 4, 3–20 (English translation in Geotectonics 40, 249–262).
Tryti, J., Sellevoll, M.A., 1977. Seismic crustal study of the Oslo rift. PAGEOPH 115, 1061–1085.
Tsikalas, F., Eldholm, O., Faleide, J.I., 2005. Crustal structure of the Lofoten–Vesteralen continental margin, off Norway. Tectonophysics 404, 151–174.
Vergés, J., Saura, E., Casciello, E., Fernàndez, M., Villaseñor, A., Jiménez-Munt, I., García-Castellanos, D., 2011. Crustal-scale cross-sections across the NW Zagros belt: implications for the Arabian margin reconstruction. Geol. Mag. Cambridge University Press, pp. 1–23 http://dx.doi.org/10.1017/S0016756811000331.
Vogt, U., Makris, J., O'Reilly, B.M., et al., 1998. The Hatton basin and continental margin: crustal structure from wide-angle seismic and gravity data. J. Geophys. Res. 103 (B6), 12545–12566.
Volozh, Y.A., Sinelnikov, A.V., Groshev, V.G., 1996. Stratigraphy of Mesozoic–Cenozoic deposits in the salt dome basin of the Peri-Caspian depression. Stratigr. Geol. Correl. 4 (4), 409–415.
Volvovski, I.S., 1973. Seismic Studies of the Earth's Crust in the USSR. Nedra, Moscow (208 pp.).
Volvovsky, I.S., Volvovsky, B.S., 1975. Cross-sections of the Earth's crust for the USSR territory based on deep seismic sounding. MGC RAS. Nauka, Moscow (268 pp. (in Russian)).
Voss, M., Jokat, W., 2007. Continent–ocean transition and voluminous magmatic underplating derived from P-wave velocity modelling of the East Greenland continental margin. Geophys. J. Int. 170 (2), 580–604.
Waight, T.E., Baker, J.A., 2012. Depleted basaltic lavas from the Proto-Iceland plume, central East Greenland. J. Petrol. 53, 1569–1596.
Walter, C., Flueh, E.R., 1993. The POLAR profile revisited: combined P- and S-wave interpretation. Precambrian Res. 64, 153–168.
Weber, Z., 2002. Imaging Pn velocities beneath the Pannonian basin. Phys. Earth Planet. Inter. 129 (3–4), 283–300.
Weir, N.R.W., White, R.S., Brandsdottir, B., Einarsson, P., et al., 2001. Crustal structure of the northern Reykjanes Ridge and Reykjanes Peninsula, southwest Iceland. J. Geophys. Res. 106, 6347–6368.
White, R.S., Jones, E.J.W., Hughes, V.J., Matthews, D.H., 1982. Crustal structure from 2-ship multichannel seismic profiles on the continental-shelf off northwest Scotland. Tectonophysics 90 (1–2), 167–178.
White, R.S., McBride, J.H., Maguire, P.K.H., Brandsdottir, B., Menke, W., Minshull, T.A., Richardson, K.R., Smallwood, J.R., Staples, R.K., the FIRE Working Group, 1996. Seismic images of crust beneath Iceland contribute to long-standing debate. Eos 77, 197.
White, R.S., Smith, L.K., Roberts, A.W., Christie, P.A.F., Kusznir, N.J., 2008. Lower-crustal intrusion on the North Atlantic continental margin. Nature 452, 460–465.
White, R.S., Spence, G.D., Fowler, S.R., McKenzie, D.P., Westbrook, G.K., Bowen, A.N., 1987. Magmatism at rifted continental margins. Nature (London) 330, 439–444.
Whitmarsh, R.B., Langford, J.J., Buckley, J.S., Bailey, R.J., Blundell, D.J., 1974. Crustal structure beneath porcupine ridge as determined by explosion seismology. Earth Planet. Sci. Lett. 22, 197–204.
Whitmarsh, R.B., Miles, P.R., Mauffret, A., 1990. The ocean–continent boundary off the western continental-margin of Iberia. 1. Crustal structure at 40°30′N. Geophys. J. Int. 103 (2), 509–521.
Wigger, P., et al., 1992. Crustal structure along a traverse across the Middle and High Atlas mountains derived from seismic refraction studies. Geol. Rundsch. 81 (1), 237–248.
Wilde-Piorko, M., Grad, M., TOR Working Group, 2002. Crustal structure variation from the Precambrian to Palaeozoic platforms in Europe imaged by the inversion of teleseismic receiver functions — project TOR. Geophys. J. Int. 150, 261–270.
Winchester, J.A., the PACE Network Team, 2002. Palaeozoic amalgamation of Central Europe: new results from recent geological and geophysical investigations. Tectonophysics 360, 5–21.
Ye, S., Ansorge, J., Kissling, E., Mueller, S., 1995. Crustal structure beneath the eastern Swiss Alps derived from seismic-refraction data. Tectonophysics 242 (3–4), 199–221.
Yegorkin, A.V., Matushkin, B.A., 1970. Crustal structure of the Caucasus and western Central Asia based on geophysical sounding data. Int. Geol. Rev. 12, 281–290.
Yegorova, T.P., Starostenko, V.I., 1999. Large-scale three-dimensional gravity analysis of the lithosphere below the transition zone from Western Europe to the East European Platform. Tectonophysics 314, 83–100.
Yilmaz, Y., Genç, S.C., Gürer, F., et al., 2000. When did the western Anatolian grabens begin to develop? Tectonics and Magmatism in Turkey and the Surrounding Area. In: Bozkurt, E., Winchester, J.A., Piper, J.D.A. (Eds.), Geological Society, London, Special Publications, 173, pp. 353–384.
Yoon, M.-K., Baykulov, M., Dümmong, S., et al., 2009. Reprocessing of deep seismic reflection data from the North German Basin with the Common Reflection Surface stack. Tectonophysics 472, 273–283.
Yurov, Yu.G., 1980. Regional cross section through the Russian platform (Kupiyansk–Kineshma profile) (in Russian). In: Zverev, S.M., Kosminskaya, I.P. (Eds.), Seismic Models of the Lithosphere for the Major Geostructures on the Territory of the USSR. Nauka, Moscow, pp. 50–60.
Zeck, H.P., 1999. Alpine plate kinematics in the western Mediterranean: a westward-directed subduction regime followed by slab roll-back and slab detachment. The Mediterranean Basins: Tertiary Extension within the Alpine Orogen. In: Durand, B., Jolivet, L., Horvath, F., Séranne, M. (Eds.), Geological Society, London, Special Publications, 156, pp. 109–120.
Zeis, S., Gajewski, D., Prodehl, C., 1990. Crustal structure of southern Germany from seismic refraction data. Tectonophysics 176 (1–2), 59–86.
Zelt, C.A., Smith, R.B., 1992. Seismic traveltime inversion for 2-D crustal velocity structure. Geophys. J. Int. 108 (1), 16–34.
Zelt, B.C., Taylor, B., Sachpazi, M., Hirn, A., 2005. Crustal velocity and Moho structure beneath the Gulf of Corinth, Greece. Geophys. J. Int. 162 (1), 257–268.
Zeyen, H., et al., 1997. Refraction-seismic investigations of the northern Massif Central (France). Tectonophysics 275 (1–3), 99–117.
Zhang, J., Langston, C.A., 1995. Dipping structure under Dourbes, Belgium, determined by receiver function modeling and inversion. Bull. Seismol. Soc. Am. 85 (1), 254–268.
Zhu, L., Kanamori, H., 2000. Moho depth variation in southern California from teleseismic receiver functions. J. Geophys. Res. 105, 2969–2980.
Zhu, L.P., Mitchell, B.J., Akyol, N., et al., 2006. Crustal thickness variations in the Aegean region and implications for the extension of continental crust. J. Geophys. Res. 111 (Article Number: B01301).
Ziegler, P., 1986. Geodynamic model for the Palaeozoic crustal consolidation of western and central Europe. Tectonophysics 126, 303–328.
Ziegler, P.A., 1992. European Cenozoic rift system. Tectonophysics 208, 91–111.
Ziegler, P.A., Dezes, P., 2006. Crustal evolution of Western and Central Europe. European Lithosphere Dynamics. In: Gee, D., Stephenson, R. (Eds.), Geol. Soc. London Sp. Publ., 32, pp. 43–56.
Zonenshain, L.P., Kuzmin, M.I., Natapov, L.M. (Eds.), 1990. Geology of the USSR: a plate tectonic synthesis. AGU Geodynam. Ser., 21.
Zonenshain, L.P., Le Pichon, X., 1986. The Black Sea and Caspian Sea deep basins as remnants of Mesozoic back arc basins. Tectonophysics 123, 181–211.
Zor, E., Sandvol, E., Gurbuz, C., et al., 2003. The crustal structure of the East Anatolian plateau (Turkey) from receiver functions. Geophys. Res. Lett. 30 (Article Number: 8044).
Zverev, S.M., Kosminskaya, I.P. (Eds.), 1980. Seismic Models of the Lithosphere for the Major Geostructures on the USSR Territory. Nauka, Moscow (218 pp. (in Russian)).